A novel fictitious sequence generation approach for fast estimations of hybrid real-time HVAC system in building performances

Prasaant Balasundaram

THÈSE

Pour obtenir le grade de

DOCTEUR DE L'UNIVERSITÉ GRENOBLE ALPES

École doctorale : EEATS
Spécialité : Automatique et Productique
Unité de recherche : GSCOP / G2ELab

Une nouvelle approche de génération de séquences fictives pour des estimations rapides de systèmes CVC hybrides en temps réel dans les performances des bâtiments

A novel fictitious sequence generation approach for fast estimations of hybrid real-time HVAC system in building performances

Présentée par :

Balasundaram Prasaant

Direction de thèse :

Stéphane PLOIX	Directeur ou Directrice de thèse
Benoit DELINCHANT	Co-Directeur ou co-directrice de thèse

Rapporteurs :

Frédéric Hamelin
Professeur des universités, Université de Lorraine
Christian Inard
Professeur des universités, Université de La Rochelle

Thèse soutenue publiquement le **« date de soutenance (23/01/2023) »**, devant le jury composé de :

Stéphane Ploix Professeur des universités, Université Grenoble Alpes	Directeur de thèse
Benoit Delinchant Professeur des universités, Université Grenoble Alpes	Co-Directeur de thèse
Frédric Hamelin Professeur des universités, Université de Lorraine	Rapporteur
Christian Inard Professeur des universités, Université de La Rochelle	Rapporteur
Gilles Fraisse Professeur des universités, USMB	Examinateur
Stéphane Ginestet Professeur des universités, INSA Toulouse	Examinateur
Seddick Bacha Professeur des universités, Université Grenoble Alpes	Président du jury

Invités :

Cristian Muresan
Ingénieur de Recherche, ENGIE CRIGEN

Titre : Une nouvelle approche de génération de séquences fictives pour des estimations rapides de systèmes CVC hybrides en temps réel dans les performances des bâtiments

Mots clés : Optimisation, simulation en temps réel, réduction de séquence

Résumé : Les simulations Hardware in the Loop (HIL) offrent un avantage de test en temps réel dans des conditions de terrain quasi réelles. Ceci est dû au fait que le simulateur HIL comporte deux parties une partie réelle et une partie virtuelle. Dans la plupart des cas, la partie réelle est le système qui doit être testé (généralement un système de chauffage ou de refroidissement), tandis que la partie virtuelle constitue l'enveloppe du bâtiment qui combine l'environnement bâti et les conditions météorologiques. On peut utiliser cette philosophie pour évaluer la performance saisonnière d'un système de chauffage/refroidissement par rapport à une enveloppe de bâtiment particulière. Les méthodologies existantes utilisent cette philosophie HIL pour évaluer l'efficacité saisonnière. Ils s'appuient sur l'idée de récupérer des jours représentatifs de test à partir des données météorologiques existantes. Ces journées types peuvent inclure des journées de différentes saisons. La sélection des jours pertinents est basée sur la technique de regroupement où les jours de différentes saisons sont utilisés pour les tests sont discontinus, ce qui a entraîné des retards supplémentaires dans la durée des tests. Ce travail de recherche propose une alternative à l'approche du jour de collecte : la conception de données météorologiques fictives représentatives peut encore être surmontée en essayant d'ajouter plus de fonctionnalités au temps de test en développant de nouvelles conditions météorologiques fictives basées sur les métadonnées de l'ensemble. données météorologiques de l'année. Ces données fictives peuvent représenter toutes les données météorologiques ou les données que nous voulons en utilisant ces conditions de test fictives. Un tel résultat est ensuite comparé avec la méthode de clustering de pointe. En bref, le problème est de développer une nouvelle méthodologie qui réduira le temps nécessaire à la simulation HIL pour l'évaluation des performances saisonnières des systèmes énergétiques. La méthodologie choisit de surmonter les discontinuités entre les jours de test en raison de la méthodologie de clustering. De plus, la nouvelle méthodologie souhaite représenter une séquence courte fictive qui représentera les non-linéarités de la saison de chauffage, assurera la convergence des rendements saisonniers du système énergétique sous test. Enfin plusieurs séquences courtes fictives sont générées pour vérifier si la méthodologie pourrait poser des incertitudes sur les performances saisonnières évaluées.

Title: A novel fictitious sequence generation approach for fast estimations of hybrid real-time HVAC system in building performances

Keywords: Optimization, Real Time Simulation, Sequence Reduction

Abstract: The Hardware in the Loop (HIL) simulations offer a real time testing advantage in near real field conditions. This is since the HIL simulator has two parts a real part and a virtual part. In most cases, the real part is the system that needs to be tested (usually a heating or a cooling system), while the virtual part forms the building envelope which combines the built environment and the weather conditions. One can use this philosophy to evaluate the seasonal performance of a heating/cooling system with respect to a particular building envelope. Existing methodologies make use of this HIL philosophy to evaluate the seasonal efficiency. They rely on the idea of picking-up testing representative days from the existing weather data. These typical days can include the days from different seasons. Selecting the relevant days is based on the clustering technique where days from different seasons are used for testing are discontinuous, which led to further delays in the testing time. This research work proposes an alternative to the picking-up day approach: the design of representative fictitious weather data. can further be overcome by trying to add more features to the testing time by developing a new fictitious weather conditions based on the meta data of the whole year weather data. This fictitious data can represent all the weather data or the data that we want using this fictitious testing conditions. Such, a result is then compared with the state-of-the-art clustering method. In short the problem is to develop a new methodology that will reduce the time taken for HIL simulation for the evaluation of seasonal performance of the energy systems. The methodology chooses to overcome the discontinuities between the testing days due to the clustering methodology. Also , the new methodology wishes to represent a fictious short sequence that will represent the non-linearities in the heating season, ensure the convergence of the seasonal efficiencies of the energy system under the test. Finally multiple fictitious short sequences are generated to check if the methodology could pose any uncertainties on the seasonal performance evaluated.

Abstract

The Hardware in the Loop (HIL) simulations offer a real time testing advantage in near real field conditions, because it has two parts a real part and a virtual part. In most cases, the real part is the system that needs to be tested (usually a heating or a cooling system), while the virtual part forms the building envelope which combines the built environment and the weather conditions. One can use this philosophy to evaluate the seasonal performance of a heating/cooling system with respect to a particular building envelope. Existing methodologies make use of this HIL philosophy to evaluate the seasonal efficiency. They rely on the idea of picking-up testing representative days from the existing weather data. These typical days can include the days from different seasons. Selecting the relevant days is based on the clustering technique where days from different seasons are used for testing are discontinuous, which led to further delays in the testing time.

This research work proposes an alternative to the picking-up day approach: the design of representative fictitious weather data. One can overcome the present testing methodology by trying to add more features to the testing time by developing a new fictitious weather conditions based on the meta data of the whole year weather data. This fictitious data can represent all the weather data or the data that we want using this fictitious testing conditions. Such, a result is then compared with the state-of-the-art clustering method.

Finally multiple fictitious short sequences are generated to check if the methodology could pose any uncertainties on the seasonal performance evaluated. The results obtained using the fictitious sequence methodology hold good different climatic conditions, different building envelopes and different test sequences. The results obtained also elucidate that the same could be applied to use cases where multiple features (signals) could be involved for both open loop and closed loop HIL applications theoretically.

Table of Contents

List of Abbreviations

HIL	: Hardware in the Loop
DUT	: Device Under Test
SUT	: System Under Test
BBT	: Black Box Testing
WBT	: White Box Testing
GBT	: Grey Box Testing
sHIL	: Signal Hardware in the Loop
CIL	: Controller in the Loop
CHIL	: Controller Hardware in the Loop
pHIL	: power Hardware in the Loop
mHIL	: mechanical Hardware in the Loop
RTOS	: Real-Time Operating System
MCU	: Micro-Controller Unit
FPGA	: Field-Programmable Gate Array
DSP	: Digital Signal Processors
GPU	: Graphical Processing Units
CPU	: Central Processing Unit
KPI	: Key Performance Indicator
AWHP	: Air to Water Heat Pump
SH	: Space Heating
DHW	: Domestic Hot Water
GSHP	: Ground Source Heat Pump
BCVTB	: Building Controls Virtual Test Bench
HVAC	: Heating Ventilation and Air Conditioning
TMY	: Typical Meteorological Year
TRY	: Typical Test Reference Year
VFD	: Variable Frequency Drive
PID	: Proportional Integral Derivative Controller
DST	: Dynamic System Testing

CTSS : Component Testing–System Simulation

CCT : Concise Cycle Test

SCSPT : Short Cycle and System Performance Test

PLPE : Prescribed Load -Performance Extrapolation

DSE : Dynamic System Evaluation

COP : Co-efficient of Performance

SCOP : Seasonal Co-efficient of performance

PCA : Principal Component Analysis

NCA : Neighborhood Component Analysis

PDF : Probability Density Function

FFT : Fast Fourier Transform

PSD : Power Spectral Density

FSG : Fictitious Sequence Generation

DFT : Discrete Fourier Transform

RMS : Root Means Square

GHI : Global Horizontal Irradiation

DE : Differential Evolution

DA : Dual Annealing

GA : Genetic Algorithm

RMSE : Root Mean Square Error

KL : Kullback Leibler Divergence

1. Overview of HIL systems and problem statement

1.1 Objectives and Problem Statement

The main operational functionality of the HIL (Hardware in the Loop) testing setup in ENGIE is to measure the efficiency of products like boilers, heat pumps, fuel cells, etc. In general, the product has two approaches to efficiency measures such as the direct and indirect methods of calculating efficiencies. Each method has its advantages and disadvantages. To decide on which type of efficiency measure to choose it is important to understand what indirect and direct efficiencies mean. In the direct method, efficiency is calculated by dividing energy delivered by the boiler by energy input as fuel.

The method most standards follow is the indirect efficiency calculation method. In this method, each loss is individually calculated, and the sum of these losses is then subtracted from 100 to give efficiency in terms of percentage. The direct method gives us more realistic efficiency values but to understand where the losses are taking place, indirect efficiency will be more helpful [1]. From the practical problem point of view, more than the losses that occur in the system efficiency is the key performance indicator when it comes to the assessment. Hence, it is better to choose the direct method of evaluation for the energy efficiency assessment.

The next step is to identify which type of energy efficiency should be measured using the direct method of energy assessment. One of the most important ways to assess the efficiency of the product is to determine if the product can operate in different load conditions throughout the year or during the heating/cooling season. Hence, the seasonal efficiency is needed to be assessed for the product that needs to be tested using the HIL setup at ENGIE. The next step would be to identify why is it so important to measure the seasonal efficiency? As explained in [2], seasonal efficiency is the actual operating efficiency that the product will achieve during the heating/cooling season at various loadings and operating conditions. Because most heating/cooling products operate at part load, the part-load efficiency, including heat losses when the product is off, has a great effect on the seasonal efficiency.

Nearly all space heating/cooling products have at least 25% to 50% more capacity than is required at peak, so most products operate at peak conditions only rarely. Heating /Cooling products operate under varying load conditions — sometimes down to approximately 10% of peak load or less. Meaning, more than testing the product at the extreme operating conditions it is important to test the product at the most recurring operating points throughout the year.

So, in short, one of the objectives of the research work are to make sure that the seasonal efficiency of a product can be estimated in the shortest time possible. For the sole reason to make sure that the product can operate at different load conditions throughout the year.

Based on the cons of the HIL system one could easily identify the two different locks in the testing method where one needs to evaluate the seasonal efficiency of the product. As explained in [3] one of the problems in the HIL system is that the simulation happens in real-time. If in case one's intention is to measure the seasonal efficiency of the product it makes little to no sense to test the product for a full season.

Hence, the first scientific lock will be to develop a testing sequence where one needs to reduce the time taken for HIL simulation in evaluating the seasonal efficiency of the DUT (Device Under Test). Again in [3] the author explains that the internal information about the DUT is not taken into account by the HIL testing system. Therefore, there is a need to ensure that there is no uncertainty on the evaluated efficiency of the DUT concerning the test bench and the methodology of testing.

Objective: Evaluation of the seasonal efficiency of using a HIL setup

Scientific Locks: Time taken for the evaluation of the seasonal efficiency in real-time and ensuring the uncertainty levels on the evaluated seasonal efficiency is at acceptable levels.

Based on the objectives and the scientific locks one could formalize the **problem statement** as follows, the important problem to be addressed is to evaluate the seasonal efficiency of the DUT using a short testing sequence that will guarantee the efficiency with the acceptable range of uncertainties on the evaluated seasonal efficiency.

The next question that comes to one's mind is what the acceptable range of seasonal efficiency could be. Moreover, the seasonal efficiency is the ratio of energy utilized to the energy consumed there is also a need to add other KPI as well based on the functionality of the test bench. The prime reason is that even with the under-evaluated efficiency levels one could achieve energy efficiency when compared to the annual results. The most universally accepted error ranges from the result are within 5% from the reference values. Hence, the main KPIs are the seasonal energy efficiency, the input, and the output energy level with a 5% error in the energy levels in comparison to the appropriate reference values. The next section will elucidate the proper short sequence reduction methods and the uncertainty evaluation methods based on the applications.

1.2 Introduction

Over the last few decades, the electronic and mechatronic systems have become inseparable parts in almost every domain. Also, in the same time frame, there has been an increase in demand to perform the validation and the verification of such complex systems that combine both the electronic and mechatronic subsystems. This is the point where the Hardware-in-the-Loop (HIL) approach comes into

the picture since it is one of the approaches that optimize the process of verification and validation of the technology. Although widely used there is still no definition for the HIL because the term is still not included and defined as per the IEEE taxonomy [4]. There are several domains where the HIL testing methodology finds purpose, these include but are not limited to the Automotive industry as stated in [5], [6], Aerospace industries where HIL testing finds its application in flight simulation, fan rocket control, etc. HIL also find their application in railway industries; power electronics domain; electrical systems; thermal power plant control systems; manufacturing and distributed automation and finally in the field of robotics as well.

Based on the initial statement that the HIL simulation optimizes the verification and validation of the technology, one could easily state that the HIL simulation is generally applied in:

- Safety-related industries where the verification and the validation process could be very complicated and expensive
- Industries where the verification and the validation process could cause damage to expensive components in a system
- Industries where the functionalities of a component could not be tested because of the real-time environment. One best example could be the building energy domain where a lot of practical problems occur once when a particular product needs to be tested for a real building.

Before going deep into the domain of building energy the next few sections give an overview of the HIL systems from a general point of view. A more mechatronic approach towards the system is given followed by the existing use cases and the applications related to the building energy domain. A rapid overview of the philosophy of the HIL systems, followed by the types of the HIL systems, platforms, and solutions are discussed in the upcoming sections. Then the same philosophy is then related to the applications in the building energy domain.

There is a lot of state-of-the-art definitions regarding the HIL systems, it is also well known in other names and description:

- HIL is a system operating real components in connection with the real time-time simulated components [7]
- HIL is defined as a non-intrusive mechanism where the environment of a SUT (System Under Test) is simulated to perform real-time tests on the SUT [8]
- HIL is a combination of simulated and real components alternatively, a real component can be emulated, i.e. replaced by an artificial component that has the same input and output characteristics in a closed-loop configuration [9]

- HIL is a synergistic combination of physical and virtual prototyping or a setup that emulates a system by immersing faithful replicas of some of its subsystems within a closed-loop virtual simulation of the remaining subsystems [10]
- HIL is a technique for combining a mathematical simulation system model with actual physical hardware, such that the hardware performs as though it were integrated into the real system[11]

There are a lot of definitions for HIL as stated by benefactors of the HIL approach. Based on all the definitions one can easily figure out the main aspects of the HIL as a system of real and virtual components that contain a model which executes in real-time and uses the control signals for creating a tradeoff between virtual simulation and the real environment.

The very next set of questions that comes to one's mind are:

- Which part of the testing system should be real and which part of the testing system should be virtual?
- What kind of testing is envisioned for black-box testing /white box testing or grey box testing?
- Is HIL testing a closed-loop or an open-loop testing approach?

1.2.1 Real and Virtual parts of a HIL simulator

In the previous section, there were multiple definitions based as stated by the benefactors of the HIL testing approach, one could already state that the HIL system is a system with real and virtual parts. Based on the definitions it could be the real controlling part and virtual processing part or virtual control part and real processing part.

Based on several literature studies the majority of the benefactors claim that the HIL system is a system with a real controller and possibly virtual sensors, actuators, and environment [10], [12]. Using the previous definitions and the intuition based on the literature studies the generalized schema of the HIL simulator can be visualized as shown in Figure 1. The HIL system contains a computer that configures the HIL device, the HIL device executes the simulation models and emulates the SUT's interface signals.

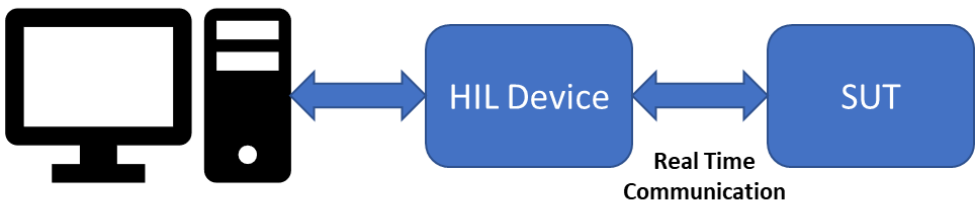

Figure 1:HIL system overview

1.2.2 Type of testing

The nature of the testing is very important, usually, the type of testing is divided into three types:

- **Black Box Testing (BBT):** A functional testing type associated with the system's specification with no understanding of its realization [13]
- **White Box Testing (WBT):** A functional testing methodology that arises from a deep knowledge of the SUT [13]
- **Grey Box Testing (GBT):** Usually GBT is in between the WBT and BBT when there is only partial knowledge on the SUT

Based on the literature the HIL is generally classified as a BBT since the HIL is mostly used for the system functional tests, which is a BBT. Most of the HIL in addition are not able to access the SUT in real-time to synchronize with its internal states. Such cases warrant a white box treatment. There are a lot of advantages of the WBT over the BBT as elucidated in [14] and so solidifying the need for implementing the WBT based HIL. Meaning that the synchronization between the HIL and the SUT is well understood and visualized for application (implementing and understating the synchronization between the SUT and HIL itself is a very big challenge), leading to the complexity of the HIL simulators, thus such kind of HIL simulators are very rare. A sample use case is explained in [15] where extra functionality is added to the main system. In an overall view, such approaches not only add complexity but add to the cost of such a HIL system. From a more practical and intuitive approach, one can conclude that the HIL is usually GBT since in most cases the test case is well known. Even though the functional testing requires BBT, in many cases using the knowledge about the system is beneficial, since one could improve the amount of covered code and execution paths.

1.2.3 HIL as an Open / Closed Loop testing system?

Most reviewed publications [10], [16] state that the HIL is a closed-loop system. However, in [17] and [18] the statement is another way around stating that it is an open-loop system. If and only if the output of the SUT is used for future evaluation and not for simulation purposes then the HIL is an open-loop system. In simple terms, the generation of the data by the SUT or the Device Under Test (DUT) by the HIL simulator is independent of the previous data of the SUT/DUT. On the other hand, if the SUT /DUT data directly influences the simulation, then it is a closed-loop simulation.

1.3 HIL Types

Based on the [19] the HIL types are divided into three broad categories, meaning that the HIL could be either established at the signal, power, or mechanical level.

1.3.1 Signal HIL

If the interconnection between the real and the virtual subsystem of the HIL system is on a signal basis then it is called sHIL (signal level HIL). This also adds to the understanding that the real part of the HIL systems is a signal processing and control unit whereas the rest of them belong to the virtual environment as explained in [16]. Based on the mechatronics system diagram the signal HIL can be represented as shown in Figure 2.

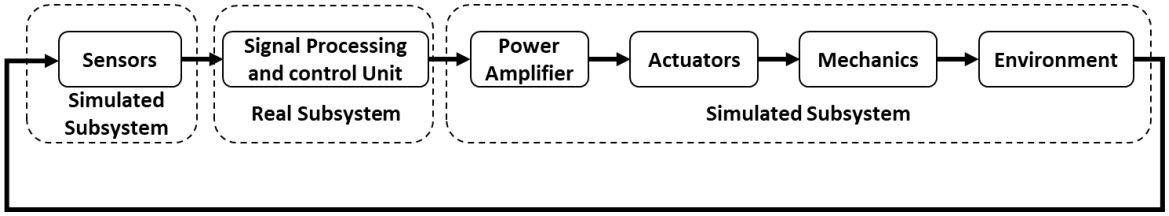

Figure 2: Signal hardware-in-the-loop(sHIL)[20]

Of all the types of HIL, the sHIL is the easiest to implement and troubleshoot, some of the other common names given for such types if HIL are Controller-In-the-Loop(CIL) [10], Controller-Hardware-In-the-Loop(CHIL)[21], and also called the component level HIL [22].

1.3.2 Power HIL

Power HIL (PHIL) in general is the type of HIL where there is a significant exchange of electrical power between the physical subsystem and the simulated subsystem. To emulate the real power as per the simulation conditions power amplifiers are used. If such power amplifiers are used which would intuitively mean that the real actuators are to be used as well, in [23] the authors discuss the different PHIL configurations for their proposal related to the hybrid electric vehicle simulation.

Based on the mechatronic diagram the PHIL can be represented as shown in Figure 3. Furthermore, the authors also explain the possibility of implementing a reduced pHIL that uses a smaller load, scaled pHIL where the power amplifier scales to one time or n times the power required based on the simulated data.

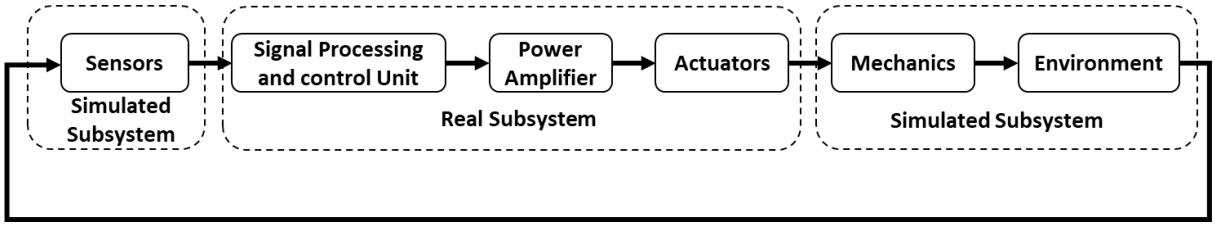

Figure 3:Power Hardware-In-the-Loop(PHIL)[20]

1.3.3 Mechanical HIL

The mechatronic diagram of the Mechanical HIL (mHIL) is shown in Figure 4, from which one could easily identify that sensor added to the HIL systems are also the real ones. Such a HIL configuration is the one that is as close to the real system that is going to be tested on the field. In such use cases, the real actuators and the real mechanics with the additionally integrated sensors can capture the dynamics of the system. Thus, only the DUT's sensors and the environment is simulated. mHIL systems are very difficult to integrate, very expensive, and are usually custom-made to suit the benefactor. But, it also gives the advantage of representing the system as close to the real-world scenario[20].

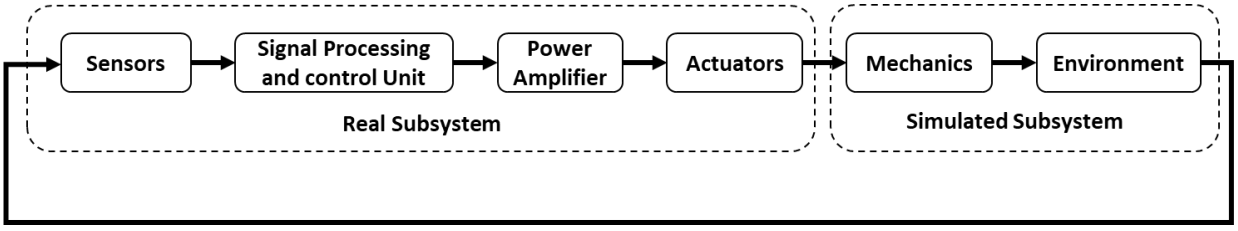

Figure 4: Mechanical Hardware-In-the-Loop (mHIL)[20]

Also, in the literature, there are other types of HIL systems that do not exactly fit into the three distinct types of HIL's. The level of abstraction remains undefined, so it could fall under any type of the already defined types of HIL, one such use case is explained in [24] where the HIL system is referred to as a component HIL.

Also, in the literature, there is another type of HIL system that gets a special mention often known by the name Platform HIL. It is a special use case where the HIL system calculates the mathematical parameters based on the hardware signals. Since it uses a signal-level communication to run the real-time simulation its level of abstraction falls under the signal HIL.

1.4 HIL system Design

In general, the HIL system designs are normally divided into two types mainly go by standard and non-standard systems design. By systems design, the implied meaning in the literature was to see what are the computational platforms that are used for the implementation of the HIL systems.

1.4.1 Non-Standard Types

Under the non-standard types, the systems are developed for user-specific applications, and such platforms are not available commercially. For example, one can make use of a personal computer (PC) based on the windows Operating System (OS) for executing the HIL tests this is entirely possible using standard communication ports (DUT and the virtual environment are connected via a serial bus such as

USB or RS232) and interfaces. This is a simple yet very cost-effective solution and one such use case for the Unmanned Aerial Vehicle (UAV) is explained in [25].

On the other hand, to ascertain the very high-frequency simulations and the accuracy one could also adopt a Real-Time Operating System (RTOS). In [26] the author exposes a use case for the control of the electric ducted fan for rocket control systems which have been implemented through an ATMEGA 2560 8 bit Micro-Controller Unit (MCU) showing that such low-cost HIL systems could also be established. Additionally HIL dedicated for the power applications make use of FPGA's (Field-Programmable Gate Array) a few use cases are demonstrated in [27], [28]. Also, another use-case is demonstrated where the MCU and FPGA are combined as explained in [29].In addition to the use of PCs, MCU, FPGA digital signal processors (DSP) are also used to realize the HIL platform as explained in [30]. Graphical Processing Units (GPUs) are very rarely used in realizing the HIL systems, a rare use case is explained and demonstrated in [31], the HIL system is implemented with the combinations of the GPU and the Central Processing Units (CPUs'). Whatever be the computational platforms in all the use cases demonstrated the PC was chosen as the standard equipment.

The problem that one could expect with a non-standard HIL system is that they were mainly implemented based on the author's domain of expertise, moreover, this also leads to one overarching question will such non-standard application be able to demonstrate the dependency between the user hardware platform and the application. Thus, leading to the investigation of the design of the standard system about the industrial needs.

1.4.2 Standard Types

In general, the commercial standard types of the HIL system design are broadly divided into two types based on their architecture types namely the simple and the complex simulators [32]. A simple simulator generally is targeted towards a single computational device like an FPGA, MCU, etc. The complex simulators are further divided into two types namely the Monolithic HIL simulators and Distributed HIL simulators [32]. The monolithic simulator as the name implies consists of a single device that is capable of interfacing with all the SUTs, while the distributed simulator on the contrary contains multiple interfacing nodes that help and aid in the executing distributed simulation model.

A Rapid Control Prototyping experimental use case is shown to demonstrate such distribution simulation as explained by the authors in [33]. Further, the standard types are divided into open and closed architecture solutions as the names imply the closed architecture systems are normally locked to one single application without any scope for further expansion while the open architecture simulator is

practically on the opposite side. The cost for the open architecture systems is the increased configuration time and higher cost as explained by the author in [34].

Some of the commercially available standard platforms are from DSpace, National Instruments, SpeedGoat, ETAS, and Opal-RT. In the case of National Instruments, they claim that their HIL system uses CPU for computation and real-time simulation processing and FPGA for electrical signals emulation [35]. SpeedGoat also proposed or use CPU for their real-time target machine [17], I/O modules based on their FPGA models for high-end realization, and MCU for the low-end realization of the HIL systems [17]. ETAS proposes to use the CPU and FPGA-based combination boards. Standing apart from all the other commercial fabricators are DSpace and Opal-RT who propose a large line of HIL devices. Both propose a large range of solutions including a processor-based board on CPU for complex calculations, a CAN interface board based on DSP. Specialized modules called “piggy modules” are used for measuring digital and analog signals.

1.5 Hardware-In-the-Loop simulations in the context of Building Simulations

The HIL simulations have two parts primarily they have part that is simulated using a PC , mostly it is building envelope while the hardware part is usually the emulator and the DUT/SUT. The simulation of the building environment is done using MODELICA and TRNSYS mostly as stated in the literature. For this section, the idea will be look at the simulation tools that are widely used and the types of interfacing methodologies that are available to execute the HIL simulations.

Throughout the previous sections the various types, aspects, architecture, and the system design of the HIL systems were elucidated by considering the different domains, the same applies to the Building Simulations context as well. In most of the HIL simulation platforms about the building energy domain perform two things one is to test products/systems for a particular Key Performance Indicator (KPI) and the second is to test control algorithms based on literature as shown in Figure 5.

Plus, also there is an added advantage regarding the communication interfacing of the HIL systems, where a lot of use cases show that there is a flexibility to use software-based communication interfacing in comparison to hardware-based communication interfacing as explained in the earlier sections.

The product assessment is generally more of a system assessment since the product is slotted into one of the heating/cooling scenarios based on the requirements of the testing. It is also to state that the application areas are not only limited to only the product and control strategy assessment but also many other applications which at this point is not under the scope of this report.

A very simple execution of the HIL system, solely for testing one circulating pump is discussed in [36], the idea is to investigate the interaction of a real circulating pump with the hydronic network of a virtual building energy and control system which is one simple use case for testing one specific product.

Another use-case is shown in [37] where the performance of a heating system (capable of delivering heat for a particular day of choice) is assessed based on the different control strategies. The idea is to measure the performance of the heating system that contains AWHP (Air-to-Water Heat Pump) that is used for delivering Space Heating (SH) and Domestic Hot Water (DHW) for a residential building.

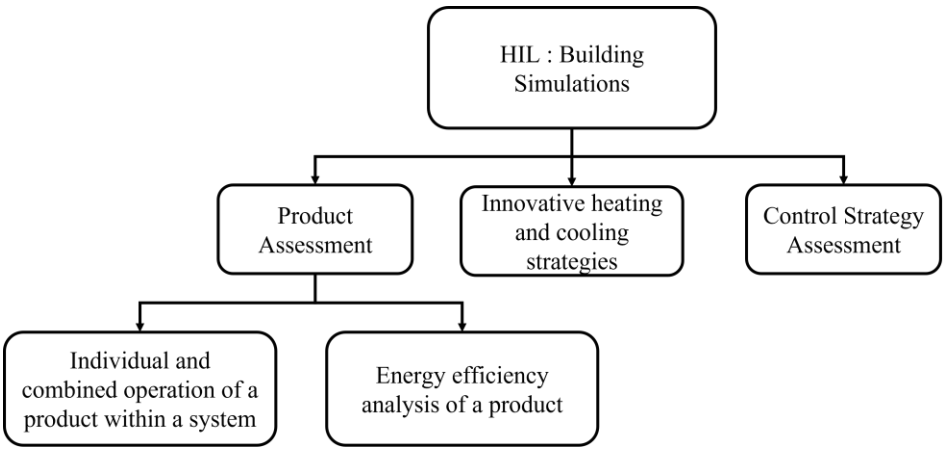

Figure 5: Application majors of HIL in building simulation context

1.5.1 Simulation tools

The simulation is done for one day and the dynamic internal conditions of the building are modeled in Modelica. The use case also shows how the HIL simulations can be used to lower the real-time required for studying the different control strategies in real-time. An experimental application regarding the usage of dual-source heat pumps for space heating and domestic hot water needs is shown in [38]. A $60m^3$ climatic chamber was used to simulate both the heat pumps, where different configurations for the heating applications were studied. The study proves that such experimental assessments prove to be less time-consuming in implementing different heating and cooling strategies.

A rather more open-source tool in close conjunction to the building simulations domain is the BCVTB (Building Controls Virtual Test Bench). The Building Controls Virtual Test Bed (BCVTB) is an open-source, freely available software that can link different simulation programs (Energy Plus, Modelica, Radiance, MATLAB/Simulink) for co-simulation. It can also link these programs to Building Automation Systems and databases for model-based operation [39]. The BCVTB can perform HIL simulations, building energy studies, HVAC, and control-related studies, it also enables the data analysis studies, more importantly, the ability to do automation network studies and wireless network studies. The

above applications on one test bend make the BCVTB one of the most versatile environments for building simulation studies. Although the BCVTB facilitates all such studies, the primary focus as stated in [39] are:

- Innovation in integrated building energy and controls systems,
- Development of new controls algorithms, and
- Formal verification of controls algorithms before deployment in a building to reduce commissioning time.

1.5.2 Interfacing methods for HIL simulations

In [40] the author explains an agent-based HIL system for testing the real-time controllers related to the building energy domain. From the literature, the author terms such systems as Controller in the Loop (CIL) testing method. The already existing methodology of CIL using hardware interfacing is elucidated as shown in Figure 6. The author establishes the fact that the hardware communication interfacing could lead to potential delays in communication due to the slowness of the interacting hardware interfacing components. Hence, the author adopts software-based communication interfacing as shown in Figure 7.

The main reasons for the use of software interfacing as stated in [40] are :

- Reduce the cost of HIL implementation
- Support different hardware, including controllers, physical equipment, and physical systems in operating buildings
- Support high volumes of data exchange between hardware and simulations
- Accommodate the use of several different simulation programs

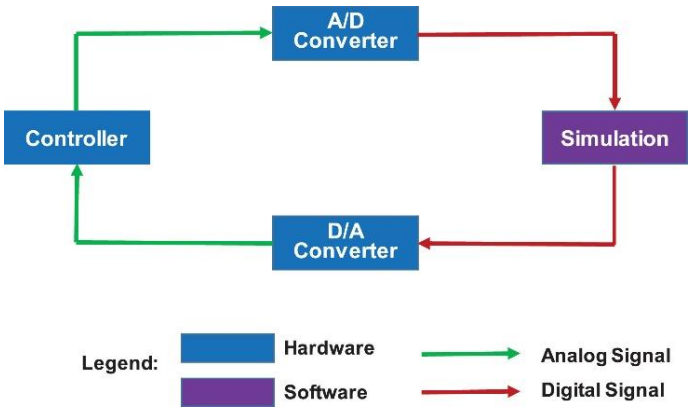

Figure 6: Controller in Loop Hardware Interface [40]

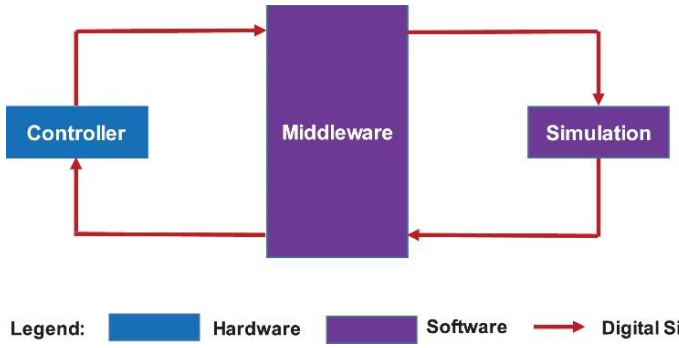

Figure 7: Controller in the Loop Simulations with software Interfacing [40]

Hence, in the building simulations domain, the earlier mechatronic diagrams representing the HIL system can be re-imagined as shown in Figure 8. For the rest of the report, the intended use of the HIL system representation would be as depicted as shown in Figure 8.

In all the use cases [36] [37] [38] [39] and [40] one can see that they are mostly non-standardized solutions of the HIL system design as elucidated in the previous sections. In the use-cases cited, mostly for the building simulation applications mostly used simulation software include Modelica, Simulink, TRNSYS, and Energy Plus.

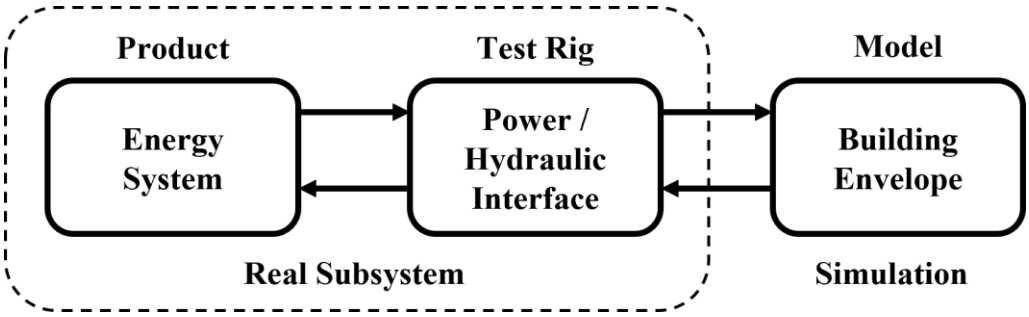

Figure 8: Schematic of a typical HIL system

The test rig that supports an emulation interface between the software and the system under test can be piloted by a different software or not, usually in most use cases a LabVIEW based software was used to pilot the test bench. The communication interface between the test rig, product and the simulation software can be done either by a software or a hardware communication interfaces. For the rest of the report the schema shown in Figure 8 will be maintained. In short, the framework of the HIL systems in the building simulations domain includes the following

- Simulation software that produces data in real-time based on the scenario of choice.
- A power/hydraulic interface that emulates the simulated scenario
- A product/system to test it could also be a controller depending upon the application

- Finally, a communication interface that could interface all the three subsystems the interfacing could be done either based on a hardware solution or a software solution.

Additional information is that the simulated model at first could be a model of the building which is exposed to the weather conditions. The weather file used could be a Typical Metrological Year (TMY) or a Typical Reference Year (TRY). The second case could be that a load profile for a particular building can be used for simulation. This load profile could carry the heating/ cooling load requirement of a building for a particular weather condition. The second approach is more like detaching the equipment from the building by slightly ceding out the dynamic capabilities of the HIL testing approach. One such use case is elucidated in [41]. The use case proposes to evaluate the performance of a renewable heating system combined with a Ground Source Heat Pump(GSHP) that is used for both space heating and domestic hot water applications.

Twelve-day testing is done with the rationale of choosing 1 typical day for each month and the energy supplied to the system for heating, the energy used for the space heating is calculated for each chosen day and the ratio of both the energies are taken to evaluate the performance factor of the heating system for each day. The total sum of the energy levels for the 12 days and its ratio is used for calculating the performance factor for one year. Although the scope and application of the HIL systems are used for a multitude of different evaluations, the prime focus on the said thesis is purely going to be about the energy efficiency evaluation of a particular product or system under test based on short-term testing.

1.6 HIL Setup in ENGIE-CRIGEN

The hardware in the loop test bench (HIL) is a Micro plan hardware platform (bench) for tests on heating or cooling systems, electrically or gas supplied, like gas boilers (space heaters), gas water heaters, chillers, etc.

The user can perform free tests of power consumption and efficiency at different operating conditions simulating the external reaction of the environment in which the appliance under test will be installed. Those tests can be performed in steady or in transitory conditions in case the user is interested to study the behavior of the system under test in case of quite rapid changes of some conditions. The HIL test bench can be used in two ways:

- Manual way: the operator can use a synoptic interface to select the circuits, open/close the valves, increase/decrease the head of the pumps and so on.
- Automatic way: the test bench is controlled by an external simulation program.

1.6.1 Structure and hardware

The HIL test system is composed of three different units as shown in Figure 9:

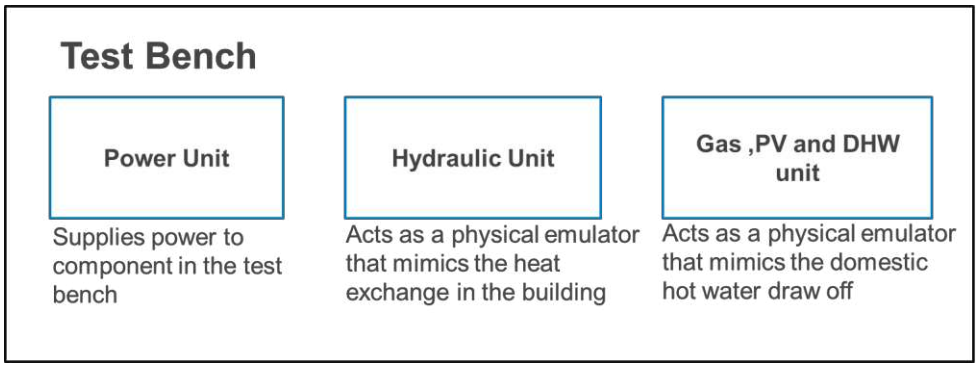

Figure 9: Three parts if the HIL system in ENGIE

- The Power Unit, the main electric cabinet, supplies the electric power to the appliance under test, and to which the programmable electrical loads are connected.
- The CH Unit, with an electric cabinet and a hydraulic section (HU) in which the main hydraulic circuits are located. The HU is composed of four different zones, arranged in order of increasing exchangeable heating power. Every zone is split into a primary circuit, connected to the appliance under test, and a secondary circuit, that adds or removes heat to the system.
- The GAS-DHW-Solar Unit, with an electric cabinet and three different circuits: the gas supply circuit, the solar panel's simulation circuit, and the sanitary circuit.

The PC and the two 24'' monitors can be remoted on a desk and the operator can work sitting. The PC is connected to the electric cabinet of the CH Unit by an Ethernet cable. The CH Unit is wired to the Power Unit and the GAS-DHW-Solar Unit via two Ethernet cables.

The electronic interface between the PC and the transducers, the valves, and the other active element in the bench is made up of a set of 16-bit Beckhoff electronic modules, connected to the control PC by an Ethernet cable. The test bench setup in ENGIE CRIGEN Labs is shown in Figure 10.

1.6.2 Heat Output and Flow Ranges

Every zone of the CH Unit is set to carry out tests at different ranges of heat outputs. The following table indicates the minimum and maximum power manageable by every single zone in two different conditions: with a differential between the inlet and outlet temperature at the primary circuit respectively of 5°C and 20°C.

The most assumption is that the flow rate at the primary and secondary circuits are similar and that the temperature difference between the inlet of the secondary circuit and the return of the primary circuit is about 17°C.

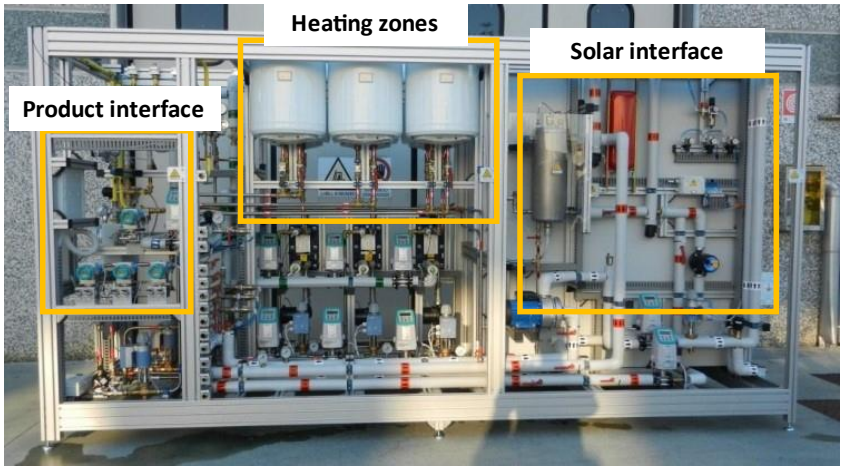

Figure 10: HIL test setup for testing products in ENGIE CRIGEN

Regarding the DHW circuit of boilers or water heaters, the range of flow rates managed by the bench is from 2 to 40 l/min. Outside these limits, the regulation capability gradually decreases. Regarding the Solar circuit, the maximum heat input that can be generated by the system is 6kW. The flow rate can be set between 2 and 30 l/min. The thermal heat ranges of each of the hydraulic zones in the test bench are shown in Table 1. All the four zones are in the heating zone part of the test bench as shown in Figure 10.

Table 1: Nominal Heat Ranges of the Hydraulic Circuit

Zone	Flow Meter Diameter	dT= 5K		dT = 20K	
1	3 mm	0.3 kW	1.3 kW	1.2 kW	5 kW
2	6 mm	0.3 kW	5.0 kW	1.2 kW	20 kW
3	15 mm	2.0 kW	30.0 kW	7.5 kW	130 kW
4	25 mm	5.5 kW	90.0 kW	22.0 kW	360.0 kW

1.6.3 The philosophy behind the test bench based on the literature study

Based on the literature survey done in the previous sections, one needs to have an idea of what the test bench is capable of and what it is not capable of. To know more about the test bench let us explore its Synoptics first. The synoptic for the information exchange for the HIL setup is shown in Figure 11

The test bench was fabricated with the main idea to emulate the power load inside the building model at each time step. Hence, the first understanding is that the test bench's primary motive is to mimic the heat flow inside the building. In more practical terms one needs to know exactly is the heat capacity at each point in time.

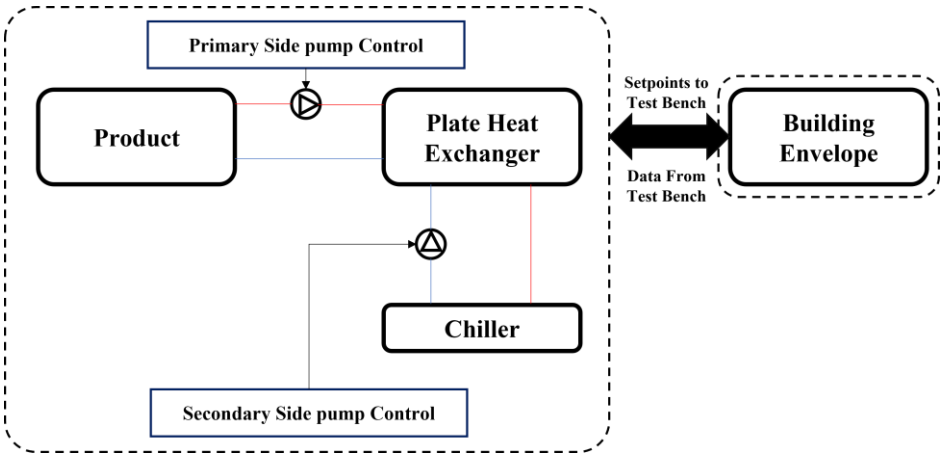

Figure 11: Synoptics of the HIL setup for space heating section in ENGIE CRIGEN Labs

Building Envelope : The part that is simulated

Parts within the dotted encasing : The parts that are real and emulated

The heat flux as data from the building model needs to be emulated at the heat exchanger in the test bench. Then, in the test bench since it is a plate heat exchanger one needs to ensure that the heat flux in the heating side and the heat flux on the cold side should be established. To maintain the heat flux at the heat exchanger level, one needs to establish a control strategy. There exist two control strategies, one on the primary side (product side) and one on the secondary side (chiller side). The control strategy on the primary side can perform two strategies:

- Control the temperature difference between the supply and the return temperatures from the product of testing (DT control, $T_{supply\text{-}product} - T_{return\text{-}product}$)
- Control the mass flow rate ($\dot{m}$ mass flow rate control, $\dot{m}_{product}$)

The control strategy on the secondary side can perform one control strategy that is to control the return temperature to the product ($T_{return\text{-}product}$). The primary side is connected to the product that needs to be tested and on the secondary side, a chiller is connected to supply cold water to emulate the heat load inside the building. A chiller is a collective unit, that not only supplies cooling water only to this test bench but also to other test benches in the laboratory facility. The chiller supplies cold water in the range of 6°C – 11°C with a cycling time of around 20 minutes, meaning that the range of the temperatures is

fixed from 6°C-11°C range. Also, based on the control strategy the mass flow rate on the secondary side is controlled to maintain the return temperature on the primary side. The actual Synoptics of the physical working of the test bench to emulate the heat load from the building is shown in Figure 12. Based on the synoptic and the information obtained one can create a table of the controlled and the manipulated variables of the hydraulic circuit of the test bench. All the possible variables that are involved in the heat transfer are shown in Figure 12 itself.

From Based on the equations and the list of variables that one can control one can understand that the primary interest of the test bench is to only control the total heat load related to a particular scenario under experimentation. Since the supply and the return temperatures of the chiller loop are partially controlled (a grey box philosophy of testing) the internal building temperatures for any scenario are partially controlled. Hence, the foremost objective of the test bench is to emulate the total heat load inside the building based on the initial analysis of the test bench.

The trade-off for such a construction is to employ the test bench for future experiments related to District Heating and District Cooling applications where products are to be tested if they can be capable of catering to the power load at that instant. Additional information is that the pumps in the primary and the secondary sides are of the same specifications. A Variable Frequency Drive (VFD) is used to manipulate the pump speeds based on PID control regulation.

Hence, from the initial analysis, the HIL system is mainly used to perform and analyze the products based on its overall ability to deliver the thermal needs at every step of time when considered if it were to be used for the analysis of the internal comfort of the buildings or microlevel studies within the building envelope.

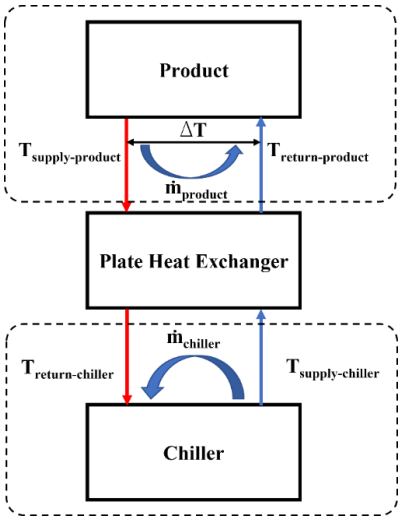

Figure 12:Physical emulation of the heat load in the test bench heat exchanger

Table 2, the list of the variables that can be controlled and manipulated on both sides of the test bench is shown. Scientifically one can see that the heat load in the building needs to be emulated and to achieve it the heat fluxes in the product loop and the chiller loop need to be matched. The thermodynamic equations are shown below in Equations (1) and (2).

$$\phi_{product-side} = \dot{m}_{product} * Cp_{product} * (T_{supply-product} - T_{return-product}) \quad (1)$$

$$\phi_{chiller-side} = \dot{m}_{chiller} * Cp_{chiller} * (T_{supply-chiller} - T_{return-chiller}) \quad (2)$$

Based on the equations and the list of variables that one can control one can understand that the primary interest of the test bench is to only control the total heat load related to a particular scenario under experimentation. Since the supply and the return temperatures of the chiller loop are partially controlled (a grey box philosophy of testing) the internal building temperatures for any scenario are partially controlled.

Hence, the foremost objective of the test bench is to emulate the total heat load inside the building based on the initial analysis of the test bench. The trade-off for such a construction is to employ the test bench for future experiments related to District Heating and District Cooling applications where products are to be tested if they can be capable of catering to the power load at that instant.

Additional information is that the pumps in the primary and the secondary sides are of the same specifications. A Variable Frequency Drive (VFD) is used to manipulate the pump speeds based on PID control regulation. Hence, from the initial analysis, the HIL system is mainly used to perform and analyze the products based on its overall ability to deliver the thermal needs at every step of time when considered if it were to be used for the analysis of the internal comfort of the buildings or microlevel studies within the building envelope.

Table 2: List of controlled and manipulated variables in the test bench

Control Side	Control Strategy	Variable to be Controlled	Manipulated Variable
Product	DT (temperature diff.)	$T_{supply-product} - T_{return-product}$	$\dot{m}_{product}$
Product	Flow Rate	$\dot{m}_{product}$	$\dot{m}_{product}$
Chiller	Return Temperature	$T_{return-product}$	$\dot{m}_{chiller}$

The other part of the test bench also emulates the domestic hot water draw-off at the required instance, generally, there are no thermal storages attached to the test bench. The idea is to test the initial

draw-offs from the device under test directly. The schema of the test bench section to emulate the domestic hot water draw-off is shown in Figure 13.

There are two types of controls for the hot water draw-off one is to control the flow rate of the hot water draw-off and the other is to control the temperature of the hot water at the domestic hot water draw-off. The solenoid valve control for the domestic hot water draw-off is done by a PID regulation for performing both the control strategies.

Overall, the same technique of establishing the heat flux for the domestic hot water draw-off is used. The regulation for the domestic hot water loop can be done at a maximum flow rate of about 40 l/min beyond this rate the regulation becomes unstable during the experiments.

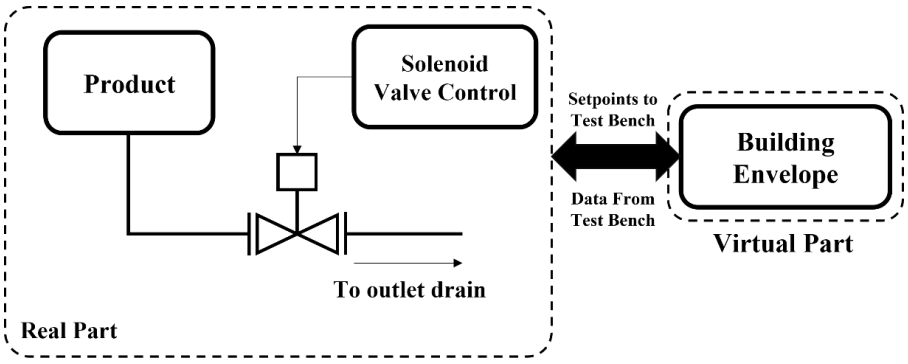

Figure 13: Synoptics of the HIL setup for domestic hot water draws off in ENGIE CRIGEN Labs

Now both the philosophy of the HIL and the capabilities of the test bench is known, hence the list of probable problems that one could face related to the context of the HIL need to be understood to establish the problem statement. In short, the test bench relies on transferring the heat flux at every time step and waiting for the DUT to respond to the heat load requirements. Plus, the test bench is used to integrate the energy levels over the testing period to calculate the energy levels and then use to calculate the appropriate efficiency indicator (could include seasonal efficiency, typical single day efficiency of the DUT).

1.7 Probable problems from the context of HIL systems and its compensating pros

In [42] the author elucidates the possible pros and cons of the HIL systems. There are a lot of pros which could be seen later in this section. The major and the important cons related to the HIL systems are that they are very few.

- The first and the most important con of the HIL system is that there is no internal information about the SUT / DUT that is under test. The HIL simulator in itself will not give any information about the state of the SUT/ DUT under test since it acts only as a black box tester [3]. Such a lock

could pose a big problem in the case of the building simulations where a product can be tested for a particular KPI where one needs to take care of the internal states of the system specifications.

- The next problem that one can face during the HIL system-based evaluations is that the simulation speed is constant. The HIL simulators operate in real-time the simulation speed can neither be accelerated nor slowed down [3]. This could also pose a problem in the domain of building simulation where one needs to measure the seasonal efficiency of a product. Usually, such efficiencies are calculated based on the yearly consumption and utilization of fuel hence this con of the HIL systems poses practical problems in this aspect.
- There are no standard solutions that can set a benchmark for the HIL systems, and slow integration [3].
- The last and the final issue that one can come across the HIL systems is very much scenario-specific rather being system-specific. They include non-perfect virtualization and non-perfect parameterization as explained in [43].

The above are the most important problems that one could face during a HIL system-based experimentation in real-time. The pros of the HIL testing system can be elucidated as follows the major advantage based on the philosophy of the HIL testing methodology is that the tests can be reproduced and automated. HIL in general is a testing methodology that enables the testing in the different virtual situations, keeping the context on maximum possible reality level that is the last option before the actual real field test. It is a trade-off between the accuracy of the test and the cost and time consumption as shown in Figure 14. Because of its semi-virtual nature, the HIL testing methodology has the following pros as listed below :

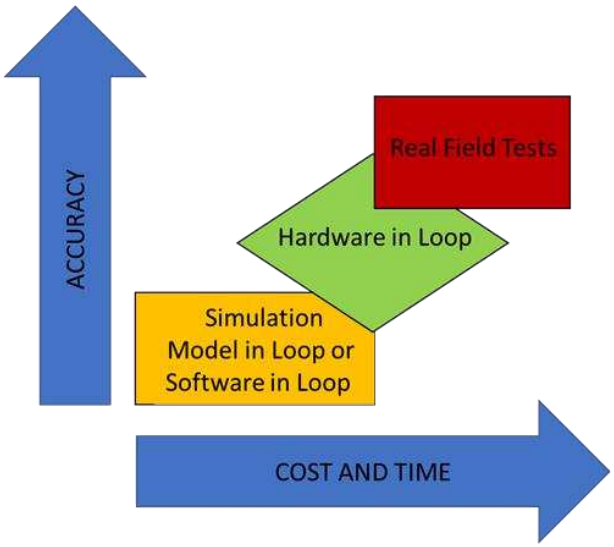

Figure 14: Testing methods as a trade-off between the accuracy of test and cost and time consumption

- The HIL testing system can run the tests without any hindrance from the unrelated systems that are attached to the actual SUT in real-time. This signifies that the HIL system could give a platform where one could make **repeatable and stable** as explained in [44].
- In cases where real-time field testing is very expensive and time-consuming the HIL system-based testing can alleviate such difficulties, HIL system-based testing can be **cost-effective** both time and cost [44].
- By prototyping in hardware components, which dynamics or other attributes are not fully understood, HIL simulators often achieve higher fidelity levels. In short, the **verisimilitude and fidelity** of the testing can be achieved [10].
- HIL simulation often makes it possible to simulate destructive events eliminating the possibility for costly destruction, hence making the **non-destructive testing** methodology feasible [45].
- HIL systems can be used to make very meticulous **parametric studies, sensitivity analysis, and optimization** is easily performable. HIL system also supports **flexibility** in testing, even if there are minor changes in the HIL system it's **versatile** enough to adjust and acknowledge changes in the behavior of the virtual system [46], [47].
- HIL testing systems can also ensure **safety** by training human operators in relatively safer working environments as compared to the real working environment [10].

From the available information, it is evident what could be the possible problems that one would have to face regarding the HIL system-based testing concerning the building energy domain. The rationale behind the problem statements and their objectives is elucidated in the next section.

1.8 Conclusion

In short, the HIL testing systems are used for the verification and validation of the systems/products that are expensive to test in terms of safety, cost, accuracy, and time. The HIL systems are made up of both real and virtual parts. The real and the virtual parts of the HIL system vary depending upon the testing requirements and the nature. The HIL system proposed could be a standard or non-standard platform-based solution.

Although from a theoretical aspect one could talk about black, grey, and white box testing philosophies and their association with HIL testing all the HIL testing systems are grey box equivalents. The HIL setup in ENGIE CRIGEN Labs is also a non-standard HIL platform whose functionality is to evaluate the efficiency of a thermodynamic product for its efficiency based on the energy levels. The basic construct of the test bench is to transfer the heat flux required at every point of time during real-time

experiments. This gives one an idea of what is to be expected out of the test bench before commencing the real-time experiments.

The final problem statement is that the HIL test setup at ENGIE needs to be used to evaluate the seasonal efficiency of the DUT and evaluate the uncertainty on the seasonal efficiency. The scientific locks that one needs to encounter in such a problem are to develop a short sequence that will estimate the seasonal efficiency of the DUT within acceptable limits and to identify the uncertainty related to such a complicated system of testing.

2. Existing methods and use case demonstration

From the earlier sections, one could conclude that the HIL simulations offer an intuitive procedure for the validation and verification of building technology evaluated under dynamic conditions. The only downside of such HIL simulation is that they are prone to time constraints when products are evaluated for their annual/seasonal performance. In such a situation, one cannot evaluate the product for a long time, one can reduce the simulation cycle based on few days that stand for the entire year by choosing the most representative n-days from the entire year.

The choice of representative days can be identified based on optimization, intuitive or iterative methods. The performance got in the short cycle is extrapolated to an entire year. The extrapolated result is then verified with annual simulation and their closeness represents the correctness of the reduced simulation cycle, as explained in [48]. The entire simulation is done on the DYMOLA (commercial Modelica platform), which allows a user to model the components in the system as close to the real-world representation. The very next problem is how to address the uncertainty on the extrapolated performance index (namely because of the numerical and experimental part of the HIL simulation or to consider the sources that are proper to the process involved).

A thorough literature study is done to form a framework to tackle distinct problems that are met while doing an HIL simulation. For the sake of explaining, the problem can be split into two aspects: the sequence reduction part followed by the uncertainty analysis part. As a first step the sequence reduction is done based on the clustering method and its pitfalls are discussed. A new fictitious sequence generation technique for evaluating the seasonal efficiency is proposed based on the pitfalls about the clustering technique used for the sequence reduction.

The flow of the chapter is shown in Figure 15 the first step will be to look at the simulation-aided validation standards followed by the state-of-the-art analysis for the simulation-based problem of short sequence reduction and uncertainty analysis about the system. The general approach is to first find existing methods that use the HIL method to evaluate the performance of a system/component. Then, finally, within the HIL method, find the suitable method to find the set of representative days that could represent the entire year / season.

In short the main problem will be to explore the literature to address the problem, which is to develop a short sequence for evaluating the performance of a product for HIL use cases and quantify the uncertainties on the evaluated performance. This literature study will explore the relevant methodologies that are existing to evaluate the performance of an energy systems, then relevant methodologies to establish a short sequence and quantify the uncertainty on the evaluated performance. Also, at the end of

the chapter one would be able to identify what are the pitfalls in the existing methods, what would be the new method and what are the problem areas that the new method proposes to address within the problem statement.

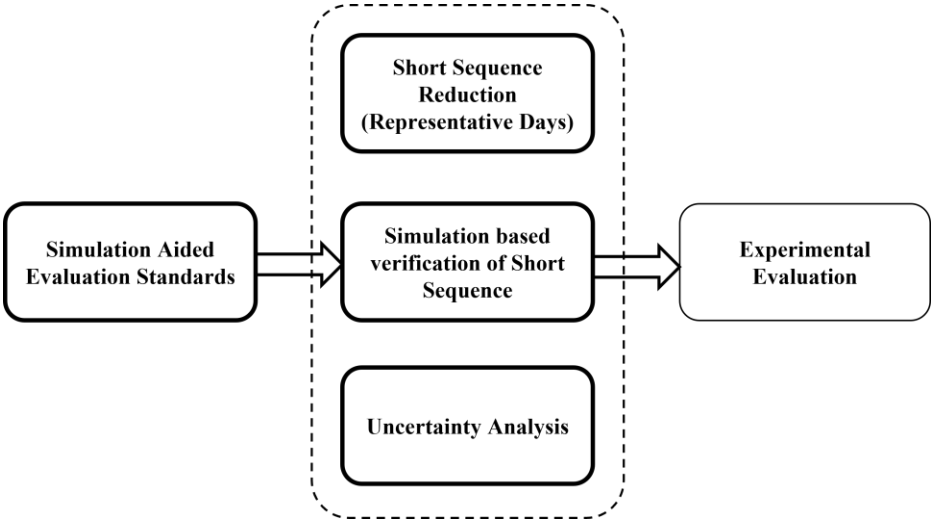

Figure 15: Workflow of the HIL evaluation-based performance

2.1 Literature analysis for Short Sequence Reduction

2.1.1 Existing HIL testing methodologies for performance evaluation of energy systems

The main idea of this section is identifying the existing methodologies both HIL and non-HIL based methodologies for the evaluation of performance of the energy systems. Identify the features and aspects of each method that are interesting and impart it towards solving the problem at hand. Finally conclude with the methods that could be worthwhile looking at.

Before going into the methodologies to find the representative days and define a short testing sequence, the first step will be to look at the simulation-aided standards. The first step will be to find the methods that support the HIL testing philosophy and the ones that do not support the HIL testing philosophy. All the methodologies based on the literature are shown in Figure 16**.**

There are three methods referred to in the literature, namely the bin method, Dynamic System Test method (DST), and Component Testing–System Simulation (CTSS) it is known these methods do not consider the HIL testing philosophy. One of the most recurring methods based on literature is the bin method of evaluating the efficiency of a particular system, which is explained in [49] with extensive definitions and calculations based on the computer simulation.

The bin method is a handy procedure to evaluate the seasonal performance of heating and cooling seasons considering the reference operating conditions. The cumulative frequency distribution of the

temperature profiles is used for the calculation of the seasonal performance parameters, along with the performance figures retrieved from both the stationery and part load conditions. All this is done whilst considering the features such as the cumulative frequencies of the outdoor air temperature and the corresponding load variations. The detailed description of the method is found in [50].

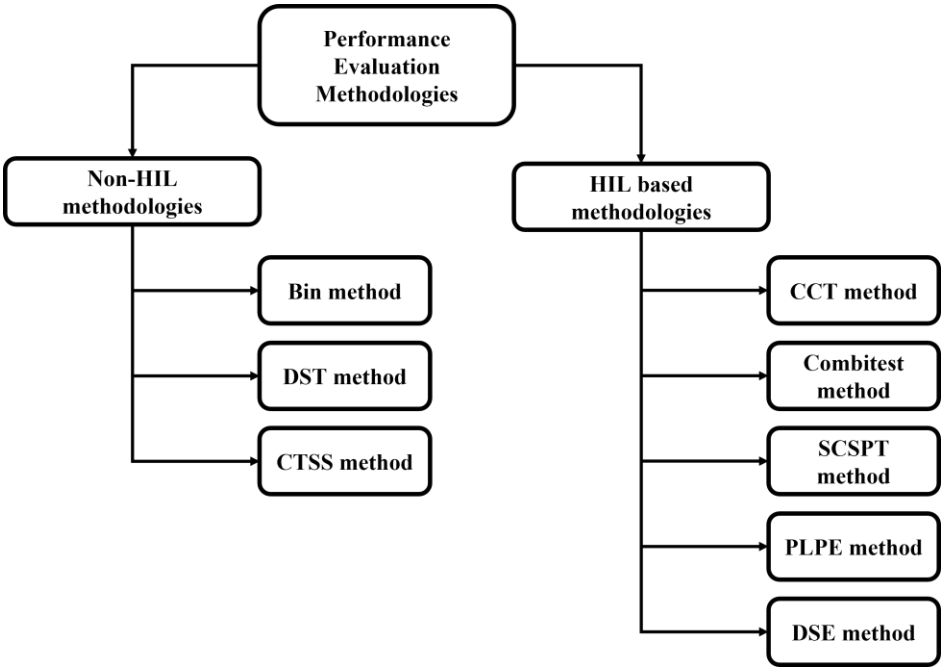

Figure 16: HIL and non-HIL methodologies for performance evaluation

Another simulation evaluation standard is the "Dynamic System Testing" (DST) method which applies to the ISO 9459-5 [51] and EN 12976-2 [52] standards, facilitating the collection of data for short solar domestic hot water (DHW) is gathered, parametrized then used as a mathematical model which is then used for dynamic simulations as explained in [53] and [54]. ISO 9459-4 [55] and EN 12977-2 [56] describe and apply the CTSS method and apply this testing method.

The CTSS method is also one of those methods that do not consider the dynamic effects just like the bin method. The tests are made on single components which are the numerically developed models based on which the seasonal performance is evaluated. The main drawback of both the bin and the CTSS methods are that they neglect the dynamic effects. Plus, in the case of the CTSS method one needs to develop individual components numerically hence, the time and the complexity in developing the models is very high for each use case. As mentioned earlier, the bin methods, DTS, and CTSS methods are not compatible with the HIL testing. They do not consider the real-time response.

The next step will be to explore the testing methodologies that consider the HIL testing philosophy. Some institutions that work on the HIL-based methodologies are the CEA at the French

National Institute for Energy (CEA-INES) in France, EURAC Research Institute for Renewable Energy in Italy, Institute of Solar Technology (SPF) of the University of Applied Sciences in Rapperswil, Switzerland, and finally the Solar Energy Research Center of Hogskolan Dalarna University in Sweden. Also, all the methodologies developed by the above research units explain that the evaluation method does not consider the thermal inertia of the system under test as explained in [57] and [58] since the non HIL methodologies test only a single component under steady-state conditions. The authors in [59] compare all the HIL based methodologies based on the following criteria they include:

- Simulation or Load Profile as Virtual Part
- Number of Test Days
- Data Exchange Frequency
- Level of detail of the building model, on which the simulation or load profile bases

The overview of the state-of-the-art HIL-based methods as described by the authors in [59] are shown in Table 3.

Table 3: Overview of the state-of-the-art HIL methods for performance evaluation [59]

Acronym	CCT	Combitest	SCSPT	PLPE	DSE
Description	Concise Cycle Test	Combitest	Short Cycle and System Performance Test	Prescribed Load - Performance Extrapolation	Dynamic System Evaluation
Institution	SPF	SERC	CEA INES	EURAC	TU Dresden, RWTH Aachen, University of Stuttgart
Country	Switzerland	Sweden	France	Italy	Germany
Load Profile/ Simulation	Simulation	Load Profile	Simulation	Load Profile	Simulation
DHW	Yes	Yes	Yes	Yes	Yes
No. of Testing Days	12–6 days	6 days	12 days	6–24 days	4 days
Data Exchange time	1/32 h	0.005h	1 minute	1-5 s	1s

In all the above methods mentioned in Table 3, the idea is to start with a simulation model making up a building envelope and weather data. Then perform an annual analysis of the model and the concerned component/system. The next step will be to find the representative days for the short sequence reduction. Finally, the authors find the pitfalls in the short sequence reduction and find suitable methods to ease them during the experimental validation of the result. The Combitest method, PLPE [58] considers the load profile of a specific building, while the CCT [60] and SCSPT [58] methods consider the model of a building which is a single zone building. The DSE (Dynamic System Evaluation) method is the latest method where a more detailed model of the building is considered for the simulation [59] and also

considers the thermal inertia of the building and the storages. In all the methods a heating use case and a Domestic Hot Water (DHW) use case is showed, also the DHW contribution to the overall energy consumption is very less when compared to the space heating use case as explained by all the individual authors who developed the HIL based simulation testing.

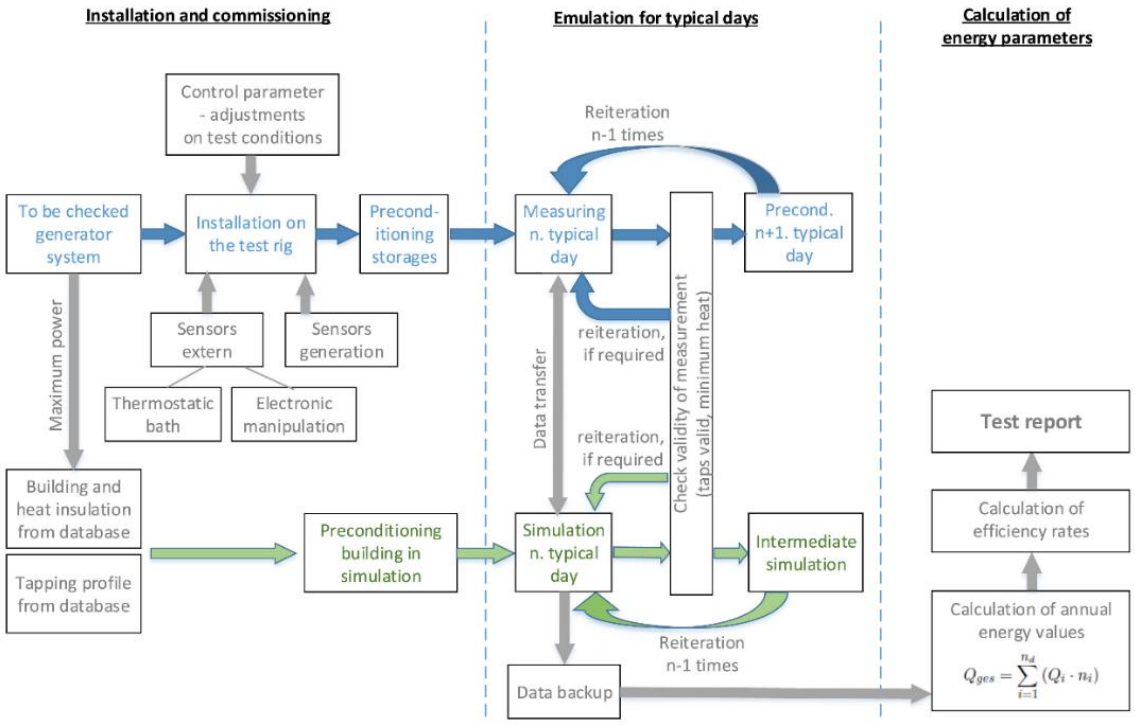

Figure 17: Procedure of the DSE method [59]

The emulation part is the test bench emulating the heat transfer within the building, while the simulation part is the part where the numerical model is being simulated. The numerical model in general generates the boundary conditions from the building envelope side using which the emulation is performed. The intermediate simulation is explained in the later sections of this chapter. In short to conclude the literature offers both the HIL and non-HIL based methods to evaluate the performance of the whole system and the individual components. The pros and the cons of the discussed methodologies are explained in Table 4 and Table 5, respectively. The conclusion is that the current work wishes to address the work in close relation to the DSE method and the CCT method. The process flow of the DSE method is shown in Figure 17. The CCT method considers the entire year's performance based on annual simulations. The point to be noted is that the component-level testing is performed by the non-HIL methodologies and the system-level performance evaluations are done by the HIL-based methodologies.

Table 4: Comparison of the model and process aspects of the different HIL methodologies

Method Aspects	CCT	SCSPT	Combitest	DSE
Building Model	TRNSYS Type 56 : Type 56 describes a building with multiple thermal zones, i.e. rooms. The model uses data from wall and window materials and thicknesses. Each room has a homogenous temperature, and radiation heat between the rooms is based on the room area [61].	TRNSYS Type 56	TRNSYS Type 56 or simplified building model based on the ISO 13790:2008 model	ASHRAE 140 standard [62]: Standard Method of Test for Building Energy Simulation Computer Programs" aims to increase confidence in the use of building energy modeling (BEM) by creating standardized and citable test procedures for validating, diagnosing, and improving the current generation of BEM software
Heat Distribution Model	The active layer of the building model is used for heat distribution, they used thermostatic valves for simulation purpose.	User-defined types with radiator distribution (Type 262) and heating floor (Type 241)	Heat distribution system developed with the building model of Type 56	User defined heat distribution system
Solar collector models	Type 301 developed by Isakson and Erikkson [63]	Type 8322 developed by Bengt Peres [63]	Type 8322 developed by Bengt Peres [63]	-
Draw off profile model	IEA Task 26 model [64]	IEA Task 26 model [64]	-	Profile L EN 16147 standards [65]
Process Involved	They assessed parameter based on the manufacturer's data. The missing parameters are fitted using a re-simulation. The numerical models of the test systems is extended to predict the seasonal performance. Experimental and the simulation results are compared shown in .	The testing procedures are developed by comparing the experimental results with the reference heating system that uses the same type of main heat source without the solar thermal energy. The measured data is used to find a simplified model of the complete system	The annual performance is evaluated by multiplying using an extrapolation factor of 365/6 and a correction factor to the eventual results got from the experimental testing is shown in	The annual performance is obtained by an extrapolation based on the cluster weights. It is then verified using a round robin test to prove the repeatability of the results as shown in Figure 17.

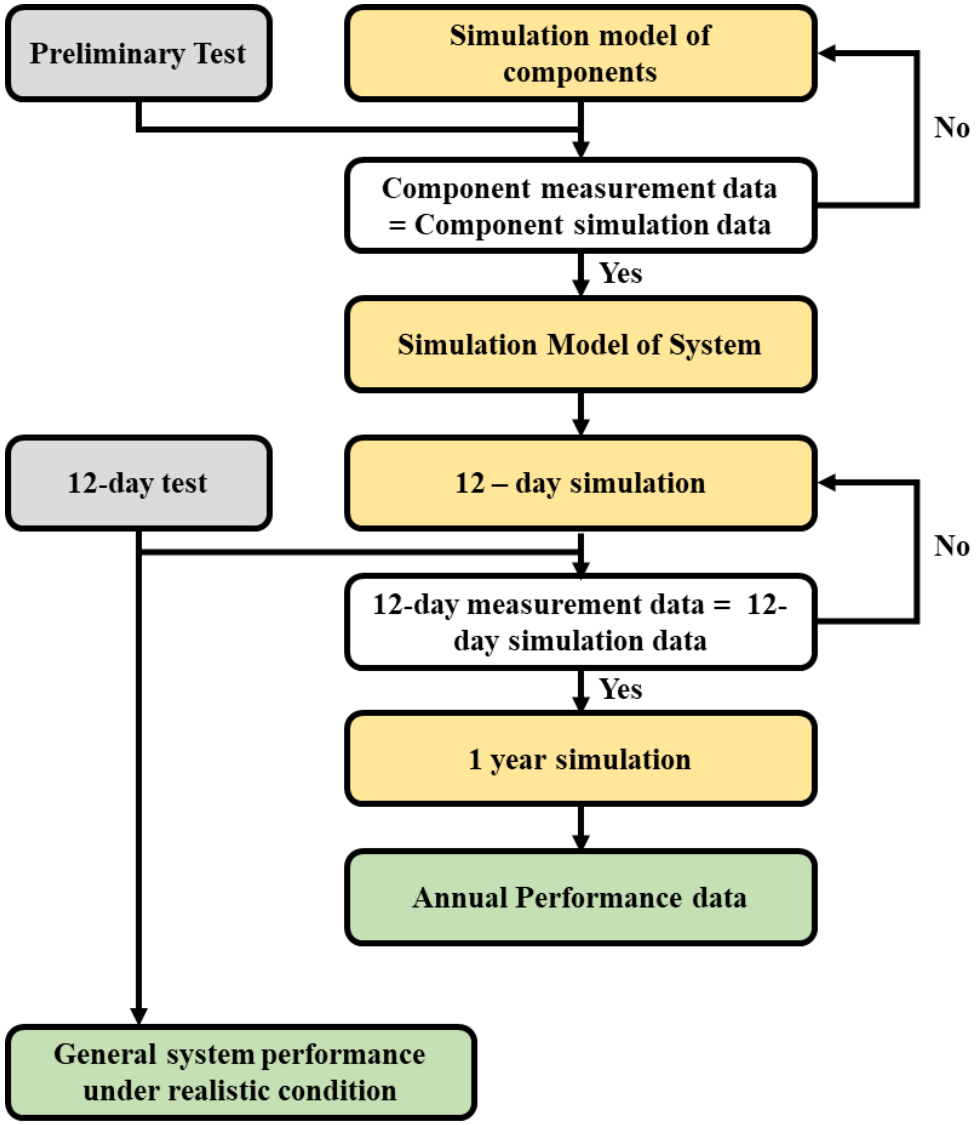

Figure 18: Process flow of CCT method [57]

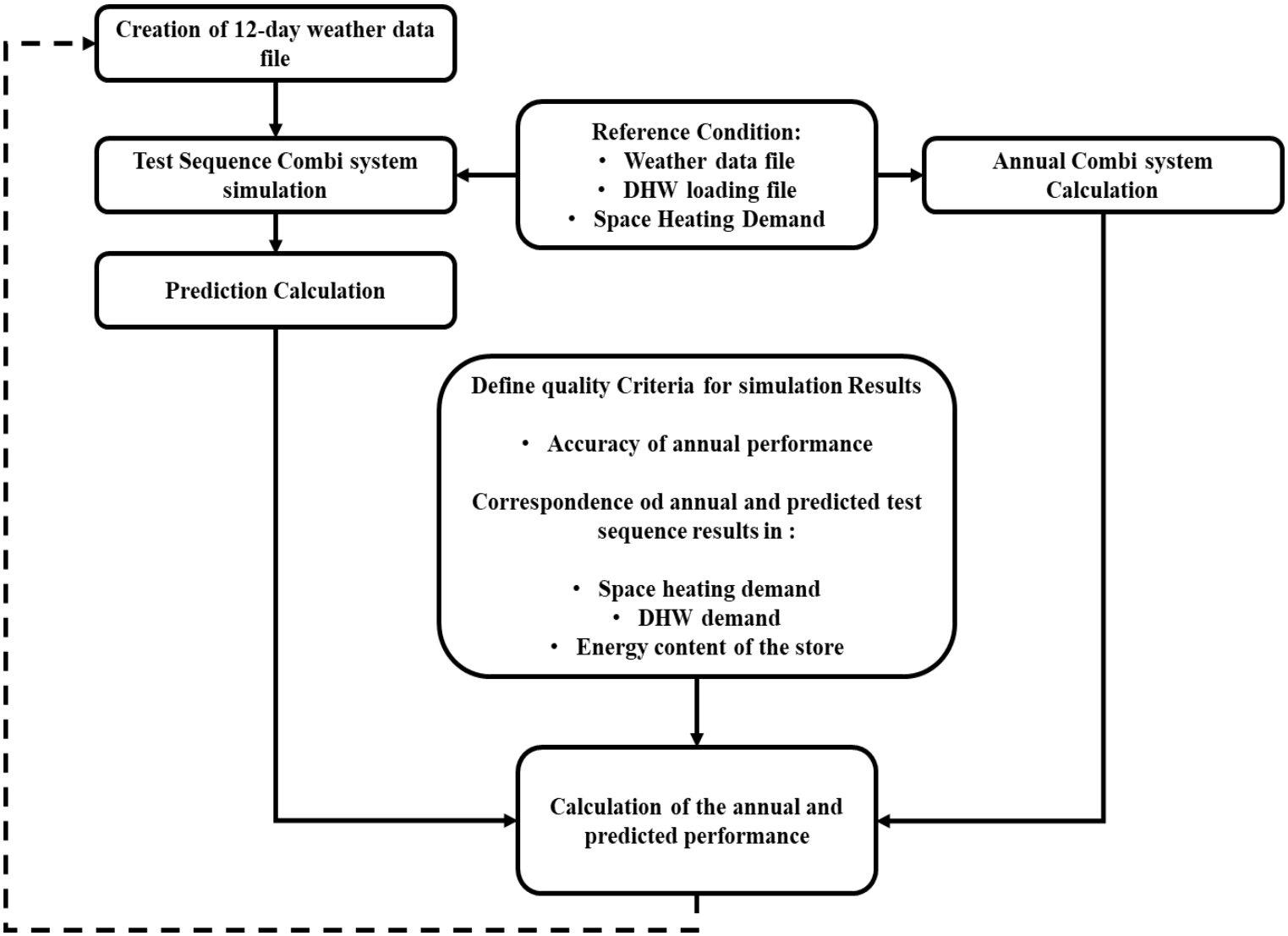

Figure 19: Process flow of SCSPT method [57]

2.1.2 Existing methodologies for finding the representative days

The literature has various methods for reducing the simulation cycles. Usually, it starts with the annual data and ends in a short testing sequence. The idea of the research methodologies is to check and verify if one can generate a fictitious weather profile data that combines multiple aspects of the weather profile and then evaluate the seasonal efficiency. Weather data and load curves are considered, other criteria include maximum power and internal temperature, the selection criteria can have several profiles (namely temporal, cumulative curves, etc.). Such methods can be grouped into three large categories, namely the Heuristic Methods, Iterative methods, and Clustering methods as explained and classified by the authors in [66].

2.1.2.1 Heuristic Method

In short, the heuristic methods are manual methods, with selection criteria based on the annual data. The idea is to select the number of periods with different load or meteorological conditions to capture a variety of unique events. The authors in [67] and [68] selected specific days to contain the hours with meteorological and load events to characterize typical system behavior for PV plant use and a building use case. The heuristic methods are used to reach immediate goals do not prove to be optimal. Overall flow of the heuristic method is shown in Figure 20.

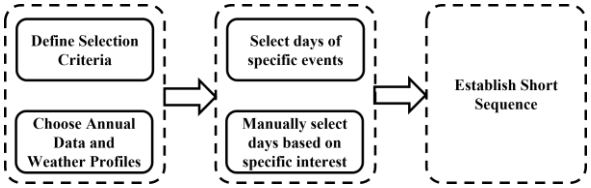

Figure 20: Process flow in heuristic method

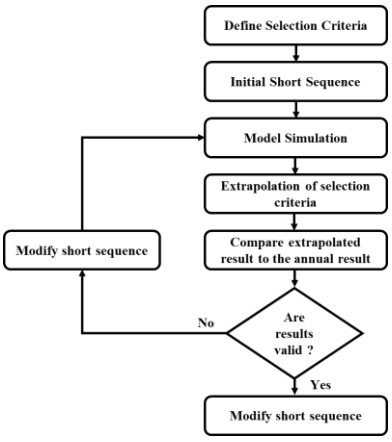

Figure 21: Process flow for Iterative Method

2.1.2.2 Iterative Method

The iterative methods search for the best optimal solution based on repetitive action and compare the quality of the result in each iteration. The Short Cycle System Performance (SCSPT) is a method developed by the French Commission of Alternative Energies and Atomic Energy (CEA), where a twelve-day reduced, sequence is used to represent an entire year that is simulated. The sequence could reproduce the annual performance with a good accuracy applicable to different models, as explained in [69] and [70]. Process flow of the iterative method is shown in Figure 21.

Table 5: Pros and Cons of state-of-the-art HIL methodologies for performance evaluation

Method	Pros	Cons
DST	• Dynamic effects and component interaction under realistic operating conditions are assessed • Less detailed components information • The seasonal performance was evaluated for different climates and buildings • The physics-based models with proper physical parametrization	• The test procedure and test facility are more demanding for evaluating each component • The predictions for a long hybrid system can be less accurate
CCT	• Dynamic effects and component interaction under realistic operating conditions are assessed • Less detailed components information • The response of heat distribution is simulated so that the effect of the thermostatic valves was considered • The tested system controls the flow temperature to the heat distribution system	• Long term performances evaluated through simulations based on real time experiments
SCSPT / PLPE	• Dynamic effects and component interaction under realistic operating conditions are assessed • The annual performance assessed easily with direct extrapolation • Different climates and buildings were investigated • Not necessary to identify some components to model the system or components	• The test results are valid only for the set-up boundary conditions, such as load and climate
Combitest	• Dynamic effects and component interaction under realistic operating conditions are assessed • The annual performance can be found via direct extrapolation • By reducing the test to a six-day sequence, the test cost is reduced	• The extrapolation to other boundary conditions is not foreseen
DSE	• Dynamic effects and component interaction under realistic operating conditions are assessed • Detailed models of buildings are used, with less testing days (4 days	• Too many interruptions during the testing time since the representative days chosen based on k-medoids clustering represent a discontinuity

2.1.2.3 Clustering Methods

Clustering algorithms employ an advanced technique of grouping days with similar attributes into clusters. The most used methods are the k–means and k–medoids clustering, as per literature. The days close to the cluster centers are chosen for the short testing sequence. One such application is showed in [60]. The method of the time reduction process directly depends on the way the extrapolation is done. The literature suggests that two different ways are possible: one is multiplying the result got in the reduced cycle by a proportion (commonly adopted in heuristic and iterative methods). The other method is to multiply the result got in the reduced cycle by the weight of the group represented by a day (usually adopted for the clustering methods).

Based on the literature studies the latest state-of-the art testing method (DSE method) firstly tries to compare all the methods for choosing the suitable set of representative days as explained in [71] where the author compares all the possible methods to find the set of suitable days. The k-means, k-medoids, dynamic time warping, are compared and finally, the k-medoids clustering is chosen since it leads to the least deviations in terms of the annual efficiency factor SCOP (Seasonal Co-efficiency of Performance) for a Heat Pump use case. Thus, the standard procedure is to associate a weight for each feature chosen for performing the clustering, namely the outdoor air temperature and the solar irradiation, as explained in [72] on a weather time series with hourly data. Process flow for the clustering method of finding the set of suitable days is shown in Figure 22.

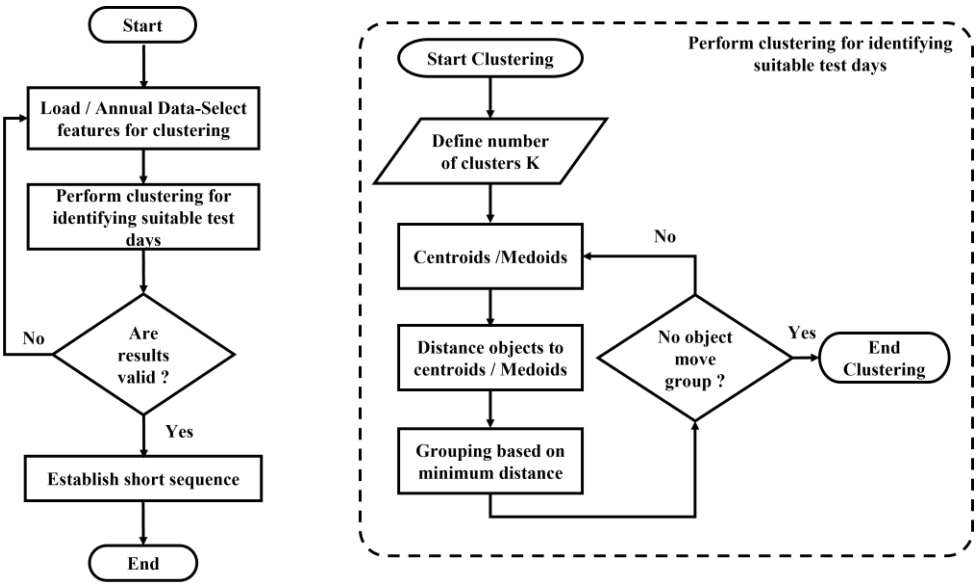

Figure 22: Clustering-based sequence reduction

2.1.2.3.1 K-Means and K–Medoids clustering algorithm

In short, the clustering method is a common technique to group similar objects into different groups. Grouping is achieved by the partitioning of the data set into subsets according to some defined distance measure [73]. Both these techniques are based on the point that the center of the cluster can represent a cluster [73]. In K- means clustering, the mean or median point of a group of points is computed, which is usually called the centroid. This centroid does not correspond to the actual data point. While, in the K–medoid clustering algorithm, the medoid is found out. This medoid is the most representative point of the cluster, which belongs to the actual group of data points. Comparison of both the clustering algorithms is shown in Table 6. The difference between the centroid and medoids in shown in Figure 23.

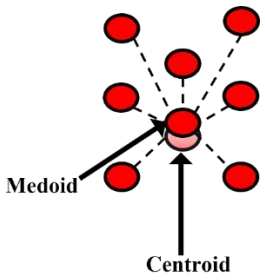

Figure 23: Clustering, identification of centroid and medoid

The K - means clustering techniques is applied to the sample use case in the upcoming section for a space heating application. Since these two techniques are the most referenced in the literature in identifying the most representative days. For the next section, simulation-based studies based on the short testing sequence is performed. In short, the first step was to identify the methods that evaluate the performance of a system using the HIL method where the DSE and the CCT are the ones related closely.

The next step will be to address the first lock within the HIL evaluation method which is the identification of the representative days. For this, mathematical optimization methods like the K–Means and the K–Medoids algorithm is chosen based on the literature.

The next section will describe the uncertainties related to the HIL testing methodologies and the main hypothesis considered in current context of the current research work. As an initial step, the idea is to implement the state of art the clustering technique and check if the seasonal efficiencies could be evaluated. Based on literature the testing is done based on choosing the representative days from already existing days. The idea of the research methodologies is to check and verify if one can generate a fictitious weather profile data that combines multiple aspects of the weather profile and then evaluate the seasonal efficiency.

Table 6: Comparison of K-means and K - medoids clustering algorithm

Aspect	K- Means algorithm	K–Medoids algorithm
Partitioning Aspect	• Partitioning is done around the centroid that does not exist in the actual data point	• Partitioning is done around the medoid, which is an actual data point
Mathematical Representation[73]	$E = \sum_{i=1}^{k} \sum_{p \in C_i} \lvert p - m_i \rvert^2$ • E is the sum of the square error for all the objects in the data set • p is the point in space representing an object • Mi is the mean of the cluster C_i • Meaning that the distance from the data point to the cluster center is squared and then the distances are summed up	$E = \sum_{j=1}^{k} \sum_{p \in C_i} \lvert p - o_j \rvert$ • E is the sum of the error for all the objects in the data set under consideration • p is the Point in the space representing an object • Oj is the object in the cluster C_i • Meaning that the distance from the center object belonging to the data point are summed up
Features of the clustering algorithm	• Minimization of the sum of the squares of the Euclidean distances	• Minimization of the sum of dissimilarities instead of the sum of the squares of the Euclidean distances
Pros	• The major advantage of K–means clustering is the favorable execution time	• Robust to outliers since only the dissimilarities are calculated outperform K- Means clustering for large datasets
Cons	• Sensitive to outliers, large data sets may distort the distribution of the data • Efficient only for the small data sets	• PAM (Partitioning Around Medoids) lacks scalability for extensive databases and its present high time and space complexity
Steps involved in the algorithm	• Step 1: Select K points as the initial centroids • Step 2: Assign all the points to the closest centroid • Step 3: Recompute the centroid of each cluster • Step 4: Repeat steps 2 and 3 until the centroids do not change’	• Step 1: Select K initial points • Step 2: Set one of the K initial points as medoids • Step 3: Replace one of the non-selected medoids with the central medoids until the convergence is achieved

2.2 Application of state-of-the-art methodology to a sample use case

2.2.1 Description about the building envelope, weather profile and heat load analysis

To evaluate the efficiency and then determine the uncertainty due to the state-of-the-art methods, a sample use case is proposed. The first step is to establish about the building envelope and perform an analysis based on the whole year simulation to identify the heat load throughout the year. The use case is a single zone building with 70m^2 of habitable area. The building has windows on all four sides that is about 10% of the wall area. There are two layers, one is a concrete wall having a thermal conductivity of 0.095 W/m^{2}K and an insulating layer having a thermal conductivity 0.038 W/m^{2}K. The windows have a single layer of glass, and the conductivity of the frame is around 1.4 W/ m^{2}K and for the single layer of the glass it is around 0.045 W/m^{2}K. The weather is chosen as Trappes, FR. The weather file is a Test Reference Year (TRY) with a one-hour resolution. As explained by the author in [60] it is better to consider a high resolution weather profile in order to achieve transient variations close to the reality as possible. But, it is always better to consider weather profiles with 1 hour resolution as explained in [59]. The external air temperature and the irradiation profile for the chosen weather profile is shown in Figure 24 and Figure 25. From Figure 24 it can be inferred that the average value of temperature is around 12°C for the whole year. The minimum and the maximum values for the temperatures being -3.5°C and 33°C, respectively. Similarly, from Figure 25 one can infer that the average Global Horizontal Irradiation (GHI) is around 130.4 Wh/m^2 the minimum and the maximum values of the GHI are 0 Wh/m^2 and 913 Wh/m^2, respectively. Also, it can be seen from an initial observation on the outside air temperature and the irradiation values that the space heating is required during the winter season.

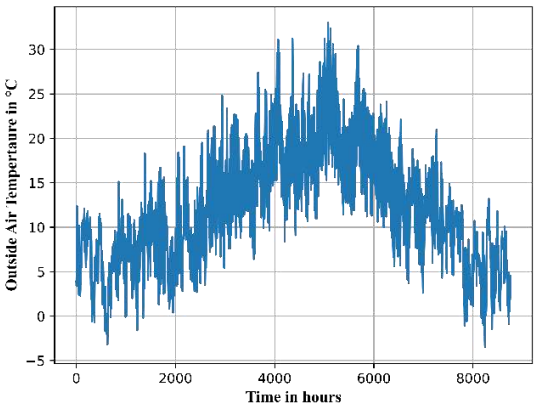

Figure 24: Full year temperature profile of Trappes

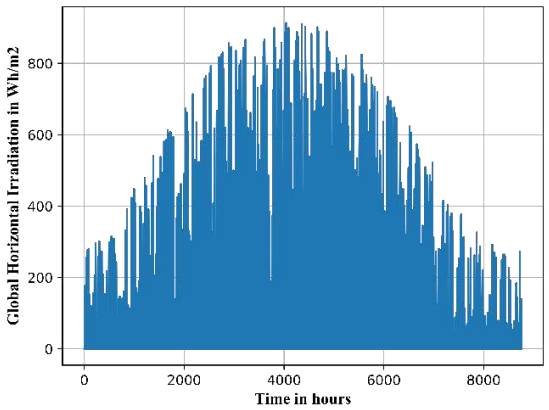

Figure 25: Full year irradiation profile of profile

In DYMOLA, the simulation environment uses the convective heat transfer source to evaluate the heating load of the building during the heating and the cooling season. The heat load requirements for the building are shown in Figure 26. The heating season is around 153 days in the whole year. The maximum

heating load for the building is around 10kW for an external temperature of around -3.5 °C, while the maximum cooling load for the building was found to be around 6.2kW for an external temperature of around 32°C. It could also be seen in Figure 26 that there are two parts to the heating season for 93 days at the beginning of the year and around 60 days at the end of the year. Also, in Figure 26 it could also be observed that there is a spike at the beginning of the heating season towards the end of the year that accounts to 12kW in power. This is due to fact that the convective heating source was designed to switch between the heating season and the cooling season, due to this the sudden change from the heating mode to the cooling mode results in the sudden spike of power this is due to the simulation environment and is not realistic in nature. Hence this spike need not be considered as a maximum value for the heat load requirement for heating and cooling applications.

The next step will be to perform an annual simulation for the building with a boiler (a condensing boiler) specifically for the heating season. The testing facility at ENGIE does not have a climatic chamber at the present time. Hence, leaving one with the ability to not test the heat pumps in real time. But for the simulation analysis a boiler uses case, and a heat pump use case is demonstrated. Both the use cases involve the space heating application for the same building and the same weather profile. The internal loads are set to 570 W during the period of occupancy and 20 W during the period of inoccupancy. The ventilation for the building is maintained at 25 m3/h/person. The temperature setpoints are 20°C during occupancy and 16°C during inoccupancy. The occupancy period for the single zone building is from 12AM to 10AM and 6PM to 12AM while the period of inoccupancy is after 10AM until 6PM for one day during the weekdays.

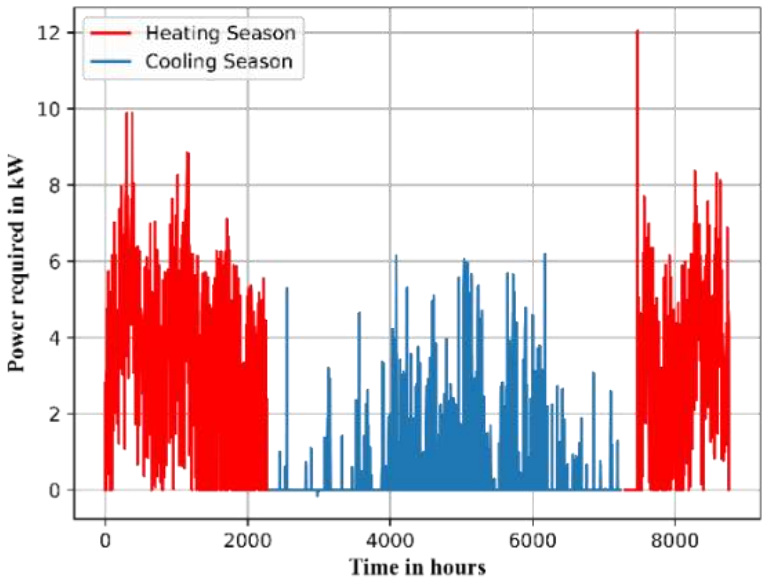

Figure 26: Heat load requirements of the building

2.2.2 Component Analysis: Boiler and Heat Pump and choice of solvers in Dymola

For the intended use case a condensing boiler is chosen to deliver the space heating required during the heating season. In Dymola the buildings library allows one to use the boiler models that are predeveloped based on the first principles of thermodynamics. The heat transfer equation of the boiler as described in [74] is :

$$\dot{Q} = y\,\dot{Q}_0\,\eta/\eta_0$$

Where $\dot{Q}$ is the heat transferred to the fluid for space heating, y is the control signal given to the boiler depending upon the conditions to provide space heating when necessary. $\dot{Q}_0$ is the nominal power that can be delivered by the boiler, η is the efficiency at the current operating point, η_0 is the efficiency when the control signal $y = 1$ ($y = 1$ represents the maximum power deliverable if the controller output is 1) or at the nominal temperature T_0. Also in [74] it is mentioned that the value of η is obtained from the efficiency curves at part loads and full loads. This efficiency curve for different load can be either obtained by experiments or from the data sheets. In short Dymola allows one to use the efficiency curves vs load as a polynomial equation in the already existing building models. The boiler efficiency in [74] (building library) is defined as shown in the equation below:

$$\eta = \frac{\dot{Q}}{\dot{Q}_f}$$

Where $\dot{Q}_f$ is the heat combustion released by the fuel and $\dot{Q}$ is the heat transferred to the working fluid. The definition for boiler efficiency η is represented using a polynomial or a constant, the idea is to use a polynomial equation since it corresponds to the description of the efficiency at different operating points the part load or in other terms at different operating points of the controller. The data for the part load vs the efficiency of the condensing boiler from SIME UNIQUA 25 Revolution data is shown in Figure 27. The part load curve for the boiler was obtained by considering a few operating points and then interpolating. From the data sheets the maximum power deliverable by the boiler is around 25kW and the minimum deliverable power is around 6 kW.

Hence, the operating range of the boiler based on the heat load curve from Figure 27 should be around 20% to 50% of the part load and sometimes at 100% of the load depending upon the start and stop cycle. Meaning the final seasonal efficiency should be around 0.88 to 0.97 during the total operation based upon the initial analysis, while the daily efficiency values could range from 0.82 to 0.97 based on the initial observations. Also, from Figure 27 it could be observed that the efficiency is higher for the lower part loads when compared to the full load. This is because in the condensing boiler the hot flue gases are captured and recycled back into the system through a heat exchanger into what is known as the

primary circuit, while the flue gases are let into the atmosphere in the non-condensing boilers. The part load curve for the boiler is shown for a supply temperature of 50°C the reason being that lower the operating temperature higher the efficiency of the boiler.

Similarly, the buildings library in Dymola allows one to use the pre-existing models of the heat pump especially the air to water heat pump. This model allows one to calculate the COP as the temperature changes as shown in the equation below:

$$COP = \eta_{Carnot,0} * COP_{Carnot} * \eta_{PL}$$

Where COP_{Carnot} is the Carnot efficiency and η_{PL} is the polynomial in the heating part load ratio y_{PL} that can consider a change in COP at part load conditions. η_{PL} is a polynomial in the heating part load ratio y_{PL} that can consider the change in COP under part load conditions. The polynomial is written in the form:

$$\eta_{PL} = a_1 + a_2 * y_{PL} + a_3 * y_{PL}^2$$

Where the coefficients a_i are declared by the parameter a.

The η_{Carnot} is defined by the equations below:

$$\eta_{Carnot,0} = \frac{COP_0}{T_{con,0} * \frac{1}{(T_{con,0} - T_{eva,0})}}$$

Where η_{Carnot} is the Carnot effectiveness, COP_0 is the Coefficient of Performance of the heat pump at nominal conditions, $T_{con,0}$ and $T_{eva,0}$ are the condenser temperature and the evaporator temperature at the nominal conditions. The heat pump considered for this application is an air to a water heat pump that can deliver 15.4kW of heat output with 4.2kw of power input with a single compressor and a nominal COP of about 4.

The heat pump chosen from the data sheet is DIMPLEX SI30TER+. The COP for the part load ratio is shown in Figure 28. Since as explained earlier, the load varies between 6–12 kW, hence the COP could vary between 2.8- 3.2 based on the initial analysis and first observation of both the curves. Like the boiler curves a few points from the data sheets are taken and interpolated using Python.

The COP for the part loads are taken for the condenser temperature of about 35°C and also for the hot water supply temperature of about 55°C .In the building libraries documentation it is recommended either to use the numerical solver Dassl with a solver tolerance of 10^{-4} and Radau solver with a tolerance

of 10^{-6}, while trying to run the simulation as mentioned in their documentation [75] for a smooth running of the simulation.

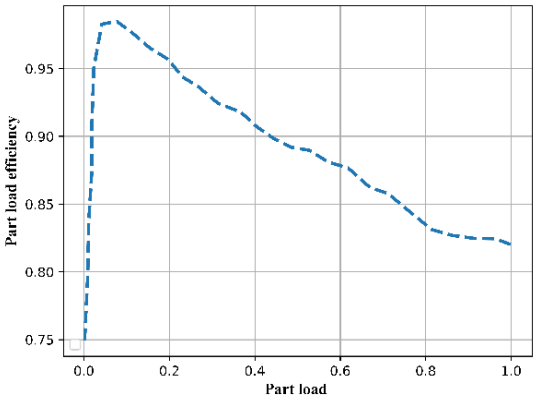

Figure 27: Part load vs Efficiency curve of a SIME condensing boiler supply temperature of 50°C

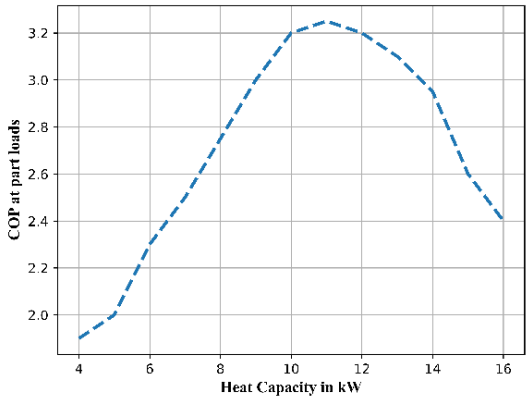

Figure 28: Part load ratio for the chosen air to water heat pump for supply temperature of 55°C

2.2.3 Full Year Simulation analysis

The control scheme for the heat pump and the boiler is based on the internal temperature requirements. Plus, the hot water sent to the radiator for heating is also controlled by the water law so that the efficiency of the system is not compromised based on successive starts and stops of the boiler/ heat pump. Also, in the models for both the boiler and heat pumps, the cycling time (the combination of the boiler run time and the off time) of the equipment's are considered. It is usually between 10 minutes–20 minutes as a thumb rule and is also modeled in Dymola. Indeed, the cycling of the equipment also contributes to the seasonal efficiency, as shown in Figure 29. The cycling times were experimented by simulation from 5,10,15 and 20 minutes. The efficiency does not increase much beyond 15 minutes, the longer the cycling time, the longer the equipment takes to provide space heating to the building.

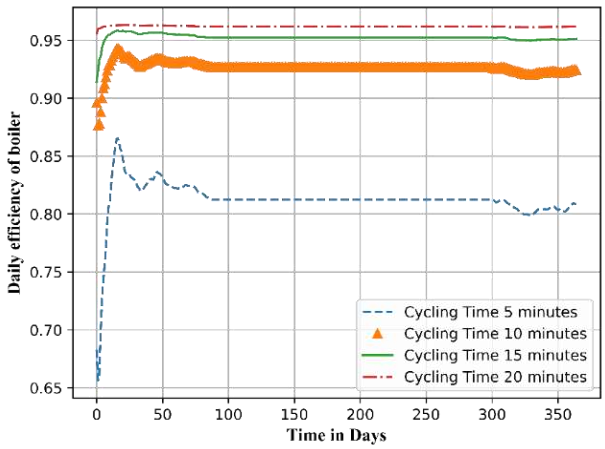

Figure 29: Effect of cycling time on the boiler efficiency

The choice of the cycling time for the simulation studies is kept at 10 minutes in the Dymola model since it offers a better tradeoff between maintaining the internal temperature and the efficiency. The internal temperature for one day is viewed for the 10-minute cycling time for the boiler as shown in Figure 29. One can see that the internal oscillates between ± 0.5°C of the set-point temperature during the occupancy period, where the internal temperature needs to be maintained at 20°C. It is due to the use of a hysteresis control. However, during the period of inoccupancy, because of the presence of high irradiation effect, the internal temperature of the building varies slightly, although it is maintained in the ± 0.5°C band from the setpoint.

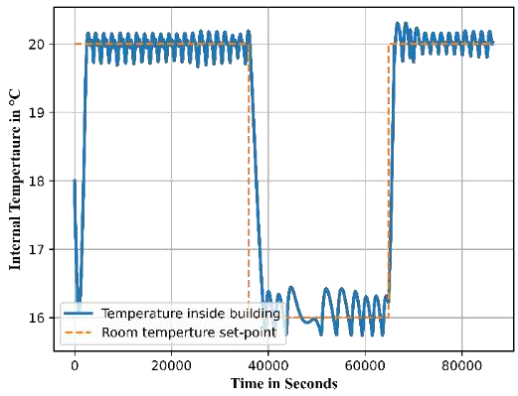

Figure 30: Internal temperature inside the building vs. setpoint for a typical starting day

Initially, one can see that the setpoint inside the building is decreasing. It is because the boiler takes some time to heat the volume of air inside the building. The windows with a single layer of glass are also contributing to the fall in the internal temperature of the building. Since the windows on all the four walls have an attribute of being 10% the area of the walls. The entire year energy consumption (cumulative) of the boiler is shown in Figure 31.

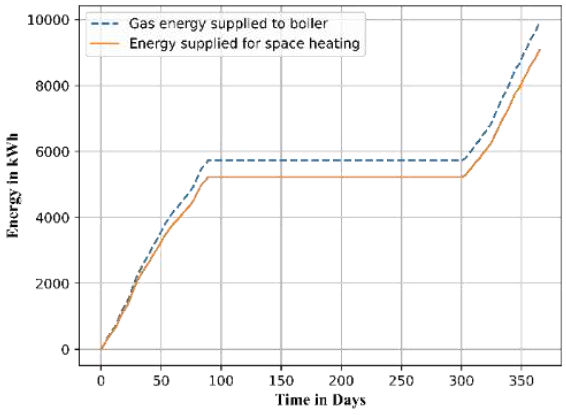

Figure 31: Cumulative energy for boiler entire year simulation

The total gas energy supplied to the boiler for the total heating season is 9926 kWh and the total energy output delivered for the space heating is around 9074 kWh. The seasonal efficiency calculated as per the direct method of calculating the boiler seasonal efficiency is around 0.914. The daily energy analysis for the boiler entire year simulation is shown in Figure 32. The daily gas energy supplied to the boiler ranges from 19.02 kWh to 110.58 kWh with an average energy supplied being at 64.872 kWh. The useful energy consumed for the space heating is in the range 17.82 kWh–105 kWh. The average energy used for space heating is around 59.30 kWh.

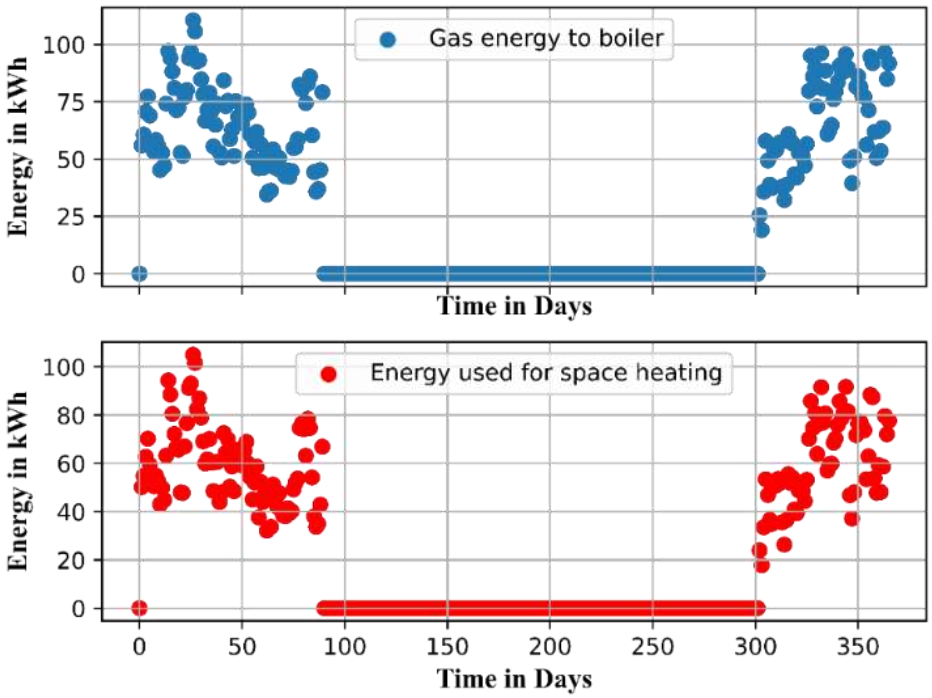

Figure 32: Daily energy for boiler one year simulation

The point to be noted is that the 75-percentile of the values for the gas energy supplied to the boiler is above 56.62 kWh while the energy used for the space heating is above or around 56.62 kWh. Similarly, the 75-percentile value is around 0.91 for the daily efficiency. The daily efficiencies for the boiler simulation ranges from 0.82 to 0.97, with the average value of the energy efficiency is around 0.92. Daily efficiency values are shown in Figure 33.

Also from Figure 31 and Figure 32 one could see that as the year starts and the mid-season approaches one could see that the values for the energy supplied and used up by the boiler decreases, while daily efficiency values also decrease this is because the boiler does not run for longer period of times and requires multiple starts and stops during the days closer to the mid-season.

It could also be explained from after the boiler stop and then the start the boiler operates at maximum operable load, leading to a decrease in the mid-season efficiency. In Figure 33 one could see that the lowest value of the efficiency occurs at the full load and the part load ratio being at 0.82. The lowest operating load being at 20 percent where the part load efficiency is at 0.97.

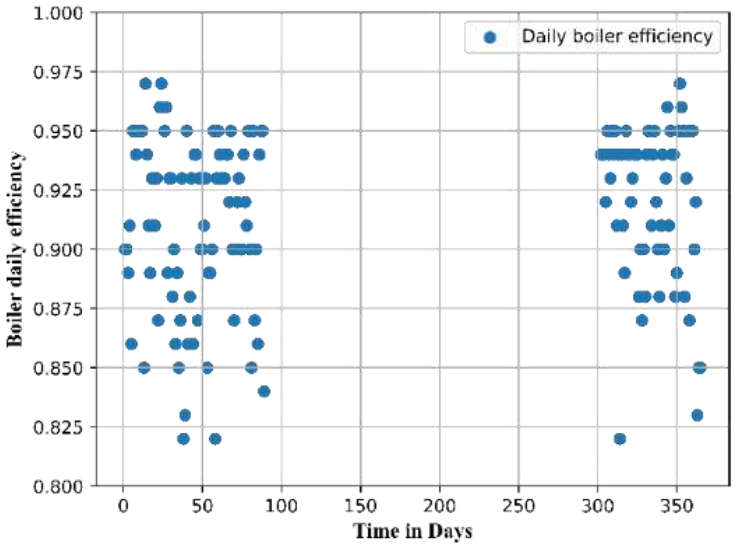

Figure 33: Daily energy efficiencies of the condensing boiler

The one-year simulation is also done for the same control setting with the component being replaced by the heat pump. The total energy used up for the space heating is around 8328.75 kWh and the electrical energy supplied to the compressor is around 2691kWh. The seasonal COP for space heating is around 3.06, the energy levels (cumulative) are shown in Figure 34.

The maximum values of the energy delivered for space heating and the electrical energy supplied to the compressor are 93.9 kWh and 35.7 kWh, respectively. The minimum values for the energy supplied for space heating and electrical power supplied to the compressor are 17.1 kWh and 4.1 kWh, respectively. The daily COP values are in the range from 2.63–3.56, respectively.

The average energy levels for the space heating and the average energy levels for the electrical power supplied to the compressor are 53.6 kWh and 17.53 kWh respectively, while the average COP values about 3.11.

As the mid-season approaches, the COP values increase, and it could be attributed to the fact that the heat pump depends on the outside air temperature. During the coldest parts of the year during the beginning and towards the end of the year, one could see that the values of COP are slightly lower when compared to the mid-season values.

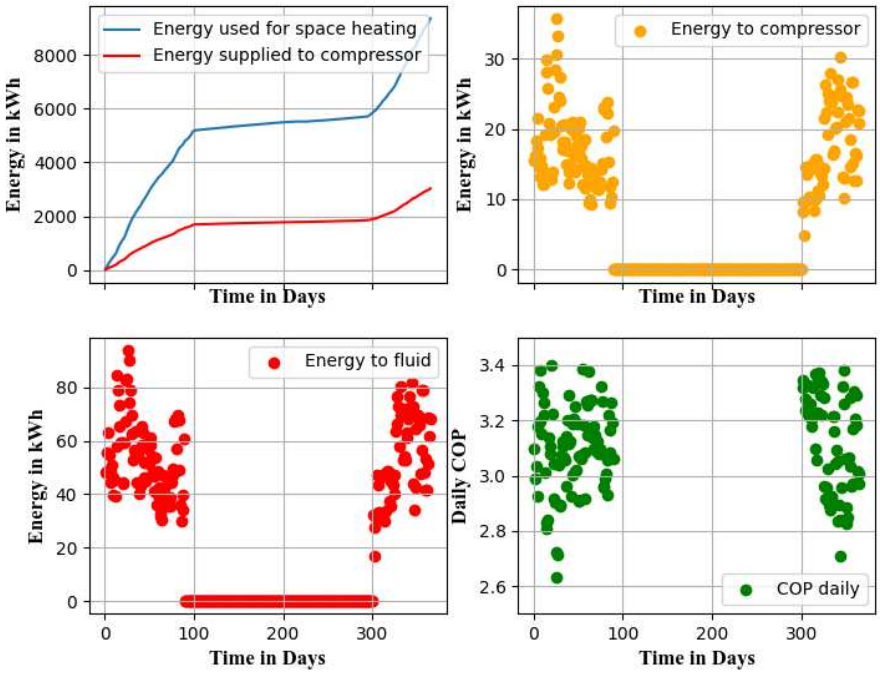

Figure 34: Heat pump one year simulation results: Cumulative energy consumed, daily electrical energy supplied to compressor, Daily energy used for space heating, Daily COP values

A statistical analysis performed on the daily COP values show that the 75th percentile values are above 3.0, the 75th percentile value for the energy levels are respectively around 47.4 kWh and 14.4 kWh. During the cooling season, where the space heating is not required, the COP values and the energy values are around zero since there is no operation required during that period, as shown in Figure 34. Values of the key performance indicators (KPI) for both the use cases are shown in Table 7.

Table 7: Values of key performance indicators from one year simulation

Key Performance Indicator	Heat Pump	Condensing Boiler
Energy supplied to equipment	8328 kWh	9926 kWh
Energy used for space heating	2691 kWh	9074 kWh
Seasonal efficiency	SCOP = 3.1	$\eta_{sesonal}$ = 0.914

2.2.4 Short Sequence Reduction - Clustering

Based on the values of the Key Performance Indicators (KPI) obtained from the one-year simulation values, the next step will be to apply the clustering method to reduce the whole heating season simulation period to a few days. To do so, primarily one needs to find the features on which one can segregate data into clusters. Also, one needs to consider the fewer number of features into account

because as the number of features increase the dimensionality of the clustering algorithm increases. Hence, the first step will be to do a component analysis to find what are the important features and the how to reduce the dimensions while performing the clusters. The most commonly used techniques are the Principal Component Analysis (PCA) [76] and the Neighborhood Component Analysis (NCA) [77].

From both [76] and [77] one can identify that the PCA is an unsupervised technique that is primarily data driven, while NCA is a supervised technique that is task driven. In [78] it is stated that the PCA is the most commonly used dimension reduction technique. Hence, the PCA is used to identify the top two/three features that are considered for performing the clustering as demonstrated for the use case under consideration in .

From the evaluation point of view, the components and the building envelope will change as per the user. Hence, the idea is to choose the representative days based on the features related to the weather data, since the outside temperature and the irradiation are the key driving features. Thus, in combination with the weighting factors for the outside temperature and the irradiation, the k-means clustering is to be applied to the weather data for the heating season for 153 days since the use case involves only the space heating.

The idea is to evaluate 1-7 testing days for the boiler and heat pump use case, then verify the KPI's from each set of testing days with that of the KPI's obtained from the annual simulation. In both the boiler and the heat pump, the supply temperature for space heating is kept at 50°C and the return temperature is dependent upon the heating needs of the building.

In [79] it is also mentioned that there is a problem with local minima in the K-means clustering, meaning that when the clustering algorithm is run each time, there is a possibility to get a set of new clusters with cluster centers. To over-come this problem, one can run the clustering algorithms for n number of times and choose the combination that occurs for most of the n times while also viewing how evenly all the clusters are distributed.

Before going into the next steps, it is better to evaluate the cluster with a metric. The most used clustering metric is the elbow method to find the optimal number of clusters before going into the actual simulation. Elbow method to evaluate the clusters is shown in Figure 35 The optimum number of clusters is around 5-7 days.

If the clustering was done right, one should start seeing a convergence around these three days, plus these testing days also being practically workable. The temperature and the irradiation profiles for

the 6-day and the 7-day sequences are shown in Figure 36. One could see that even though with the increase in the number of days almost remains the same in both the sequences.

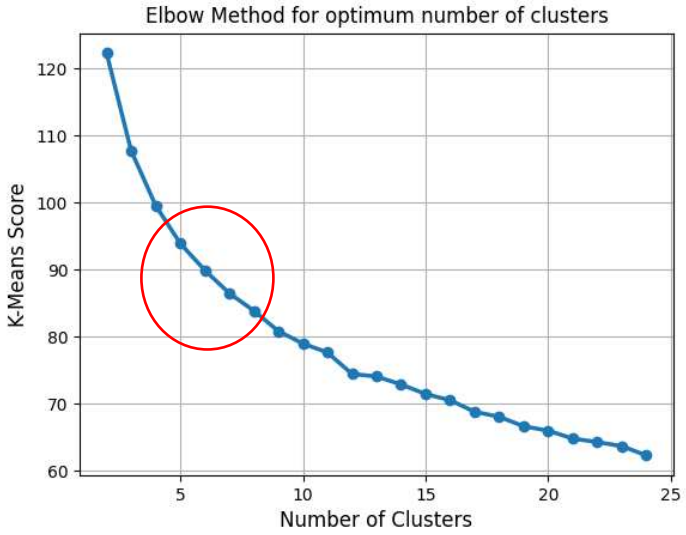

Figure 35: Elbow method for optimum number of clusters

Also, one could see from Figure 36 that there is a discontinuity between the days if they are arranged in the calendar order. The discontinuity is due to selected days are from the different time periods of the heating season. In such case one could observe in Figure 36 there is a huge temperature difference between each day.

One such example is the case after the 5th day where one could see the temperature difference between end of the 5th day and the starting day of the 6th day being 8°C.The problem of discontinuous days present two problems, one leading to energy shifting in the buildings and also in the thermal storages as explained in [59].

2.2.4.1 Energy shifting in buildings:

If a cold day is followed by a warm day, the heating load requirement for the cold day could be partially recovered because of the building's internal storage. Hence, one needs to first check the sequence of testing days by suitably re-arranging the days, so the phenomenon does not occur. During simulation, the simulation could be done for a set of virtual days prior to the actual test day, to solve this issue during the simulation studies.

During the actual HIL simulation, one could decouple the model from the HIL setup and use a heating supply according to a typical heating curve as explained in [59]. Also, one can simulate the days in between the actual test days based on the calendar this approach can be used depending upon the software used for the simulation as explained in [59].

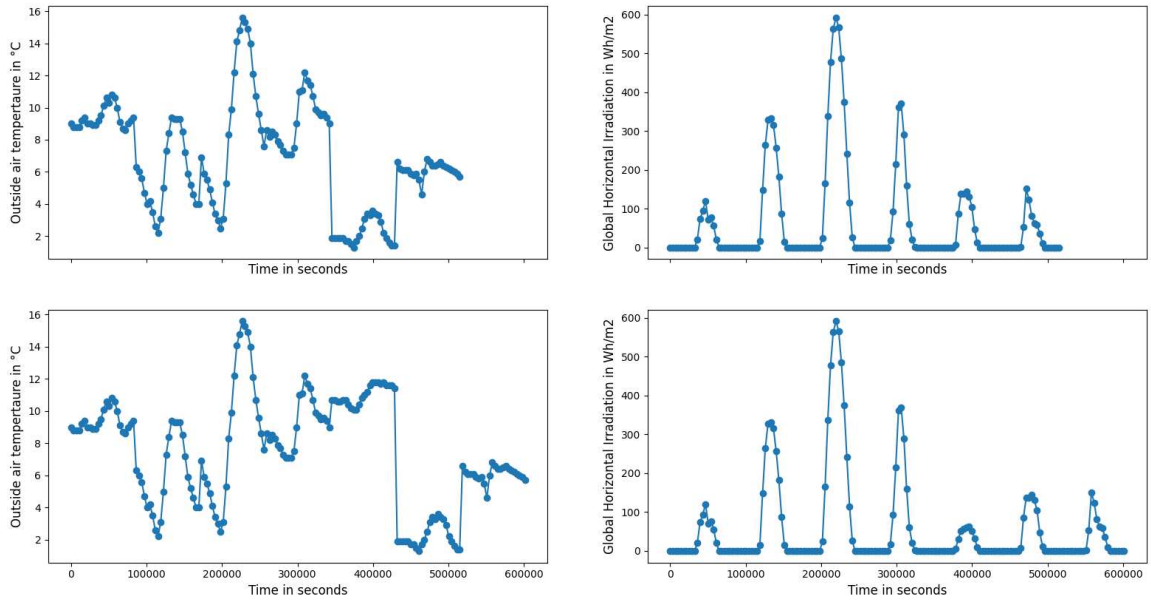

Figure 36: Temperature and irradiation profiles for a 6 day and 7 day sequence

2.2.4.2 Energy shifting in thermal storages:

Due to the discontinuity between the test days, the thermal charge inside the thermal storage tank could pose a problem. At the beginning of the simulation the thermal storage inside the tank could be adequate and if a warm day is followed by a subsequent cold day, then this could pose a problem because the tank is over charged for the warm day. This proves that the system could behave differently due depending upon the different arrangements of the testing days.

The second problem is more coincidental meaning that the tank could have a state of charge in between its minimal and the maximal charge inside the tank at the end of a typical test day. As a result, if an electrical heater is used for heating the tank this electrical energy expended could represent the wrong day. In both the cases the model needs to be decoupled and then the required thermal energy is consumed or supplied depending upon the situation.

As explained in [80] in order to tackle the energy shifting in thermal storages the different combinations of the days involved the short sequence are experimented using simulations. From those results the combination with the least deviation in the internal energy of the thermal storage tank is chosen as the short testing sequence. In the use case demonstrated there is no thermal storage involved.

An experimental use case related to the energy shifting in thermal storages for the heat pumps is demonstrated in [81]. The simulative study in [80] reveals that the order from warm to cold and then back to warm days leads to the least deviation in the shifted internal energy of the thermal storage.

The energy levels for the boiler use case is shown in Figure 37 and the seasonal efficiency values are shown in Figure 38. The efficiency levels are always under the 5% error bounds and the energy levels are within 5% error bounds for all the different sequences, this is because the gas boiler has a very narrow operating range and always delivers the space heating with the same efficiency.

Hence, for the boiler use case a 6–7-day short sequence is required to replicate the heating season performance. The results obtained from the 6 to 7-day short sequence are extrapolated by multiplying the result for each testing day with the weight of that appropriate cluster. The six days and the seven days testing results are shown in Figure 37 and Figure 38. Also, it can be noted that as one increases the number of testing days it could be observed that the values converge as close to the annual values.

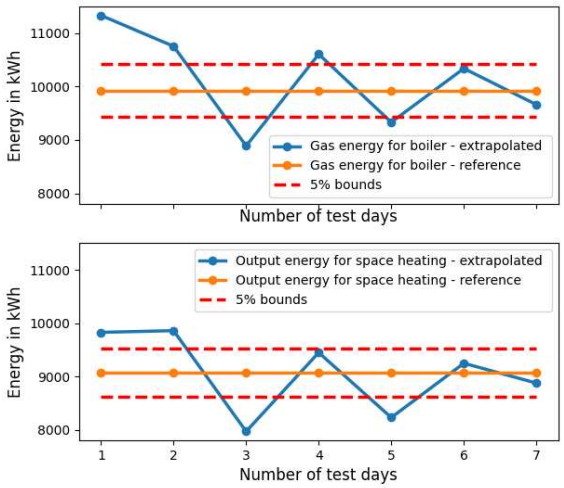

Figure 37: Energy levels short sequence values vs. annual reference values

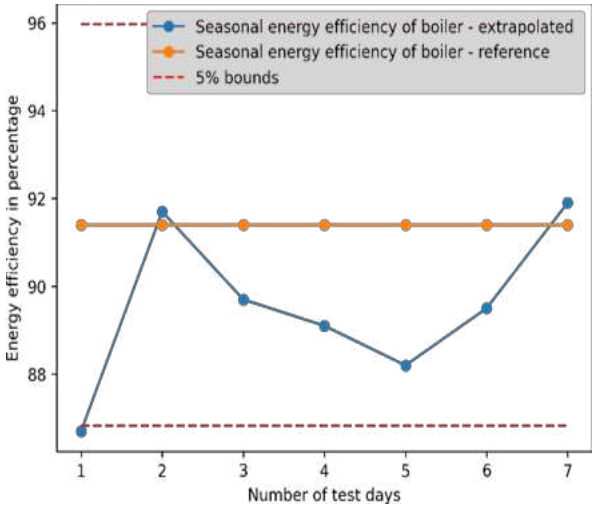

Figure 38: Seasonal efficiency short sequence vs. annual reference values

In Table 6 $E_{in\ 6\ days}$ is the gas energy supplied for the boiler for 6 days and $E_{out\ 6\ days}$ is the energy used for heating the fluid for space heating for 6 days. The results obtained for each day is multiplied by the weight of each cluster. Similarly, the results for a 7-day testing sequence are shown in Table 7.

Table 8: Results for 6-day test sequence for condensing boiler

Day	$E_{in\ 6\ days}$ kWh	$E_{out\ 6\ days}$ kWh	Weight	$E_{in\ extrapolated}$ in kWh	$E_{out\ extrapolated}$ in kWh
1	55.39	50.21	47	2603.49	2359.86
2	64.50	55.30	23	1483.57	1271.97
3	44.67	37.77	11	491.36	415.52
4	52.86	47.04	19	1004.37	893.74
5	90.32	84.82	29	2619.15	2459.64
6	82.22	71.16	24	1973.29	1707.82

Table 9: Results for a 7-day test sequence for condensing boiler

Day	$E_{in\ 7\ days}$ kWh	$E_{in\ 7\ days}$ kWh	Weight	$E_{in\ extrapolated}$ in kWh	$E_{out\ extrapolated}$ in kWh
1	55.39	50.21	37	2049.56	1857.76
2	64.50	55.30	21	1354.56	1161.36
3	44.67	37.77	23	1027.39	868.82
4	50.43	44.84	11	554.68	493.20
5	53.42	43.68	18	961.64	786.29
6	98.50	87.54	14	1379.01	1225.55
7	81.92	70.90	29	2375.59	2056.18

One could also see that the convergence to the values take place for either a 6 day or 7-day sequence as per the criteria as discussed earlier for the KPI's. Similarly, the results for the heat pumps can be seen in Figure 39 and Figure 40 respectively. The same pattern could be observed as it was observed for the condensing boiler use case. The 6–7-day sequence have a good convergence for all the three KPI's.

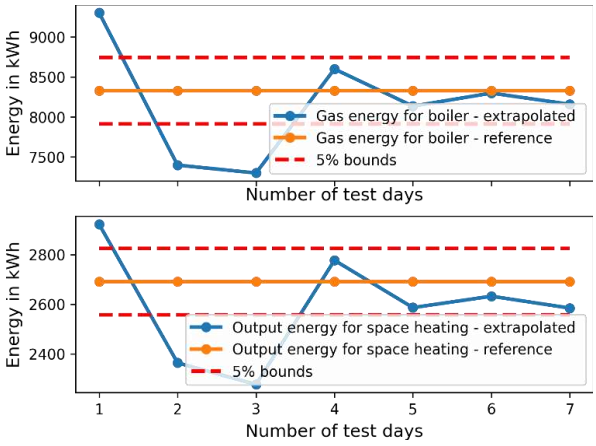

Figure 39: Energy levels for the short sequence vs the annual reference values

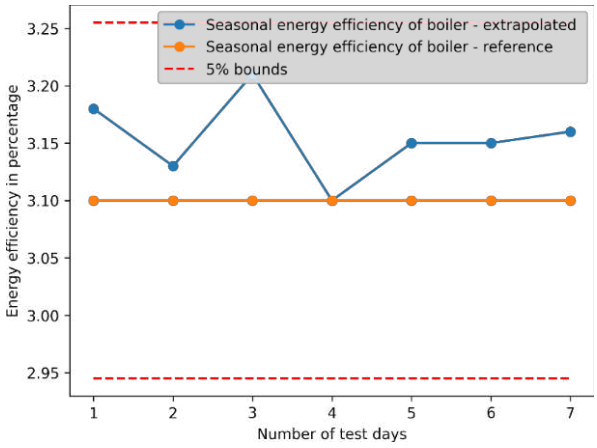

Figure 40: SCOP of short sequence vs. the annual reference values

Similarly, the SCOP for the heat pump for the heating season is always under the 5% error bound from the annual reference value. The convergence for all the three KPI's are shown in Figure 41. From the simulation studies it could be seen that the short sequence could be achieved based on the clustering technique with good convergence. Since the days chosen to represent the entire year is from different parts of the year this poses a discontinuity between the days.

These discontinuities then introduce two problems: the thermal energy shift in the building and in the thermal storages. These problems are a bit complicated to handle during the real time simulations since constant decoupling of models are required as explained in [59].

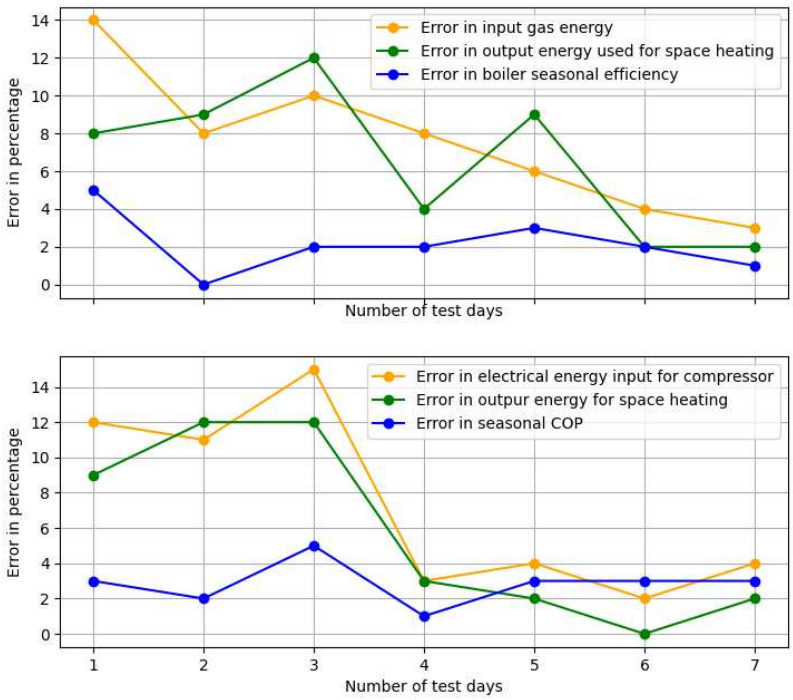

Figure 41: Convergence for the heat pump and boiler use case

These not only increases the testing time as the number of test days increases but also require an elevated level of monitoring of the closed loop simulations. The next point one could also ask is why number of days and why not reduce the test hours to a matter of few hours. Hence, the idea is to generate a fictitious temperature and irradiation profiles that are continuous and are hour wise.

This fictitious sequence is generated using an optimization algorithm. The generated weather profiles are then verified by simulation experiments and then compared with the annual reference simulations values to validate the short sequence. This will be the covered in the entirety of the Chapter 3.

2.3 State-of-the art on uncertainty analysis related to HIL Simulation

From the state-of-the-art review of the HIL simulation one can say that there are two parts associated to the HIL simulation, one being the real part where the emulator and the system to be tested are present and the other part being the virtual part that comprises the scenario / building envelope.

Based on the research work done on the uncertainty related particularly to HIL simulation, there are two parts where the uncertainty analysis can be in a HIL simulation [82]. There are two key areas, they are:

- Simulation Modeling Uncertainty (SUM) because of the numerical part of the HIL simulation.
- Simulation Running Uncertainty (SRU) because of the experimental environment and design.

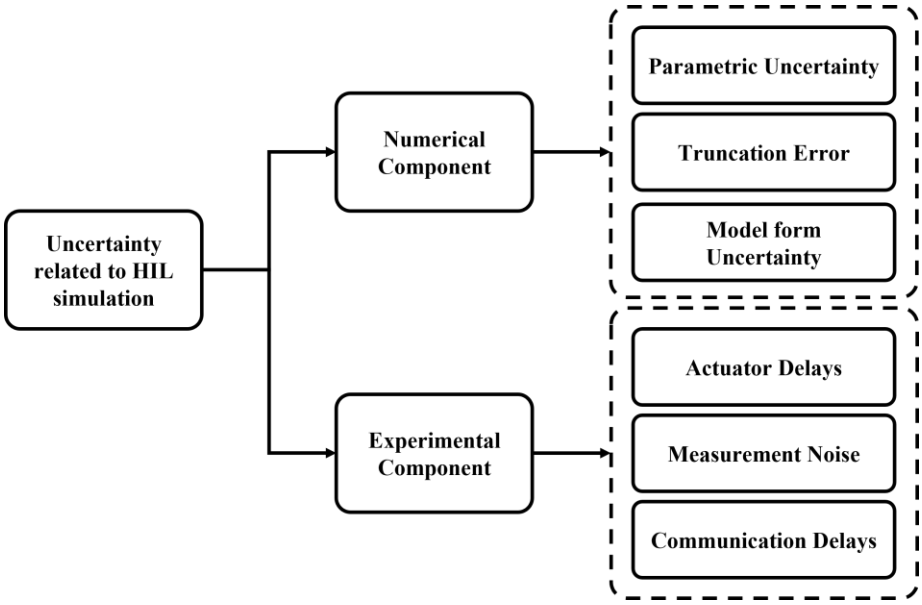

Figure 42: Uncertainty in HIL simulation

2.3.1 Simulation Modeling Uncertainty (SUM)

The process of Simulation Modeling Uncertainty terms of a general context involves the following parts. As shown in Figure 43, they include the numerical part of the HIL simulation.

- Step 1: Models of the system, which comprises a computational model where one has to develop the model, either numerical or metadata-based model on which computation has to be performed.
- Step 2: Quantification of sources of uncertainty and Parametric Evidence.
- Step 3: Uncertainty propagation.
- Step 4: Iteration based improvement.

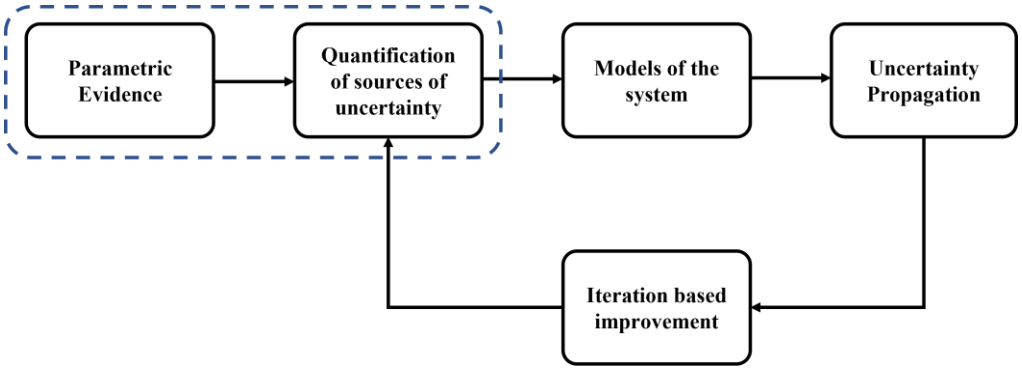

Figure 43: Process of Uncertainty Analysis

Figure 43 explains the steps involved in uncertainty quantification, the above said steps correspond only to the uncertainty related to the numerical system. In building energy simulations, the methods to

propagate uncertainty are both probabilistic and non-probabilistic. The forward uncertainty propagation (shown in Figure 44) it is quite acceptable to do a probabilistic uncertainty propagation. The first step is to develop a model. The model can be based on first principles, or it can be based on multi-physics tool like Modelica. The second step is to identify the uncertain parameters and assign a method to represent them based on the literature (a probability density function).

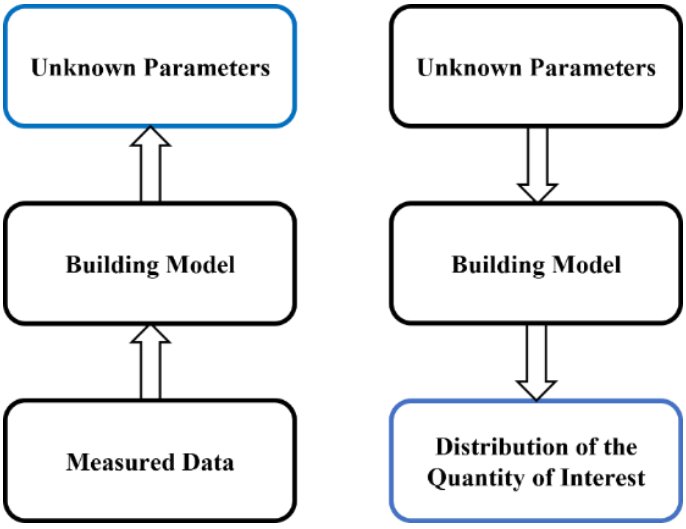

Figure 44: Inverse and forward uncertainty propagation

The most probable choice of probability density function for uncertain parameters is normal distribution [83] and [84]. Gaussian distributions need truncation where necessary to avoid unfeasible values (for instance, a negative value or zero for thermal resistance). Uniform distribution is commonly used in presenting the change of various building design strategies [85] and [86].

In case of large number or uncertain parameters, it is very essential to do a sensitivity analysis to identify the list of influential parameters, [87] shows a case where sensitivity analysis is performed to identify the 10 most influential parameters out of 139 parameters regarding their effect on the air temperature.

The third step is to run the simulation based on the different samples allocated. Monte Carlo method is the most used method, other variations of Monte Carlo Simulation include 2D–Monte Carlo Simulations, and then Surrogate Model based Monte Carlo Method are the most common techniques.

In [88], the outer loop has 30 realizations using the random Monte Carlo Simulation, and the inner loop generates 80 realization per outer loop sample using the Latin Hypercube Sampling method (an example demonstration of 2D Monte Carlo Simulation). Hence, 2400 building energy models simulated for future climatic scenarios being one of the use cases explained.

One can categorize surrogate models into two types: Data fit models and Reduced Order Models. The data fit models are based on regression methods to derive the relationships between inputs and outputs from a set of simulation results from high–fidelity models.

The linear regression methods are the most commonly used methods to construct surrogate model to capture building energy behavior [89] and [90]. To capture non–linear behavior related to building energy simulations MARS models are constructed as with [85] to emulate daylighting simulation models and airflow network models for passively designed domestic building.

In [91] the author summarizes five different data fit models, and compared the performance of these methods applied to a specific case. Then, we have the Reduced Order Model (ROM), in short, ROM is generated by using higher dimensional states and parameters onto the reduced dimensional subspaces. Some of the commonly used model order reduction methods as per literature are, eigen functions, snapshot-based methods, all of which are used to construct reduced base functions. Detailed mathematical descriptions of the methods can be found in [92].

The part of the uncertainty in the numerical component is due to the uncertain parameters. The sources of uncertainty in the simulation modelling uncertainty are shown in Figure 45. The main conclusion is that to evaluate the uncertainty in the simulation model under study one must develop the numerical model of the system under consideration. The next step would be to identify the parameters that are uncertain and represent them suitably based on the nature of the uncertainty. The final step would be to propagate the uncertainties using a suitable uncertainty propagation methodology.

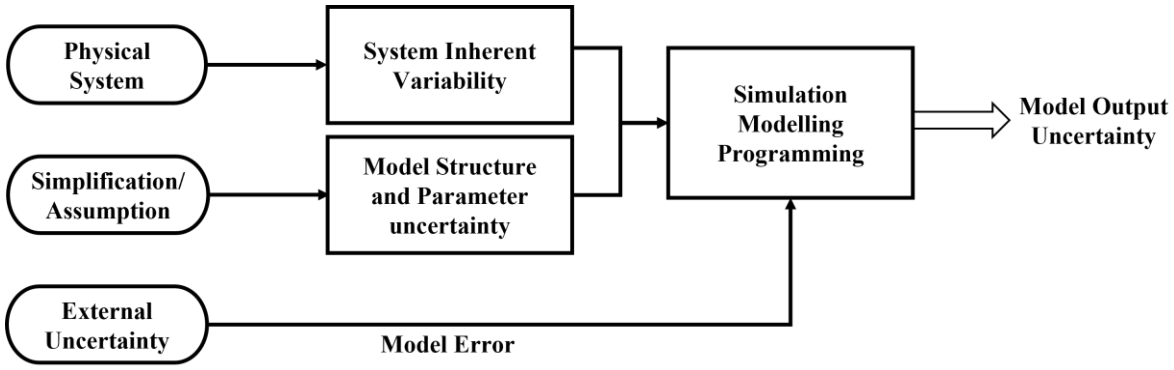

Figure 45: Simulation Modelling Uncertainty [82]

2.3.2 Simulation Running Uncertainty

The last step is to consider the experimental uncertainty related to the HIL simulation environment itself. The common sources of uncertainties related to the HIL simulation environment are, namely the actuator delays and noise in sensor measurements. Some of the errors mentioned here are

strongly affected by the closed loop nature of hybrid simulation and might be amplified and dependent on each other. Furthermore, communication delays may result in additional errors.

In [93], the author demonstrates the use of Polynomial Chaos Expansion (PCE) in treating actuator delays. First a PCE is modeled without actuator delay to determine the order of the PCE, and the next step would be to calculate the coefficients and the number of samples. Some other errors like truncation error in the numerical component can be neglected because they do not form a major part.

In [82] the author explains that the uncertainty due to the simulation running is due to the following factors, they includes the simulation environment as mentioned in [93] and also due to the experimental design. The uncertainty in the simulation environment is due to the combined comprehensive effect of all the three factors which includes the uncertainty due to the simulation model, the uncertainty due to the emulating devices and finally the uncertainty due to the DUT (Device Under Test).

In short it is to say that there is uncertainty due to input uncertainty, the internal uncertainty, and the output uncertainty. By following the process shown in the Figure 43 one can make the model of the entire system and thereby evaluate the uncertainty by using suitable quantification and propagation methods as proposed in [82].

The other rationale is that there could be uncertainty due to the process adopted for a particular HIL testing methodology or due to the design of the experiment of the HIL simulation. This is further explained because the experimental designs could not cover all the scenarios. Moreover, the author in [82] states that such type of uncertainties due to the environment is valid or considered for a quantification process depending upon the area of application such as the aircraft based application where the testing environment is crucial.

The main hypothesis of the current work is to consider the uncertainty due to the parameters of the test bench since it is the prime requirement of ENGIE as a first step. Meaning the uncertainty due to simulation model and the simulation environment is not considered but the uncertainty due to the test bench parameters are alone considered as a first step. Then as a second step is to consider the uncertainty due to the methodology for evaluating the seasonal efficiency using the fictitious sequence.

2.4 Uncertainty analysis due to the test bench parameters

2.4.1 Hypothesis

The hypothesis for this work is only to consider the parametric uncertainties related to the test bench. The model of the HIL test setup is developed in Modelica.

The first step is to develop the computational model through which one must propagate the uncertainties. The second step is to identify the sources of uncertainty and then represent the uncertainties using either probabilistic or non-probabilistic methods based on the type of uncertainty considered [94], [92].

The third step is uncertainty propagation. The uncertainty propagation can be forward or inverse propagation, as shown in Figure 46. Forward uncertainty analysis (also called uncertainty propagation) focuses on quantifying the uncertainty in the system outputs propagated from uncertain input variables through mathematical models, while the purpose of inverse uncertainty analysis (also called model calibration) determines unknown variables through mathematical models from measurement data.

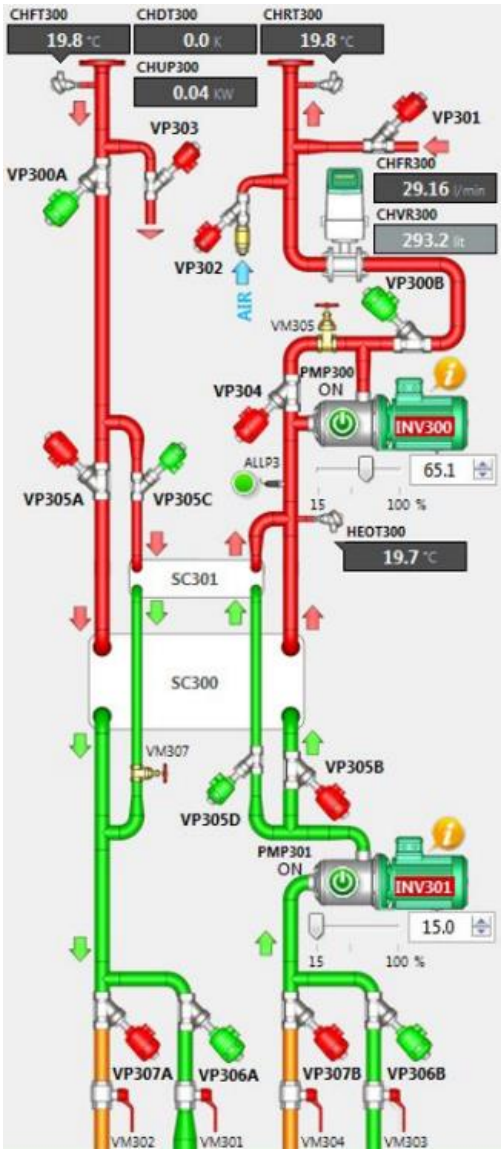

Figure 46: Test-bench layout of the chosen hydraulic loop

The last step is to perform a sensitivity analysis to find out the most important parameters that affect the Quantity of Interest (QoI). The uncertain parameters of the test bench model are represented using the Probability Distribution Functions (PDF) [95]. There are a lot of other methods to represent the uncertainties a detailed explanation is given in [95].

The choice of PDF is explained in detail in [95] the normal distribution is used to represent the uncertainties, the rationale being that most of the natural processes can be represented using a normal distribution. If in case one has to go through the added rigors of defining the parameters for the normal distribution, one can opt for the uniform distribution to represent the uncertainties as explained in [96].

In this body of work, actuator delay is also considered, verifying the effect of such delays on the QoI through simulations. For simplicity, the actuator delay is considered being uniform, although in real-time the actuator delay could be a variable and not be uniform. Then one also must address the experimental uncertainties. For propagating the uncertainties, Monte Carlo Simulation is considered (a propagation method based on random sampling).

2.4.2 Modeling

The modeling of the HIL setup is done in Modelica. The model of a building is a single zone building with a habitable area of 70m2. The total window area of the building is 24m2. The weather profile chosen for the simulation is for Trappes, France with a resolution of 1 hour. The ventilation for the building is $50m^3/h$ for two people. The heater inside the building can deliver thermal power up to 10kW. The boiler models are already available in the building's library in Modelica [74]. The boiler can deliver power up to 24kW for space heating.

The manufacturer curves of the boiler are used to obtain the relationship between the efficiency and the part-load capacity of the boiler. Then equation between the part-load capacity vs efficiency is used in the already existing model of the boiler (the equation of the efficiency vs the part load ratio is replaced in the existing model) that is already given by the building library model in Modelica.

The layout of the test bench is shown in Figure 46.The accuracy of the model is designed with all the possible known details. The parameters for the equipment and devices in the test bench are developed using the data sheets. The inner diameter and the lengths of the pipes are measured and the data about the bends are taken from the piping and instrumentation layouts of the test bench.

There are two heat exchangers (SC301, SC300 - choice of heat exchanger based on power delivered) that are used to emulate the power simulated by the building in real-time. There are two pumps one on the primary side (INV300 -the loop in red where the boiler is connected), one on the secondary side (IN3401 - the loop in green where cold water is supplied).

The pump on the primary side is used to control the mass flow (CHFR300) delivered by the controller from the building envelope. The pump on the secondary side is used to control the return temperature (CHRT300) to the boiler which varies according to the heating needs of the building.

The same is modeled in Modelica, the manufacturer sheets for the pumps are used to model the electrical and hydraulic characteristics of the pump [97]. The pipe lengths and diameters were measured manually to incorporate them into the Modelica model.

The cold-water supply is replaced by a boundary condition in the Modelica model to reduce complexity. The cold water to the test bench varies from 6°C to 14°C the same is incorporated in the Modelica model. For the actuator delay, a first-order delay is used to replicate the one in real-time to the model.

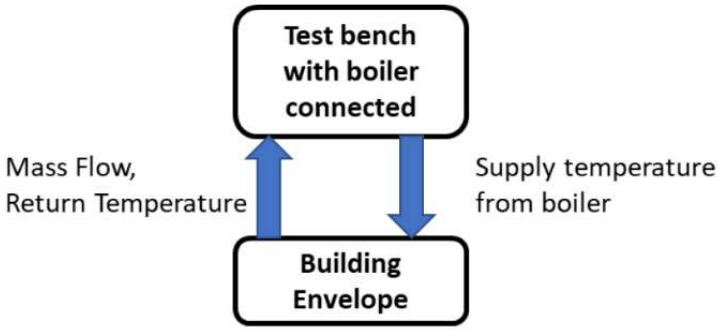

Figure 47: Schema of the model simulation

The schema of the HIL scenario in the Modelica model is shown in Figure 47. The controller in the building envelope controls the flow of hot water to the room heater. This mass flow rate is used as a setpoint to the primary pump controller.

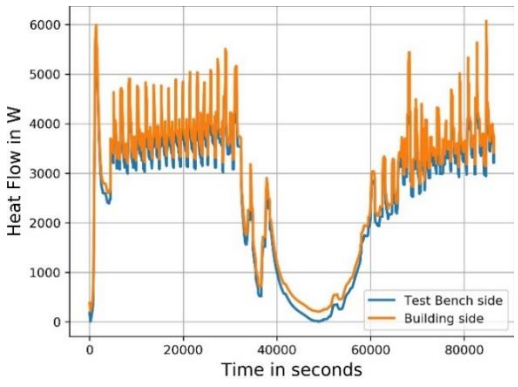

Figure 48: Heat exchanged in the test bench vs building before control parameter adjustment – a sample

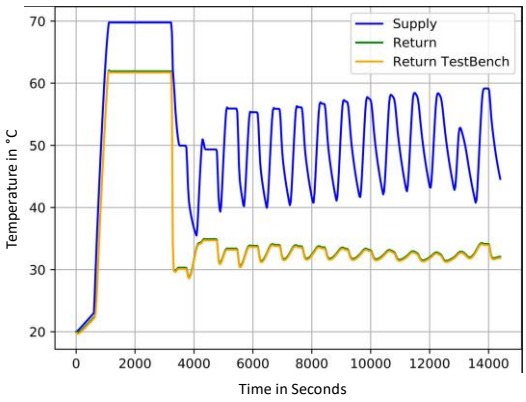

Figure 49: Return temperature test bench vs building

The return temperature from the building is given as the setpoint for the secondary pump controller. To verify the validity of the model, the supply, and the return temperature profiles in both the

test bench and from the building are verified as shown in Figure 49. Plus, the heat flow in the test bench and the heat required in the building are compared as shown in Figure 48.

There is a minor variation of 200W on average between both curves. The oscillations in both curves are because of the model of the boiler where the cycling time approximately 12 minutes as shown in Figure 50. The return temperature from the building and the test bench is almost the same both have a difference of about 0.2°C as shown in. This explains the fact that there is a minor variation in the heat flow between both cases. This variation in the heat flow was adjusted by setting the proper controller gains in the test bench controllers. The Mean Squared Average error is also around 200W. This is rectified after adjusting the controller gains on the test bench side so that both the curves are the same. Then the next step is to identify the sources that are uncertain, represent them, and perform uncertainty propagation.

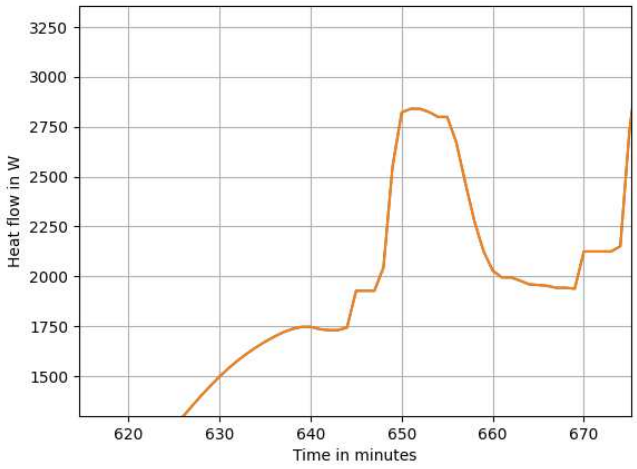

Figure 50: Cycling time of the boiler

2.4.3 Uncertainty propagation due to the test bench parameters

For the uncertainty analysis, it is important to consider the following hypothesis. For the actuator delay, a uniform delay is considered (although in the experimental phase it could be variable, the simulation is just to study the effect of the actuator delay on the efficiency). The uncertain parameters are represented using the probability distributions for the propagation of the forward uncertainty propagation Monte-Carlo analysis is adopted [96]. The choice of uncertainty distribution for the unknown parameters can be either normal distribution or uniform distribution [96], in the case considered, uniform distribution is used.

In the model of the heat exchanger that the Modelica library offers, it is necessary to specify the nominal heat exchange coefficient so that the Dymola compiler can do the simulations [97]. The uncertain

parameters are shown in Table 10. There are around twenty bends and 20 pipe diameter parameters altogether there is around 62 parameter which is assumed to be uncertain.

Table 10:Uncertain parameters and ranges

Uncertain Parameters	Distribution Range
Bend diameter (two sizes)	[39mm-41mm], [33mm-36mm]
Pipe diameters (two sizes)	[39mm-41mm], [33mm-36mm]
Heat exchanger nominal efficiency	0.85-1.0
Actuator Delay	0-1.0 minute
Radius of Curvature of bend (two sizes)	[46mm-50mm], [36mm -40mm]

The design library in Modelica allows one to perform the Monte Carlo simulations. The basis of a Monte Carlo simulation is that the probability of varying outcomes cannot be determined because of random variable interference. Therefore, a Monte Carlo simulation focuses on constantly repeating random samples to achieve certain results.

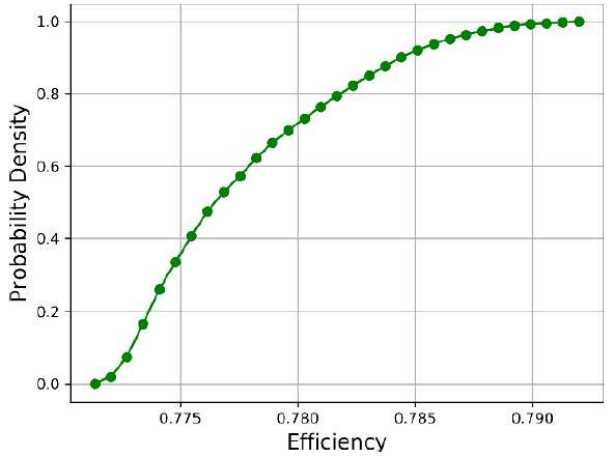

Figure 51: Cumulative Distribution for 10000 samples

A detailed explanation of the Monte-Carlo method is explained [98]. Monte Carlo-based simulation is the most widely used uncertainty propagation method in the area of building energy assessment [96]. This is because this method is very intuitive and easy to implement compared to other uncertainty propagation approaches.

Moreover, the sampling-based method is usually regarded as the most reliable uncertainty technique since it can be applied to most simulation environments and deal with different types of probability functions of input variables, even for correlated variables [96].

The main disadvantage of this method is the slow convergence rate with numerous function evaluations, which incurs a high computational cost. The number of samples chosen N = 10000. With such a detailed model the computation complexity increases both on a computation and temporal basis. The cumulative distribution function after 10000 simulations is shown in Figure 51. The mean value for the efficiency is 0.777 and the standard deviation is around 0.0047.

From the result, the physical test bench parameters do not have a big effect on the efficiency that is being measured. It is also observable that almost 80 percent of the time the efficiency is less than or equal to 78 percent. In Table 11 it is observed that over the different number of samples there is not much variation in the variance, clarifying that the test bench parameters do not have a huge effect on the efficiency measured.

Table 11: Monte Carlo simulation for different samples

Number of Samples	Mean Efficiency	Standard Deviation
100	0.7798	0.00440
500	0.7785	0.00450
1000	0.7780	0.00452
5000	0.7781	0.00462
10000	0.7770	0.00470

2.5 Conclusion

From the sample use case demonstration, one could see that the clustering methods delivers good result, but the idea is to check if the number of testing days can be reduced and avoid the discontinuity problems. Hence, the idea is to generate a new fictitious sequence based on the statistical and the frequency domain data of the weather data and check if one could achieve the results based on the KPI's of choice within 5 percent error range explained in Chapter 3. The fictitious sequence for the testing proposes to solve the soft identifiability issue for the seasonal efficiency. Represent the dynamic non-linearities in the weather profiles. Finally, the new sequence generation method also proposes to ensure that the convergence on the KPIs is guaranteed. It could be seen that the test bench parameters do not pose any uncertainty on the efficiency evaluated. Hence, the idea will be to verify the uncertainty due to methodology of evaluating the efficiency explained in Chapter 6.

3. Philosophy of fictitious sequence generation

The idea of this chapter is to give the underlying philosophy about the fictitious sequence generation methodology based on a few hypotheses. The idea will be to explore the nature of the problem leading to the identification of the optimization method to be used for the fictious sequence generation among the existing methods. Also, one thing to be seen is that instead of choosing existing days the idea is to generate correlated sequences for the individual weather variables which differs from the already existing state of the art method.

3.1 The nature of problem to be solved

Before going into the actual method of generating the short sequences using the fictitious sequence generation method once again has to investigate the problem statements and the nature of the problem to be solved. The idea is to generate a short sequence that will satisfy the multiple criteria that are considered which includes the reproduction of the seasonal efficiency and the energy levels well within the 5% error range. Generally the tests in ENGIE are designated to be replicated with a 5% error range.

The main problem areas to be addressed are the soft identifiability issue associated with the efficiency parameter. The efficiency parameter could be treated as an identifiability issue because as explained in [99] " Practical identifiability not only depends on the model structure but is also related to the experimental conditions together with the quality and quantity of the measurements".

One way to address the soft identifiability issue would be to run the experiments with different initial values and then finally observe if the convergence is suspicious with the data sets that are obtained as explained in [99]. Also, based on simulations done in the previous chapter one can observe if the short sequence can be able to consistently reproduce the same efficiency values or within the desired error ranges.

The most important problem area that one needs to address is the non-linearities associated with the process, for example, there could be static and dynamic non-linearities. The static non-linearities could be the maximum and the minimum values associated with the temperature or the irradiation profile for example. For example, if one wants to obtain seasonal efficiency and test the product for its operation under extreme conditions as well then one must find the suitable characteristic of the signal that will allow one to do so. The dynamic non-linearities could be due to the transient behavior of the system under test or due to the variations in the weather profiles that are not represented in the short sequence.

The other non-linearities associated could be due to the random behavior which causes reproducibility issues. The reproducibility issue could be also addressed by repeating the experiments for

a different number of sets as possible as explained in [99]. The most important out of all the problems stated here is the convergence of the parameters that are considered, in this case, the energy levels and the seasonal efficiency. This brings one back to the global problem, where the idea is to evaluate the seasonal energy efficiency and the energy levels where one must make sure that the convergence on the parameters considered is made possible while addressing the non-linearities and the identifiability associated with the methodology.

The idea is to define an optimization problem that will ensure that the convergence of the KPIs is addressed along with the representation of the non-linearities as well. In short in the process of evaluating the seasonal efficiency, one must address the static, dynamic non-linearities, and ensure reproducibility and convergence of the multiple criteria under consideration. This leads one to the next section where one needs to specify the optimization problem.

The problem under consideration is non-linear. The reason is that one needs to define an objective function that will successfully reproduce the criteria when a DYMOLA simulation is performed. It is self-explanatory in one way that the result one expects out of the short sequences cannot be represented by linear relationships for both the objective functions and the constraints [100], [101]. The objective function will be used to generate the short sequences for the temperature and irradiation short sequences, by using the hourly minimum and maximum values in the heating season correspondingly.

The number of variables to be optimized is very high, since one must generate the temperature or irradiation in short sequences based on the hourly values, making it a mono-objective problem, to begin with. The temperature and the irradiation short sequences are generated separately hence, one needs to add a non-linear constraint that describes the hourly correlation between the temperature and the irradiation profiles. Also, the nature of the optimization problem is convex since the idea is to minimize the value of the objective function between the generated short sequence and the weather profiles of the heating season.

3.2 Introduction to fictitious sequence generation

In the previous chapter, one could see the use case demonstration of the K-Means clustering methodology was able to produce satisfactory results for a 6-days use case and a 7-days use case based on simulations. The idea is to check if one can eliminate the discontinuities between each testing day by adopting a new sequence generation methodology and reducing the number of test days. The idea is to use the characteristic of a signal in the statistical-time or frequency domain (the distribution of the signal in the statistical domain and the FFT/PSD in the frequency domain) and generate a sequence of the optimized weather variables namely the outside air temperature and the global horizontal irradiation. In

DYMOLA the two main weather variables required for running a simulation include the external temperature and the solar irradiation. The newly experimented methodology is elucidated in Figure 52.

In short before going into the details of generating the short sequence it is imperative to define what the short sequence should do, based on the problem definition from Chapter 1: the idea is to generate an optimized short sequence that will satisfy the chosen criteria namely to produce results that are within the 5% error deviation in the annual energy levels and the seasonal energy efficiency ratio. The philosophy of the newly developed method is explained based on the following rationales, the literature shows one can use a statistical optimization method like the clustering algorithm [66]. The author chooses to explain the clustering algorithm as a statistical algorithm based on the literature from [73]. The literature also shows one can use an iterative method for finding a short testing sequence [66].

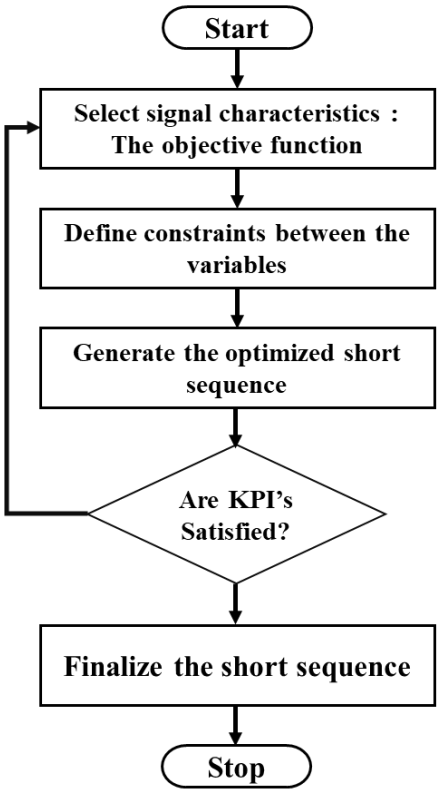

Figure 52: Process flow of the newly developed methodology

Finally, also based on the literature studies from Chapter 1 the HIL methodology is a widely used method to evaluate and experiment using the black box philosophy [20]. The general steps involved in the optimization philosophy are as follows:

- Fixing the optimization problem using a suitable optimization algorithm based on the signal characteristics in either the statistical or frequency domain.

- After fixing the optimization problem, the idea will be to choose the constraints and the bounds.
- Finally, use the sequence generated from an optimization method to verify if the methodology yields proper results by simulation.
- If the results are not met, then proceed with the problem definition again to find other characteristics of the signal in its corresponding domains that will yield the expected result.

3.3 Signal Domains and choice of objective functions

In general, there are two main important domains to identify the characteristics of a signal, they are the statistical-time and the frequency domain as explained in [102] and [103]. The steps followed are iterative, hence the idea will be to check if one can find out the characteristics of the signal that will yield the closest possible results within the 5% error.

The first approach is to check from a purely statistical-time domain point of view if the signal generated can yield the closest possible results. In general, the distribution of the signal is the most important representation of the signal in the statistical domain as explained in [104]. This is due to the reason that the distribution itself gives the most information about the first-order statistical moments of the signal.

As explained previously stated the non-linearities due to the extreme values need to be looked upon and the non-linearities due to the variations within the temperature and the irradiation profile in the heating season as well. Hence, from this point onwards one could think of distribution as a statistical domain best representing the static linearities.

While the FFT could be thought of as the representative characteristics in the frequency domain for the dynamic non-linearities. In terms of dynamic non-linearities, one can treat the profiles as random vibration signals with multiple frequencies where one can use the power spectral density. In general power spectral density specifies the power levels of the frequency components present in a signal.

The PSD specifies the power of various frequencies present in the signal and one can determine the range of power over which the signal frequencies are operating at. As explained in [105] generally the outside air temperature is usually made up of normal distribution, while other physical quantities (wind speed and irradiation) take up the Weibull distribution.

The mathematical equations of both the distributions are shown in equations and , both the distributions are represented as shown in Figure 53 and Figure 54. In the equation, μ is the Mean of the data set and σ is the Standard Deviation of the data set also based on the values of the mean and the

standard deviation the higher order statistical moments like the skewness and the kurtosis can also be found.

Where, the mean is represented by the equation $\beta\Gamma\ (1 + \alpha^{-1})$, and the standard deviation is represented by the equation $\beta^2[\Gamma\ (1 + 2\ \alpha^{-1}) - \Gamma^2(1 + \alpha^{-1})]$, α is the shape factor, β is the scaling factor. For irradiation, the β value is usually around 0.5. The Weibull distribution is a family of distributions that can assume the properties of other distributions. For example, depending on the shape parameter you define, the Weibull distribution is used to model the exponential and Rayleigh distributions, among others.

The Weibull distribution is very flexible. When the Weibull shape parameter is equal to 1.0, the Weibull distribution is identical to the exponential distribution. The Weibull location parameter lets one set up an exponential distribution to start at a location other than 0.0. When the shape parameter is less than 1.0, the Weibull distribution becomes a steeply declining curve as explained in [105]. The minimum input requirements are that the scale factor is a value greater than zero and the shape factors at least

$$f(x) = \frac{1}{\sqrt{2\pi\sigma}}\, e^{-\frac{(x-\mu)^2}{2\sigma^2}} \qquad (1)$$

$$f(x) = \frac{\alpha}{\beta}\left[\frac{x}{\beta}\right]^{\alpha-1} e^{-\left(\frac{x}{\beta}\right)^{\alpha}} \qquad (2)$$

greater than or equal to 0.05 [106].

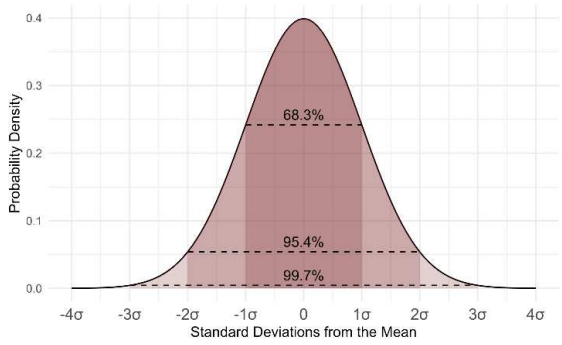

Figure 53: Representation of normal distribution

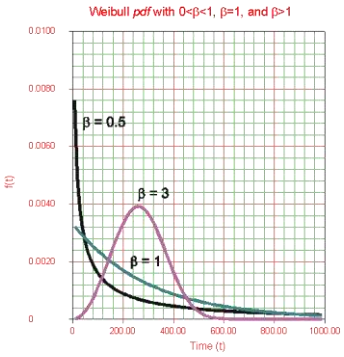

Figure 54: Representation of Weibull distribution

One of the reasoning to choose the mathematical distribution of the temperature and its hourly variation is because 68% of the values are distributed around the mean value. As one moves away from the mean value the values become fewer and fewer representing the extreme values that are represented in the heating season. The important rationale behind measuring seasonal efficiency is to evaluate the equipment under normal operating conditions throughout the year rather than in extreme conditions [103].

In the frequency domain, the most important characteristic to be analyzed is the strength of each frequency component. This can be done in two ways as per the literature one is to perform an FFT analysis (Fast Fourier Transform) and the other method is to perform the Power Spectral Density analysis (PSD) as explained in [107] and [108]. The FFT is an optimized algorithm for the implementation of the "Discrete Fourier Transformation" (DFT).

A signal is sampled over a period and divided into its frequency components. These components are single sinusoidal oscillations at distinct frequencies each with its amplitude and phase. This transformation is illustrated in Figure 55. While the PSD in simple terms is the measure of the signal's power content versus frequency, PSD is derived from the FFT auto-spectrum. As explained in [109] the FFT computes the discrete Fourier transform (DFT) using a reduced number of arithmetic operations as compared to brute-force evaluation of the DFT.

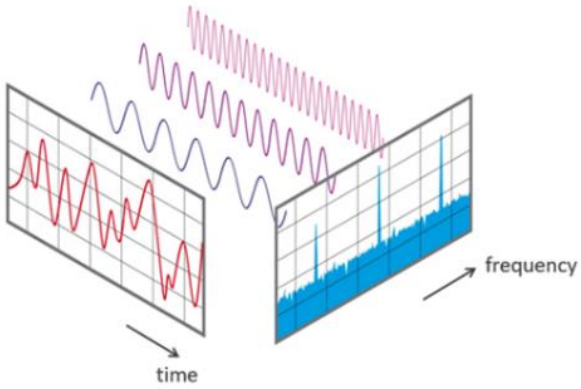

Figure 55: Signal variations over time and the frequency domain

The method is efficient because it eliminates redundancies that result from adding certain data sequence values after they have been multiplied by the same factors of fixed complex constants during the evaluation of different DFT transform coefficients. The DFT is represented using the equation for a discrete and periodic as shown in equation (3).

$$X_k = \sum_{n=1}^{N-1} e^{-i\frac{2\pi}{N}kn}\, x_n = \sum_{n=1}^{N-1} W_N^{kn}\, x_n \qquad (3)$$

$$X_k = \sum_{n=1}^{N-1} e^{-i\frac{2\pi}{N}kn}\, x_n = \sum_{n=1}^{N-1} W_N^{kn}\, x_n \text{ Where}$$

$$X_{PSD}(f) = \lim_{\Delta f \to 0} \left[\frac{1}{2} \frac{X(f)\, X^*(f)}{\Delta f} \right] \quad (4)$$

This one-half factor is needed to convert the amplitude from the square of the peak value per Hz to the square value of RMS per Hz which highlights another benefit of PSDs, calculating this cumulative RMS is also a helpful way of seeing which frequency components are contributing most of the amplitude. Or in other words, PSD gives the strength of variations as a function of frequency. The frequency step is finite in practice and is the inverse of the total measured duration.

$$\Delta f = \frac{1}{T}$$

This frequency step is the smallest sine wave frequency that can be resolved. A wider Δf gives greater PSD confidence in terms of smoothing the spectral components. Also, it would be important to check if the short sequences generated using the frequency domain characteristics could not have the same frequency spectrum but converge towards a good value of energy efficiency and energy levels.

3.4 Choice of bounds and constraints

The idea of the methodology is to generate a fictitious sequence that will lead to a good estimate of the parameters or KPIs under consideration, namely the energy efficiency and their energy levels. The generation of the fictitious sequences will be based on the hourly maximum and minimum values within whose bounds the weather variables need to be generated. The hour-wise maximum and minimum temperature values are shown in Figure 56 and Figure 57 for the corresponding heating season comprising 153 days. For example, for the first hour, one can see that the minimum temperature value is around -2.3°C and the maximum value of temperature is around 14.1°C, hence the bounds for the first hour is from -2.3°C-14.1°C.

In general, the temperature range for the heating season temperature range is about -3.5°C to 21°C. Similar bounds are then found for the Global Horizontal Irradiation (GHI). In general, the minimum value of irradiation is 0 Wh/m^2 for the first 7 hours and the last 4 hours of the day. The maximum change in hourly temperature is 4°C while the mean value is around 0.2°C. Also, the minimum possible value for the hourly temperature value is -4°C.

The important constraint to be considered is the hourly variation in the temperature for the heating season while generating the temperature sequence. For considering the temperature variation one of the methods would be to choose the distribution of the hourly temperature variation for the whole heating season.

The first step would be to generate using the temperature signal with the constraints namely to generate the temperature sequence such that the hourly temperature distribution is also as close to the hourly temperature distribution of the original signal. The next step is to identify the correlation between the GHI and the external temperature. Then using the correlation between the temperature and the GHI, the GHI sequence is generated using the optimization algorithm. Because the rationale stems from the fact that there is always a correlation between the weather profiles. At the end of the simulation analysis, it could be interesting to verify if the same results could be reproduced without the correlation constraints.

The hourly correlation between the GHI and the outside air temperature is shown in Figure 58. The next step is to identify which optimization algorithm to use initially for the generation of the short sequence. In short for the fictitious sequence generation method based on the distribution, the objective function will be to produce a short sequence whose distribution is like the heating season.

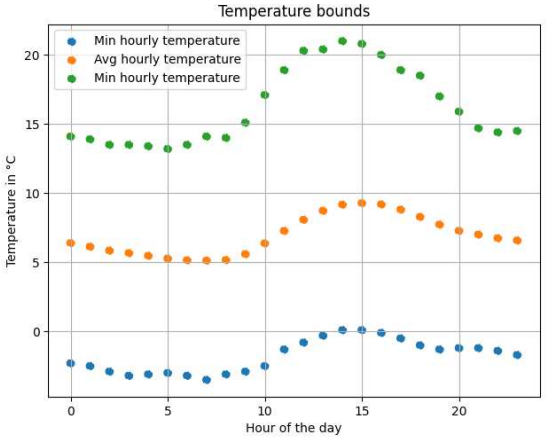

Figure 56: Hourly bounds for the temperature

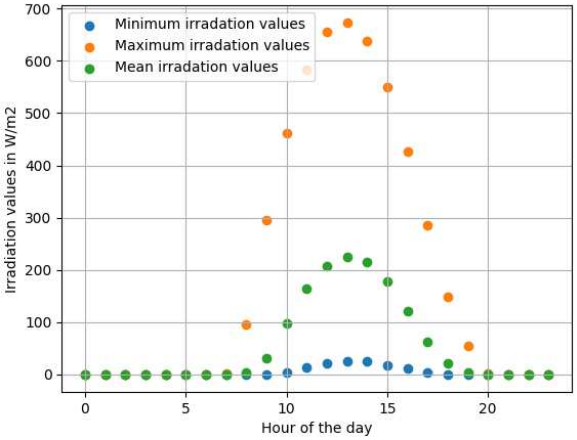

Figure 57: Hourly bounds for the global irradiation

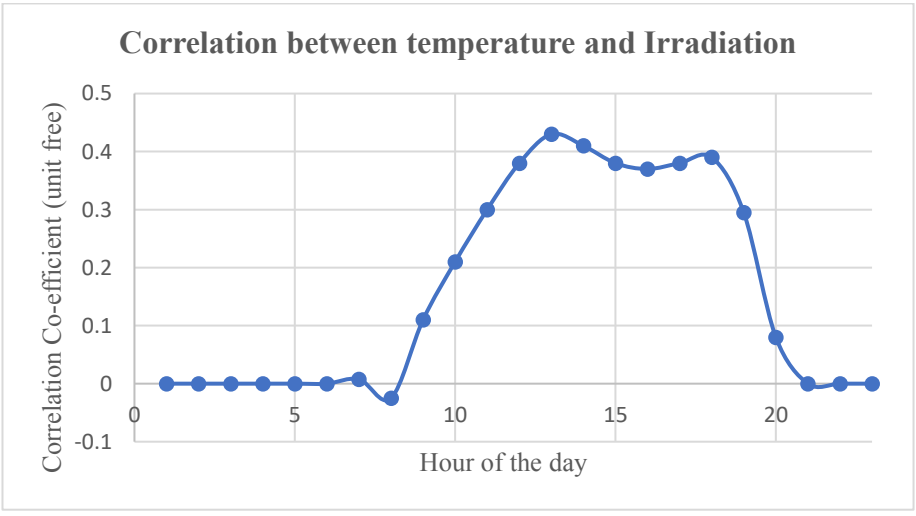

Figure 58: Hourly correlation between outside air temperature and the global horizontal irradiation

The constraints are the hourly temperature variations and the hourly correlation between the temperature and the irradiation profile. For the frequency domain-based, the objective function will be to reproduce the FFT / PSD of the heating season with only one constraint the hourly correlation between the temperature and the irradiation profile. Since the idea is that the FFT / PSD will take care of the hourly variations of the temperature profile.

3.5 Choice of the optimization algorithm

3.5.1 Existing optimization methods

In [110] the author explains the existing optimization methods. The two broad classifications of optimization methods being the combinatorial optimization and continuous optimization methods. Continuous optimization means finding the minimum or maximum value of a function of one or many real variables, subject to constraints as explained in [111]. The constraints usually take the form of equations or inequalities. While Combinatorial optimization is the process of searching for maxima (or minima) of an objective function F whose domain is a discrete but large configuration space (as opposed to an N-dimensional continuous space) as explained in [112].

Based on the constraint, one can observe that the correlation is not strictly linear as shown in Figure 58, since it varies for each hour concerning the temperature. Hence, the idea will be to choose a continuous, non-linear optimization. Under the non-linear optimization method, one must see if the problem requires a global search method vs the local search method.

The local search method searches for the local minimum of a function which is a point where the function value is smaller than at nearby points but possibly greater than at a distant point as an example. While the global search method searches for the global minimum which is a point where the function value is smaller than at all other feasible points.

The complete taxonomy of the optimization methods is shown in , the idea is to generate a short sequence that will reproduce the same results consistently, hence a global-meta-heuristic optimization approach is preferred. Based on the problem statement in 3.1, one can see that the problem requires a non-linear optimization, with constraints between both the temperature and the irradiation profile. Also, from the nature of the problem, one can see that there is no linear relationship that can be established between the seasonal efficiency values and the variables that cause it, rather one could observe the correlation between the seasonal efficiency and the variables causing it. Hence, for generating the short sequences one has opted for the Meta-heuristic algorithms namely the single solution-based search and the population-based search algorithms.

Based on [113] optimization algorithms are defined as the procedure of discovery that provides the minimum or maximum value of a function. Among the available algorithms, Differential Evolution (DE) is a stochastic algorithm for solving numerical continuous optimization problems. Since its inception, the DE algorithm has become a powerful global optimizer. The reason why a global optimizer is needed is that in the case of the short sequence generation the idea is about reducing the time is mainly on the real-time experiments and not on the generation of the short sequence. In short, the computing time is not critical for the generation of the short sequence and the emphasis is given to finding the truly global solution that is of concern as explained in the problem statement.

Developed by Kenneth Price in 1994, DE is a promising optimization algorithm that could help one to achieve results close to convergence without using significant amounts of resources. Furthermore, its performance was validated in the evolutionary domain by the IEEE Conference on Evolutionary Computation (CEC) in 1996 [114]. In a unique application related to the electrical networks as explained in [115], the author compares the performance of the Genetic Algorithm (GA), Particle Swarm Optimization (PSO), and Differential Evolution (DE) algorithm.

The idea in [115] is to mitigate unbalance and reduce the total power loss by optimizing load distribution among phases. Finally, the efficiency of these algorithms is evaluated for the proposed unbalance mitigation technique, and it is found that the proposed technique using the DE algorithm can reduce a significant amount of unbalance at all the buses of the distribution grid with less computational effort. Also in [117], the author explains why the DE algorithm is the most simple yet effective algorithm to find the global minimum and why it is promising to use it mainly for engineering problems.

In short, the author in [117] has compared the performance of the DE algorithm to that of some other well-known versions of genetic algorithms: PGA (Principal Geodesic Analysis), Grefensstette, and Eshelman. In simulation studies, De Jong's test functions have been used to compare the performance of all the algorithms. From the simulation results, it was observed that the convergence speed of DE is significantly better than genetic algorithms. Therefore, the DE algorithm seems to be a promising approach for engineering optimization problems.

3.5.2 Differential evolution algorithm

Based on the domain analysis and the choice of the bounds one can say that the stopping criterion in the statistical domain could be the degree of closeness between the probability distribution of the annual sequence and the short sequence obtained from the best vector returned by the DE optimization method. While for the frequency domain it is the FFT/ PSD that must be matched with the original signal.

Moreover in [115], the authors conclude that the DE algorithm shows greater homogeneity around the mean compared to GA and PSO. PSO also shows more effective performance than GA. However, DE is more robust and consistent than GA and PSO. The DE algorithm not only improves power quality but also requires less computational speed.

Also, as explained in [118] DE has exhibited very good performance in a variety of optimization problems from various scientific fields. It belongs to stochastic population-based evolutionary methods and like other evolutionary algorithms, it uses a population of candidate solutions, and the search is done in a stochastic way by applying mutation, crossover, and selection operators to drive the population toward better solutions in the design space.

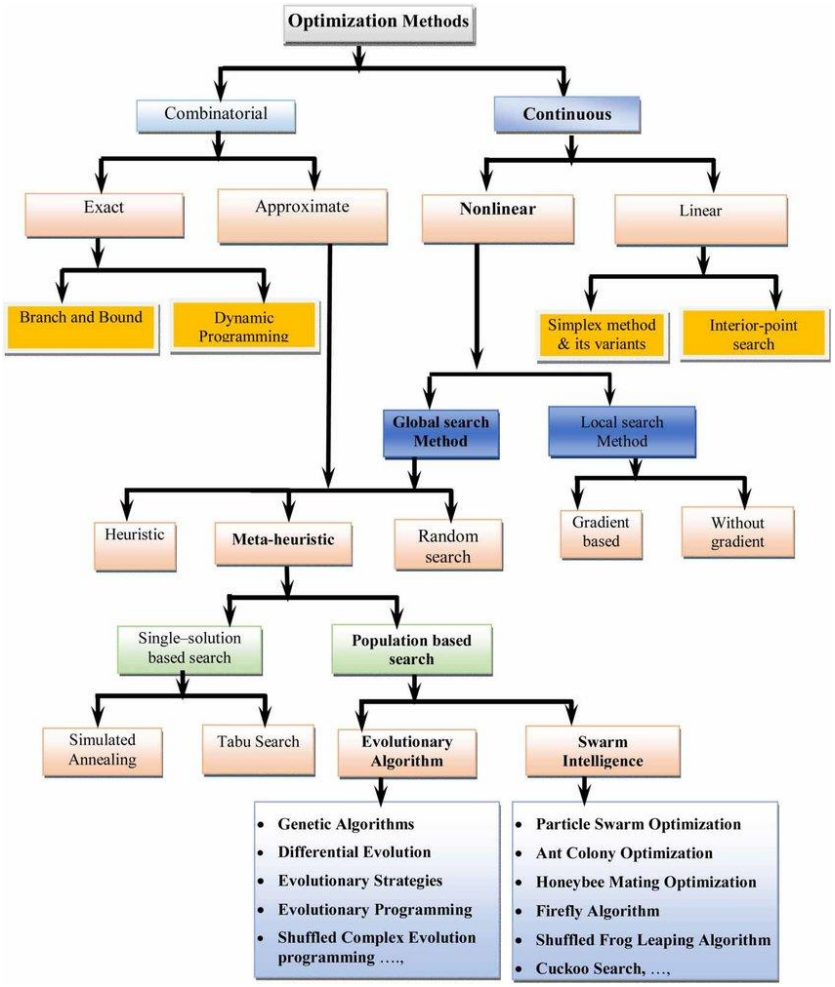

Figure 59: Taxonomy of optimization methods [116]

Also, there are only three important control parameters that need adjustment namely the population size NP, the mutation factor F, and the crossover probability CR. The flow involved in the differential evolution algorithm is shown in Figure 62.

If one is seeking the optimum for X^* which is demonstrated by the vector X_i^*, i = 1,..D, $X \in \mathbb{R}^D$ where D is the dimension, within the boundary constraints $L \leq X \leq H$. Initialization of the population is a crucial step that assumes that there is no previous information about the optimum solution. The initial population is represented by $P_{i,j} \in \mathbb{R}^{[D \text{ X } NP]}$ and the initialization starts within the lower L and the upper H boundaries for the available population.

The population can be initialized by:

$$P_{i,j} = L + (H - L).\, rand_{i,j}[0,1], \qquad i = 1,2, \ldots . , D \; ; j = 1,2, \ldots . , N_p$$

After the initialization, the next steps are mutation, cross-over, and selection. The most classical approach consists of selecting three random vectors v_1,v_2, and v_3 that are selected from the population. Also in [119], it is explained that many mutation strategies can be used to perform the differential evolution algorithm. The mutation strategy that is best recommended is the DE/best/1/bin as mentioned in [120], the reason stated being that the "objective function values to generate trial individuals, can produce an exploitation function". DE stands for differential evolution best represent the best vector that is selected, 1 stand for the number of distance pairs ($v_1 - v_2$), while the last term represents the crossover either exponential (exp) or binomial (bin).

The other best method is the DE/rand/1/bin as mentioned in[119] and [120], the reason being that "the random selection of parents for a trial enhances exploration capabilities. Thus, the locations of individuals carry information about the fitness landscape. Therefore, an effective mutation strategy that leads to uniform random vectors represents the entire search space well,." The pseudocode for the DE algorithm with the DE/best/1/bin mutation strategy is shown below.

The lower and the upper bounds correspond to the hourly maximum and the minimum values of the temperature and GHI. The problem size is 24*n meaning there are hourly bounds for the 24 hours each, and n is the number of days from 1 to n until the stopping criterion is met.

Meaning as the number of days increases more is the time taken for the computation, since the number of variables to optimize increases. As explained in [119] the problem size increases the dimensionality of the algorithm thereby increasing the computation time taken for the convergence or satisfying the stopping criterion.

The population size can be fixed based on the problem to be solved, initially starting from 10 and then increasing in order. In [121] the authors explain that the choices of F and C_R are only evaluated based on experimentation. The recommendation for the population should be slightly low as possible. Since the population parameter defines, the total population of candidates is 24 * n.

As the number of days n increases the number of individuals in the population increases, hence it would be useful to find by incremental experimentation the least possible population value as explained in [121]. In short, the global problem is to find the signal characteristics that will be able to reproduce the energy efficiency in the heating season within 5% error bounds.

Table 12: Optimization problem to solve and constraints to be addressed

Domain	Statistical	Frequency
Objective Function	Match the distribution of the short sequence with the temperature and irradiation profiles of the heating season. By minimizing the KL divergence value between both.	Match the FFT / PSD of the short sequence with that of the heating sequence. By minimizing the RMSE error between them.
Constraints	Match the distribution of the hourly temperature difference distribution Match the correlation between the temperature profile and the irradiation profile in the short sequence to that of the heating season.	Match the correlation between the temperature profile and the irradiation profile of the short sequence to that of the heating season.
Bounds	Hourly maximum and minimum values of temperature and irradiation	Hourly maximum and minimum values of temperature and irradiation

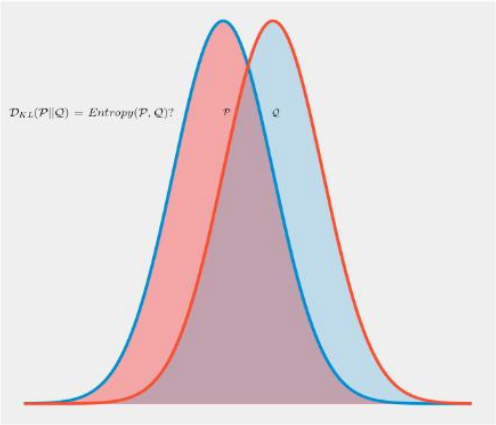

Figure 60: Comparison of two PDFs [122]

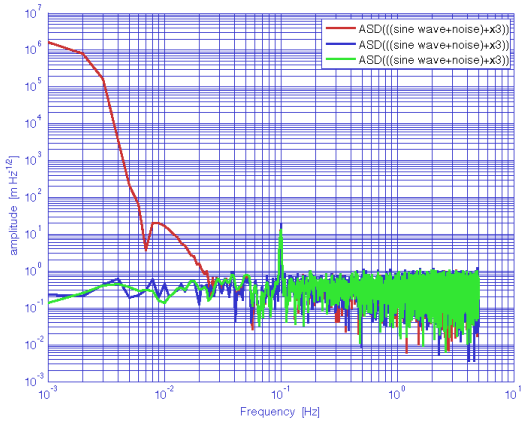

Figure 61: Comparison of multiple PSD [123]

The optimization problem can be defined as shown in Table 13. Hence, in short, the optimization algorithm chosen is the DE algorithm. The objective function to be solved is to match the distribution of the annual temperature and the GHI to that of the short sequence generated in the statistical domain (shown in Figure 60) and the FFT/PSD in the frequency domain (shown in Figure 61).

The constraints would be to consider the distribution of the hourly differences in the temperature to that of the same with the generated short sequence in the statistical domain and the FFT of the same if required in the frequency domain.

The upper and lower bounds are the hour-wise maximum and minimum values of the GHI and the outside temperature. The mutation strategy chosen for the DE algorithm is the DE/randtobest/1/bin since it returns the final vector that is the best fit for the chosen problem to be solved and exploits the available population based on random initialization.

The best idea is to initialize the population with a random vector and use the best vector for the next generation mutation thereby exploring and exploiting the available population to find the final vector of the best fit.

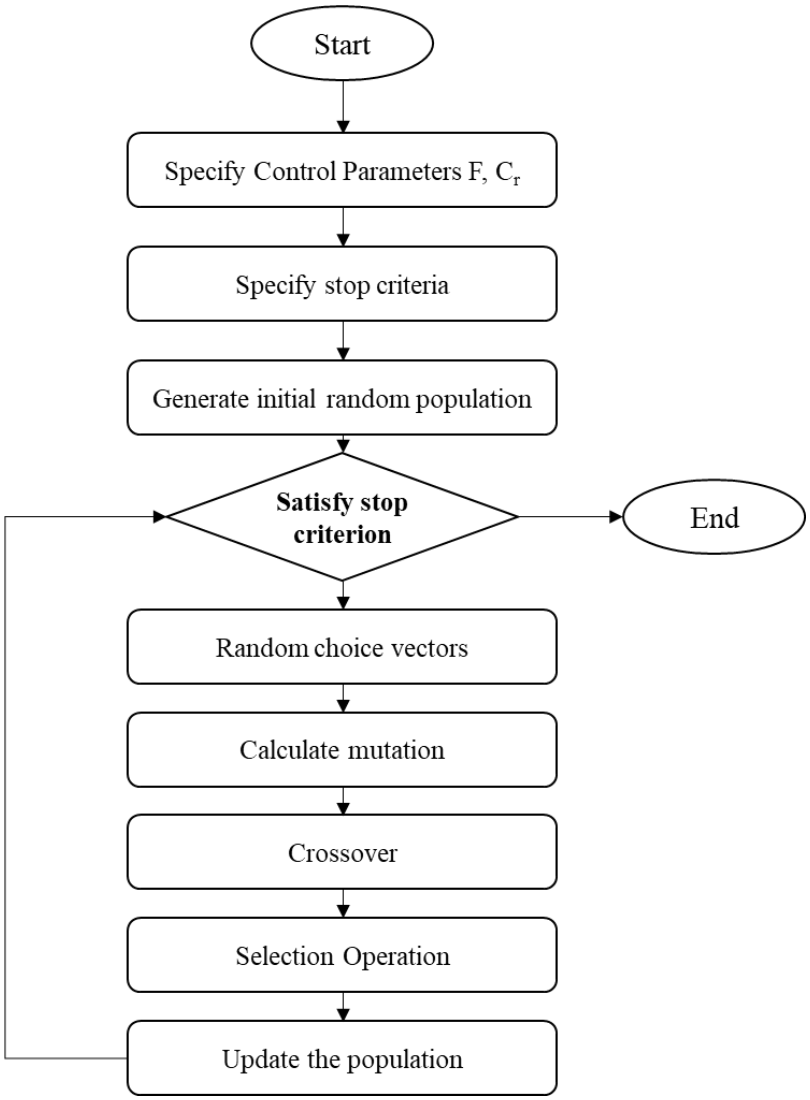

Figure 62: Flowchart for the DE algorithm [119]

Algorithm 1. Pseudocode for the differential evolution algorithm

Inputs: Population size NP, Problem size D, Mutation rate F, Cross Over Rate C_r, Stop Criteria, Upper Bound 'U,' Lower Bound 'L'

Output: Best Vector that satisfies the criteria

```
1  Population = Initialise Population (NP, D, U, L)
2  While (Stop Criteria ≠ True) do
3          Best Vector = Evaluate Population (Population)
4          v_x = Select Random Vector (Population)
5          Index = Find Index of Vector (v_x); //specify row number of a vector
6          Select Random Vector (Population, v_1, v_2, v_3) where v_1 ≠ v_2 ≠ v_3 ≠ v_x
7  V_y = v_1, + F (v_2 − v_3) // mutation strategy DE/best/1/bin
8          For (i = 0; i++; i < D − 1) //Loop for starting Crossover operation
9                  if (rand_j [0, 1) < C_r) Then
10                 u[i] = v_x [i]
11                 Else u[i] = v_y [i]
12         End For Loop//end crossover operation
13         If (Cost Function of Vector(u) ≤ Cost Function of Vector (v_x)) Then
14         Update Population (u, Index, Population)
15 End; // While loop
16 Return Best Vector.
```

In the next chapter, the generation of the short sequences is explained in detail, and then the analysis of the short sequences is done. Based on the simulation studies the results are analyzed and finally, all the approaches are compared based on the results obtained.

3.6 Conclusion

The problem to solve involves reproducing the KPIs within the 5% error bound, i.e the seasonal efficiency and the energy levels using the proposed method. The nature of the problem to be solved involves three important areas to be addressed one is to ensure the convergence of the KPIs for the short sequence, and the next includes the addition of non-linearities into the short sequence so that the short sequence is representative of the entire heating season. Also, the third important part will be to ensure that the repeatability of the results is ensured this part will be addressed in the fifth chapter onwards.

4. Fictitious Sequence Generation – Statistical domain

The main idea of this chapter is to demonstrate the Fictitious Sequence Generation (FSG) based on the statistical domain. The main idea of the chapter is to check if the philosophy of the FSG can reproduce the required results like the state-of-the-art clustering methodology. At the end of the chapter, it is conclusive that the statistical method is only capable of reproducing the seasonal efficiency but not the energy levels. The main problem to be solved is that one must evaluate the seasonal efficiency of the system among with its energy levels while addressing the reproducibility and the non-linearities.

4.1 Statistical domain-based sequence generation and analysis

The process flow for the short sequence generation in the statistical domain is shown in Figure 63. The idea in this statistical domain is to match the distribution of both the heating season (for both the temperature and irradiation) and the short sequence generated from the optimization method. The first step is to find the metrics that can be used to compare the two distributions.

Based on the literature [92] the simplest metric that can be used for measuring the similarity between both the probability distribution is the KL divergence. The reason a divergence function is chosen is that it is based on the rationale it is better to quantify the disagreement between both the respective distributions.

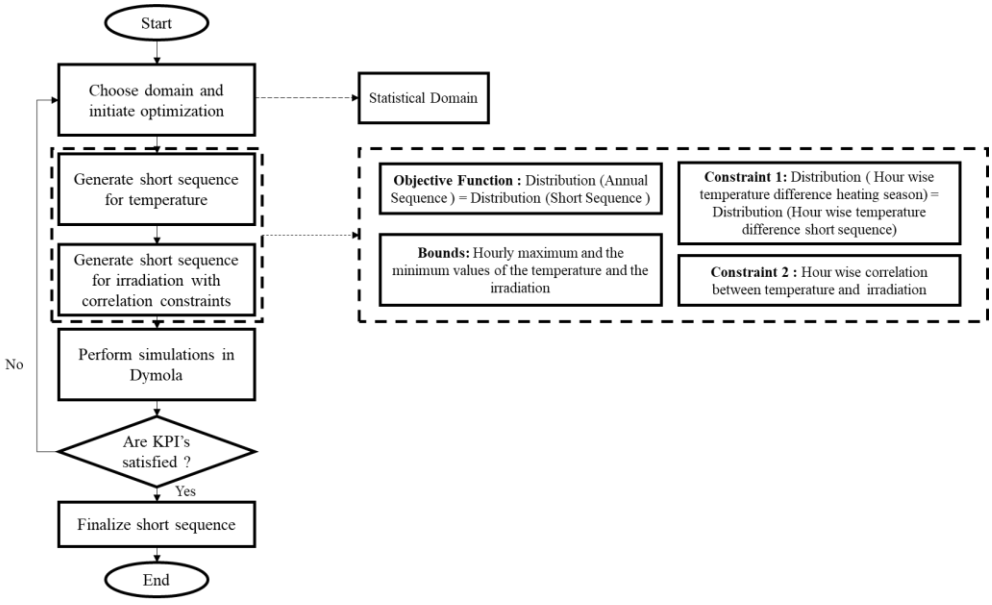

Figure 63: Process flow for fictitious sequence generation in the statistical domain

The KL-divergence is defined as the relative entropy of probability distribution P to probability distribution Q and quantifies the information lost when moving from P to Q as shown in Figure 64.

Although throughout the literature the KL divergence is not mentioned as a true metric, it is one of the simplest metrics to identify the divergence between two distributions. KL Divergence is the expectation value of the logarithmic difference between the two probability distributions as computed with weights ∏ as explained in equation (5) where i stands for the individual samples:

$$K(P \parallel Q) = \sum_i P_i \log\left(\frac{P_i}{Q_i}\right) \tag{5}$$

In general, the values of the KL divergence take the values in the range from 0 to +∞ , the values near zero mean that both the distributions are evenly distributed with one another, and the positive value means greater the divergence. Also, there are other metrics like the KS test that are considered true metrics, but it has a huge dimensionality constraint [124]. It is very much suited for one-dimensional datasets with a lesser number of data points as explained in [125]. The KL divergence is used to compare both the distributions of the temperature and the hour-wise temperature difference distribution.

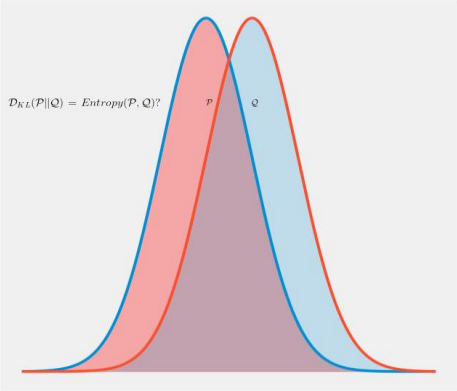

Figure 64: KL - divergence between two distributions

4.1.1 Temperature short sequence generation and analysis – statistical method

For the generation of the sequences, the Python SciPy library is used [126] where one can make use of the DE function that is already written and ready to be used. Before going into the generation of the sequences the first step is to choose the parameters for the population size, crossover function, and recombination factor. The population size can be chosen by first initially fixing the other two parameters and then sequentially increasing the population size.

By default, the population size is set to 15 - 200, the reason being to find a short sequence that is consistent. This can be based on the rationale as on increases the population size thereby increasing the population candidates one can fix on the population size, this being one of the simplest approaches as explained in [127] where the authors use an Artificial Neural Network (ANN) to tune the parameters of

the DE parameters. For the application considered it would be easy to consider the simplest approach since the optimal tuning of the parameters would be out of scope in the considered framework. Based on the approach one can fix on the parameters as population size as 100. Only from 100 onward one can see the same temperature sequence for a one-day sequence. Finally based on a trial-and-error basis, the mutation rates were fixed to 0.5 and the cross-over rates fixed to 0.8.

The one-day temperature sequence generated using the DE algorithm is shown in Figure 65. The difference between the distribution of the total heating season and the one-day short sequence is shown in Figure 66. From the short sequence generated for the one day, it can be noticed that the one-day temperature sequence is not having a regular cycle for the day as generally desired. This means that the temperature is slightly higher at the beginning and the end of the day and lower during the mid-day which is vice versa in an otherwise normal day.

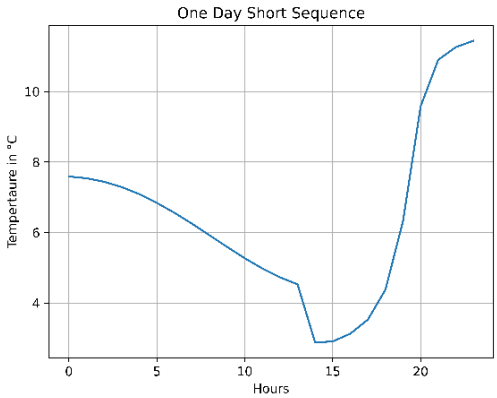

Figure 65: One-day short sequence

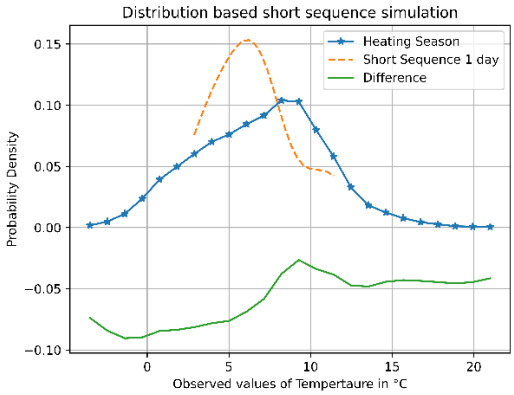

Figure 66: Distribution of heating season vs 1-day sequence

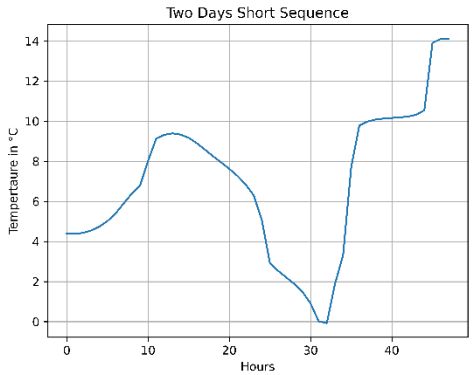

Figure 67: Two-day short sequence

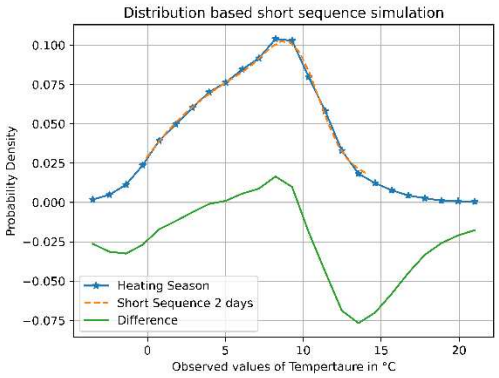

Figure 68: Distribution of heating season vs 2-day sequence

Also, when the distributions of the heating season to that of the day generated by the optimization method do not match exactly. Also, based on visual inspection it can be noticed that the distribution of the

one-day sequence can be seen generated around the mean value. Hence, before going into further statistical analysis a 2-day/48 hours sequence is generated. The two-day sequence generated is shown in Figure 67 and the distribution compared for the heating season and the 2-day short sequence is shown in Figure 68.

Compared to the one-day sequence the two-day sequence satisfies the statistical parameters when compared to the entire heating season to some extent. Also, the DE algorithm produces the short sequence that starts dispersing out from the mean value of the distribution as shown in Figure 69. In one way it can be observed that the DE algorithm will proceed to add hours based on the mean value of the entire heating season in the short sequence that the DE algorithm produces.

Also, based on the difference between both the distributions plotted in Figure 69 it could be observed that the difference between the distributions reduces as the number of days increases in the short sequence. It can also be noted with the further increase in the days in the short sequence the difference between both the distributions does not reduce much, showing that there could be some theoretical limitations associated with the distributions. The statistical moments of the first order and the higher order are verified between the heating season and the short sequences for the temperature are shown in Table 13. From Day 3 onwards the statistical moments almost match up with the heating season, barring the extreme values. In the context of the testing methodology reaching the extremities does not add much value to the testing hence, it can be seen as a compromise like the clustering technique. Moreover, one can see from Figure 69, that extreme conditions contribute to a smaller number of hours in the whole heating season.

Also, the main difference between this fictitious sequence method and the clustering method is that in the clustering method the already existing days are chosen while in the fictitious sequence method a fictitious testing sequence is generated. Also, from Figure 70, it could be seen that as the number of days increased the difference between the distribution of the heating season and the short sequence decreased. The difference between the clustering method and the fictitious sequence-based methods is that the clustering picks up the centroid/medoid. The fictitious sequence method chooses the average value of the entire heating season signal, while also making it a possibility to represent the extreme values with a shorter sequence length when compared to the clustering approach.

Since the clustering picks up the actual value from the existing days it would be easy to identify the frequencies that the short sequence can represent when compared to the fictitious sequence generated using the distribution. From the comparison table with just an increase in another 24 hours, the important statistical moments are almost matching with the heating season (Table 13). Hence, this also confirms the

basic philosophy with the increase in the number of days the heating season is better represented in the short sequence as shown in Figure 70.

The short sequences generated could be considered as a global optimum because, before generating the short sequences the parameters were tuned to give the same short sequence (Figure 71), even though one restarts the optimization. The only initial value is changed while the entire profile is the same, this aspect is discussed in detail in Chapter 4. The only downside to such an approach is that the time taken for generating the short sequence is very high, but it is a very good trade-off considering if one can reduce the number of testing days in real-time

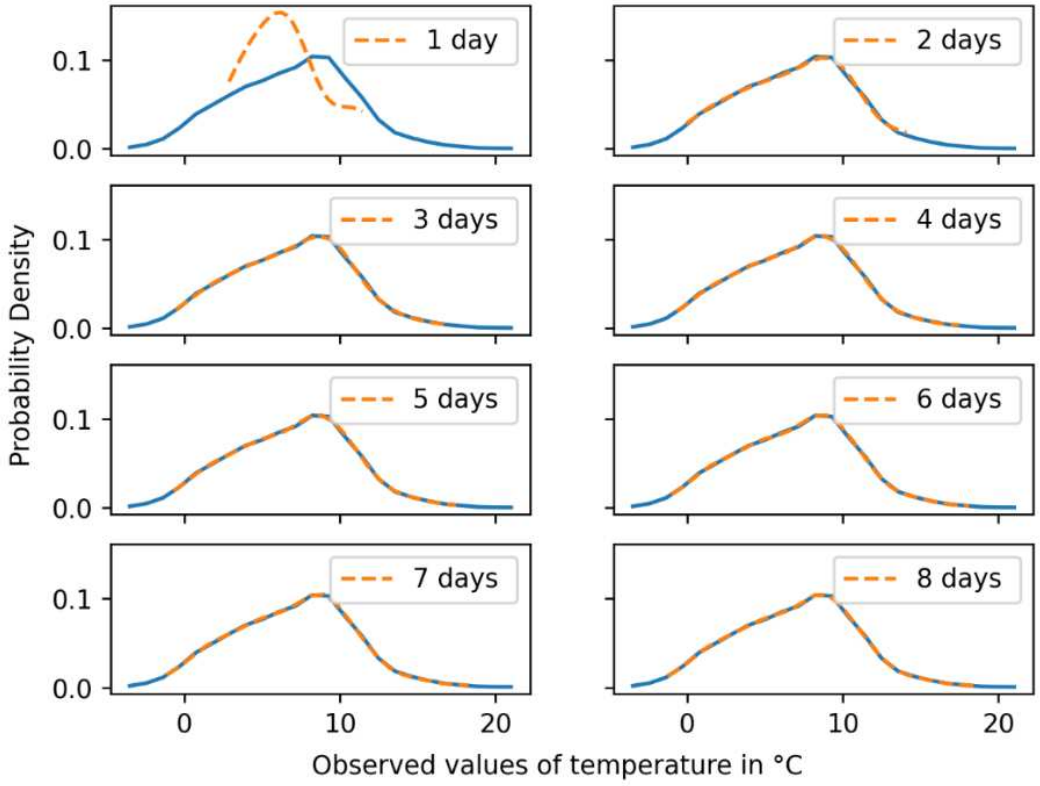

Figure 69: Temperature distribution of heating season vs short sequence

Also, for the entire season, the ranges for the percentage of the temperature values (based on the 68-95-99% rule) covered can be seen from the distribution of the heating season. 68% of the temperature values fall in the range of 3.07°C – 10.79°C, 95% of the temperature values fall in the range from -3.65°C – 18.51°C, and 99% of the values fall in the range of -0.79°C – 14.65°C regarding the statistics related to the heating season.

Based on the data from Table 13, it could be seen that for the one-day short sequence the range of the temperature values is from 2.9°C – 11.4°C meaning that the one-day short sequence is not capable of

covering at least 68% of the temperature values comprising the heating season. For the two-day short sequence, the range of temperature values is from -0.07°C – 14.1°C. This means that the two-day short sequence is almost covering 95% of the values comprising the heating season. From day 3 onwards one could see that 99% of the temperature ranges are also covered, signifying the theoretical limitation of the distribution-based method where the extreme 1% of the temperature ranges are not covered.

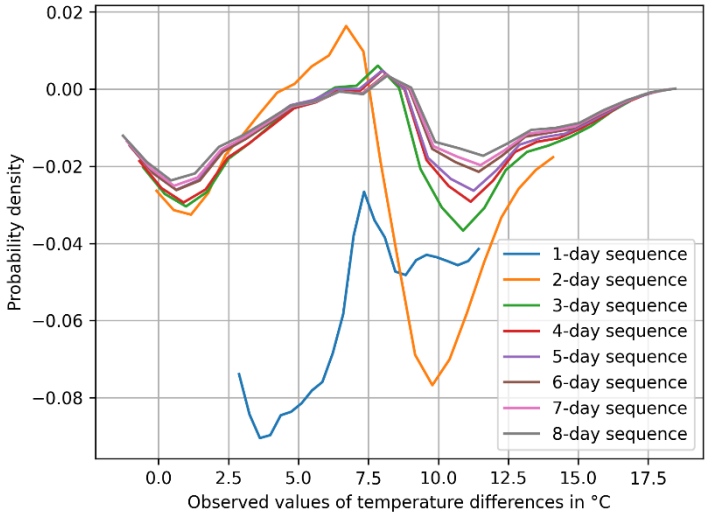

Figure 70: Difference in distribution heating season vs short sequence

All the temperature short sequences generated are shown in Figure 71. It can also be seen from the short sequences that as one increases the number of days one can see that the DE algorithm adds different temperature profiles. The other identification that one can make is that also by increasing the number of days for the short sequences one can see that the day added to the sequence contains days with the mean values of the temperature from the heating season.

Table 13:Comparison of the statistical moments of the temperature sequence for heating season vs short sequence

Statistical Moments	Heating Season	1 Day	2 Day	3 Day	4 Day	5 Day	6 Day	7 Day	8 Day
Hours	3664	24	48	72	96	120	144	168	192
Mean	6.93	6.42	6.90	6.94	6.94	6.94	6.94	6.93	6.93
Standard Deviation	3.86	2.49	3.60	3.65	3.67	3.68	3.70	3.70	3.71
Minimum Value	-3.5	2.88	-0.07	-0.54	-0.68	-1	-1.02	-1.13	-1.27
25% Percentile	4.1	4.68	4.42	4.50	4.33	4.40	4.33	4.29	4.15
50% Percentile	7.2	6.29	7.45	7.59	7.10	7.48	7.26	7.41	7.33
75% Percentile	9.5	7.47	9.49	9.43	9.28	9.30	9.35	9.34	9.34
Maximum Value	21	11.44	14.1	16.98	17.47	17.80	18.09	18.25	18.47
Skewness	0.01	0.60	-0.13	0.02	0.02	0.02	0.02	0.01	0.01
Kurtosis	-0.18	-0.16	-0.54	-0.22	-0.2	-0.2	-0.2	-0.2	-0.2

One of the prime reasons why the profile of the temperature sequence does not follow the general temperature profile shape is that the distribution gives an insight into the overall statistical characteristics of the data set but not the dynamic characteristics of the dataset. One of the later steps will be to check if the profile generated by the DE algorithm has some sort of resemblance to any of the days from the heating season. The immediate next step will be to analyze the constraint criteria for the hour-wise temperature difference distribution.

The distribution of the hour-wise temperature difference is shown in Figure 72. From the visual inspection, it could also be seen that both the sequences do not have the same mean as the heating season. For the one-day short sequence the average hour, wise temperatures are around 0.16°C and 0.2°C respectively for the two-day sequence for the heating season the average hour-wise temperature difference was around 0°C.

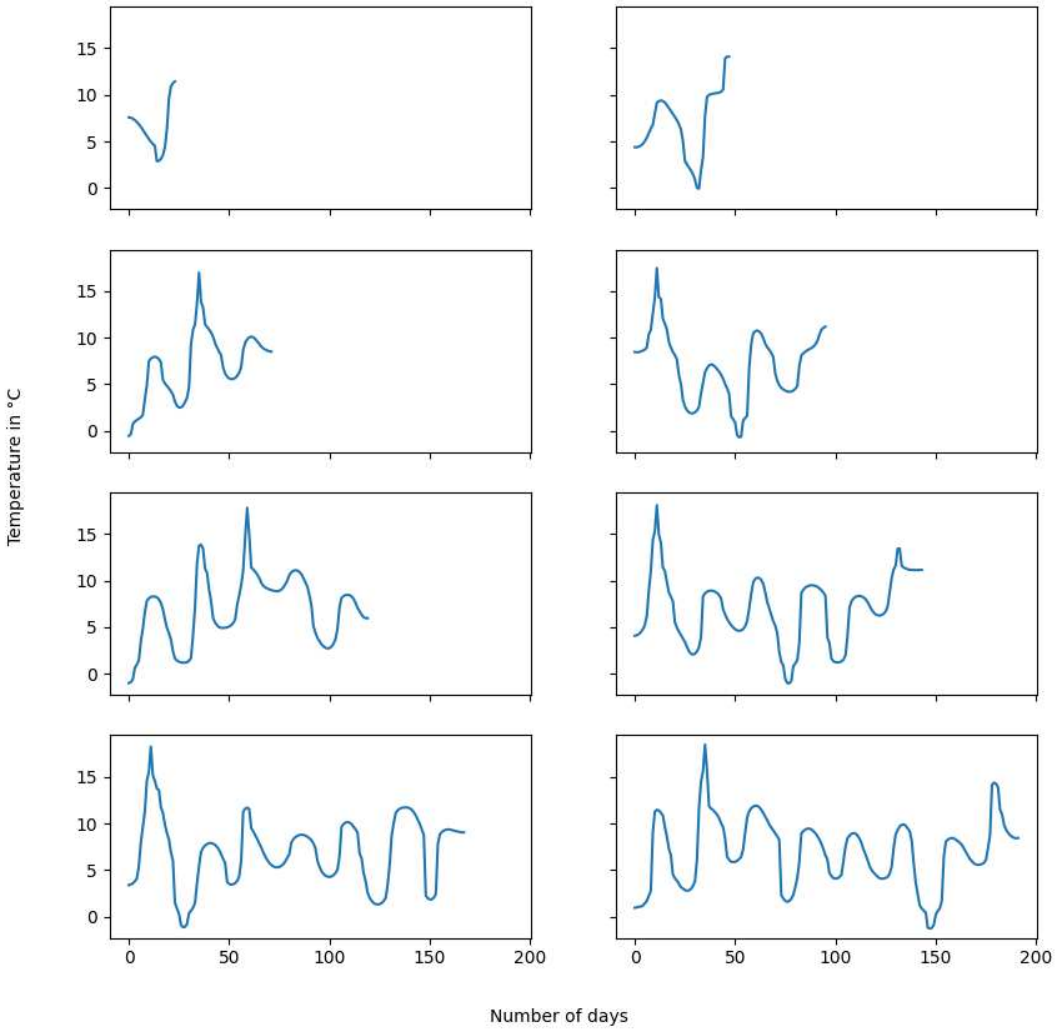

Figure 71: Temperature short sequences generated, in the order (Day 1 to Day 8)

Also, it can be seen from Figure 72 that to match the entire hour-wise temperature difference range of the heating season, at times the temperature difference is overcompensated at the right extremes of the distribution towards the right tail of the distribution. This was bound to be expected, it is because the DE algorithm tries to solve for the temperature ranges in the temperature distribution as shown in Figure 69. To catch up with the temperature ranges at times the hour-wise temperature difference from the lower temperature's values is increased more often than expected.

At times that could be the reason that one can see that in Figure 72 towards the right tail of the distribution one can see the over-representation of the values in the short sequences.

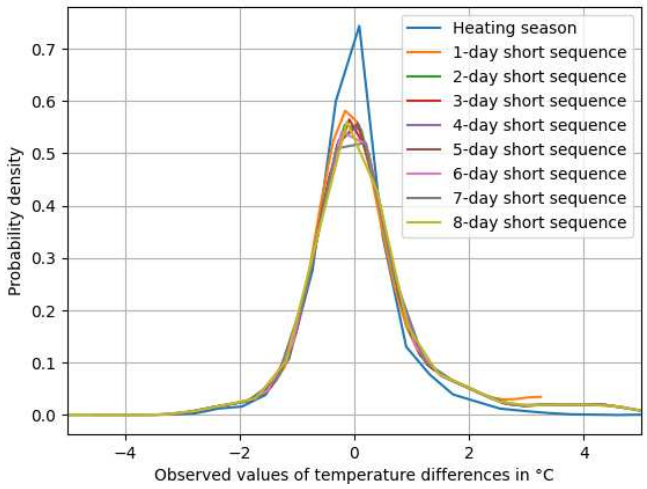

Figure 72: Distribution of hour-wise temperature difference for heating season vs short sequence

It could also be seen that the higher statistical moments vary because of the over-representation towards the right-hand tail, the area under the mean, and the unrepresented part towards the left-hand tail of the distribution. Another observation made is that one can notice that with the increase in the number of days, the density of representation under the mean value represented becomes smaller in the short sequence.

Also, it is to be noted that the time taken for increasing the number of days in the short sequence takes more time to produce the sequence since there is an objective with many unknowns. Hence, the time is taken for the convergence to return the best vector that best represents the heating season increases as the number of days increases.

4.1.2 Irradiation short sequence generation and analysis

The immediate next step will be to generate the irradiation sequence along with the hour-wise correlation between the temperature and the irradiation as shown in Figure 75 and Figure 75. The

irradiation short sequences that are generated are shown in Figure 73. It could be seen that the limitation of the distribution-based method of generating the short sequence shows up.

The GHI for all 8 days is similar and there are hourly variations for the profiles that are quite questionable. Even though with the increase in the number of days one is not able to observe cloudy days, this is because the distribution has a mean value of around 400 W/m^{2,} and the short sequence is generated using the distribution that serves as a representation of the values in the signal and not the dynamics that are represented in the signal.

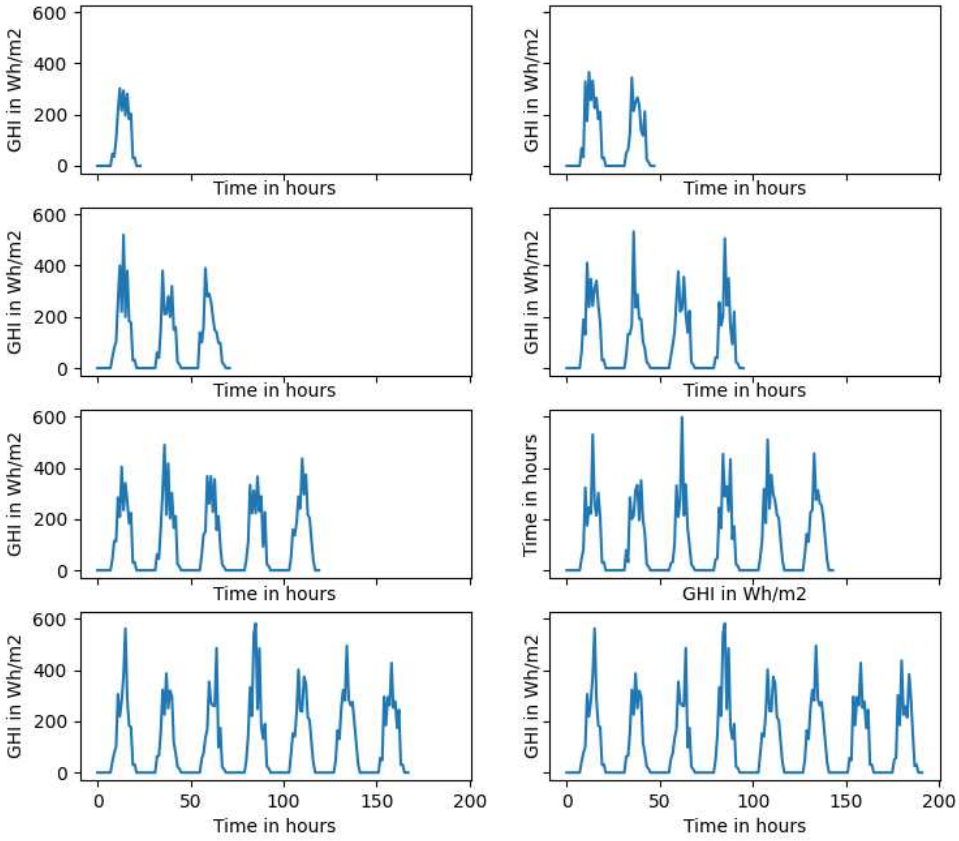

Figure 73: GHI short sequences generated, in the order (Day 1 to Day 8)

The distribution of the heating season GHI and those of the short sequence are compared as shown in Figure 74. One could also see that the DE algorithm reproduces the short sequence from the mean value of the heating season. This is also seen as the overrepresentation of the values in the range from 50 Wh/m2 to 400 Wh/m2. As expected since the DE algorithm reproduces the short sequences for the value around the mean value of the heating season the statistical moments of the heating season and the short sequence do not match at all. The same would be the other way as well since (if the irradiation

sequence was to be generated first), for both the irradiation and the temperature sequence the parameters have been fixed based to give the same short sequences based on experimentation.

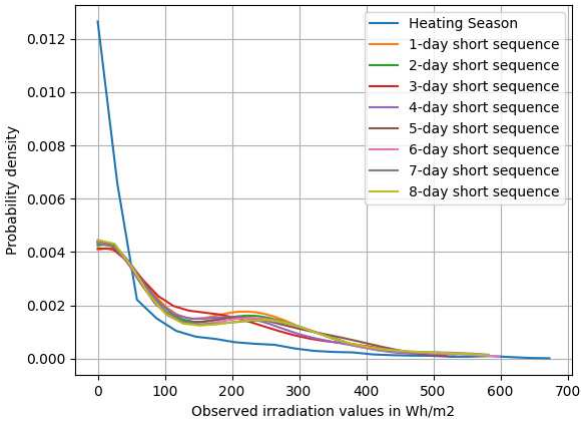

Figure 74: Distribution of GHI heating season vs short sequence

Like the temperature short sequence as one increases the number of days in the short sequence, one can observe that extreme values could be reached. Also, the area represented from 50 Wh/m^2 to 400 Wh/m^2 decreases but based on the type of the distribution the number of days increases. In the case of the temperature distribution the statistical moments could be reached after a few days (starting from n = 3). But, in the case of the Weibull distribution, it could take a greater number of days to converge to the actual distribution of the heating season, since the distribution is not spread out as in the case of the normal distribution. The distribution is skewed towards zero since a greater number of days in the heating season correspond to more hours having zero irradiation. Since the short sequence represents better the other areas namely the region from 50 Wh/m^2 to 400 Wh/m^2 in the distribution curve the statistical moments do not match with the distribution of the full year.

The next step will be to verify the constraint parameters visually, the hour-wise correlation of the outside air temperature and the GHI are compared for both the heating season and measure the RMSE (Root Mean Squared Error) between both the correlation data sets. The correlation between GHI and the outside air temperatures for the heating season vs the short sequences is shown in Figure 75. The reason to do this is that the individual weather variables are generated based on the optimization , hence , one needs to consider the hourly correlation between both the variables. One can see that as one increases the number of days in the short sequence the correlation is better represented. For the 8 days short sequence one could conclude that the correlation constraint is the same as the one corresponding to the heating season. It is also understood that the correlation between the one-day and two days short sequence does not correspond with that of the total heating season it is based on the rationale that not much data is available for comparison when the sequences have one or two days. From the three-day short sequence,

one could see that the correlation is respected with that of the heating season. The RMSE between the correlation for the heating season and the short sequence is shown in Figure 75. The main idea of the correlation plot is to check how the correlation of the short sequences measure up against the original heating season between the temperature and the irradiation. It could be observed that as the number of days in the short sequence increases the correlation between both the temperature and the irradiation is like the whole heating season.

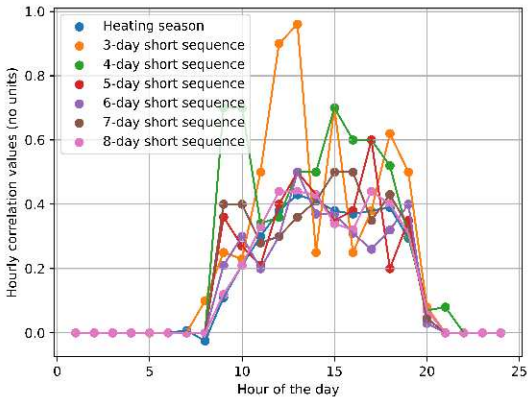

Figure 75: Correlation of the GHI and temperature for the heating season vs short sequences

The RMSE values for the one-day and the two-day sequence do not seem to be extremely high it is because almost 12 hours of the sequence have zero irradiation values, this is one of the reasons why there is not an extremely high value of RMSE being shown.

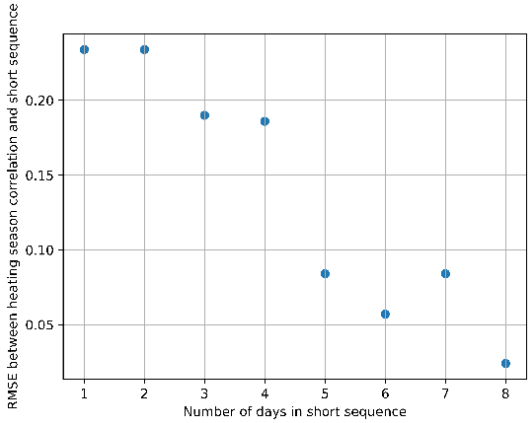

Figure 76: RMSE between short sequence and heating season hour-wise correlation between GHI and outside air temperate

As the number of days is added to the short sequence for evaluation it could be seen that the RMSE value decreases. More the number of days better the correlation between the GHI and the outside air temperature in the short sequence. The next step would be to make use of these short sequences to

perform simulations on the boiler and heat pump use case and check if one could achieve the KPIs under consideration within a 5% error value.

One can either create a weather file .epw extension using the elements weather file creator or one could use the values of temperature and the GHI values directly as inputs to the weather file reader using an input connector. Since the number of days represented in the heating season by the short sequence is not known, the extrapolation factor used is 153/n. The results for the generated sequences are seen in the next section, compared with the clustering results.

4.1.3 Simulation Analysis for fictitious sequences generated using the statistical domain

The simulation is performed on the same use case as explained in the previous chapter. The results for the boiler use case are shown in Figure 77 and Figure 78. From the results, it could be seen that the fictitious sequence returns the seasonal energy efficiency of the boiler more accurately than the clustering methodology from Figure 77. But when the energy levels are verified for the boiler use case, it is seen that the energy supplied to the boiler and the energy used for space heating do not fall within the 5% bounds.

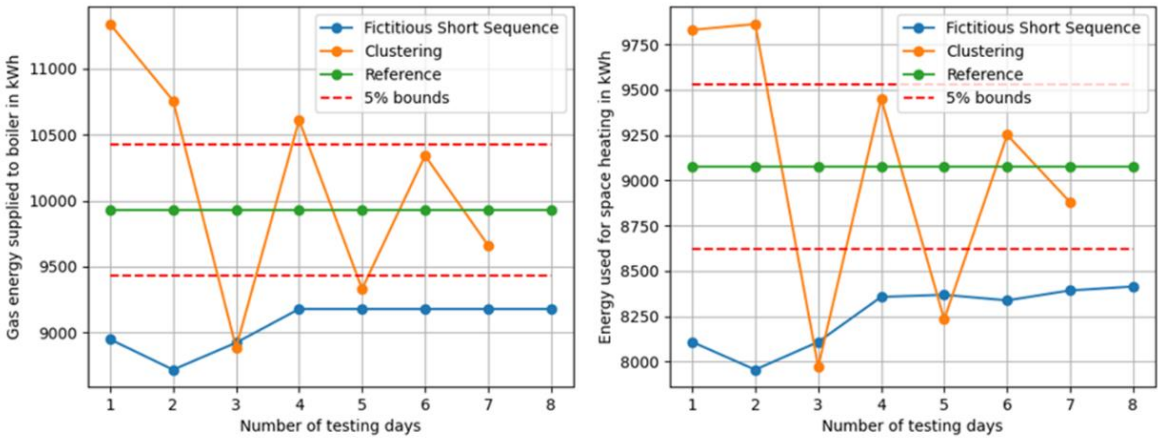

Figure 77: Energy levels Clustering vs Distribution method (Left - gas energy supplied to the boiler, right – Output energy used for space heating)

The error values for the clustering methodology and the fictitious short sequences are compared for the energy levels of the boiler and the season energy efficiency as shown in Figure 79. The result converges faster in comparison to the clustering methodology, from day 4 onwards. In the case of energy efficiency when compared to the clustering methodology the FSG (Fictious Sequence Generation) - Distribution-based method produces results well under 1% error for all 8 days of testing.

As far as the energy level goes it could be seen that there is a convergence at an 8% error for both the input and output energy levels. In the case of the clustering methodology, the error decreases within the required bounds as one increases the number of clusters. The reason the energy efficiency is less than 1% for the boiler could be due to the case that the gas-fired boiler could produce similar efficiency rates throughout the year. Also, the average values are added to the short sequences based on the methodology of generating the short sequences as seen in the previous case.

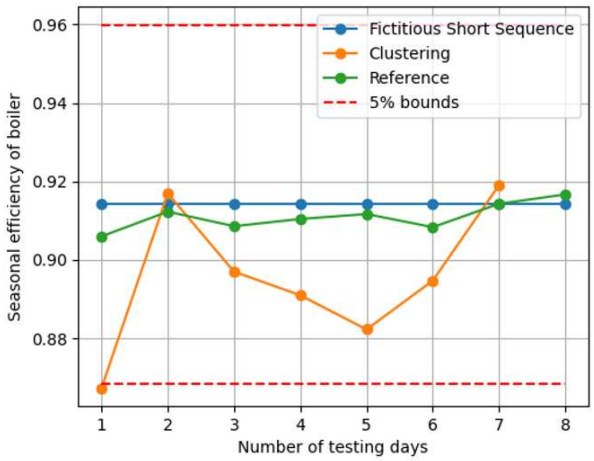

Figure 78: Seasonal efficiency of boiler clustering vs fictitious sequence (distribution)

Moreover, the entire dynamics of the heating season are not represented by the distribution. Also, based on the analysis done on the short sequence even after increasing the number of testing days the distribution of both the temperature and irradiation does not change much, this could explain the fact why the energy levels were not respected along with the dynamics not being represented by the distribution.

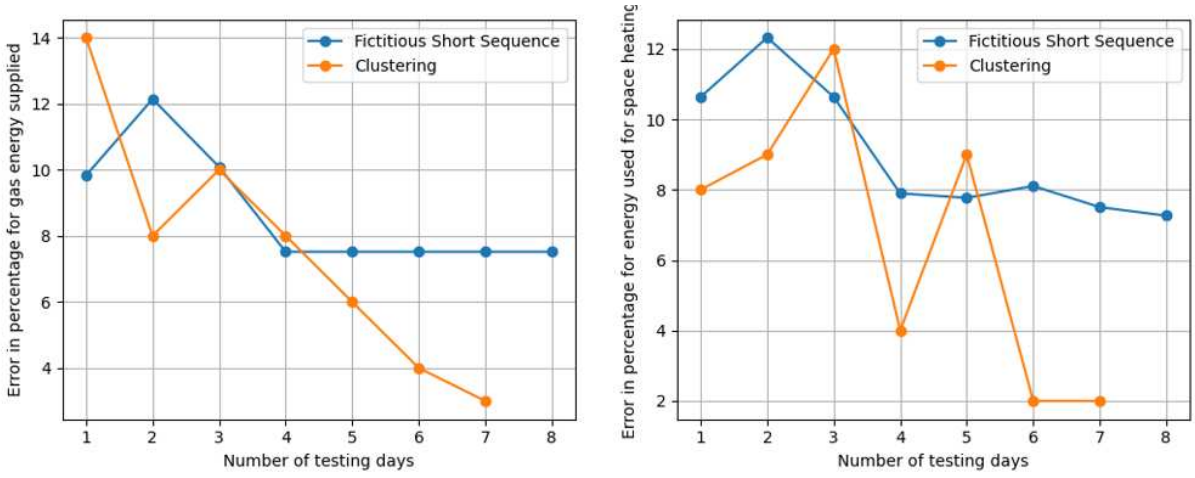

Figure 79: Error comparison for the boiler clustering vs fictitious sequence (left – input gas energy error, right – output energy error)

The simulation is also done for the heat pump use case to verify if the same analysis holds good as well. The results for the heat pump use case are shown in Figure 81, for the corresponding energy levels. Like in the boiler use case the SCOP here is reproduced with 1% accuracy as shown in Figure 82. While the energy levels for the heat pump do not fall within the expected bounds of 5%.

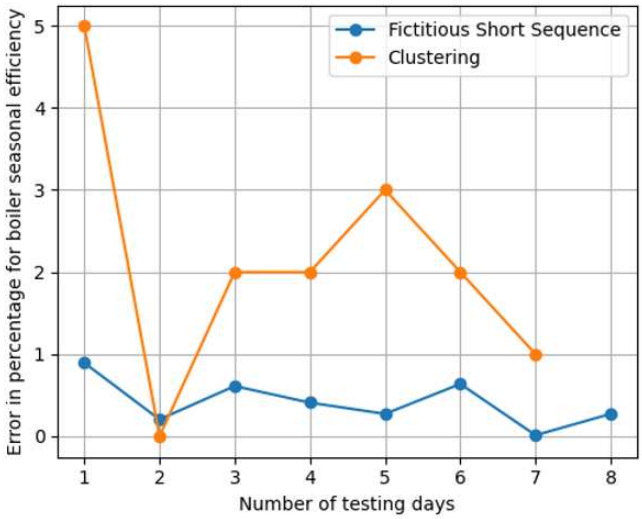

Figure 80: Error for boiler seasonal efficiency clustering vs fictitious sequence (distribution)

Based on the analysis performed on the short sequences that were generated one can conclude that the distribution method might not satisfy energy levels because the distribution captures the range of the temperature values but not the dynamic associated with it. This could be verified using simulation and check if this method of generating the short sequences could help.

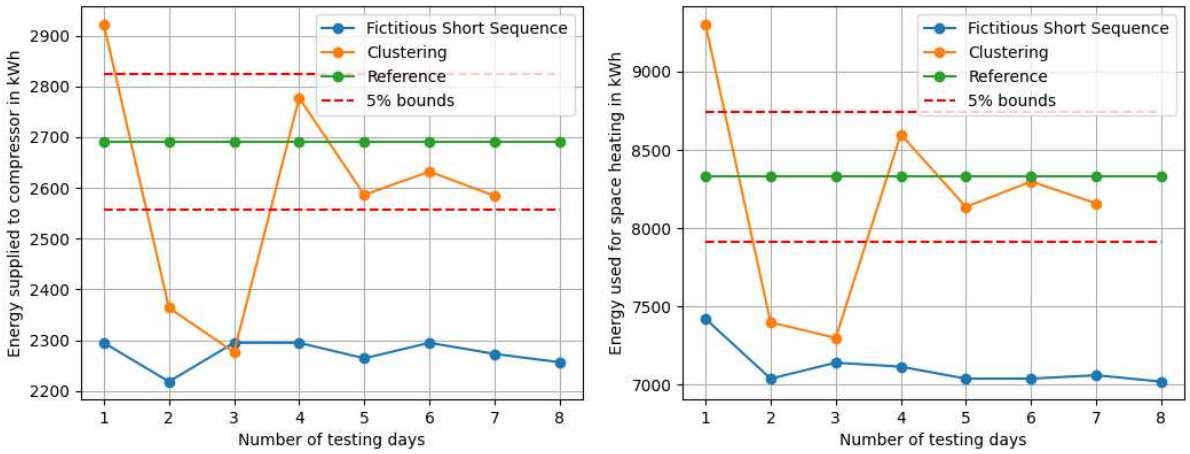

Figure 81: Results for heat pump use case simulation-Energy levels

The error in the energy levels and the SCOP of the heat pump are shown in Figure 83. Like the boiler use case, one could see that the convergence happens at a higher energy level. In the boiler use case, the energy levels converged at 7% - 8% of the annual energy levels. In the case of the heat pump use case, the energy levels are higher at 16% for the error in the energy levels.

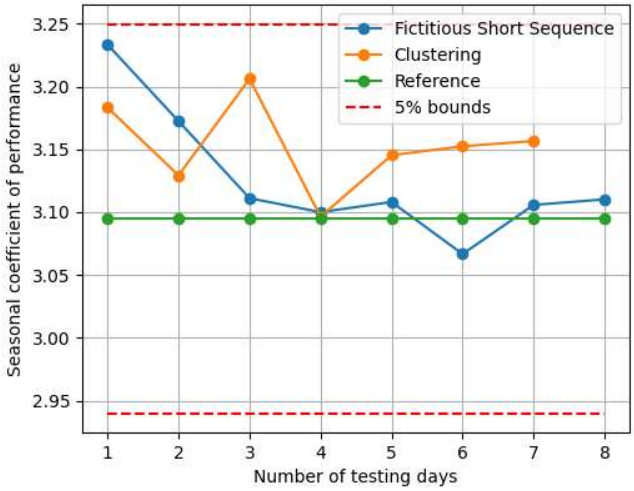

Figure 82: SCOP for the heat pump use case, clustering vs distribution method

As seen in both cases the distribution method has some limitations, one of the key limitations being the ability to not reproduce the annual energy levels. This is explained by the fact that the distribution gives only the statistical representation of the signal, but the dynamics of the signal are not represented by the distribution. Plus, from Figure 69 difference between both distributions does not reach zero there is always some residue left out in the case of the optimization process, this also signifies that there is always a theoretical limitation associated with the distribution methods.

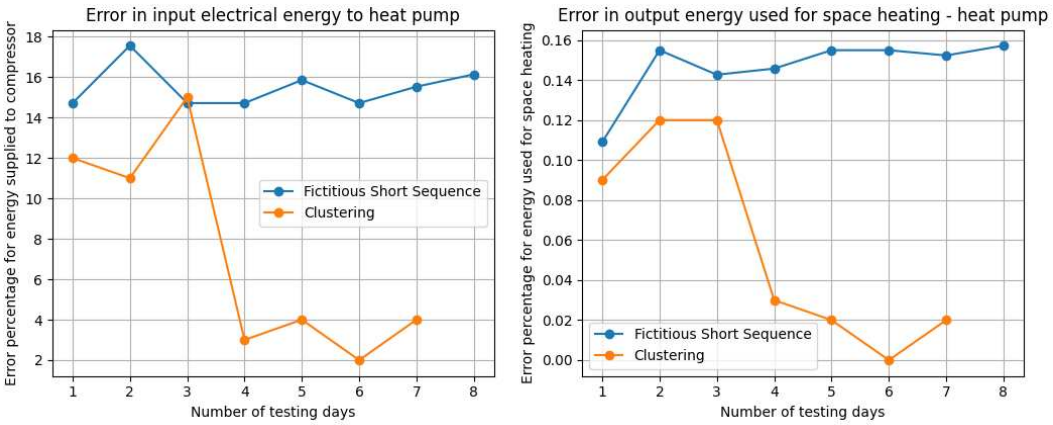

Figure 83: Error in energy levels clustering vs Fictitious Sequence (Distribution method – heat pump use case)

The objective function values for the temperature and the irradiation short sequences for all the 8-day use cases are shown in Figure 84 and Figure 85. It could be seen that the KL-values decrease as the number of days decreases, one could also question why the values are very less for the irradiation sequence when compared to the temperature sequence since the temperature sequence has the best fitting distribution when compared to the irradiation sequence. This is because the KL-Divergence is only a divergence estimate but not a true estimate.

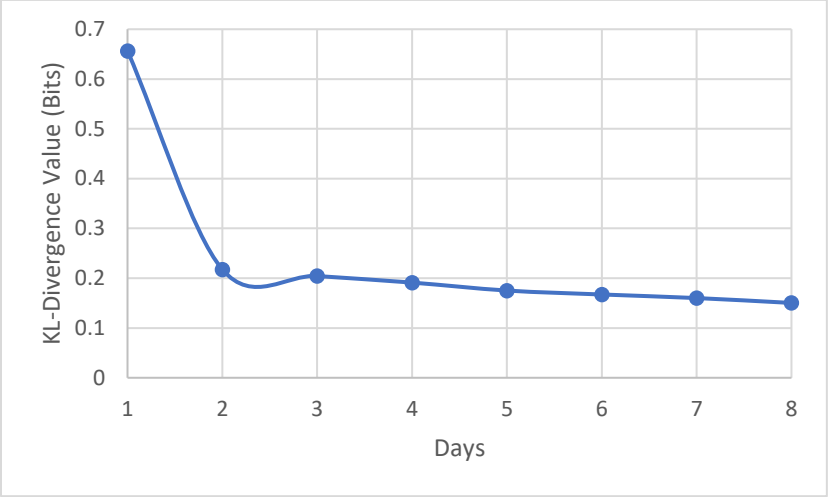

Figure 84: Objective function values for the temperature sequence

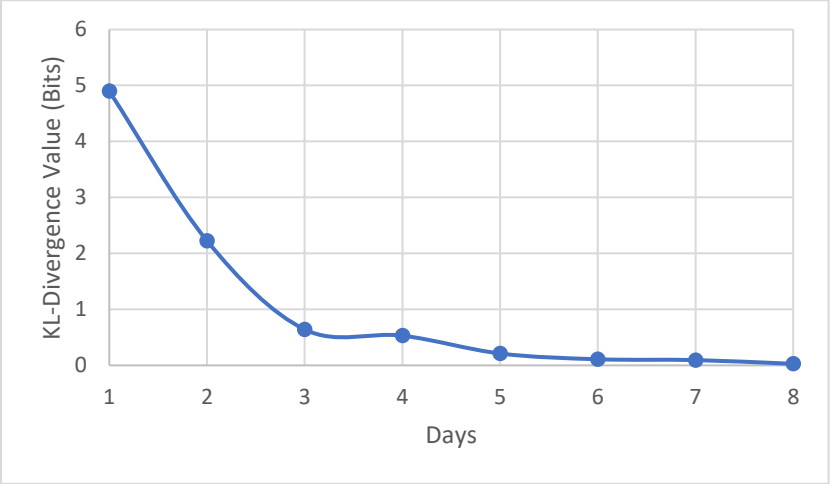

Figure 85: Objective function values for the irradiation sequence

To capture all the dynamics in the whole heating season the next idea will be to generate a short sequence based on the frequency domain parameters. The idea will be to match the FFT or PSD of the sequence and generate the short sequence. In short, the distribution method is good enough to generate the seasonal efficiency within a 1% error, while it is not the same for the energy levels.

4.2 Conclusion

The FSG (Fictitious Sequence Generation) based on the time domain method can produce the seasonal efficiencies within the 5% error range. The energy levels were not reproduced when compared with the heating season values. The main reason is the distribution although represents the characteristics of the signal it doesn't represent the variations that are present in the season. Hence , the next step would be to investigate the frequency domain characteristics so that the energy levels of the heating season could also be replicated. In short the distribution method produces the signals based on mean value and then spreads out from the mean value of the distribution. When one calculates the average value of the signals and compare them to the average of the seasonal value both remains the same. Hence, once can conclude that the fictitious seqeunce based on the time domain distribution reolicates the average seasonal value efficiently . To include the extremities on has to specify a lot of constraints which inturn increases the time taken for generating the signals. The next step will be to investigate the frequency domain so that one can be able to reproduce the signals which replicate the variations in the heating season as wel, explained in the next chapter. The main idea will be to replicate the frequency domain characteristics of the heatin season signal with that of the short signal generated by the optimization algorithm.

5. Frequency domain-based sequence generation and analysis

The main idea of this chapter is to demonstrate the Fictitious Sequence Generation (FSG) based on the frequency domain. The main idea of the chapter is to check if the philosophy of the FSG can reproduce the required results like the state-of-the-art clustering methodology. At the end of the chapter, it is conclusive that the FSG method based on the PSD is only capable of reproducing the seasonal efficiency but not the energy levels. The main problem to be solved is that one must evaluate the seasonal efficiency of the system among with its energy levels while addressing the reproducibility and the non-linearities.

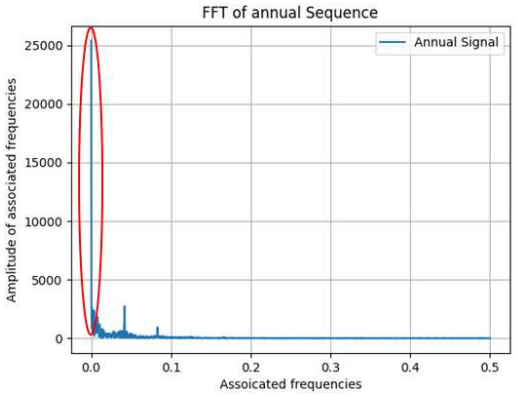

Figure 86: FFT of the temperature signal with an offset

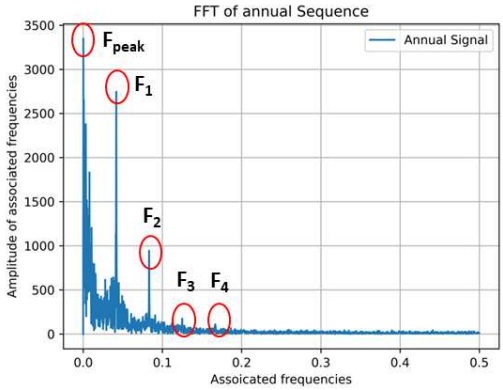

Figure 87: Frequency components of the temperature signal

The first step for this method will be to analyze the FFT of the temperature sequence and analyze the frequency components of the signal. The frequency components of the signal are shown in . The important frequencies include the 24-hour (0.0416 Hz), 12-hour (0.0833 Hz), and 8-hour (0.125 Hz) frequencies, etc.

The idea of the short sequence generation would be to generate the signal that matches the FFT of the original signal of both the temperature and the irradiation sequences. The constraint to be considered is the correlation between temperature and irradiation. To compare the FFT of the short sequence and the heating season, the FFT of the heating season is divided by the total number of samples available. The short sequence is then zero-padded and then the FFT is compared with the heating season. This needs to be done because the comparison of the FFTs is of signals having different lengths. The temperature short sequences generated for one day are shown in and . From the one-day short sequence, the frequencies are not matched based on the visual inspection. Even the 24-hour cycle for one day is not satisfactory.

The next step will be to add one more day to the short sequence and check if the short sequence can add a few more frequency components to the short sequence. The FFT for the two-day short sequence is shown in and . From both figures, the FFT of the short sequence does not match exactly with the FFT

of the full heating season. But one could see that the new frequencies are getting added to the short sequence as compared to the one-day sequence. As one can see the increase in the number of days increases the key frequencies namely the 24-hour frequency match, but it does not include all the frequencies in one whole heating season.

The FFT of the other short sequences are also compared but the FFT does not match up for all the sequences, but the other frequencies of the heating season do get added up. The FFT of the other sequences during the heating season is shown in , , , , , and . The important frequencies are added as the length of the short sequence increases but the FFT of the heating season and the short sequence do not match. This could be due to the method of generating the short sequence based on finding an array of values that satisfy the FFT of the heating season.

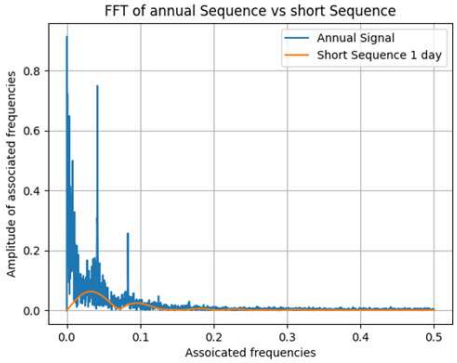

Figure 88: FFT of the short sequence vs the heating season

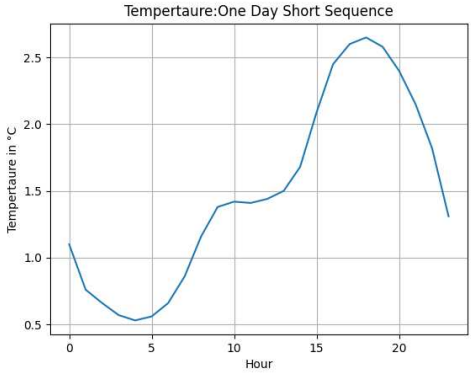

Figure 89: One day short sequence generated using FFT

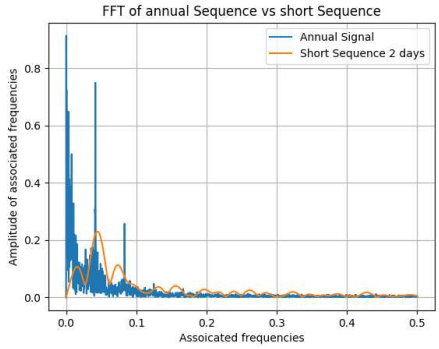

Figure 90: FFT heating season vs two-day short sequence

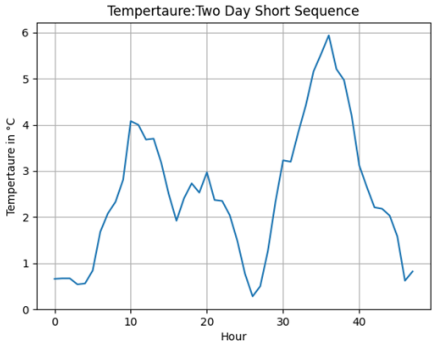

Figure 91: Two-day short sequence (temperature)

Similarly, by comparing the FFT of the irradiation of the short sequence with that of the heating season it could be seen that as increasing the number of days in the short sequence the important peak frequencies are added to the short sequence such a case for the 4-5 day short sequence is shown in and . Also, one of the main things to notice is that the irradiation for each day remains the same, this could also be attributed to the fact that the optimization algorithm searches for an array of values that satisfy the FFT of the heating season. Also, it can be seen for both the cases of the irradiation and the temperature short

sequence, the FFT of the short sequence does not exactly match that of the heating season. From this one can see that the heating season is not represented properly as per our criteria.

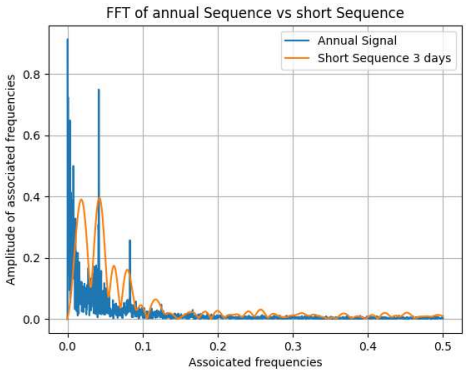

Figure 92: FFT heating season vs short sequence (3 days)

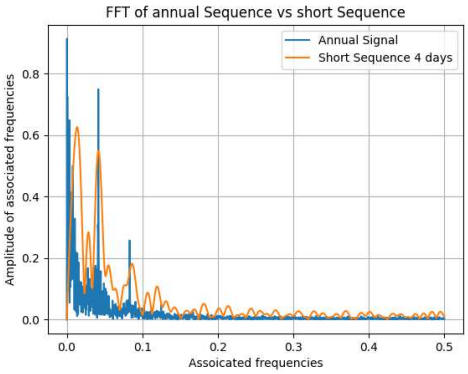

Figure 93: FFT heating season vs short sequence (4 days)

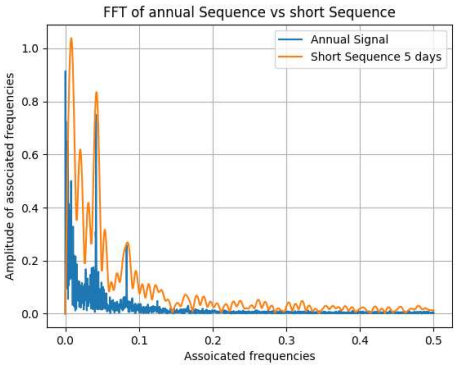

Figure 94: FFT heating season vs short sequence (5 days)

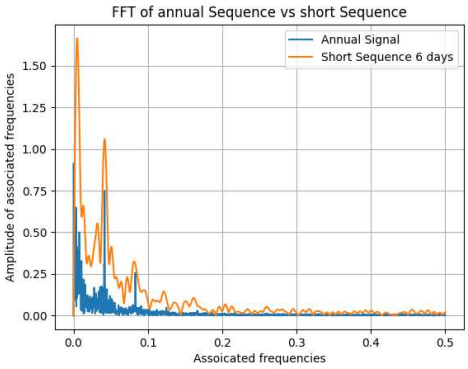

Figure 95: FFT heating season vs short sequence (6 days)

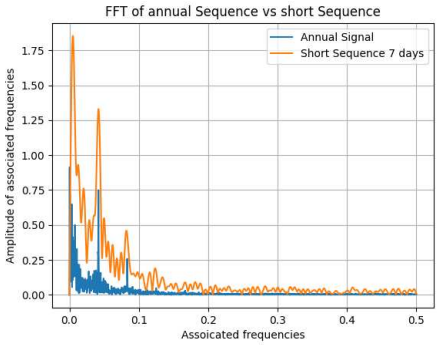

Figure 96: FFT heating season vs short sequence (7 days)

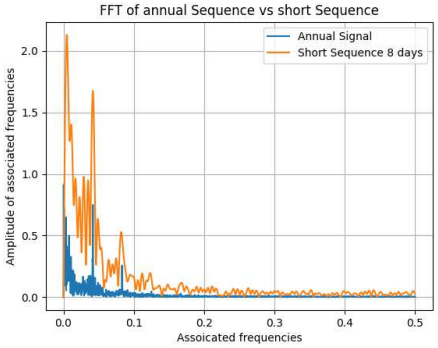

Figure 97: FFT heating season vs short sequence (8 days)

The other reason is that the FFT is not represented meaning that the dynamics of the heating season are also not accurately represented. This could also mean that the energy level might not be reproduced by the short sequence within the five percent limit. Also, based on the FFT comparison the 24-hour and the 12-hour frequency is achieved from the 3-day short sequence onwards. Meaning that from this day onwards one could see some sort of convergence. Also, one can note that with the increase

in the number of days the amplitude increases signifying that there could be missing components that could not be addressed only with the FFT alone. The results for the energy levels of the boiler use case are shown in , there is a large deviation in the energy levels. As expected, each day is represented as a cloudy day leading to an extremely high variation in the energy levels. As one increases the number of testing days, the energy variation decrease. But even after 8 days of testing, there is no convergence at one point.

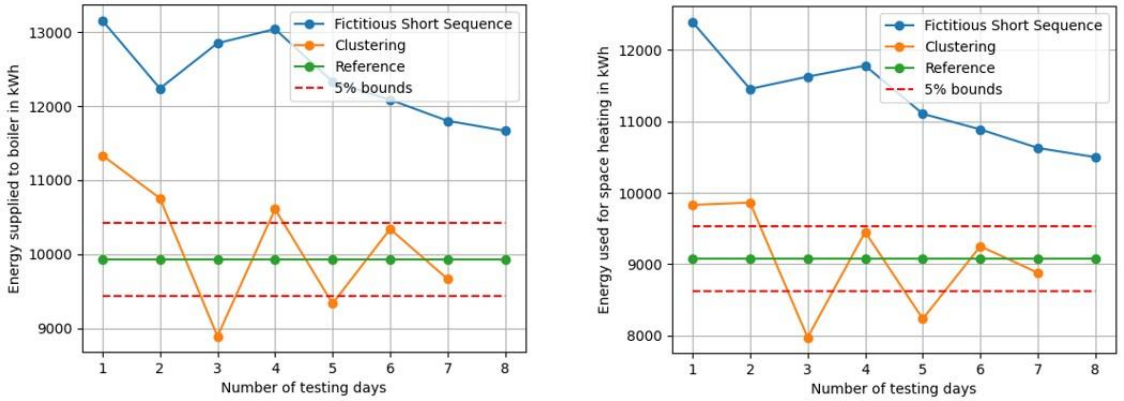

Figure 98:Boiler energy levels for FFT-based fictitious sequence

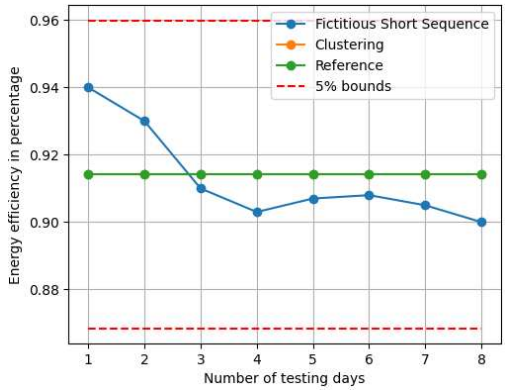

Figure 99:Boiler energy efficiency for FFT-based fictitious sequence

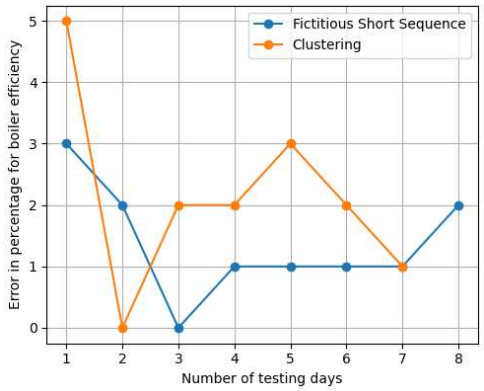

Figure 100: Error for boiler efficiency clustering vs FFT-based fictitious sequence

The energy efficiency of the boiler is shown in , as in the previous method of generating the fictitious sequence one could see that the efficiency of the boiler does not deviate by much. For the entire 8-day testing sequence it could be seen that the error in the seasonal energy efficiency is always sub 3%. But the same could not be said for the energy level of the boiler use case.

The error deviations are as high as 35% as shown in . This still does not satisfy our criteria of having a 5% error deviation in the considered KPIs. The FFT method also does not seem to produce the

best-desired result with a 5% error on all three KPIs. The same need not be experimented with for the heat pump because the idea is to reproduce the same results for both use cases. But the FFT method does not lead to convergence for all three KPIs. Hence, the next step will be to try the PSD method of generating the fictitious sequence.

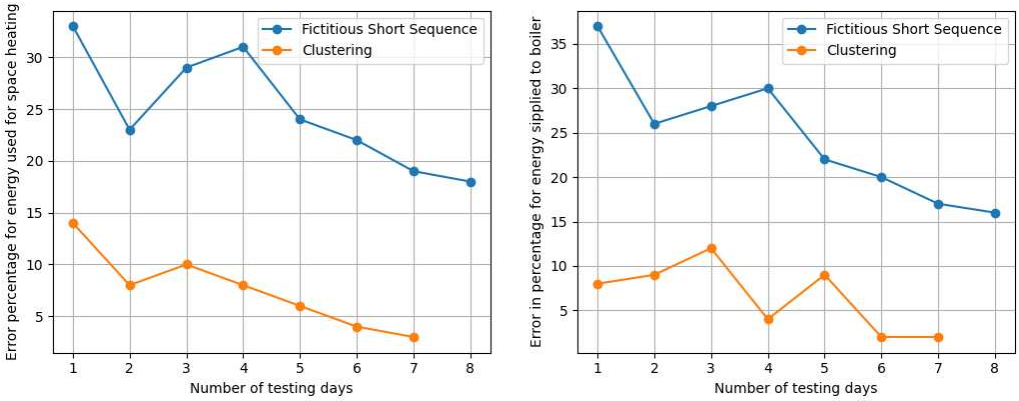

Figure 101: Error in energy levels for the FFT-based fictitious sequence generation method

5.1 Frequency domain-based sequence generation and analysis (PSD-based)

The next step in the fictitious sequence generation is to use the PSD as the objective function to generate the short sequence. The idea will be to match the PSD of the short sequence with that of the heating season. The constraint between the temperature short sequence and the irradiation short sequence will remain the same. If FFT can identify and estimate the dominant powers of the frequencies then PSD is useful for identifying the spread of the distortions on the specified signal along with the most dominating frequencies. This could also be a logical explanation for why in the FFT method of sequence generation, one was not able to reproduce the results as same as the heating season.

In short, what does the PSD represent one can ask, PSD represents the power density of the different bands of frequencies. Welch's method is used for the estimation of the PSD of the temperature signal and the short sequence. Welch's method computes an estimate of the power spectral density by dividing the data into overlapping segments, computing a modified periodogram for each segment, and averaging the periodograms as explained in [128] and [129]. The PSD of the original temperature signal and the one-day short sequence is shown in Figure 102 and the generated one-day short sequence is shown in Figure 103.

One can see that the PSD of the one-day short sequence is not able to match that of the whole heating season, plus it can also be seen that the spectral bandwidth associated with the temperature signal includes the frequency ranges until 0.0416 Hz (24-hour cycle).

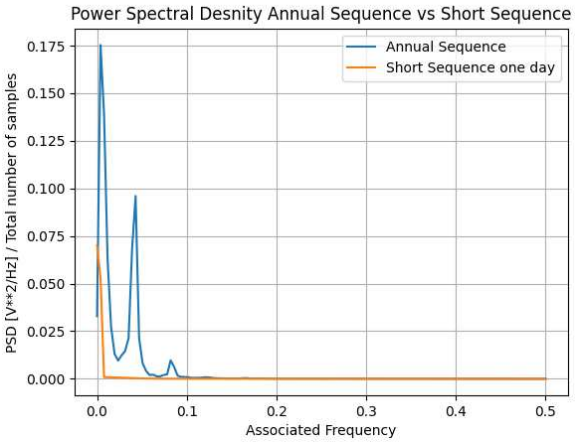

Figure 102: PSD heating season vs one-day shot sequence

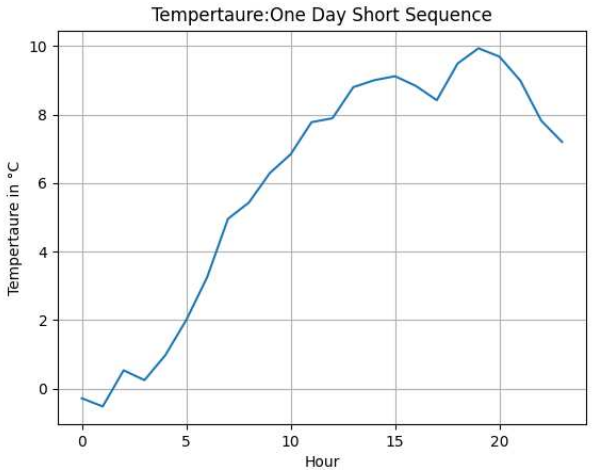

Figure 103: One-day temperature short sequence

From Figure 102 and Figure 103 it can be seen that the 24-hour cycle is not respected in the one-day short sequence one can see that there is a straight increase in the temperature from the start of the day to the end of the day.

The generated short sequence of the temperatures is shown in Figure 104. From the 3-day short sequence onwards, one can see three types of days represented. The first day starts with a very cold day, the second day is a day with many variations, and finally, a third day which is the same as the second day.

Unlike in the distribution method where the lowest temperature value reached was 1.27°C, in the PSD method the lowest possible value reached was around -3.0°C. The highest temperature value reached was around 18.9°C for the distribution method, whereas in the PSD method it was around 16°C.

The reason is that the distribution considers only the statistical moments of the signal while the PSD is more like treating the temperature signal as a random vibration signal. Hence, it considers both the temperature ranges and the dynamics associated with the temperature signal. When one cross-examines the PSD of the heating season with the PSD of the 3-day short sequence as shown in Figure 106 the 3-day short sequence covers most of the PSD spectrum in comparison to the heating season.

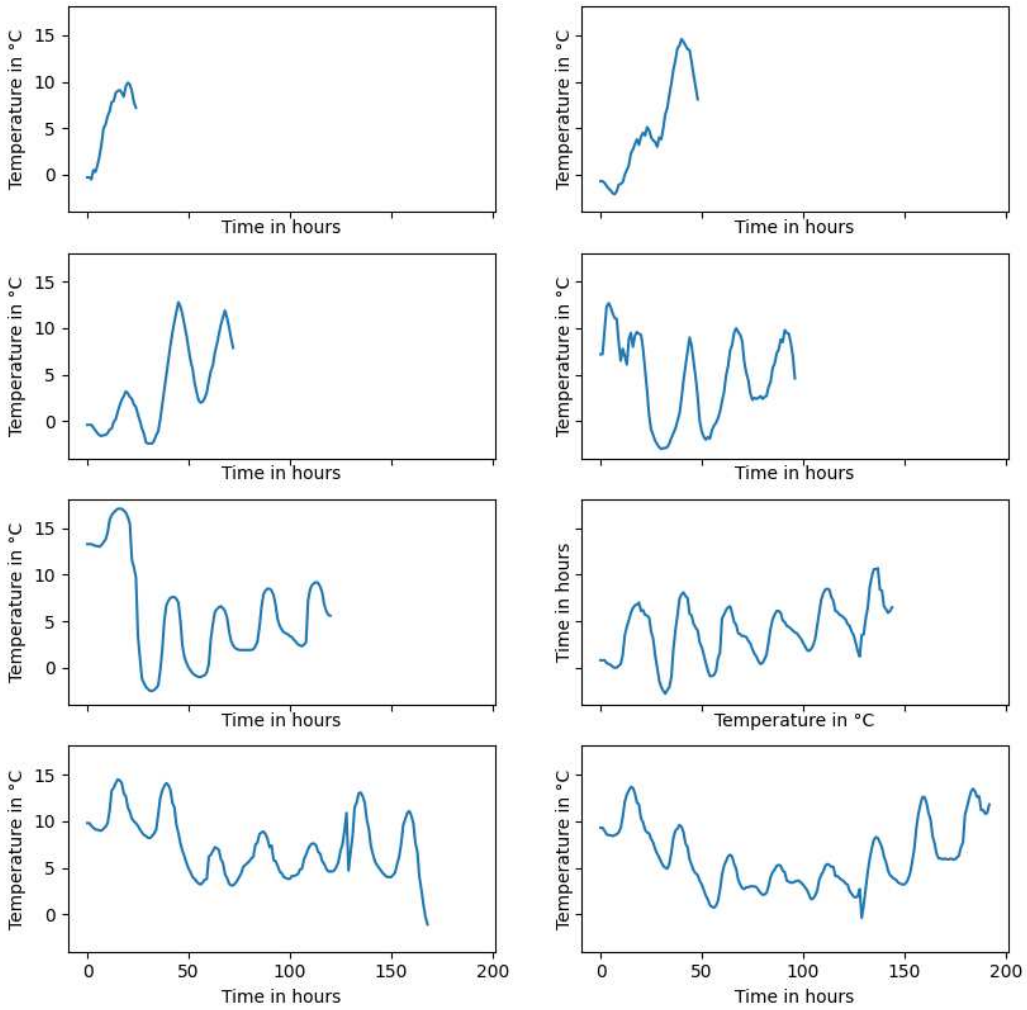

Figure 104: Temperature short sequences generated using the PSD methods from 1 day – 8 days

As one increases the number of days it could be observed that the PSD of the short sequence catches up with that of the heating season. The 4-day short sequence is the minimum number of days required to mimic the PSD of the heating season as one could see from Figure 107.

As one can observe from Figure 108 the five-day short sequence almost matches the PSD of the heating season. It could also be observed that there are few extra dynamics are also added to the short sequences. The phenomenon could be observed in Figure 108 where one can see that the part where the power spectrum distribution has zero density for the heating season is not the same for the short sequence where one can see some changes which have some values in that distribution area.

This keeps increasing as one increases the number of days hence one can conclude that the changes added might or might not cause many variations in the KPIs considered.

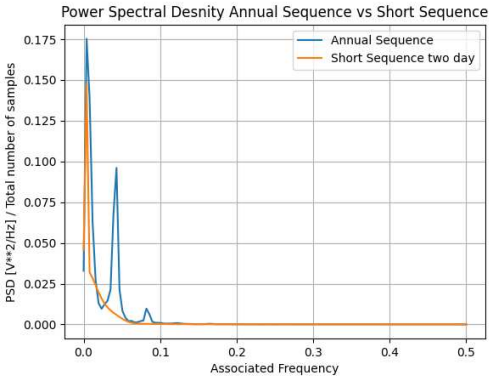

Figure 105: PSD heating season vs 2-day short sequence

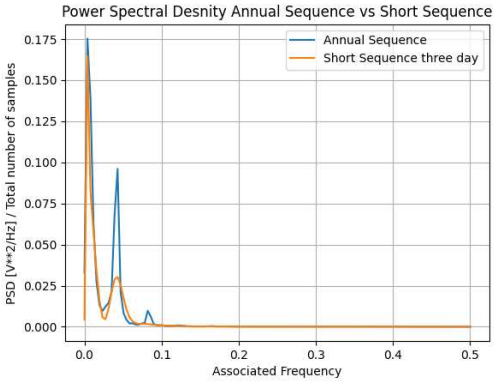

Figure 106: PSD heating season vs 3-day short sequence

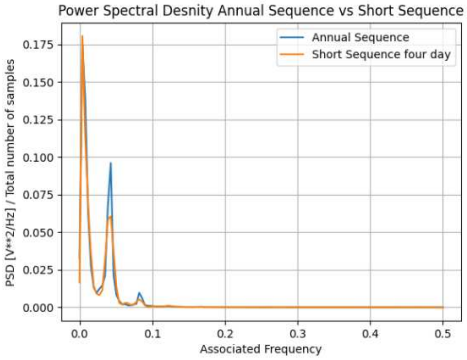

Figure 107: PSD heating season vs 4-days short sequence

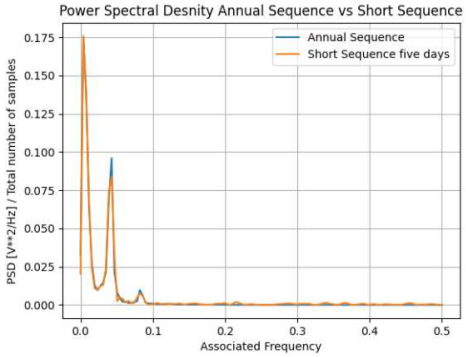

Figure 108: PSD heating season vs 5-day short sequence

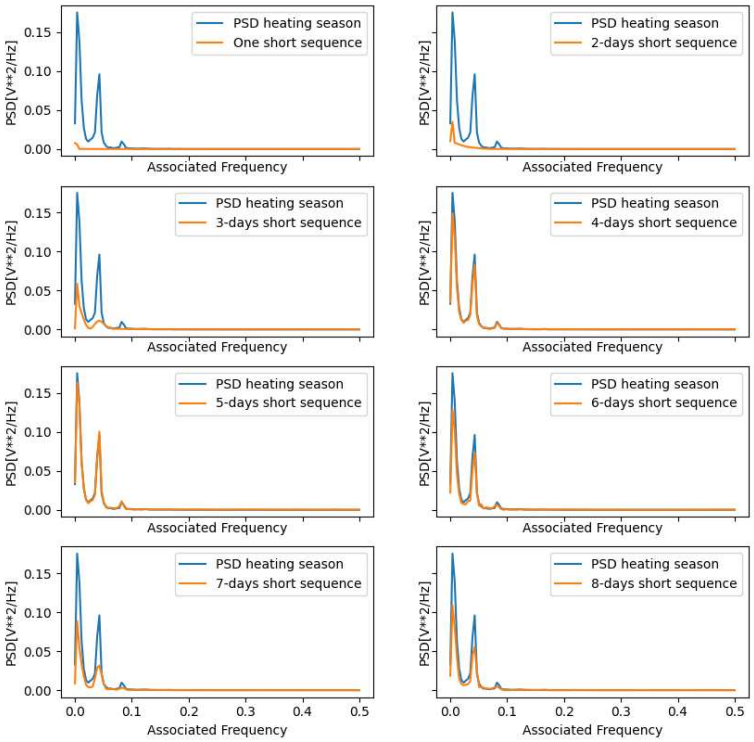

Figure 109:Comparison of PSD for temperature profiles heating season vs the short sequences

The irradiation sequences generated by the PSD method are also shown in Figure 110. When compared to the other methods of generating the short sequence the PSD method produces short sequences of the irradiation profiles with different days.

The representation of different days was not possible in the previous methods. But as the testing sequence crosses beyond 6-days on can see in both the temperature and the irradiation sequence that the optimization becomes computation heavy as the number of variables increase.

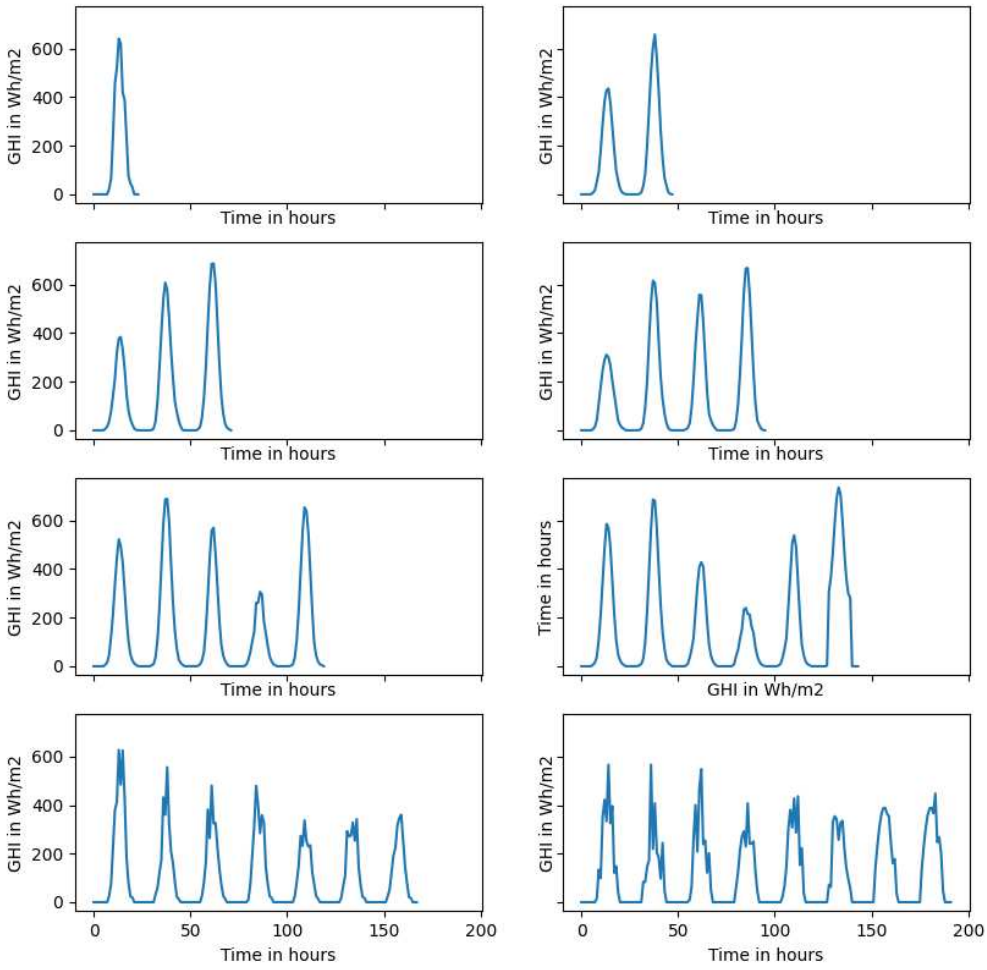

Figure 110: GHI short sequences produced by the PSD method

This could be due to the reason that the PSD take not only into account the FFT but also the noise distribution around the FFT. But one can also note that as the number of days increases the short sequence is not smooth, the same case that was seen in the temperature short sequence where there were two discontinuous patterns that were observed in the same point of time in the 7-days and the 8-days sequence as shown in Figure 110. The PSD of the irradiation sequences related to the short sequence and the

heating season are shown in the Figure 111. As seen with the temperature sequence, it can be noticed that the PSD method is capable of reproducing PSD like the heating season until 5-days short sequences. After that the accuracy if the optimization is not particularly good since the number of variables increases and the also there is a constraint to respect.

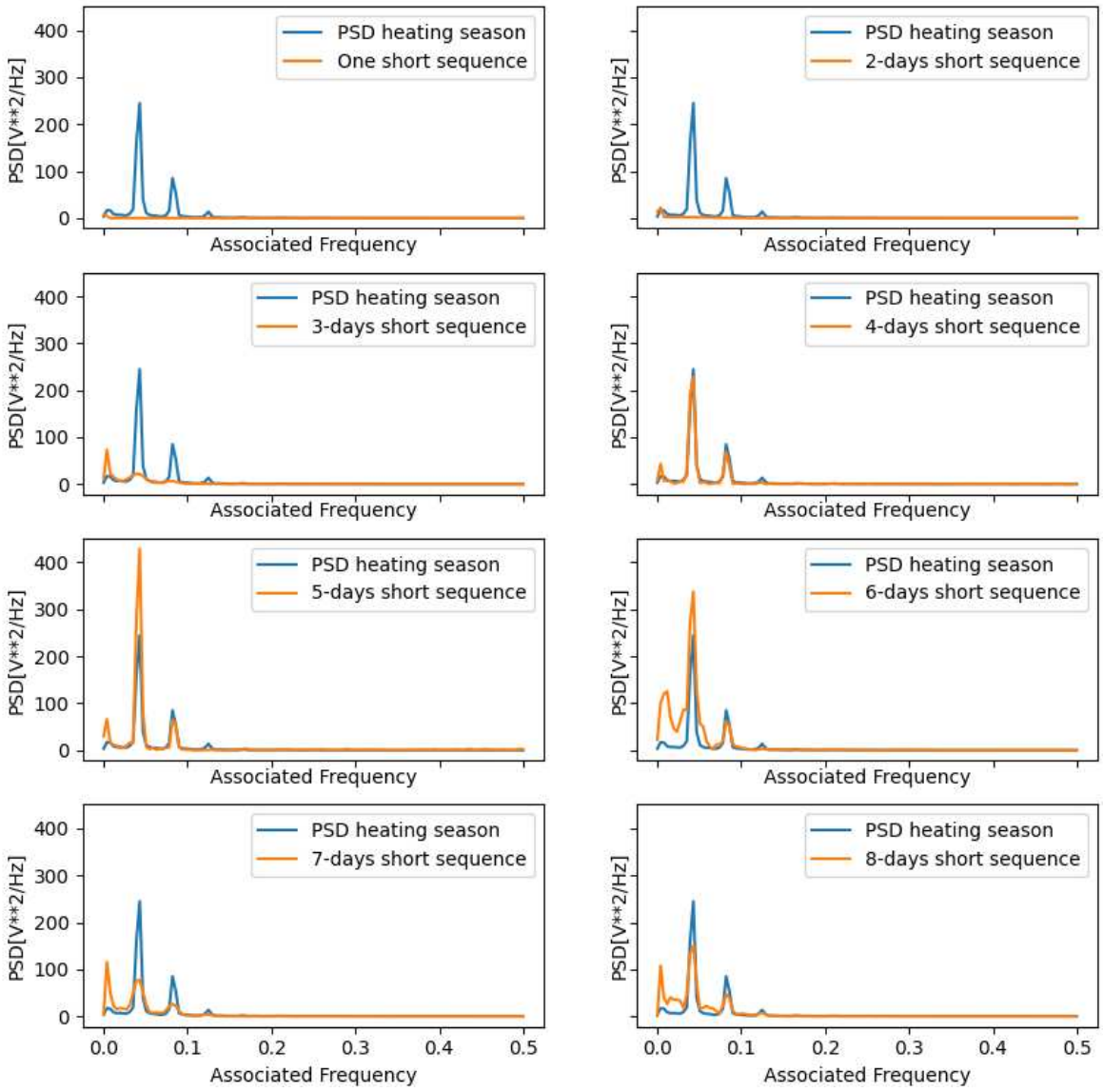

Figure 111: Comparison of PSD for irradiation profiles heating season vs short sequences

From the PSD of the heating season, the major contributing frequencies to the heating season are the 24-hour, 12-hour, and 8-hour frequency components shown in Figure 111. Also, one can see the decreasing order of the peaks with the most contributing frequencies in the heating season. Meaning that these dominant frequencies are enough to represent the whole heating sequence equivalent to the short sequence. For both the temperature and the irradiation sequence the most dominant frequencies to be

represented in the short sequences can be observed from the PSD of the heating seasons, unlike in the FFT where the entire ranges of all small frequencies are represented.

The objective function for both the short sequences is evaluated using the RMSE between the heating season PSD and the short sequence PSD. The main point to be noticed is that in both the use cases the 4-day short sequence seems the one closest to the actual heating season this could either mean that from the 4-day sequence onwards one could see a convergence. The other point to be understood is that there are over and under representations of certain frequencies and check whether this could cause a problem with the convergence for those short sequences. Meaning, that for the short sequence until the 3-day short sequence there is no representation in the dominant frequencies for the 5-days and 6-day short sequence.

By simulation one needs to check if there is only a minimum representation required for the PSD in the short sequence or should the PSD of the short sequence should match exactly with the heating season. While there is overcompensation for the 24-hour frequency in the 6-day short sequence. The RMSE values when compared with the PSD of the heating season for both the temperature and the irradiation sequences are shown in Figure 112 and Figure 113.

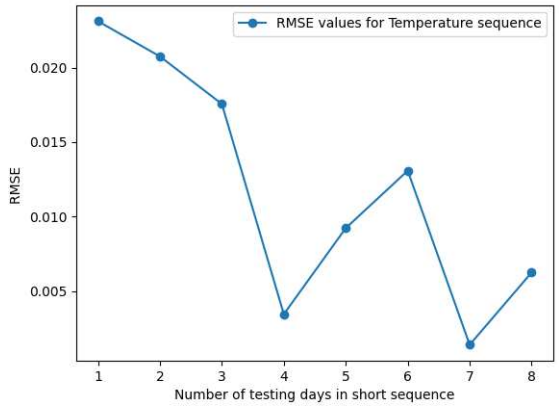

Figure 112: RMSE values for temperature sequence

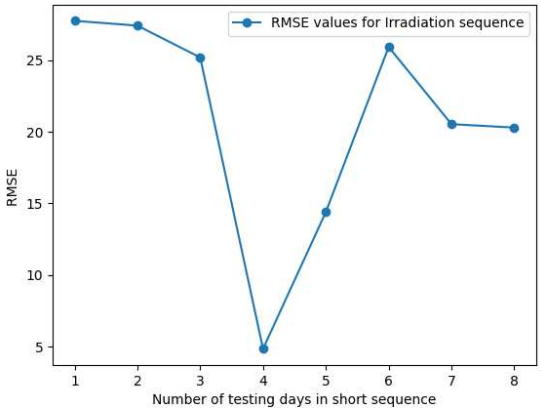

Figure 113: RMSE values for irradiation sequence

From both, cases it can be seen there is a downward trend but not exactly a completely decreasing trend. The next step will be to verify the correlation between both the short sequences with that of the whole heating season as shown in Figure 112 and Figure 113. Unlike in the statistical method, there is no need to specify a second constraint on the temperature sequence since one operates in the frequency domain. The correlation between temperature and the irradiation sequence is shown in Figure 114, one can see that although the correlation does not match exactly with that of the heating season as one increases the days the correlation catches up with that of the heating season. Although the PSD of the

short sequences is not the same when the number of days is increased the correlation constraint catches up as the number of days increases.

The results for both the boiler and the heat pump use case are shown in Figure 115 and Figure 116. For the boiler use case, the PSD method reproduces the KPIs within the 5% error bounds. As expected the convergence starts from the 4-day short sequence onwards also there is no need to exactly represent the PSD of the heating season, a small representation of the important frequencies is enough to reproduce the results for the heating season. For the boiler use case, the convergence starts to happen from the 4-day sequence onwards if the PSD method is used, while a 6-day short sequence is required minimum to reproduce the heating season results.

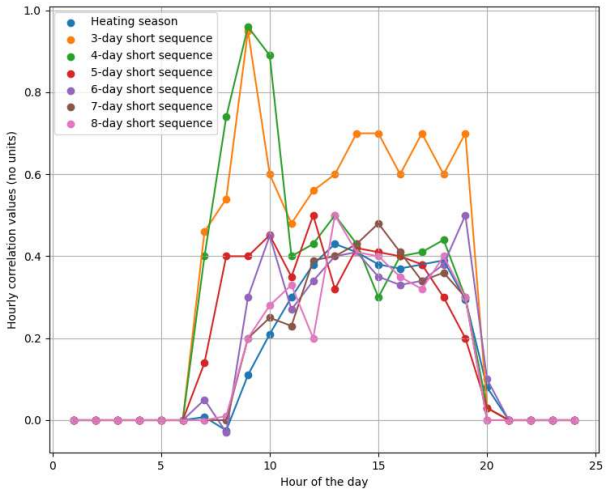

Figure 114: Comparison of hourly correlation for temperature and irradiation, heating season vs short sequence

The same could also be said for the heat pump use case as shown in Figure 116, which is identical to the boiler use case scenario where a 4-day short sequence best reproduces the results achieved in the heating season in a noticeably short testing period. Moreover, as one can see that convergence happens on a very lesser number of days as well. The convergence happens if there is a minimum representation of the PSD with the important frequencies namely the 24-hour frequency, 12-hour, and 8-hour frequency for a few days, in this way one could reproduce the KPIs for the actual heating season.

To find and represent the most dominating frequencies of the heating season, it is better to use the PSD instead of the FFT with the underlying philosophy to treat the signal as a random vibration signal. Moreover, as one can see that convergence happens on a very lesser number of days as well. The convergence happens if there is a minimum representation of the PSD with the important frequencies namely the 24-hour frequency, 12-hour, and 8-hour frequency for a few days, in this way one could reproduce the KPIs for the actual heating season. To find and represent the most dominating frequencies

of the heating season, it is better to use the PSD instead of the FFT with the underlying philosophy to treat the signal as a random vibration signal.

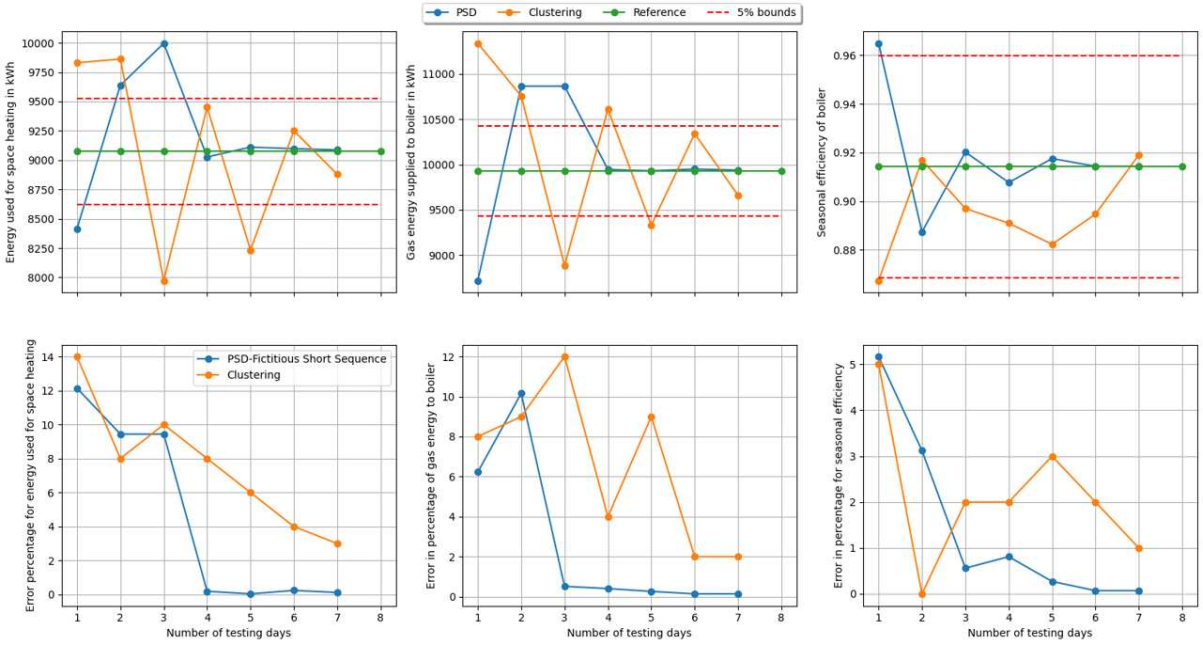

Figure 115: Results for boiler use using PSD-based fictitious sequence generation

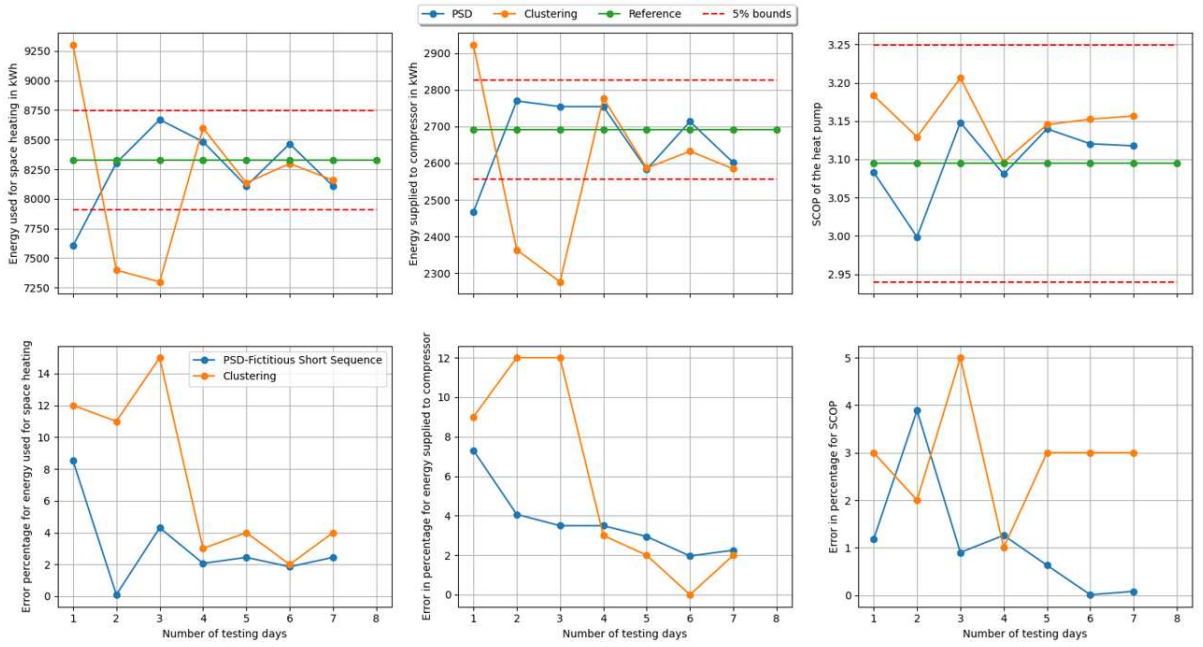

Figure 116: Results for heat pump use case – PSD - based fictitious sequence generation

Also, it could be confirmed that the idea will be to find the minimum number of days to represent the PSD of the heating season. The representation of the PSD after that minimum number of days does

not change the result which could be seen from the seven-day and the eight-day sequences. In one way one could conclude that the PSD method gives consistent results because mostly after the 4-day short sequence, the results are the same without much deviation, leading to better convergence for both the boiler and heat pump use case. Thus, the FSG-PSD method not only reduces the time taken for reducing the simulation time, plus also manages to represent the non-linearities in the signal and can converge to the required error bounds as explained in the section (nature of the problem to be solved).

5.2 Observations

While comparing all three methods with one another, the statistical method of FSG produces seasonal efficiency very close to the heating season, while the energy levels are not represented properly. While the PSD method based FSG can reproduce the results of the heating season with better accuracy. Moreover, the results obtained using this method seem consistent for the use case under consideration as shown in Figure 117 and Figure 118. From both the figures, one can see that the FSG-PSD method is better in terms of reproducing the energy levels and the seasonal efficiencies in a lesser number of days. The clustering method also reproduces the same results as the PSD method does but in more days. The FSG-Distribution method better reproduces the seasonal efficiency as close to the heating season. But it does not reproduce the energy levels.

The next point to be noted is that the distribution method can be used to represent the static-non linearities like the maximum and the minimum values in the weather profiles. But the dynamic non-linearities like the hour-wise weather variations are difficult to represent since the distribution of the signal does not represent the dynamic non-linearities in the signals. While the FSG-PSD method can represent the intensity vs the frequency of a signal, which makes it easy to represent the dynamic-non-linearities. The static non-linearities like the maximum value and the minimum values of the temperature need not be represented since in a heating season the number of hours the system needs to operate in extreme conditions is very less.

The very next observation that one can make is the time taken for the optimization algorithm to produce the short sequence. The time taken for the one-day sequence for the FSG-PSD and the FSG-Distribution is around 15 minutes. While the time taken for a 4-day short sequence is around 1 hour respectively for the FSG-PSD method. For a 7-day short sequence for the FSG-PSD method and the FSG-Distribution, a few hours were taken for the generation of the short sequence.

The next observation that one could make is that the short sequences that are produced by the optimization method are consistent, in one way one could assume that the short sequences generated can be considered the global optimums.

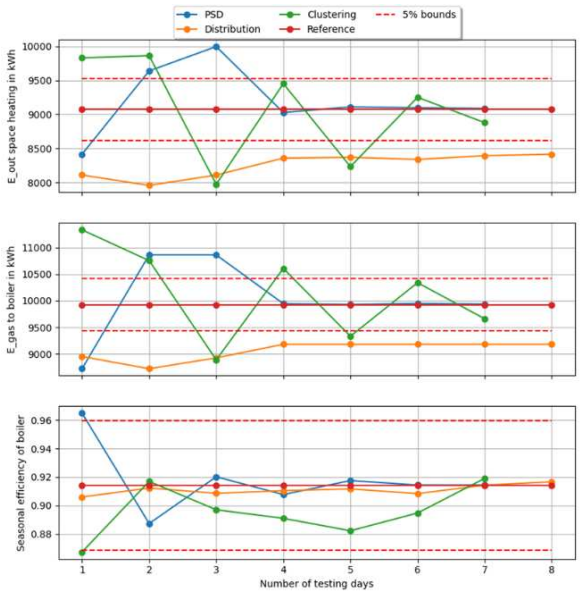

Figure 117: Comparison of methods for the boiler use case

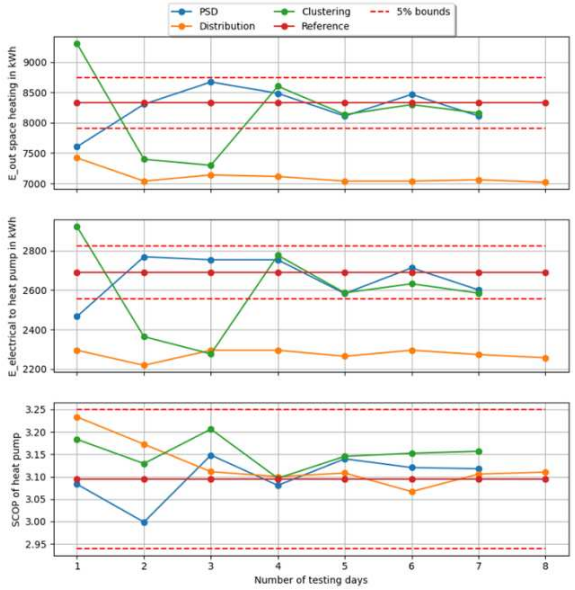

Figure 118: Comparison of methods for heat pump use case

5.3 Conclusion

The FSG method of generating the short sequences was able to reproduce satisfactory results for the use cases under consideration, for a short number of days without any discontinuities between them. But, the main problem involves generating multiple sequences, too many variables to optimize, plus also a very time-consuming process.

The average time taken for generating one short sequence was around 10-minutes. While the 7-8 days short sequence was generation took several hours, this part of this method requires a workaround. Also, only the temperature and the irradiation sequences were generated since the DYMOLA simulation environment needs these two variables as a minimum physical phenomenon to run the simulations.

The next step will be to verify if the same PSD method works for other weather conditions and a different building use case based on simulations which will be covered in the next step. Also, it would be useful to see if the process could pose any uncertainties on the final ranges of the KPIs. Also, it would be useful to see if such a process would represent some uncertainties in the result obtained during the simulation. This would take us again to the nature of the problem that is being solved. The idea was to generate a short sequence that would enable one to reduce the heating season results with a smaller number of days possible with no discontinuities. The non-linearities in the temperature and the irradiation signal are represented by the FSG-PSD method. The method guarantees the convergence of the KPI, and the reproducibility of the results need to be ensured. This step will be addressed in the next chapter of this thesis.

6. Verification of the short sequence methodology

6.1 Introduction

In the previous section one could conclude that the power spectral analysis based fictitious sequence generation yields the best results for the KPI's under consideration for one weather use case. The next step will be to check what could be the uncertainties related to the methodology of reducing the short sequence. The reason being that the test bench by itself does not introduce uncertainties on the result as explained in Chapter 2. Hence, the next logical step would be to check if the methodology of reducing the short sequence could pose any significant changes on the results. This chapter is dedicated in analyzing the KPIs in four different avenues, they are:

1. Verify if the short sequence philosophy can reproduce the seasonal efficiency for a different climatic condition
2. Verify if the short sequence can reproduce the same results for a different building envelope (RT2012)
3. Analyze the results based on the parameters of the Differential Evolution algorithm (DE algorithm)
4. Analyze the uncertainty and sensitivity due to the choice of the optimization algorithm (Differential Evolution vs Dual Annealing)

The main rationale is that there are two parts that are to be addressed, one is the verification part where one must verify if the same methodology will hold good for another climatic conditions. For example, Trappes is in the norther region of France characterized by higher variations in the weather profiles. It would be beneficial to see if the same could be applicable for another climatic condition in the other regions of France.

The second sub part of the verification process will be to verify if the same short sequence generated for Trappes will be able to generate the same results for another building environment with different insulation settings (a building with RT2012 standards). The first use case was a building without proper insulation which was very reactive to the external weather conditions, since there was not much insulation, leading to higher energy consumption and it would be useful to check how the short sequence will hold for buildings with better insulation. For both the climatic and building envelope verification, the main result area would be to check if the short sequence is able to reproduce the same results that were produced in the entire heating season. This could also confirm that the results produced for the Trappes, and the single zone use case is not only limited to one use case.

The third step will be to make a noticeably short uncertainty analysis based on the methodology, of which one must generate several sequences and then verify from the results what are the possible uncertainty bounds. This can be done by trying to evaluate different parameters of the DE (Differential Evolution) algorithm. The main result that one would need to check is that if all the sequences generated would reproduce the KPIs within the 5% error range or if there could be outliers.

The last step will be to check using another algorithm different from the DE algorithm that will be able to re-produce the same result for the 4-day short sequence scenario. This is done to ensure if the method of optimization might or might not pose any significant uncertainty due to the change in the optimization algorithm. Since the optimization algorithm is the one that is generating the short sequence based on the objective functions and the appropriate criteria that need to be verified by simulations. If the short sequences produced by the optimization algorithm (other than the DE algorithm) can consistently reproduce the same results or within the 5% error bounds for all the KPI's or results like the DE algorithm. Then one could conclude that the optimization does not induce much uncertainty.

The flow of the chapter is organized in the same order and in the conclusion of the chapter few of the concluding remarks on the methodology of adoption are explained. After all these steps the next step will be to verify by experimentation if the same results could be achieved using the HIL test bench in the next chapter if possible.

6.2 Verification of KPIs for different climatic conditions

6.2.1 Choice of weather data and full year simulation analysis

The main aim of this section is to check if the short new sequence reduction will work for another climate in another region. For the initial use case the weather data of choice was Trappes which belonged to the HI region in France, usually H1 regions are characterized by territories with the coldest winter temperatures. This area corresponds to the eastern and northern departments of France under the influence of a semi-continental climate.

The weather data of choice is for La Rochelle since the summers are comfortable, winters are very cold and windy, and it is partly cloudy around the year and belongs to the H2 region. The approach adopted is like the use cases shown in the second and the third chapters, the first step will be to analyze the weather data for the chosen weather file. The temperature distribution and the irradiation distributions for the heating season are shown in the Figure 119 and Figure 120, from which one can see that the ranges of outside air temperature varies from -3.5°C to 25°C and 0 W/m2 to 900 W/m2 for the irradiation respectively.

From the distribution of the temperature one can say that for most parts of the heating season the temperature is from the range 2.5°C to 13°C. In short one can say that if the short sequence can effectively represent this temperature range one can be able to see the results close to the entire heating season simulation.

The results for the entire heating season concerning the boiler use case simulation are to be analyzed, the gas energy supplied to the boiler during the heating season daily is shown in the Figure 121. The lowest possible energy value is around 8kWh while the highest possible value is around 130kWh, with the average energy levels being 31.3 kWh. The energy used for the space heating ranges from around 6kWh – 122 kWh, with the average value being 28kWh for the energy used for the space heating purpose. Also, one could observe that as the transition happens from the winter season to the mid-season one could see that the energy level goes down. It is interesting to see if the short sequence can represent this average energy levels during the short sequence simulations.

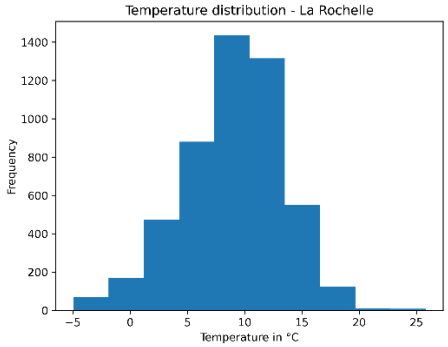

Figure 119: Temperature distribution for La-Rochelle

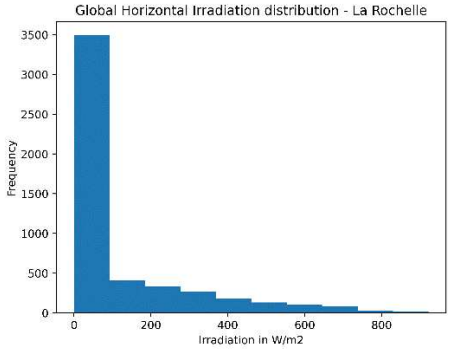

Figure 120: Irradiation distribution for La-Rochelle use case

From Figure 123 one can see the range of boiler seasonal efficiency values from 0.77 to 0.96 for the days that are cold one can see a decrease in the efficiency values since for the condensing boiler one must operate at 100 percent loads which leads to lesser efficiency. While the seasonal energy efficiency of the boiler is around 0.895. The total gas energy supplied to the boiler for the entire heating season is around 11387 kWh, while the total energy used for space heating is around 10187 kWh.

Similarly, the annual simulation results for the heat pump are shown in the Figure 124, Figure 125 and Figure 126. The results are obtained from the building model that were introduced in Chapter 2, where there was a single zone building with a single layer of insulation.

The total energy supplied to the compressor for the heating season is shown in Figure 124, the maximum energy supplied to the compressor heat pump is around 39kWh, while the lowest value is around 3kWh, the total energy supplied to the compressor is around 2854kWh. The scatter plots give us

the idea of the energy consumption and utilization factor over the heating season, it is useful to see which parts of the heating season demands average and extreme operating conditions.

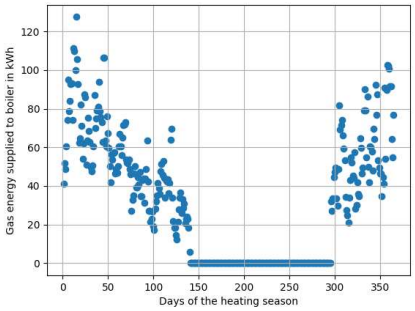

Figure 121: Gas energy supplied to boiler

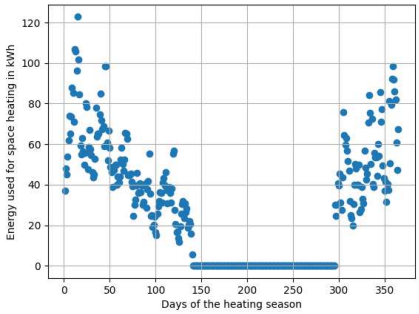

Figure 122: Energy used for space heating- boiler use case

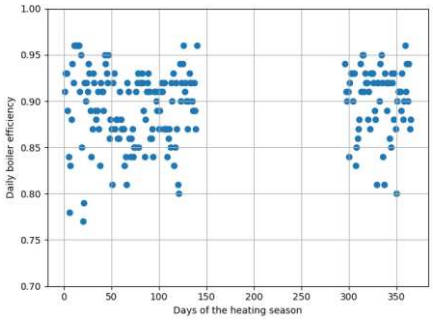

Figure 123: Daily energy efficiency of the boiler for the heating season

The daily values for the energy used for the space heating is shown in Figure 125, the most required energy for space heating is around 105kWh, while the minimum value is around 10kWh. The total useful energy used for the space heating is around 9108kWh. The daily COP values for the heating season are represented in Figure 126. The range of values for the daily COP are from 2.7 to 3.7. The seasonal COP for the heating season specifically for the heat pump is around 3.19.

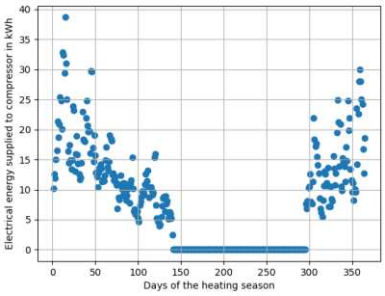

Figure 124: Energy supplied to the compressor–heating season

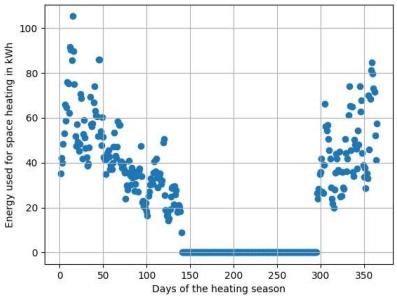

Figure 125: Energy used for space heating - heating season

It could be seen from all the three plots at the beginning of the year when there is a winter season one can see higher energy levels and continues a decreasing trend as the mid-season approaches and after the

summer as one could see an increasing trend because of the approaching winter season. Simultaneously one could also see that the daily COP values are lower at the starting of the heating season due to the outside air temperature being low. As the mid-season approaches one can see that the COP increases as the outside conditions improve from winter to the mid-season.

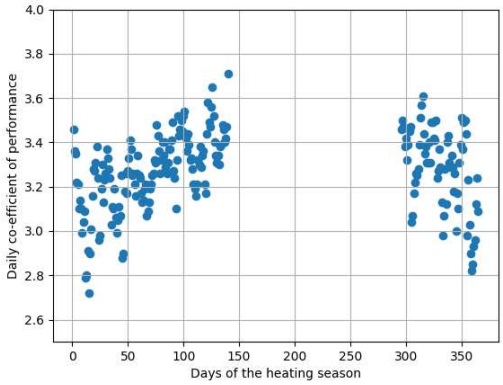

Figure 126: Daily COP during the heating season

Also, one can see that at the end of the summer one can see a downward trend in the COP leading towards the winter season for the air-to-water heat pump. The summary of the annual simulations for the La Rochelle use case for the same buildings and the equipment's are shown in the Table 14.

Table 14: KPI's for La Rochelle use case – space heating for heating season

KPI	Boiler	Heat Pump
Energy supplied to equipment	11387 kWh	2854 kWh
Energy used for space heating	10187 kWh	9108 kWh
Seasonal efficiency	$\eta_{sesonal}$ = 0.895	SCOP = 3.19

6.2.2 La-Rochelle weather use case short sequence generation

The total number of days in the heating season is around 210 days. The next step will be to generate the short sequence based on the power spectral density method of fictitious sequence generation. The generated temperature short sequence is shown in Figure 127. From the short sequence the ranges of the temperatures covered are from -2.5°C to 18°C. The first day has high-temperature variations for each hour, this must be considered because of the method of optimization, since the aim is to match the power spectral density of the heating season with that of the power spectral density of the 4 days short sequence.

The three other days are very cold days. The other point to be noted is that to match up with the PSD of the heating season , the PSD-FCG method introduces two days that are like one another, to match the amplitudes of the power spectrum. As with the previous use case for Trappes the time take for the optimization to produce the short sequence is high (around 90 minutes). The reason being that the number of variables to optimize for the temperature sequence is around 96 for four days.

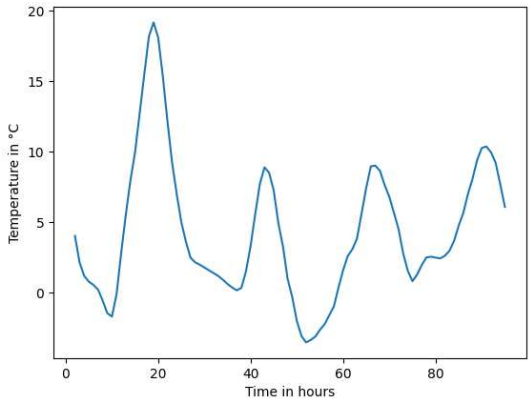

Figure 127: Temperature short sequence for La Rochelle use case (4-days)

There are 210 days and 4-days are used to represent the heating season as a short sequence. This has an implication on the first day. The first day of the sequence when analyzed, one can see that the day has extreme cold hours combined along with the mid-day where the temperature reaches 18°C.

Also, the point to be noted is that the temperature variations are also huge for each hour. But it does not exceed the maximum hourly variations possible in the heating season (which is 3.5°C for the entire heating season), the overall observation being that the first day is a hybrid day that combines multiple aspects of the heating season. The power spectral density of the temperature profile of the heating season and the short sequence is shown in Figure 128.

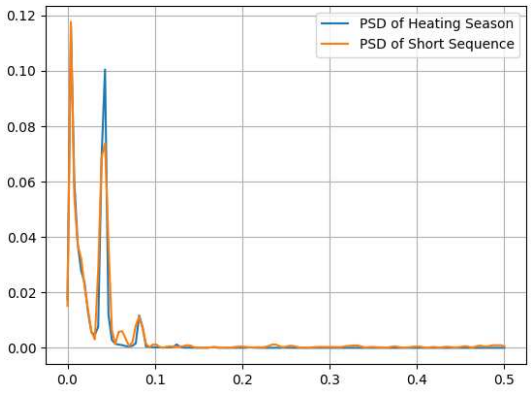

Figure 128: PSD heating season vs short sequence La-Rochelle use case

As seen that the initial peak corresponds to the whole season as explained earlier due to this one was able to see a hybrid day combining multiple seasonal aspects in first day of the short sequence. The second peak corresponds to the 24-hour frequency , while the smaller third peak corresponds to the 12-hour frequency. When compared to the FFT where one had all the possible frequencies , the PSD method is useful in representing the most important frequencies of the heating season along with the added advantage of representing the energy per unit frequency.

It is seen that the power spectral density is not exactly as same as the heating season, but it should be able to reproduce the results to some extent or at least within the 5% error bounds. The next step will be to generate the hourly temperature correlation between the temperature and the irradiation sequence as a constraint to produce the short sequence. The generated irradiation short sequence in correspondence to the heating season is shown in Figure 129.

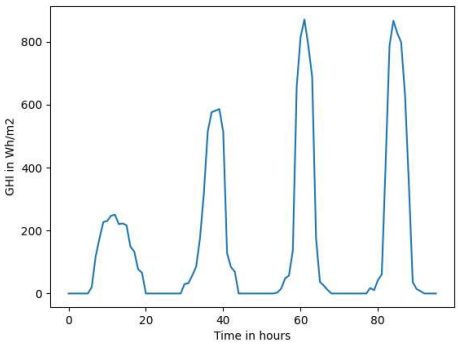

Figure 129: Irradiation short sequence for La-Rochelle use case

From the short sequence it can be noted that the short sequence represents three distinct types of days. One being the cloudy day where the irradiation is very less. The second day being the average day with normal irradiation while the last two identical days have two identical irradiation patterns. The PSD of the irradiation sequences for both the heating season and the short sequence are shown in the Figure 130.

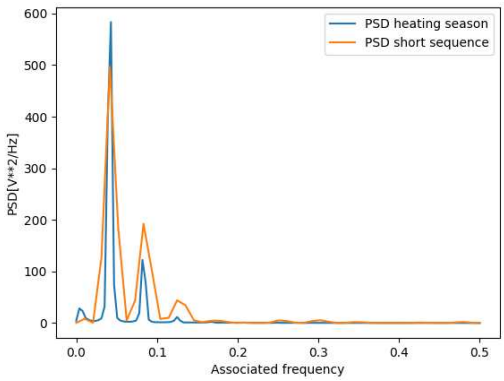

Figure 130: PSD for irradiation sequences, heating season vs short sequence

One could notice that there is a representation for the 8-hour frequency the fourth spike in the power spectral density, this is due to the 8 hours each day where there is irradiation. This is what is observed from the small 5-hour peak in the power spectral density.

6.2.3 Simulation result analysis-La Rochelle Use case

The short sequences that are generated are used for the simulation for the single zone building (single layer of insulation) use case with the boiler and the heat pump, respectively. The extrapolation factor is 210/4 since, in this power spectral density based fictitious sequence generation method does not have the same distinction as the clustering methodology where one is able to obtain the weight on each of the representative days under consideration.

The comparison of the energy levels for both the boiler and the heat pump are shown in Figure 131. One can see that the energy levels do not vary much and are within the 5% error bounds for the energy levels on the first glance.

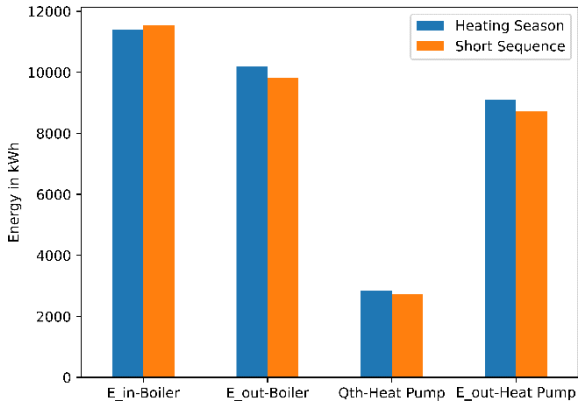

Figure 131: Comparison of energy levels for heating season vs short sequence

The SCOP (Seasonal Co-efficient of Performance) and the seasonal energy efficiency of the boiler are compared between the heating season and the short sequence are shown in Figure 132. The values for the seasonal efficiencies for both the use cases seem to be well under the 5% error ranges. The short sequence for 4 days is minimum enough to reproduce the results like the heating season.

The results for the short sequence for each day are shown in Table 14,where $E_{Gas\text{-}Boiler}$ is the gas energy supplied to the boiler, $E_{Out\text{-}Boiler}$ is the energy used for the space heating related to the boiler, $E_{Out\text{-}Heat\ Pump}$ is the energy used for space heating , $Q_{Electrical\text{-}Compressor}$ is the electrical energy supplied to the compressor. From the Table 15 although the short sequence can produce the results within the desired error ranges one can see that all the days are similar in the energy consumption patterns.

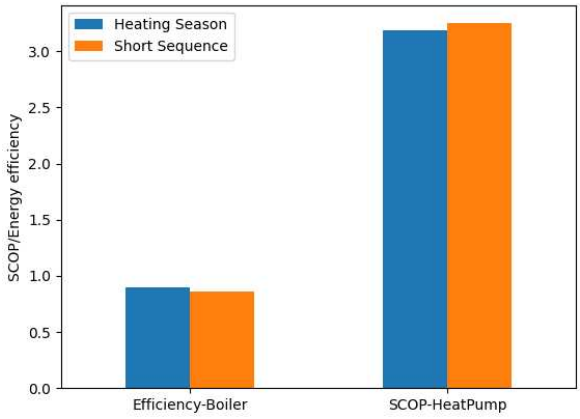

Figure 132: Seasonal efficiency/SCOP heating season vs short sequence

Meaning that the short sequence produced based on the fictitious sequence might not be able to well represent all the micro details within that heating season or during that test year. Also, from the short sequence generated for the La-Rochelle use case shown in Figure 127 one can see that all the four days in the short sequence had cold temperature hours. The extreme days are not represented enough, but most of the days fall between the range where the daily energy efficiency ranges of the boiler are from 79%-92%.

Table 15: Short sequence results for each day

Day	$E_{Gas\text{-}Boiler}$ (kWh)	$E_{Out\text{-}Boiler}$(kWh)	$\eta_{sesonal}$	$E_{Out\text{-}Heat\ Pump}$ (kWh)	$Q_{Electrical\text{-}Compressor}$ (kWh)	COP_{Daily}
1	55.60	49.96	90%	46.96	14.69	3.20
2	59.05	47.71	81%	40.76	13.09	3.11
3	51.81	40.92	79%	36.73	11.46	3.20
4	52.69	48.42	92%	41.55	12.65	3.28

Also same is the case when one looks at the daily results for the heat pump use case, most of the daily COP values fall between 3.1-3.3. But, when one looks at the energy consumption pattern the same analogy does not hold good when compared to the daily COP/ daily efficiency values. Hence, one could conclude that although three KPI's of the heating season are reproduced well the micro details of the heating season are not accurately represented as shown in Table 16 and Table 17. From both the tables one could also see that the short sequences could just reproduce the results for the heating slightly under the 5% error band and this is due to the reason that the 4-day PSD did not accurately match with that of the heating season for both the irradiation and the temperature short sequence.

The reason being that a fictious sequence is used for running the tests instead of the exact days from the full year / heating season. The next step will be to verify if the same results can be reproduced

for another building use case namely a well-insulated building based on the RT2012 standards. This could confirm that despite having the short comings of not representing certain micro details corresponding to the heating season, the short sequence could better the KPI's related to the overall heating season. If the PSD-FCG method could produce the expected results the next step will be to see what the uncertainties on the results could be.

Table 16:Results for heat pump use case-space heating

KPI's for heat pump use case	Heating Season	PSD-FCG short sequence	Error
$Q_{Electrical\text{-}Energy\text{-}Compressor}$	2854 kWh	2730 kWh	4.3%
$E_{Out\text{-}Heat\ Pump}$	9108 kWh	8715 kWh	4.3%
SCOP	3.19	3.2	3.0%

Table 17: Results for boiler use case – space heating

KPI's for boiler use case	Heating Season	PSD-FCG short sequence	Error
$E_{Gas\text{-}Energy\text{-}Compressor}$	11387 kWh	11550 kWh	1.4%
$E_{Out\text{-}Boiler}$	10187 kWh	9817 kWh	3.6%
$\eta_{sesonal}$	0.895	0.86	3.9%

Although, a real round robin method of testing is required to establish the actual uncertainties related to the experimental analysis as demonstrated in [59].

6.3 Verification of KPIs for a different building envelope

6.3.1 Model description and use case analysis

The next step will be to verify if the generated 4-day short sequence can reproduce the results for another building use case. A building with RT2012 standards is chosen for the use case demonstration. For a better understanding the idea will be to first check by short sequence what are the results that are obtained from the extrapolation and then try to analyze the one-year results to check by simulation if the obtained short sequence can reproduce the same results.

In short the building is slightly larger form the last use case, the habitable area of the building is around 100m^2. The building model is a detailed model of the building with different rooms the building has living are, three rooms, a grange , a veranda, and a bath area. The interior wall of the building has three layers of insulation while the external wall has two layers of insulation. The thermal conductivity for the 2 layers of insulation in the external wall are 0.2 and 0.032 W/m^2K. The thermal conductivity values for the internal wall for the three layers are 0.013 W/m^2K, 0.1 W/m^2K and 0.013 W/m^2K,

respectively. For the window area the U value of the frame is 1.4 W/m^{2}K. There is only one insulation layer for the ceiling whose U value is 0.2W/m^{2}K.The floor also has two layers of insulation whose corresponding U values are 0.06 W/m^{2}K and 0.15 W/m^{2}K, respectively. When compared to the earlier use case where there was only one single layer of insulation the building in this use case is well insulated, meaning that the energy levels could be very less when compared to the previous use case. The maximum values of power for the radiators in the living area is around 1800 W, for the three chambers they are 1000W, 900W and 1100W, respectively. The maximum radiator powers for the bath area and the veranda are fixed at 800W and 1000W. The spatial-temporal variation of the radiators is fixed at 0.7 The boiler use case is chose for this scenario. The power required at each time step is calculated by considering the heating needs of all the rooms. Based on the power required the boiler is operated based on the simple ON/OFF control meaning this could reduce the efficiency of the boiler , the efficiency of the same condensing boiler with ON/OFF control was demonstrated in the uncertainty analysis in the second chapter, where the seasonal efficiency of the boiler was found to be around 0.7, more or less the same result should be applicable for the chosen use case well. The weather profile for this use case verification is Trappes , Fr.

The boundary conditions for the building are the maximum supply temperature of hot water from the boiler is fixed at 60°C while the maximum allowable return temperature back to the boiler is around 50°C. The temperature in the living area during the period of occupancy is 22°C and 16°C during the period of inoccupancy. While for all the three other rooms the boundary conditions for the internal air temperature are around 20°C during occupancy and 16°C during the period of occupancy. The boundary conditions for the temperature are same as the three other rooms, 20°C during the period of occupancy and 16°C during the period of inoccupancy. The next step will be to analyze the temperature and the energy profiles of the building to check if the building model is simulating what is required.

6.3.2 Building model Analysis

The model is analyzed for a one-day simulation to see if the temperature set points are respected in each of the rooms and the corridors etc. A typical one-day analysis is done to ensure that the temperature set-points are respected along with the comfort levels. The temperature for all the other rooms apart from the living area is shown in Figure 133 from which one can see that the insulation of the building provides a better thermal comfort. The temperature is always maintained under the comfortable range, apart from room 2 where there is an offset of 1°C due to the control strategy. The strategy is to calculate the power required for a particular room as a proportion of the total power at that time, based on this the boiler is either turned ON/OFF. Initially one could see that the heating is not required for the zone, hence one could see a decrease in the temperature slope, from 22°C onwards to the 19°C set point

mark. Also, one could notice that during the transition from the occupancy to inoccupancy period, unlike in the previous model one could see the slow transition in the temperature of the set-points. This also being one of the reasons one could anticipate a lower consumption in energy because there is no need to operate the equipment during the period of inoccupancy.

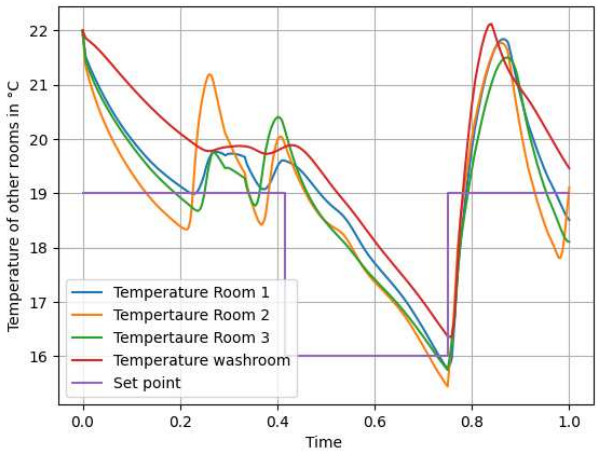

Figure 133:Temperature for other rooms in a typical day

Also, one could see that until the first 5 hours (0.2 day) mark there is no heating required since the building is initialized at 22°C and due to the thermal insulation of the building there is a retention of heat leading to the maintenance of temperature well within the comfort zone. The temperature in the living area is shown in Figure 134, it could be seen that temperature is well regulated in the living area, but there is a little lag during the period of transition from inoccupancy to occupancy.

Also, for all the zones the starting temperature point is parametrized at 22°C. From both the Figure 135 and Figure 136 at the start of the day and just until 5 hours one can see that due to the thermal insulation of the building the heat is retained better compared to the scenario in the previous case where there is a steep drop in the room temperature.

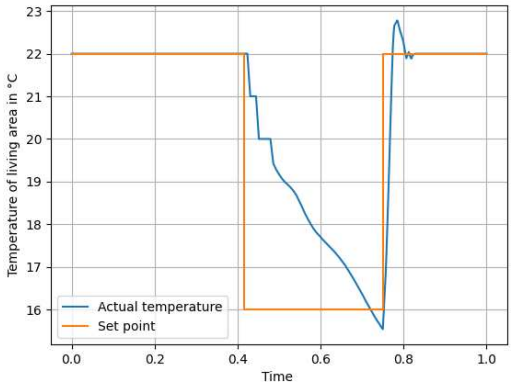

Figure 134: Temperature in living area

Also, after the 5-hour mark (0.2 day), it is seen that the boiler is turned on, because of the heating needs in room 1, and room 2. The heating need of each area is calculated as a proportion of the total heating need at that time step. Also, the boiler is turned ON around the 18h (0.67day) mark, this is due to the occupancy settings in the evening. It is seen that the return temperature nears 0°C during the time of no operation. This is typically due to the outside temperature being extremely low. Also, there is slight bump in the supply and the return temperature curves close to the 9-hour mark (0.4 days).

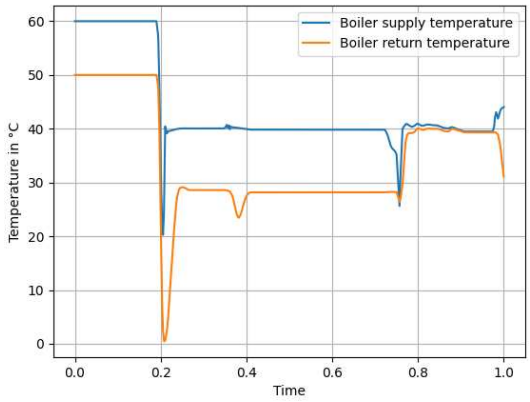

Figure 135: Supply and return temperatures for the boiler

The slight bump in the curves is due to the reason that the actual temperatures in room 2 and room 3 are less than the required setpoint temperature of 19°C. The same could be observed from the energy profiles of the building, as shown in Figure 136. It is seen from Figure 135 one could see that after 18h mark, one can see that the boiler is turned on due to heating requirements, also after once the heating set-point is reached and beyond that the supply and the return temperature almost remains the same. The reason being that no heating is required, this also signifies that there could be times in the whole heating season where such phenomenon could occur. The next step will be to perform the short sequence simulation followed by the full heating season simulation analysis.

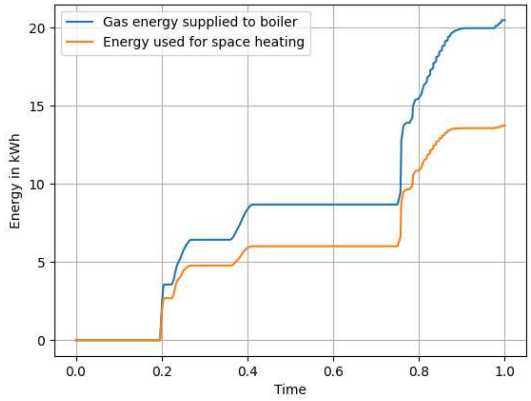

Figure 136: Energy levels observed in one typical day

6.3.3 Simulation result analysis for RT 2012 building use case

As explained earlier the first step will be to obtain the simulation results using the short sequence and then perform the annual simulation to verify the results. The 4-day short sequence generated in the previous section is used, and the same simulation solver and the tolerance values are assigned to the Dymola simulator. For the simulation, the buildings library is used for the simulation the same tolerance value of 10^{-6} is used and the Radau solver is used. The results for the 4-day short simulation pertaining to the boiler use case is shown in Table 18, form which one can see that the short sequence is effectively able to reproduce the simulation for days that have the daily efficiencies from 0.72 – 0.83.

For daily gas energy consumed the energy ranges are from 14 kWh to 40 kWh approximately and for the daily useful energy used up for the space heating is from 10 kWh to 30 kWh. As observed in the previous cases the idea will be to check if the short sequence is able to reproduce the KPI's alone but not the micro details within the heating season. When the results are extrapolated from the results for the short sequence using an extrapolation factor of 153/4. The gas energy supplied $E_{in\_extrapolated}$ = 4590 kWh , the energy used for space heating $E_{out\_extrapolated}$ = 3595.5 kWh , the seasonal efficiency $\eta_{seasonl\_extrapolated}$ = 0.78. The next step will be to verify from annual simulations if the results obtained fall within the required 5% error range.

Table 18. Short sequence simulation for boiler use case -FSG – PSD method

Days	$E_{in\ daily\ short}$ (kWh)	$E_{out\ daily\ short}$ (kWh)	η_{daily}
1	14.1	10.1	72%
2	34.3	28.6	83%
3	39.0	30.3	78%
4	33.0	25.0	76%

Also, one more crucial step will be to analyze if the results obtained are only limited to the three KPI's or is the short sequence is also able to reproduce the micro details within the heating season.

The annual simulation results for the RT 2012 use case are shown in Figure 137, Figure 138 and Figure 139. From Figure 137, one can see that the daily energy supplied to the boiler ranges from 10 kWh – 48 kWh, also there are three days towards the end of the heating season where the boiler operation is zero , the reason being that the energy from the previous days are conserved for those three days. For those three days the average temperature is around 14°C. Based on the result obtained from the short sequence one can see that the 2 days have 30kWh, 1 day has approximately 40kWh and 1 day has 14 kWh of energy consumption by the boiler. Meaning that the days below 14 kWh are not effectively

represented, proving that the micro details within the heating season are not well represented using the fictitious sequence generation method, this same analysis holds good for all the use cases demonstrated so far. The total energy supplied to the boiler during the heating season is around E_{in} = 4442 kWh while the extrapolated value is around $E_{in\_extrapolated}$ = 4590 kWh. The error between the extrapolated values and the heating season is around 3.3%.

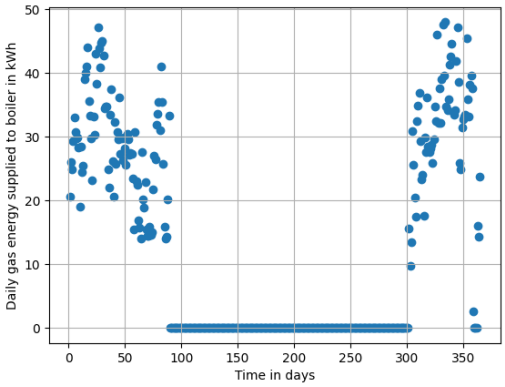

Figure 137: Daily gas energy supplied to boiler

From the Figure 138, one can see that the useful space heating energy supplied by the boiler to the building is in the range 6 – 40 kWh. Based on the results obtained from the short sequence one could see that out of the 4 testing days 2 days have the energy levels in the 20's range while the other two days have the energy levels at 10 kWh and 30 kWh, respectively.

Meaning that the days within the energy range 10 kWh – 30 kWh are represented using the short sequence. But, as usual the days below the energy levels of 10 kWh and above 30 kWh are not well represented, again confirming that the short sequence based on fictitious sequence generation method well reproduces the energy levels and the seasonal efficiency chosen for the heating season but not the micro details within the heating season.

The reason being that the micro details in the heating seasons are characterized by a lot of intraday and inter-day variations. These intraday variations require data with more resolution either in the 20 min or 10 min resolution. To generate a one-day short sequence then one would have to generate 144 variables thereby increasing the time take for the optimization. This could form a future work in the generation of the fictitious sequence method of generating short sequences for testing.

The total useful energy used up for the space heating is around E_{out} = 3464 kWh , while the extrapolated energy level is around $E_{out\_extrapolated}$ = 3595.5 kWh. The error between the results obtained from the heating season and the short sequence is around 3.7%.

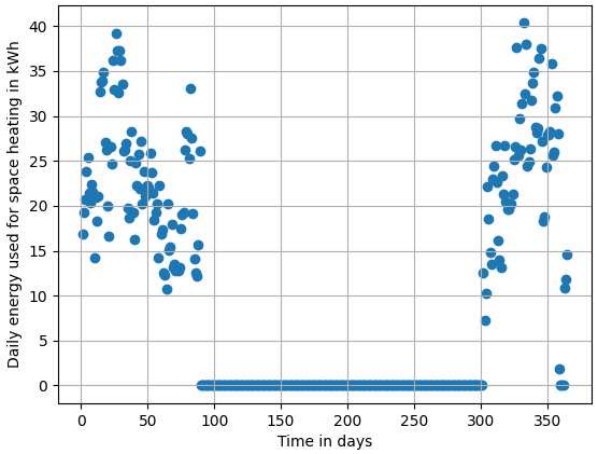

Figure 138: Daily space heating energy supplied by boiler

Similarly, the from the annual simulation results the daily efficiency values of the boiler are shown in Figure 139, one could see that the range of the daily efficiency varies from 0.57 – 0.91. The short sequence better represents the ranges from 0.72 – 0.83. Unlike the energy levels where a considerable number of days were not represented by the short sequence, from the results based on the daily energy efficiency values one could see that there are a smaller number of days above 0.83 and below 0.70 as well. This could also be seen as a problem with the FCG based methodology of generating the short sequences.

The seasonal efficiency of the boiler based on the whole heating season simulation is around $\eta_{seasonal} = 0.783$ while the $\eta_{extrapolated} = 0.75$. The error between the reference value and the short sequence is around 4.2%. The summary of the results obtained for the RT 2012 building use case is shown in Table 19. From the summary in Table 19 it is understood that the four-day short sequence generated using the power spectral density – fictious sequence can reproduce the results like the heating season.

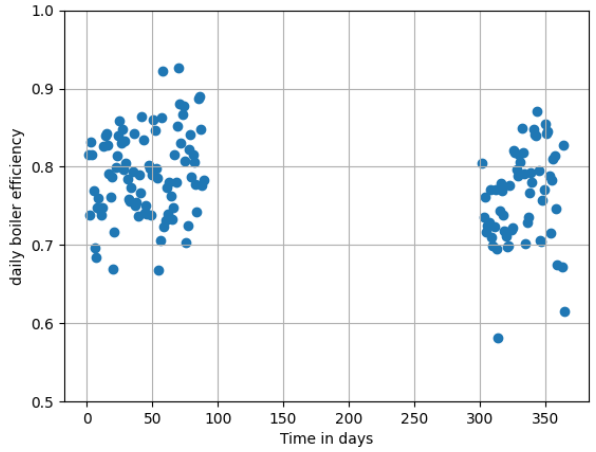

Figure 139: Daily efficiency of the boiler in the heating season

The next step will be to verify the uncertainty due to the methodology of the generating the short sequence, the idea will be generating a set of short sequences and identify the maximum and the minimum error ranges possible. The same 4-day short sequence is considered, since it is the minimum number of days onwards where the convergence starts happening for the boiler and the heat pump use case.

Table 19: Summary of results for boiler use case – FSG -PSD method

KPI	Heating season	4-day short sequence
E_{in} (kWh)	4442	4590
E_{out} (kWh)	3465	3595.5
$\eta_{seasonal}$	0.783	0.75
$E_{in\text{-}error}$ in %	3.3	
$E_{out\text{-}error}$ in %	3.6	
$\eta_{seasonal\text{-}error}$ in %	4.2	

6.4 Uncertainty Analysis due to the methodology of short sequence reduction – DE algorithm parametric analysis

One of the important steps will be to check if the uncertainty is due to the methodology, in this case being the power spectral density based fictitious sequence generation method of short sequence generation. The idea will be to check if there are many short sequences generated with the same optimization technique would it reproduce the same results within the 5% error.

The short sequence generated in the previous chapters were done after tuning the parameters namely the mutation, population, and the recombination parameter. Hence , this section will analyze more about the short sequence generation due to the parameter sensitivities.

During the tuning of the parameters for the differential evolution algorithm, the population parameter was fixed at 100 since, it is the least population value onwards which the DE algorithm started producing consistent short sequence profiles. The mutation and the recombination values were fixed at 1 and 0.7, respectively. Any change in these values of the mutation and recombination led to a very erratic profile as shown in Figure 140. From Figure 140 one can see that the generated sequence resembles more of a noise signal rather than a temperature profile, with huge hourly variations making it meaningless to test the methodology for measuring the annual efficiency under test.

Hence, one of the next steps will be to change the population variables in incremental steps and generate multiple short sequence profiles as possible within the given parametric limitations and then try to plot the distribution concerning the range of the criteria under consideration. The idea is to run as many simulations as possible in order to experiment on the limits of the results as explained in [82], where the author explains that in order to confirm to the process related uncertainty it is better to perform repeated analysis based on the process to find the ranges of the desired criteria's that include the energy levels and the seasonal efficiency.

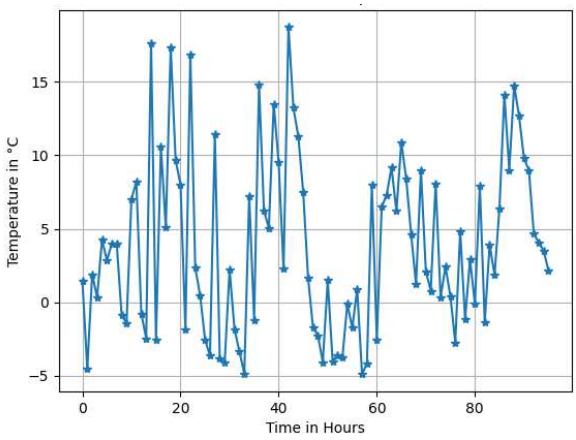

Figure 140: A sample 4-day short sequence for different mutation and recombination values for PSD based method

To start with the idea is to choose a 4-day short sequence and then try to generate more 4-day short sequences as possible keeping in consideration the time to generate the short sequences. The different short sequences are generated by increasing the number of population values in an incremental step starting from 15 until 100.

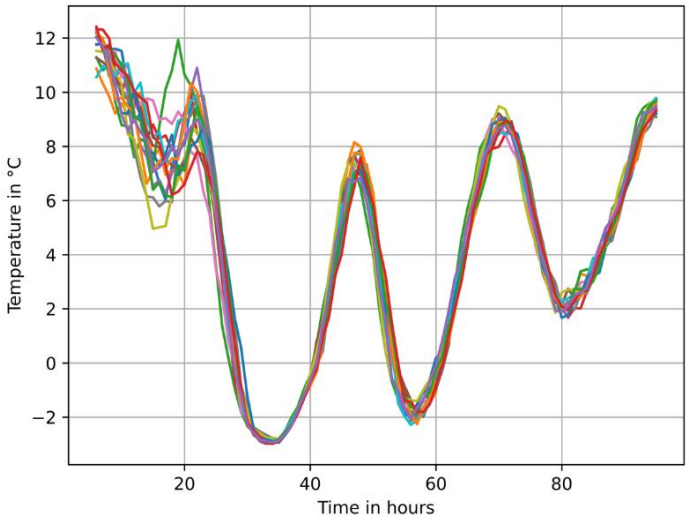

Figure 141: Generated set of temperature short sequences 1-15 FSG-PSD method

A set of 15 short sequences are generated as shown in the Figure 141. One can see that as the population is lesser starting with the sequence 1 the profile retains the shape, but the hourly variations of the temperature are not the same but vary much more than the original 4 -days short sequence. This is due to the assumption to treat the temperature as a random vibration signal to match the power spectral density of the heating season with that of the short sequence.

As one keeps on increasing beyond the population parameter above 100 one can see that the shape of the temperature changes drastically and after that the temperature profile remains constant irrespective of the increase in the population value as shown in Figure 142.

From Figure 142 it is seen that the profile of the temperature remains the same for the next 15 set of the short sequences. But one of the points to be noticed is that the first hour of each of the 15 short sequences are not the same, this is because of the random initialization and returning the best possible array of values as the DE mutation strategy.

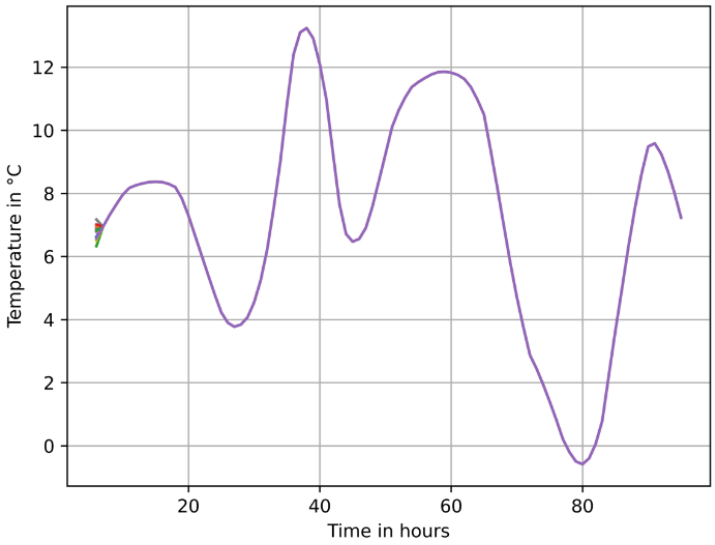

Figure 142: Generated set of short sequences 16-30 FSG-PSD method

The next step will be to use the same approaches and the same parameter settings to generate the irradiation sequences. The first 15 sequences generated for the irradiation sequences are shown in Figure 143, one can observe that for the smaller values of the population parameters the irradiation sequences are a bit erratic and as the population parameter increases the values become smoother and smoother. The next 15 sequences generated for keeping the population values above 100 is shown in Figure 144, it could be observed similar to the temperature signal the irradiation sequences are a bit consistent, but the correlation constraint has an effect of the short sequences generated which could be visible upon taking a look at the irradiation short sequences.

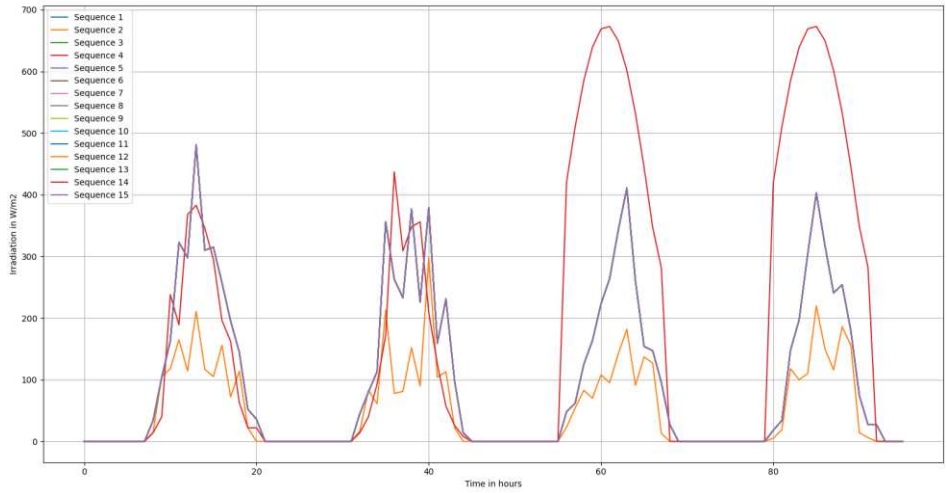

Figure 143: Generated 4-day irradiation short sequences 1-15 FSG-PSD method

The correlation constraint could not be respected for the lower population values. That could be seen as the hour wise changes in the irradiation short sequences corresponding to the lower population values. The next step will be to run the simulation for all the 30 short sequences and then verify of the results all fall within the desired bounds for the KPI's. Before doing it after the population was increased beyond 100 one could see that the profiles got consistent. The next question that raises is that will this 4-day profile be retained if one wanted to generate a 5-day profile.

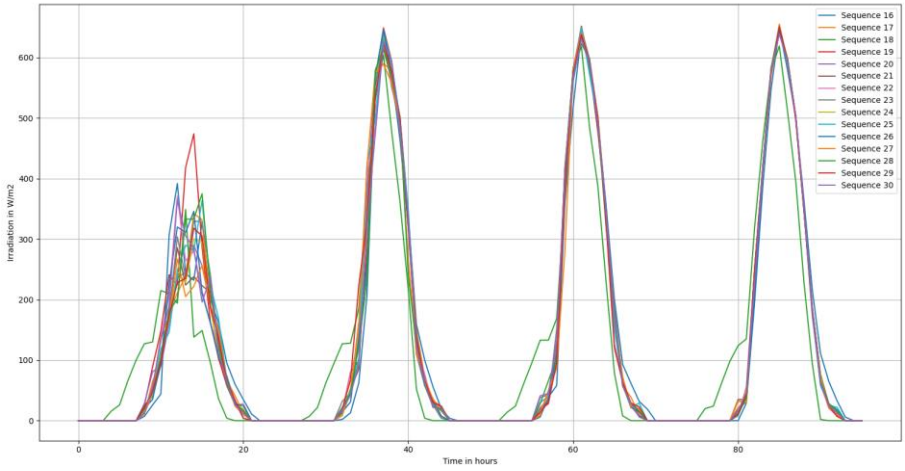

Figure 144: Generated 4-day irradiation short sequences 16-30 FSG-PSD method

The same was verified by generating 15 5-day short sequences as shown in the Figure 145. It could be observed from Figure 145 that the results are same as the 4-day use cases. The first hour is different plus there is another sequence that follows the same profile pattern, but the values are slightly changed. The previous short sequence profiles are retained as well. This also confirms that beyond a certain value of the

population the profiles remain the same but comes with a ridiculously huge cost of time consumption since there are more evaluations to make.

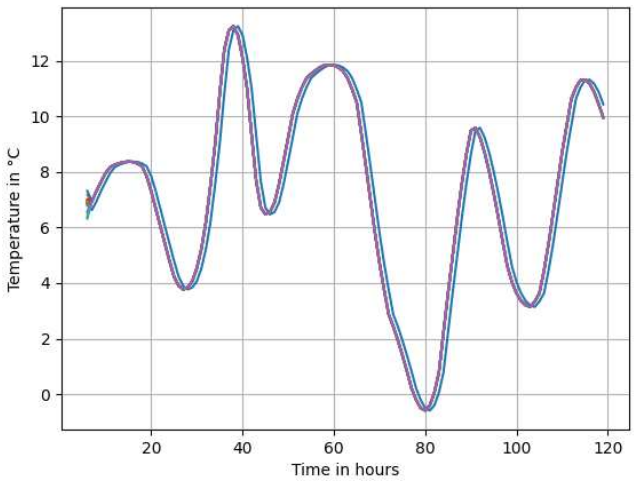

Figure 145: Generated 5-day temperature short sequence 1-15 FSG-PSD method

The results for the 30-different short sequences for the boiler and the heat pump use case are shown in Table 20 and Table 21.

Table 21Before going into the analysis on can see that two separate sets of fifteen 4-day short sequences were used for performing the experimentation. Meaning that there is a possibility of seeing the distinction of the two sets of data. From the Table 20 and Table 21 one could see that for the sequences from 16-30 the results do not vary much and are very much consistent for both the boiler and the heat pump use case. For the boiler use case one could see that for the sequences from 16-30 the gas energy supplied to the boiler hits consistently the 9500kWh, while the energy used for the space heating consistently hits the 8800kWh mark, while for the seasonal efficiency of the boiler the value consistently hits 0.92.

While for the other 15 sequences there are slight variations due to the nature of the short sequences generate with lesser population parameters that induced certain hourly variations in temperature and the irradiation short sequence. The same could be said for the heat pump use case well. For the heat pump use case one could see that the similar for the sequences from 16-30 the electrical energy supplied to the compressor consistently hits 2693 kWh.

For the energy used for the space heating purpose 8450 kWh is the consistent point, while for the SCOP it is 3.13. Also, one could also conclude if the distribution of all the above-mentioned parameters is to be plotted one can be able to see two different peaks, making it effectively a multimodal distribution.

Table 20: Simulation results for boiler use cases

Sequence	$E_{in\ extrapolated}$ (kWh)	$E_{out\ extrapolated}$ (kWh)	$\eta_{sesonal\ extrapolated}$	$E_{in\ error}$ in %	$E_{out\ error}$ in %	$\eta_{sesonal\ error}$ in %
1	10327.5	9562.5	0.93	4.04	5.08	1.19
2	9562.5	8797.5	0.92	3.66	3.32	0.55
3	10251	9333	0.91	3.27	2.56	0.50
4	9562.5	8797.5	0.92	3.66	3.32	0.55
5	10021.5	9524.25	0.95	0.96	4.66	3.87
6	9562.5	8797.5	0.92	3.66	3.32	0.55
7	10404	9524.25	0.92	4.82	4.66	0.05
8	9524.25	8797.5	0.92	4.05	3.32	0.95
9	9447.75	8874	0.94	4.82	2.48	2.65
10	10289.25	9524.25	0.93	3.66	4.66	1.16
11	9524.25	8797.5	0.92	4.05	3.32	0.95
12	10365.75	9562.5	0.92	4.43	5.08	0.82
13	9486	8874	0.94	4.43	2.48	2.24
14	10251	9486	0.93	3.27	4.24	1.13
15	9409.5	8912.25	0.95	5.20	2.06	3.51
16	10174.5	9524.25	0.94	2.50	4.66	2.30
17	9562.5	8950.5	0.94	3.66	1.64	2.30
18	10212.75	9065.25	0.89	2.89	0.38	2.99
19	9562.5	8912.25	0.93	3.66	2.06	1.86
20	10193.625	9007.875	0.88	2.70	1.01	3.42
21	9581.625	8969.625	0.94	3.47	1.43	2.31
22	10231.875	9466.875	0.93	3.08	4.03	1.12
23	10270.125	9466.875	0.92	3.47	4.03	0.74
24	9543.375	8969.625	0.94	3.85	1.43	2.72
25	10203.1875	9084.375	0.89	2.79	0.17	2.69
26	9543.375	8969.625	0.94	3.85	1.43	2.72
27	10164.9375	9438.1875	0.93	2.41	3.72	1.48
28	9581.625	9007.875	0.94	3.47	1.01	2.75
29	10279.6875	9514.6875	0.93	3.56	4.56	1.16
30	9581.625	9007.875	0.94	3.47	1.01	2.75

Table 21: Simulations results for heat pump use case

Sequence	$E_{out\ extrapolated}$ (kWh)	$Q_{compressor\ extrapolated}$ (kWh)	$SCOP_{extrapolated}$	$E_{out\ error}$ in %	Q_{error} in %	$SCOP_{error}$ in %
1	8529.75	2792.25	3.05	2.42	3.76	1.46
2	8568.00	2754.00	3.11	2.88	2.34	0.36
3	8491.50	2811.38	3.02	1.96	4.47	2.57
4	8587.13	2822.85	3.04	3.11	4.90	1.87
5	8635.32	2830.50	3.05	3.69	5.18	1.59
6	8644.50	2815.20	3.07	3.80	4.62	0.95
7	8654.18	2791.10	3.10	3.92	3.72	0.02
8	8636.85	2737.55	3.15	3.71	1.73	1.77
9	8721.00	2807.17	3.11	4.72	4.32	0.22
10	8510.63	2811.38	3.03	2.19	4.47	2.35
11	8636.85	2815.20	3.07	3.71	4.62	1.03
12	8612.75	2807.55	3.07	3.42	4.33	1.04
13	8698.82	2819.03	3.09	4.45	4.76	0.46
14	8581.77	2799.90	3.07	3.05	4.05	1.13
15	8690.40	2796.08	3.11	4.35	3.90	0.26
16	8453.25	2715.75	3.11	1.50	0.92	0.41
17	8434.13	2696.63	3.13	1.27	0.21	0.89
18	8437.95	2700.45	3.12	1.32	0.35	0.80
19	8430.30	2692.80	3.13	1.23	0.07	0.99
20	8449.43	2688.98	3.14	1.46	0.08	1.36
21	8434.13	2696.63	3.13	1.27	0.21	0.89
22	8437.95	2700.45	3.12	1.32	0.35	0.80
23	8430.30	2692.80	3.13	1.23	0.07	0.99
24	8449.43	2688.98	3.14	1.46	0.08	1.36
25	8434.13	2692.80	3.13	1.27	0.07	1.04
26	8437.95	2688.98	3.14	1.32	0.08	1.23
27	8430.30	2692.80	3.13	1.23	0.07	0.99
28	8449.43	2688.98	3.14	1.46	0.08	1.36
29	8415.00	2692.80	3.13	1.04	0.07	0.81
30	8415.00	2688.98	3.13	1.04	0.08	0.95

The box plots for the energy levels concerning the boiler use case is shown in Figure 146 and the corresponding distribution ranges of the energy levels are shown in Figure 147 and Figure 148. From the box plot one could see that the median value for the gas energy supplied is around 10000 kWh and most of the values fall well within the desired 5 % deviation. This also signifies that the interquartile range is big and most of the values fall between the 25% and 75% quartile.

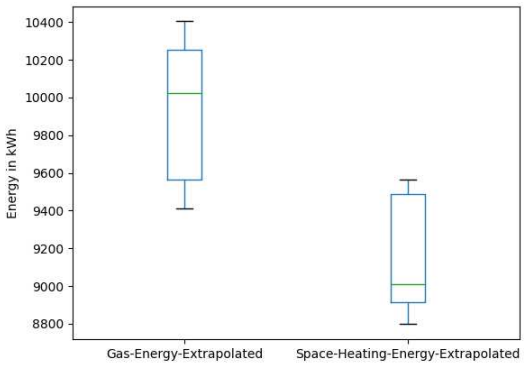

Figure 146: Box plot for the energy levels - boiler use case – FSG – PSD method

The maximum values and the minimum values of the gas energy supplied to the boiler are 10416 kWh and 9416 kWh respectively and there are no outliers in this case from the observed box plot since all the values obtained based on the simulations are well within the 5% error range. For the energy used for the space heating one could observe that the median value is around 9010 kWh. While the maximum and the minimum values are 9564 kWh and 8978 kWh. Also, one could see that there are more values in between the median and the maximum values for the space heating. For both the energy levels most of the values fall well within the first and the third quartiles which can be observed form the box plot.

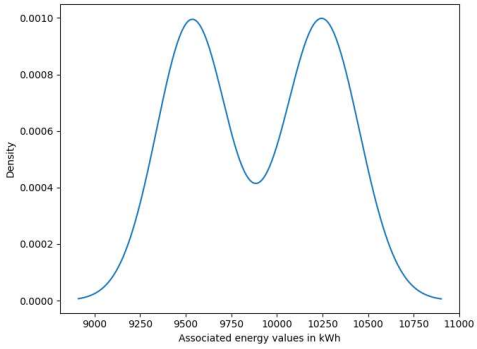

Figure 147: Distribution of E_{gas} supplied to boiler FSG – PSD method

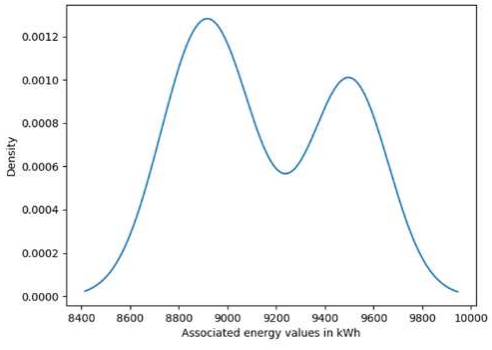

Figure 148: Distribution of energy used for $E_{Space\ Heating}$ FSG – PSD method

From the distribution of both the energy levels one could see that the distribution has taken form of the multi modal form with two distinct peaks. This was expected because two diverse sets fifteen 4-day short sequences were used for the simulation. As expected on can see that the values are 9500 kWh and

10250 kWh meaning that these are the two values that are most frequently repeated in the simulations. Similarly in the distribution related to the energy used for the space heating one can see the same multimodal distribution with 8800 kWh and 9400 kWh being the most frequent values. Also, one could notice from the box plot of the seasonal efficiencies as shown in Figure 149 the median values are at 0.925 while the maximum and the minimum values are 0.95 and 0.91, respectively. Also, one could notice that there are three outliers below the 0.90 mark with all three values being approximately 0.89. From the distribution plot of the boiler seasonal efficiency, one could conclude that the that the most frequently occurring values are 0.925 and 0.89, respectively.

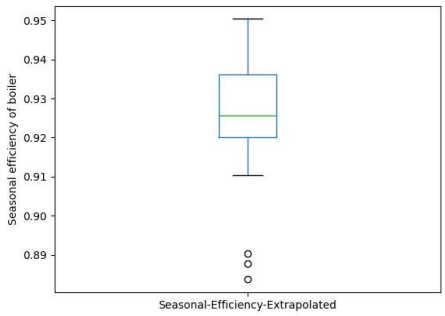

Figure 149: Box plot of boiler seasonal efficiency -FSG -PSD method

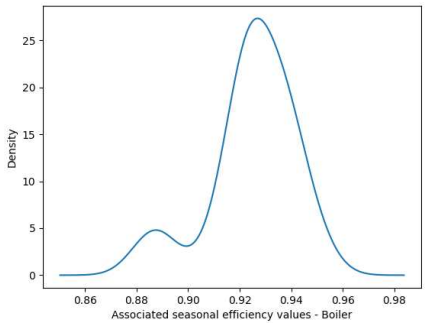

Figure 150: Distribution of boiler seasonal efficiency – FSG – PSD method

The peak at 0.89 includes the values that are distributed around the outliers while for the peak at 0.925 signifies that most of times the value occurs at this point onwards. This also signifies that for all the thirty short sequences combined the error is well under the 5% mark. The multimodal form of the distribution for the seasonal efficiency is not due to the data sets but due to the presence of the outliers below the minimum possible values from the inter quartile range. This could also signify that the boiler can produce the seasonal efficiency irrespective of the operating conditions, since the boiler operates within a narrow band during the space heating. This could be the same for the heat pump use case as well, the box plots of the electrical energy supplied to compressor is shown in Figure 151, from the box plot one could see that there are no outliers. The median value for the energy supplied to the compressor is around 2730 kWh the maximum and the minimum values are 2830 kWh and 2690 kWh. Also, like the boiler use case most of the values are within the first and the third quartile range.

From the distribution of the electrical energy supplied to the heat pump as shown in Figure 152, one could see the same multi modal distribution where the peaks could be observed at the 2830kWh and 2690 kWh which are the most frequently occurring values. Both the box plot and the distribution plot show that the values obtained from the simulation are well within the 5% error range. Similarly the same could be said about the energy used for the heat pump use case where there are no outliers and the values

are well within the 5% error range, as seen from Figure 153 and Figure 154. Similarly, from the box plot for the SCOP one could observe that the median value for the SCOP is 3.12 since for the sequences 16-30 the values are consistent since the temperature and irradiation remain the same based on the short sequences generated. The results shown below are for the FSG – PSD method.

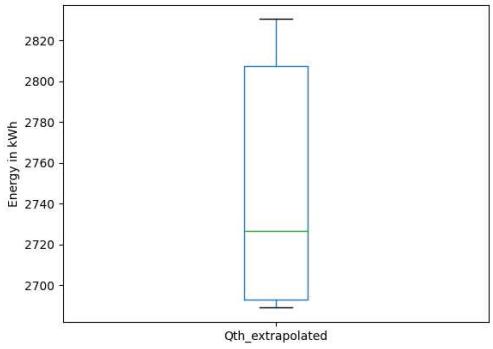

Figure 151: Box plot for electrical energy - heat pump

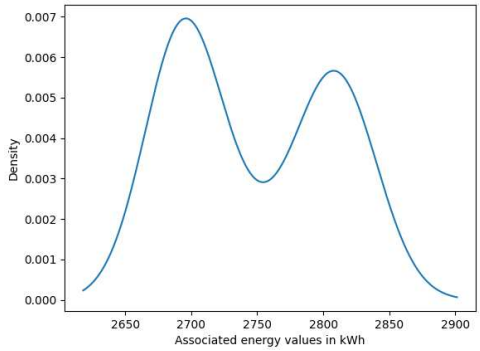

Figure 152: Distribution of electrical energy supplied

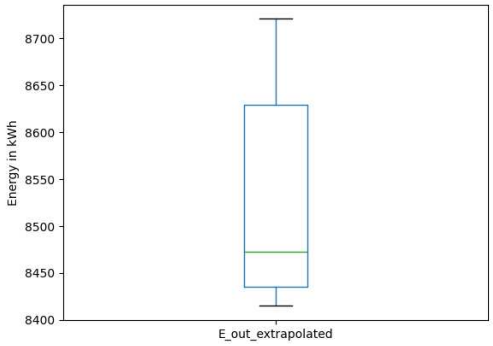

Figure 153: Box plot for energy used for space heating

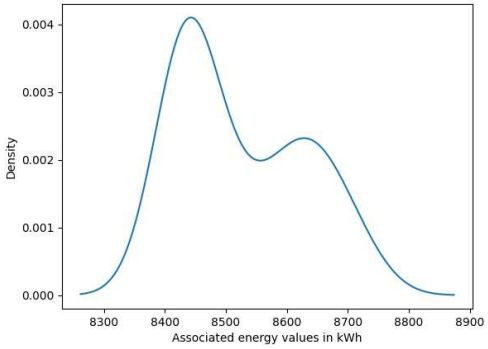

Figure 154: Distribution of energy used for space heating

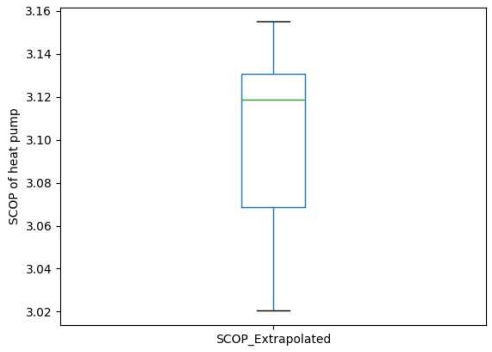

Figure 155: Box plot for SCOP - heat pump

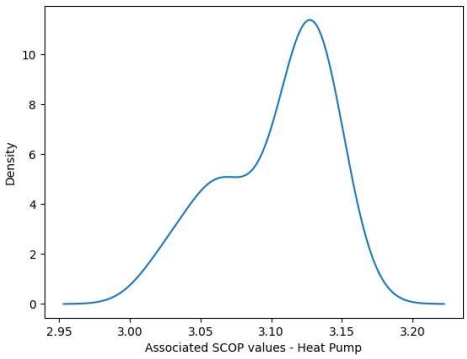

Figure 156: Distribution for SCOP heat pump

Similarly, the distribution plot of the SCOP also is multi modal and the two dominant peaks are at 3.06 and 3.12 that are the most frequently occurring values. Also, the error ranges for all the KPI's are shown in Figure 157 and Figure 158, from Figure 157 one can see that the possible error range for the electrical use for space heating varies from 1% - 4.8 % with the median value being around 1.8% For the

electrical energy supplied to the compressor of the heat pump is from the range 0.1% to 5.1%, meaning that there is one use case where the value does not fall exactly within the 5% error range. For the SCOP of the heat pump obtained from the data of 30 simulations one can see that there are two outliers namely at the 2.3% and 2.5%. It could also be observed that most of the values all fall under the 2% error range that there could not be a lot of uncertainty related to the methodology when DE algorithm is used for generating the fictitious sequences to evaluate the system under test. Similarly, when the ranges of the KPI's are analyzed for the boiler use case one could see that there is one use case where the energy levels are at the 5.1% mark.

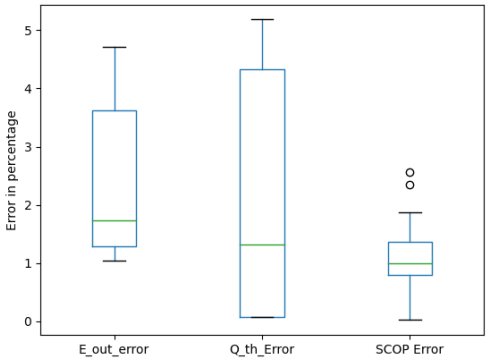

Figure 157: Box plot for the error ranges - heat pump use case

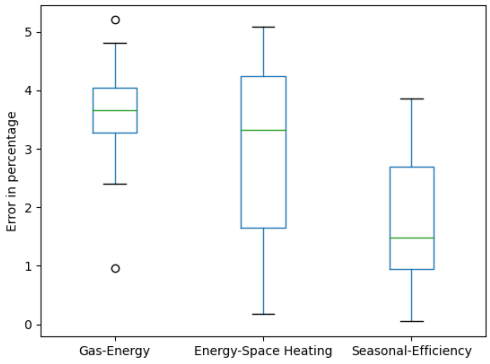

Figure 158: Error ranges for the chosen KPI's - boiler use case

Hence, one could conclude that the methodology when using the DE algorithm does not produce much uncertainty of the result based on the simulations. The next step would be to verify if the change in the optimization algorithm could lead to uncertainty. For this one-use case is generated with other algorithms and then the same is compared with the result obtained using the DE optimization algorithm. The distribution for the error ranges is shown from Figure 159 - Figure 164, it can be observed that similar to all the distribution plots seen before the same multimodal distribution can be observed. For the energy supplied to the boiler one can see that the 4% error value is the frequently repeated value.

While for the useful energy used up for the space heating, the most repeated error percentages are around 4% and 2%. For the seasonal efficiency of the boiler the most frequent error percentages are 0.9% and 1.9% respectively. Similarly, the electrical energy supplied to the compressor of the heat pump the frequently occurring error ranges are around 1.2% and 3.5%. For the energy used for the space heating related to the heat pump use case, the most frequently occurring error percentages are around 0.1% and 4.5%. The error rates with respect to the SCOP frequently occurs at 1%. Hence, from the distribution curves one can conclude that the error bounds are well within the 5% bounds for all the 30 short sequences that were generated for a 4-day short sequence.

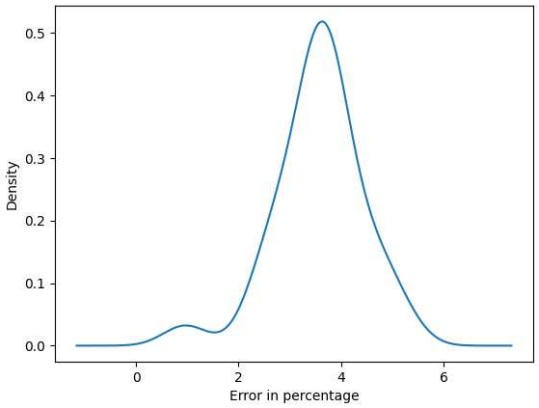

Figure 159: Distribution of error ranges $E_{in\text{-}boiler}$

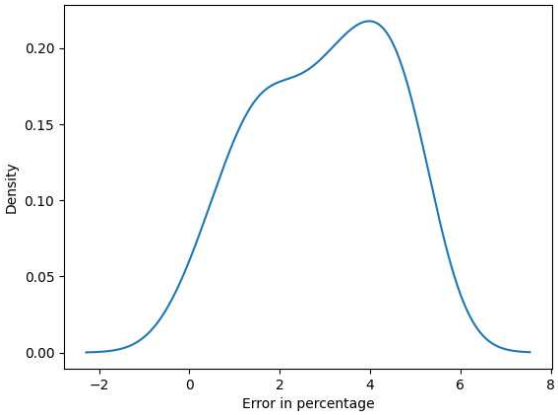

Figure 160: Distribution of error $E_{out\text{-}boiler}$

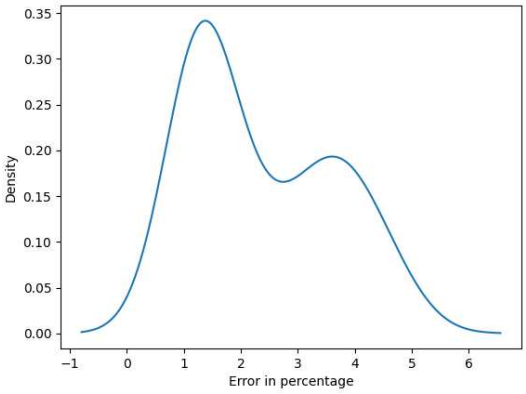

Figure 161:Distribution ranges for error $Q_{electrical\text{-}energy}$

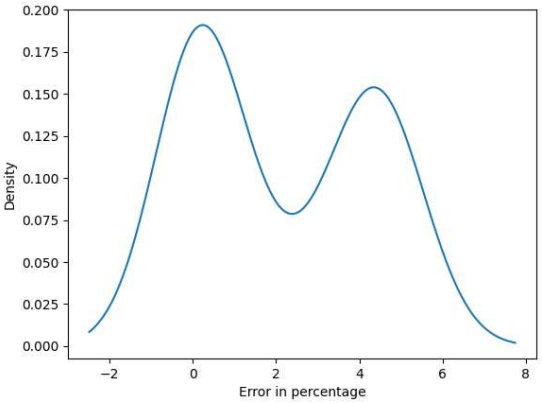

Figure 162:Distribution on error ranges for E_{out} heat pump

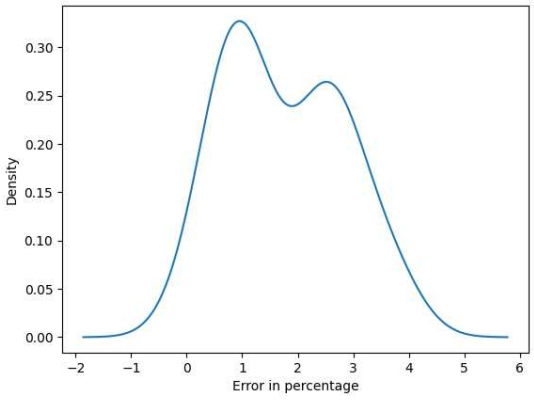

Figure 163: Distribution of error for $\eta_{sesonal}$

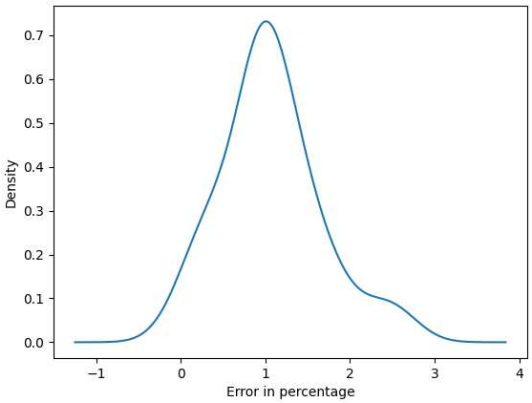

Figure 164:Distribution of error ranges for SCOP

The next step will be to check if the results obtained using the DE algorithm could be reproduced using another optimization algorithm. The algorithm of choice is Dual Annealing (DA) since it is also a global optimization algorithm. Few assumptions that one can make before generating the short sequences

using DA algorithm are , the PSD of the short sequence could be same as the heating season either under the 4-day mark or above the 4-day mark.

Since DA is also an algorithm that works on finding a global optimum philosophy one could expect the profiles of temperatures and the GHI to have a similar trend or similar values. The DA method could yield better result that the DE algorithm this could be only confirmed after the simulations. The time take for the generation of profiles could be like the time taken by the DE algorithm. Finally, the profiles generated, the power spectral density, the results of the dual annealing algorithm are compared with the differential evolution algorithm to see if the change in the optimization algorithm could yield different results.

6.5 Uncertainty Analysis due to the methodology of short sequence reduction – Change in optimization algorithm

6.5.1 Dual Annealing and choice of parameters

DA (Dual Annealing) is a stochastic global optimization; the DA algorithm combines both global and local search procedures for non-linear optimization problems as explained in [130]. In [131] the author defines the DA algorithm as a continuous global optimization algorithm with an use case demonstration using R. The dual annealing algorithm combines both the FSA (Fast Simulated Annealing) [132] and CSA (Classical Simulated Annealing) [133]. The steps involved in the simulated annealing algorithm is explained as follows :

Step 1: Generate new candidate solution from the current working solution (depends on the step size parameter)

Candidate = Solution + random (length(bounds)) * step size

Step 2: The next step will be to evaluate the candidate solution with the objective function

Candidate evaluation = objective(candidate)

Step 3: Check evaluated solution,

If candidate evaluation < best evaluation

Store best candidate

Step 4 : Replace the current working solution

Evaluate the difference between objective function and current solution

Difference = Candidate evaluated – current evaluation

Step 5 : Calculate the current annealing temperature using fast annealing schedule

T = temp / float (i + 1)

Step 6 : Evaluate the likelihood of accepting the solution with worse performing than the current working solution

Metropolis = exp (-difference / T)

Step 7 : Accept the current solution if it best satisfies the objective function , decision based on probability

If diff < 0 or random ( ) < metropolis

Store the current solution as the best solution

The above are the steps involved in the simulated annealing process, but the dual annealing process is implemented with a minor change being the refining of the best solution is done based on the Cauchy-Lorentz(CL) visiting distribution instead of the metropolis method of refining the solution. The shape of the CL distribution is controlled by the shape parameter q_v also known as the visiting parameter.

$$g_{q_v}(\Delta x(t)) = \frac{[T_{q_v}(t)]^{-\frac{D}{3-q_v}}}{\left[1 + (q_v - 1)\frac{\left((\Delta x(t))\right)^2}{[T_{q_v}(t)]^{\frac{2}{3-q_v}}}\right]^{\frac{1}{q_v-1}+\frac{D-1}{2}}}$$

Where t is the artificial time Δx(t) is used to generate the trial jump distance of variable x(t) under the artificial T_{qv}(t). The same dual annealing algorithm is available in the SciPy package in python , the building functions of the dual annealing algorithm is explained in detail in the SciPy documentation [134]. The next step will be to generate the short sequences, but before that the objective functions and constraints remain the same as in the case of power spectral density based fictitious sequence is generated based using the differential evolution algorithm. The only problem here is that he correlation constraint between the irradiation and the temperature is added as part of the objective function making it a multi-objective function. Since the package does not support the addition of constraint parameter in the DA function. But one should be able to see the same results if the philosophy of the method adopted holds good.

Before going into the generation of the short sequence the crucial step is to parametrize the DA algorithm the most important parameters are the initial temperature, the acceptance probability values and the restart temperature ratio. The initial temperature and the restart temperature combination acutely decides the restarting of the annealing process [135]. A high value for the initial starting temperature is often required and a very low value for the restart temperature is normally accepted [135]. In this case the initial temperature is maintained at 6000 and the restart temperature is chosen to be extremely low around 1x 10^{-7}. Hence, the restarting of the annealing process occurs at the 0.00006. Finally, one of the most

important parameters is the acceptance probability parameter, lower the values better the probability of not accepting the wrong solutions. The acceptance probability parameter is set at -1 x 10^4 the lower the acceptance parameter better is the process of not accepting solutions that are not global optimum. All the parameters were chosen manually although there are several other methods of tuning the parameters for the dual annealing described in the literature. The very next step will generate the short sequences for the irradiation and the temperature profile.

6.5.2 Short sequence generation – FSG – PSD method (Dual Annealing)

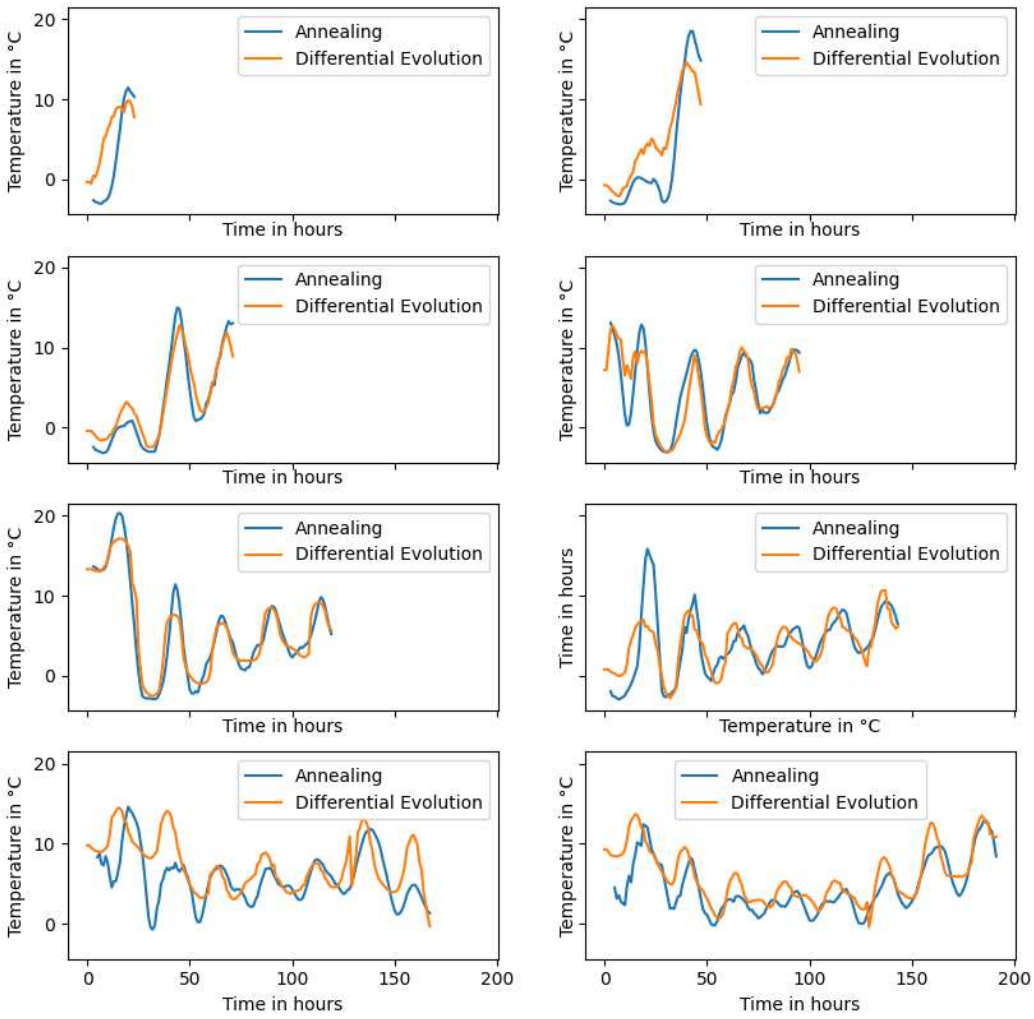

Figure 165: Temperature short sequence DA vs. DE algorithm

The temperature short sequences generated by the dual annealing algorithm is shown in Figure 165, one could observe that although the temperature ranges for all the profiles are not the same the trend of the temperature is somewhat like the temperature profiles generated by the differential evolution algorithm. This confirms the underlying philosophy of the methodology plus the next step will be investigate the

power spectral density to have a first understanding if the results could be like that of the differential evolution algorithm. The power spectral density of the temperature sequences generated by the dual annealing algorithm in comparison with the differential evolution algorithm are shown from Figure 166 to Figure 173.

The power spectral density for both the differential evolution and the dual annealing algorithm are for the 1-, 2- and 3-day sequences do not match up with that of the heating season. For the DE algorithm the convergence started happening from the 4-day sequence onwards, but the 4-day sequence generated by the dual annealing algorithm does not match up with the heating season. The 5-day short sequence is the point where the power spectral density of the short sequence generated by the dual annealing algorithm starts catching up with the PSD of the heating season.

Hence, one could anticipate the good results to be simulated from the 5-day sequence onwards or in other terms one could say that for the short sequence generated by the DE algorithm a minimum of 5 days is required to achieve the criteria for both the boiler and the heat pump use case. One could anticipate that the results could be same for the 5-, 6-, 7- and the 8- days short sequence simulations to be like that of the results generated by the DE algorithm. Also, it was observed that the time taken for the generation of the short sequences are higher than that of the DE algorithm. The optimization metrics for each of the short sequences are shown in Table 22.

Table 22: Optimization metrics for temperature short sequence

Days	Objective function	Function evaluations
1	3.12	49851
2	1.59	101146
3	1.057	151374
4	0.787	202477
5	0.625	255005
6	0.517	309171
7	0.440	368280
8	0.383	414109

The next step will be to generate the short sequences for the irradiation profiles with the constraint on the correlation between the temperature and the irradiation being added to the objective function as a multi objective criteria. The ratio between both the objective functions are adjusted manually based on different simulations in python. The short sequence profiles of the irradiation sequences generated using the DA

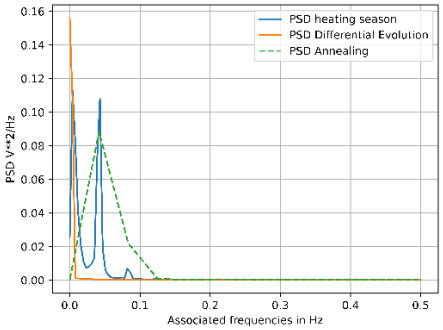

Figure 166: PSD heating season vs 1-day short sequence

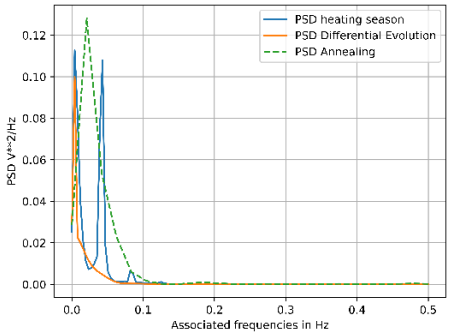

Figure 167: PSD heating season vs 2-day short sequence

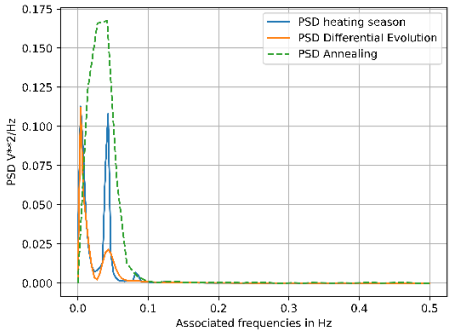

Figure 168:PSD heating season vs 3-day short sequence

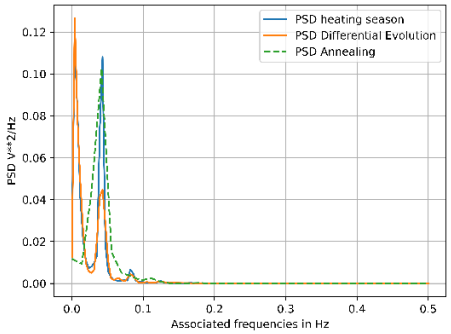

Figure 169: PSD heating season vs 4-day short sequence

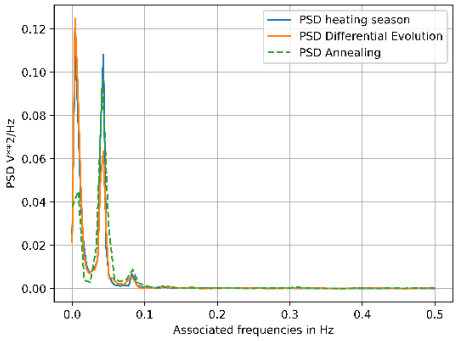

Figure 170: PSD heating season vs 5-day short sequence

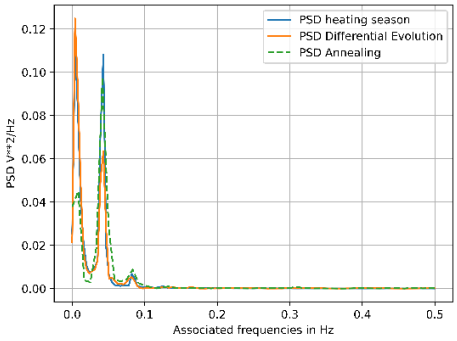

Figure 171: PSD heating season vs 6-day short sequence

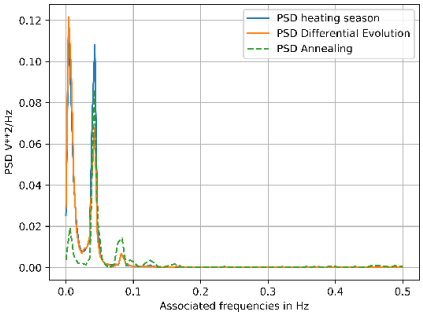

Figure 172: PSD heating season vs 7-day short sequence

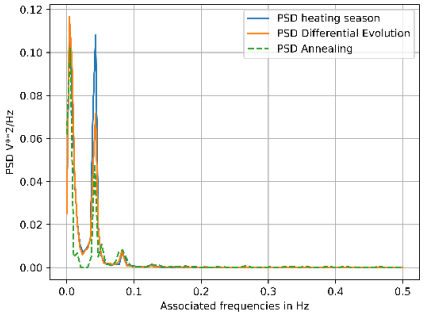

Figure 173: PSD heating season vs 8-day short sequence

algorithm is shown in Figure 174. The profiles of the irradiation sequences are like that of the ones obtained using the DE algorithm.

Also, it could be observed that like the previous case, where the ranges of the temperatures were not the same , but the trend of the profiles were , it is also a similar case with the irradiation sequence generated by the DA algorithm. The next step will be to look at the PSD of the irradiation short sequences generated by the DA algorithm with that of the DE algorithm and the heating season, to have a first understanding on what could be happening. The PSD of the irradiation sequences for both the DA, DE algorithms in comparison with the PSD of the heating season is shown in Figure 175, one can observe that the PSD patterns are like the temperature profiles generated by the DA algorithm.

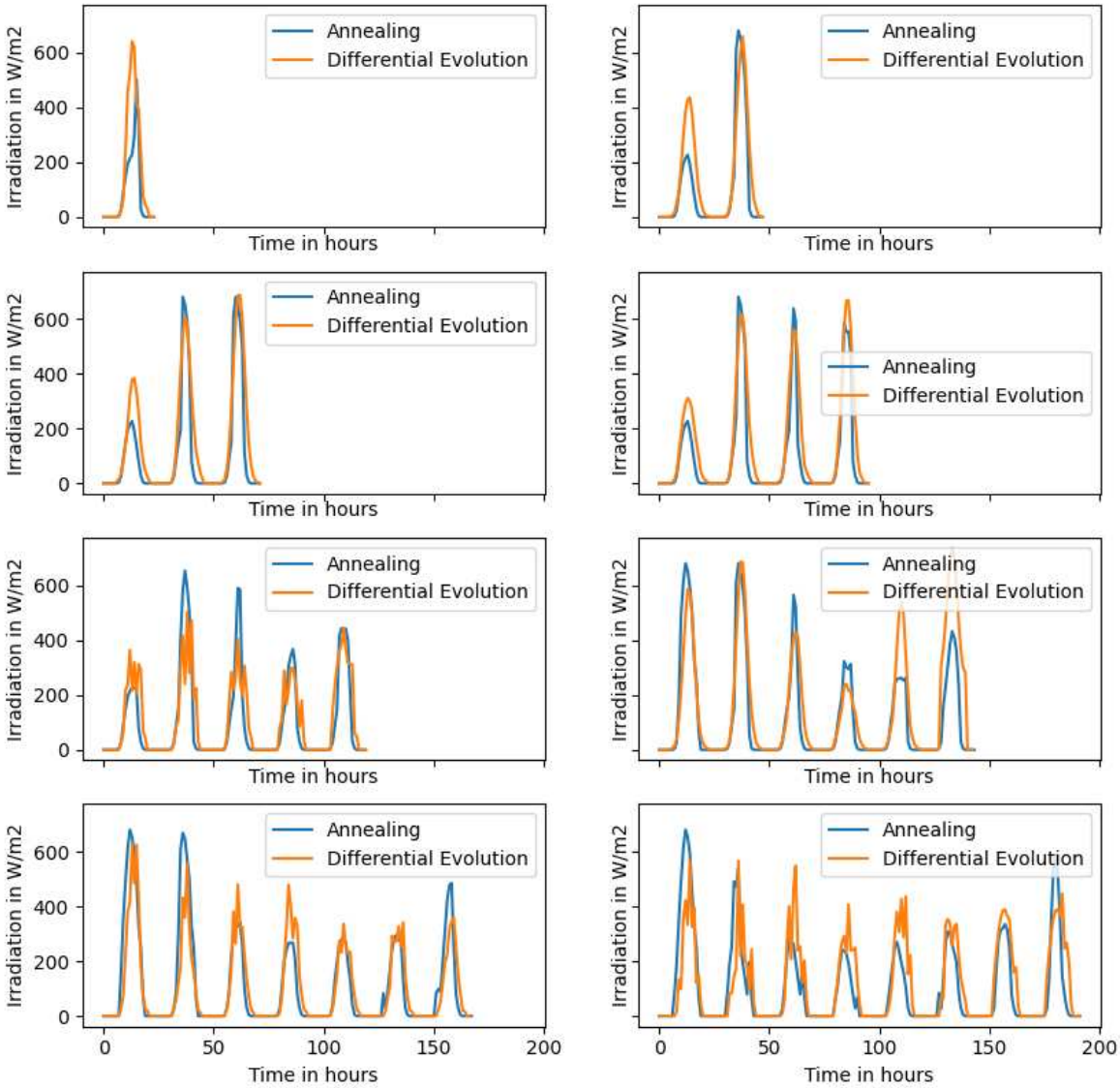

Figure 174: Irradiation sequences generated using DA vs DE algorithm – FSG – PSD method

One can observe that from the 5-day short sequence onwards the power spectral density of the dual annealing algorithm catches up with the heating season. From both the PSD comparisons one could make a pre assumption that from the 5th day onwards one could see a convergence towards the result. The optimization metrics of the DA algorithm for the irradiation sequence is shown in the Table 23.

From the optimization metrics one could observe that the difference between the error in the optimization function decreases with the increase in the number of days. As usual one can conclude that from the 5-day sequence on wards the error of the objective function reduces, and one could see that as the number of days increase the function evaluations increase by 50000 evaluations for the increase in one day in the short sequence.

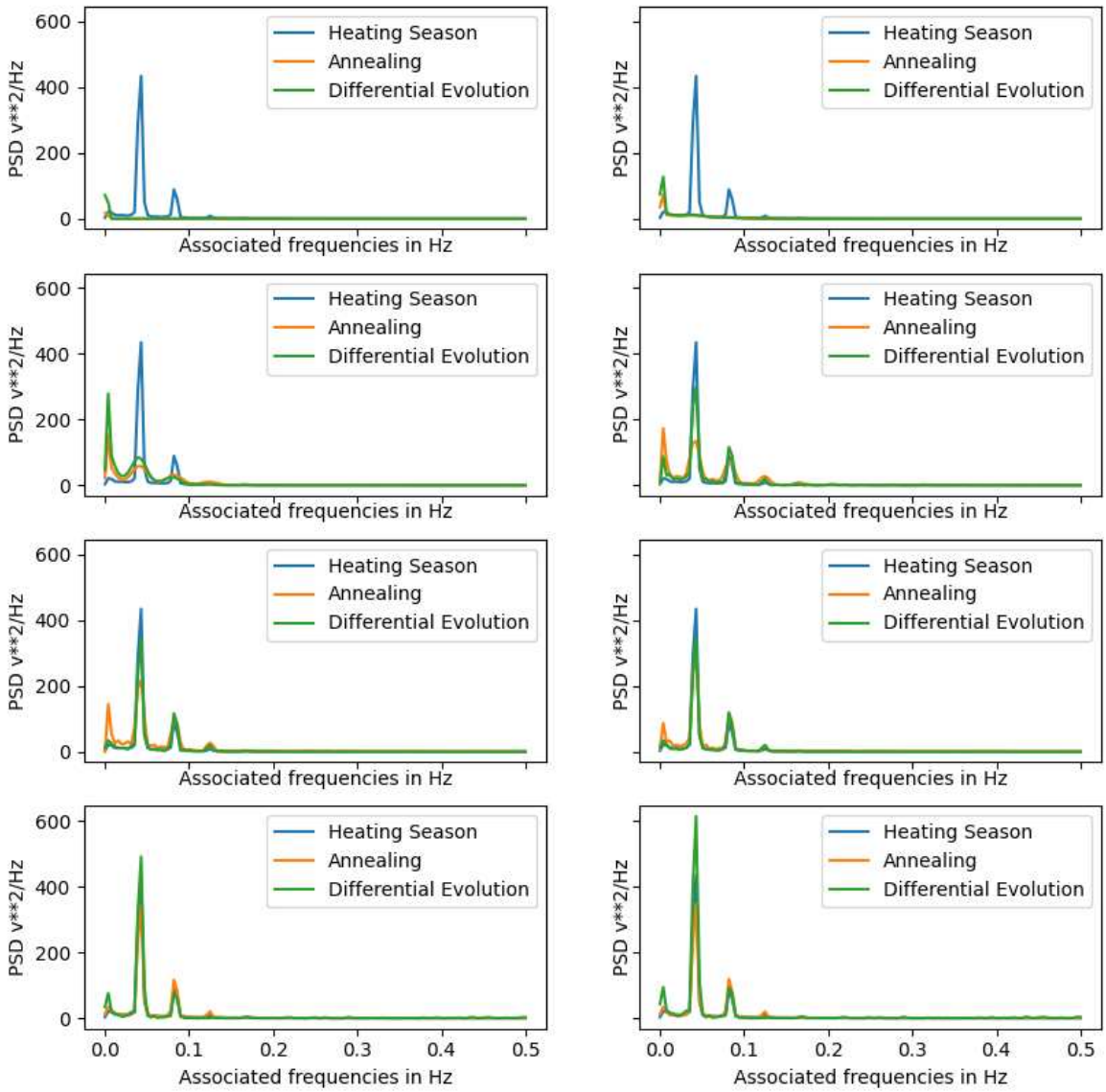

Figure 175: PSD of irradiation short sequences DE vs DA algorithms- FSG – PSD method

The next step will also be to verify the correlation between the temperature and the irradiation, since the trend remains the same and the ranges are different one could see a difference in the correlation pattern as compared to the correlation for the short sequences generated by the DE algorithm. The correlation plot between the irradiation short sequence and the temperature short sequence is shown in Figure 176. The correlation does not coincide with the actual correlation with that of the heating season, but one can see that as the number of days increase correlation of the short sequence very slowly converges towards the correlation of the gating season.

Table 23: Optimization metrics for irradiation short sequence

Days	Objective function	Function evaluations
1	28.2	57701
2	27.4	98059
3	23.5	145169
4	18.9	194135
5	12.8	249439
6	5.9	296991
7	1.3	351402
8	0.96	399055

This could also be attributed to the fact that one is trying to replicate the correlation of the heating season with a short sequence having few days. Conserving the short sequences as it is the next step will be performing the simulation analysis of the short sequence and compare it with the other methodologies.

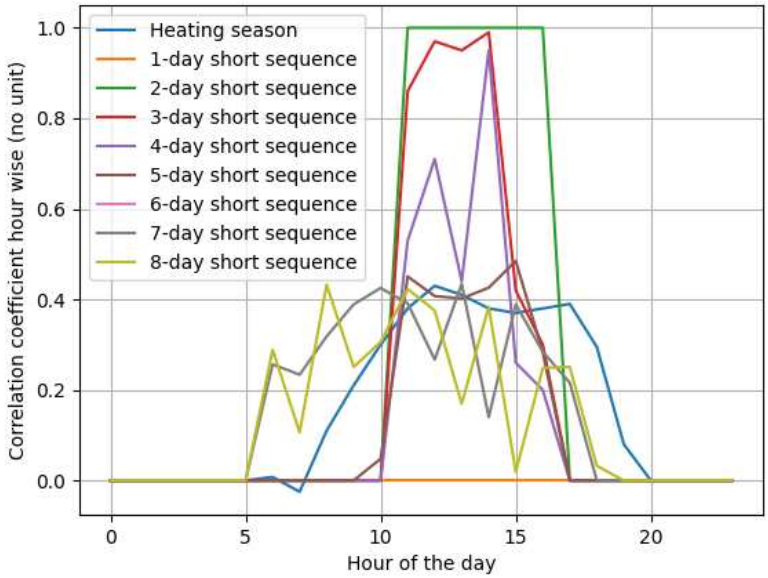

Figure 176: Correlation between temperature and irradiation sequences

6.5.3 Simulation analysis of short sequences generated using dual annealing algorithm

In this section, the main idea is to check by simulation if the sequences generated by the dual annealing algorithm can reproduce the criteria within the 5% error deviation. The reason to do this is to check if the change in the algorithm could cause any uncertainty on the results that are produced. The simulation analysis is done for the building uses cases with less insulation and the one that is well insulated using the RT 2012 standards.

The results for the boiler use case and the heat pump are shown in Figure 177, one can see that as expected the convergence starts to happen from the 5-day sequence onwards. Based on the PSD comparison between the short sequence generated by the DA algorithm and the one could conclude that the 5-day and the 8-day short sequences were the ones that best represented the PSD of the heating season. The same is reflected on the simulation results the error ranges for the 5-day and the 8-day sequences are the smallest in comparison to the other short sequences. The simulation results for the boiler use case is shown in Figure 178.

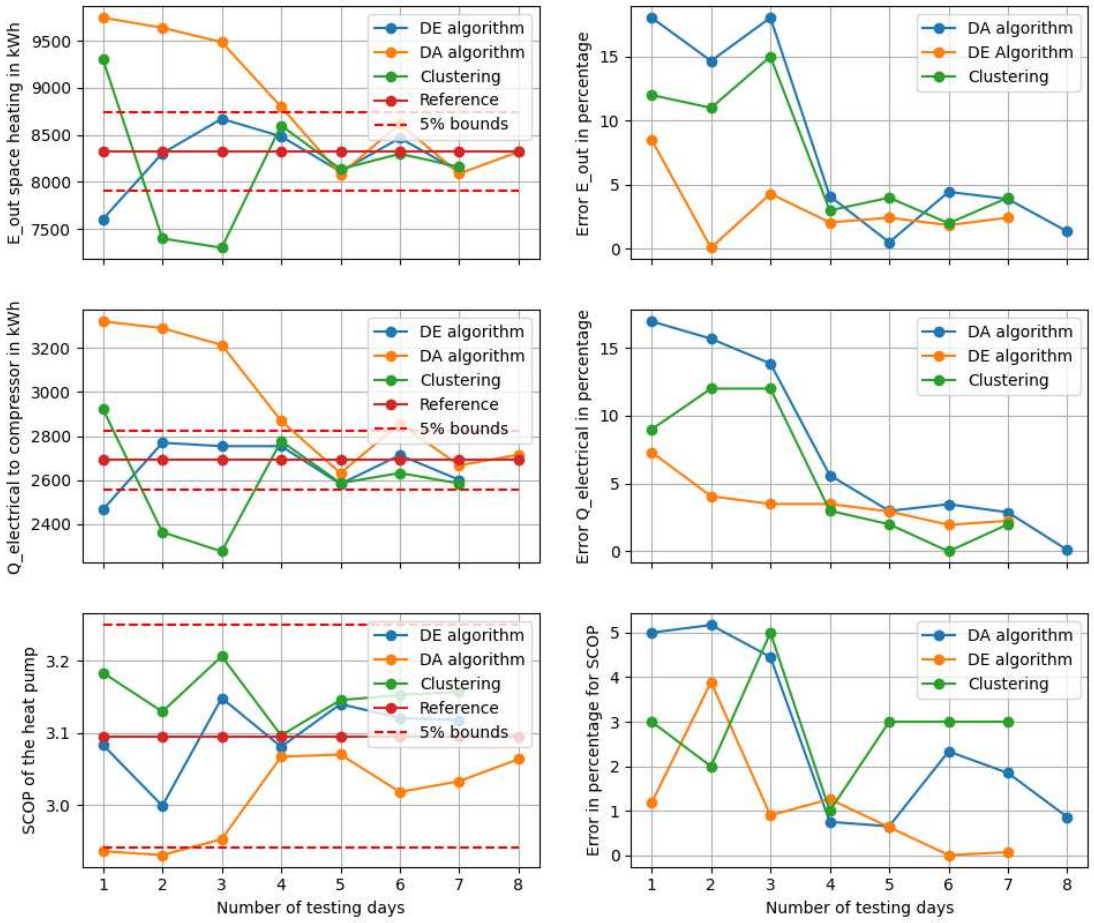

Figure 177: Simulation results for heat pump use case using DA algorithm

From the results for the boiler use case one can observe that from the 5-day sequence onwards one could see the convergence for all the three KPI's. Hence, one could say that the philosophy works irrespective of the algorithm. The biggest question that one must answer will be, how many testing days depending upon the optimization algorithm of choice.

As in the case of the DE algorithm the optimization was performed efficiently than the DA algorithm, where a four-day short sequence was able to reproduce the KPI's like the heating season within the 5% error bounds. The DA algorithm requires at least 5 days to reproduce the same results as the heating season. Like in the case of the heat pump use case, the boiler use case also best reproduces the KPI's results like the heating season.

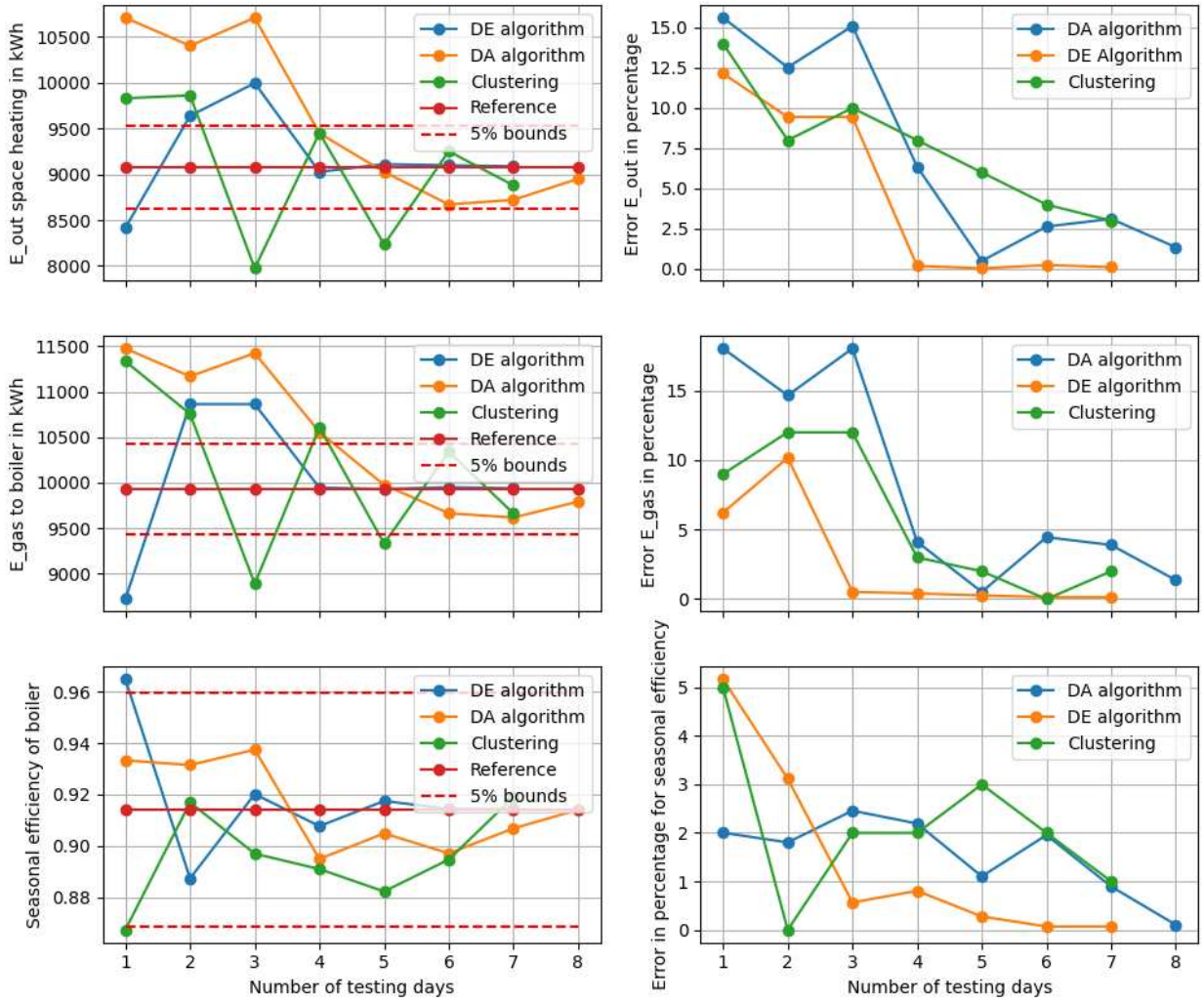

Figure 178: Simulation results for boiler use case using DA algorithm

In the future another optimization algorithm could be explored to reduce the number of testing days where a different short sequence could be generated to satisfy the criteria under consideration. The

other future work would be to consider different optimization algorithms and classify algorithms based on the minimum number of days required to reproduce the results of the heating season. This part would be interesting to check because dual annealing algorithm requires a 5-day short sequence to reproduce the results. Another algorithm could reproduce the results in lesser number of days when compared to both differential evolution and dual annealing algorithm.

6.5.4 Simulation analysis for RT2012 use case – for dual annealing short sequences

The next step will be to check if the short sequence generated could reproduce the results for the building with better insulation. A 5-day short sequence will be used for evaluating the seasonal efficiency of the boiler, since a 5-day short sequence is the point where the convergence started to happen.

The results for the RT2012 residential building with a boiler for space heating use case is shown in Table 24 and Table 25. It can be observed that the 4-day sequence from the dual annealing algorithm is not able to reproduce the same results from the heating season.

The error on the evaluated seasonal efficiency is extremely high. When, the simulation using the 5-day sequence was performed, it can be observed that the values are quite close to the 4-day short sequence generated by the DE algorithm. From the above results one can conclude that although the philosophy of the short sequence reduction can be achieved on the different optimization algorithms, it remains to be seen what the uncertainty on the number of testing days could be ?

To answer this question a lot of algorithms must be explored upon, there by one can identify the number of minimum testing days required which can be used as a base and then quantify the range of the minimum number of testing days required.

Table 24: Summary of results for boiler use case DE vs DA algorithm for 4-day sequence

KPI	Heating season	$DE_{4\text{-day short sequence}}$	$DA_{4\text{-day short sequence}}$
E_{in} (kWh)	4442	4590	4708
E_{out} (kWh)	3465	3595.5	3275
$\eta_{seasonal}$	0.783	0.75	0.70
$E_{in\text{-}error}$ in %	-	3.3	5.9
$E_{out\text{-}error}$ in %	-	3.6	5.4
$\eta_{seasonal\text{-}error}$ in %	-	4.2	10.6

Table 25: Summary of results for boiler use case DE vs DA algorithm for 5-day sequence

KPI	Heating season	DE 4-day short sequence	DA 5-day short sequence
E_{in} (kWh)	4442	4590	4620
E_{out} (kWh)	3465	3595.5	3457
$\eta_{seasonal}$	0.783	0.75	0.748
$E_{in\text{-}error}$ in %	-	3.3	4.0
$E_{out\text{-}error}$ in %	-	3.6	0.2
$\eta_{seasonal\text{-}error}$ in %	-	4.2	4.4

Also, one could also assume that even without the correlation constraint between the temperature and the irradiation there could be a possibility to achieve the convergence on the required results as close to the heating season under consideration. Also, the daily energy and the efficiency values of the 5-day simulation is shown in the Table 26.

Table 26:Short sequence simulation for boiler use case using DA algorithm

Days	$E_{in\ daily\ short}$ (kWh)	$E_{out\ daily\ short}$ (kWh)	η_{daily} in %
1	7.4	5.5	75.4
2	27.7	21.4	77.2
3	41.9	32.9	78.5
4	38.5	25.6	66.5
5	34.6	27.4	79.4

The energy ranges (shown in Figure 138 and Figure 137) of the annual simulations are compared with the result obtained from the 5-day short simulation. The range of energy represented in the 5-day energy sequences are from 7 – 40kWh for the gas energy supplied to the boiler. On a closer inspection it is typically today in the 30-kWh range, 1 day in 20 kWh range, and 1 day in the sub 10 kWh range. Effectively the day above the 40 kWh ranges is not represented. Similarly, for the energy used for the space heating one can see that the range of energy represented is around 5 kWh – 30 kWh. The days above 30kWh are not effectively represented. The daily efficiency ranges for the boiler are in the range 0.65 – 0.79 until 0.8 the days are better represented. There are outliers pertaining to the method, which is the reorientation of the micro-details corresponding to the heating season. This could be considered as a drawback to this method. But, on the other hand if one were to increase the number of days one could attain a shorter testing sequence including the extreme conditions as well. The rationale is that when one

looks at the simulation results one could see that the days represented have a mix of average days and days closer to the extreme days. Hence, one could conclude that the short sequence if generated to a greater number of days could easily represent the extreme conditions as well.

6.6 Segmentation: A brief overview and generation of short sequences

The idea behind the segmentation method is to consider the dynamic non-linearities in the weather variables by representing the signal in terms of segments. The segments in a signal are defined by three parameters in a signal, namely the slope of the signal, the duration, the initial starting value, and the final maximum value. The idea is to first define each segment and then group the segments that are alike in the next step. The definition of a segment is shown in Figure 179, where one could see that a segment is defined by the maximum value, the slope, and the duration.

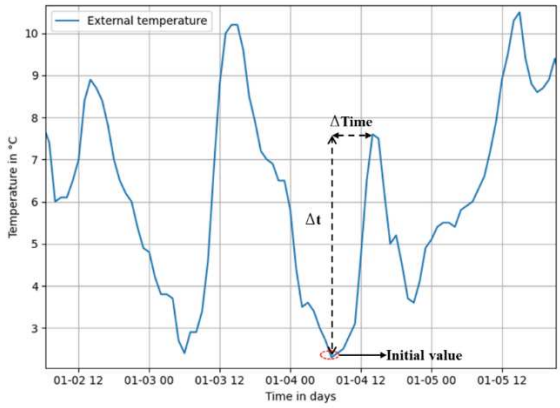

Figure 179: A sample segment from the temperature signal

The first step will be to perform the segmentation on the appropriate signal. Then the next step will be to perform a discretization on the segments based on the initial value the final value and the duration of the segments. This discretization will allow one to decompose the segmented signals into different levels and help in grouping the likely segments together for the final short sequence. Finally, the segments are joined together using genetic optimization algorithm where the problem is to reduce the discontinuity between one segment and another. The discretization level helps identify two pieces of information one is the number of types of segments and the number of segments per level. Meaning, that the signal is decomposed into 20 levels meaning that there could be n types of segments and k amount of data per segment. The data is the information about the segment that contains the slope, duration, and maximum value in that segment, while the type of segments being that the segments that have similar values for the parameters that define the slope.

In short, the idea is to perform segmentation on the whole year signal/heating season signal based on the maximum values, the duration, and the slope of the signal. Then collect all the segments and

discretize them based on different levels so that the likely segments can be grouped. Finally, perform an optimization

After various experiments, the number of levels is fixed to be 20. The discretization level of 20 guarantees round about 1 data per segment and the least number of types of segments for the short sequence. Plus, also the short sequence can be extended to the number of intended days with 1 segment contributing to 1 hour. Meaning in a short sequence for 1 day there are 24 segments of n types. The analysis for a one-day use case is shown in Figure 180, and Figure 181. As one could see from Figure 180 that for a level of 20 there is one segment per level and there is one type of segment for level 20 and the values also become the same after 20 levels.

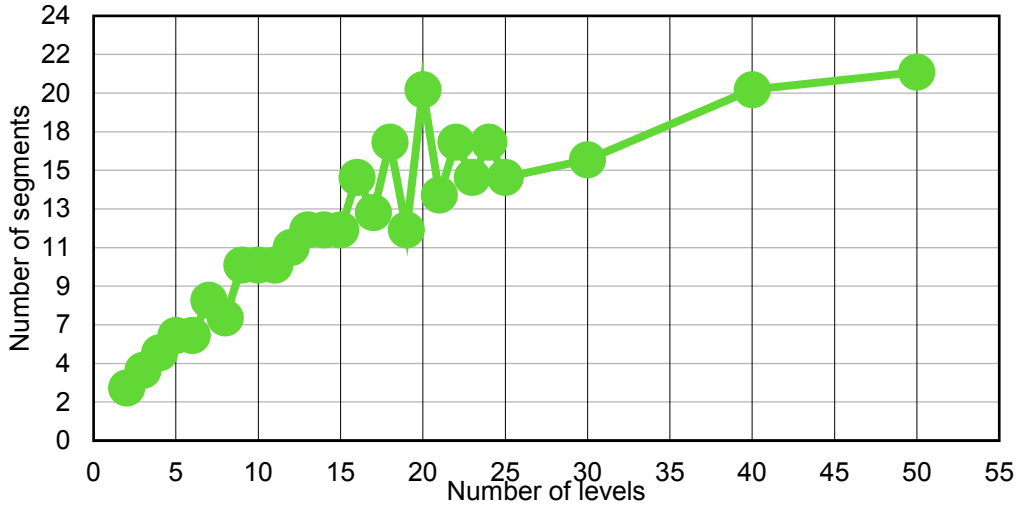

Figure 180: Number of segments vs Number of levels – a 1-day short sequence

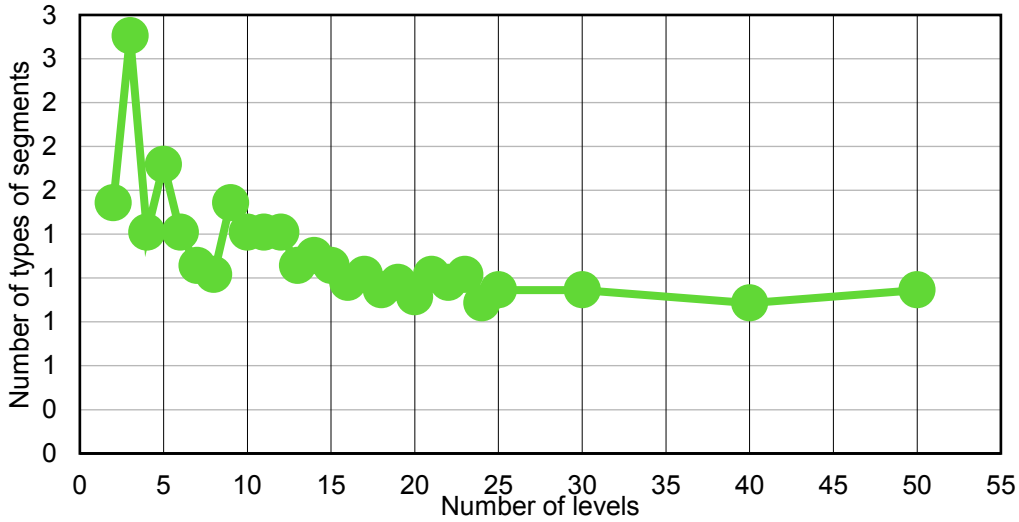

Figure 181: Number of types of segments vs Number of levels – a 1-day short sequence

The temperature short sequences generated for the temperature are shown in Figure 182, where one can see the short signal obtained by segmentation is shown in the blue curve. The orange-colored curve is the short signal obtained by the optimization of segments using the genetic algorithm. The curves in red and green are the curves obtained by the smoothing of the segmentation curves obtained after the optimization. The short sequence for the irradiation was all zeroes for the one-day short sequence since there are too many hours with zeroes in the longer sequence. A minimum of three days is required to generate the irradiation without only zeroes as shown in Figure 183. The number of segments in the short signal for the one-day temperature sequence is around 20 while for the full heating season there are around 2736 segments. For the three days short sequences the total number of segments in the whole heating season is around 750 while for the reduced short sequence is 5.

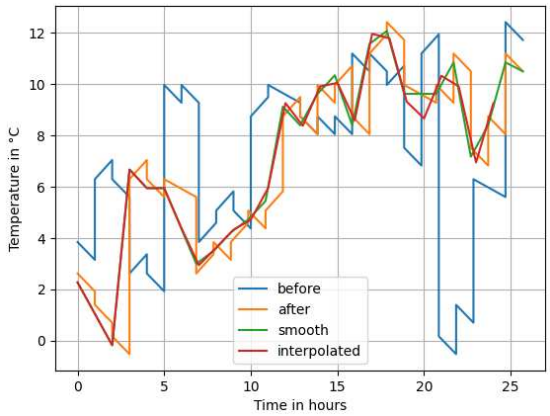

Figure 182: Temperature short sequence generated using segmentation method 1-day sequence

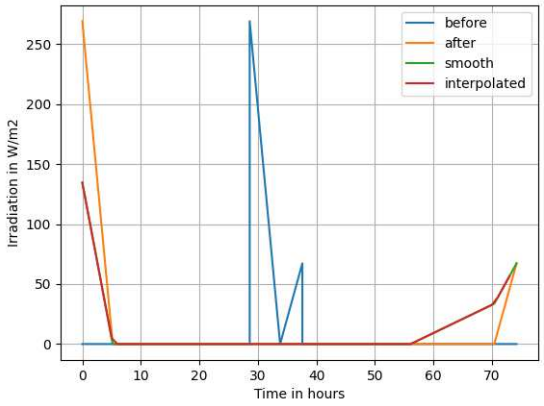

Figure 183: Irradiation short sequence generated using segmentation for 3-day sequence

The temperature and the irradiation short sequences generated by the segmentation methods for the 2 days to 4 days short sequence are shown in Figure 184 to Figure 189. One can see that as one increases the number of days better the representation of the irradiation sequences by the segmentation method.

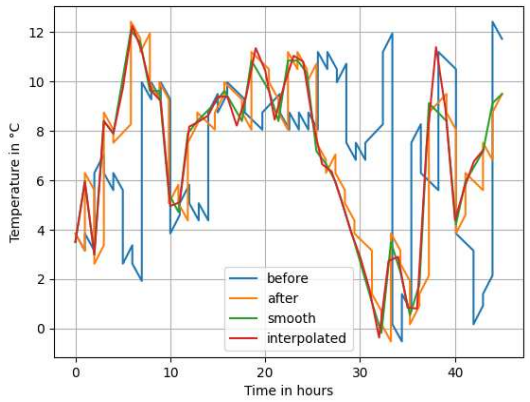

Figure 184: 2 - day temperature short sequence

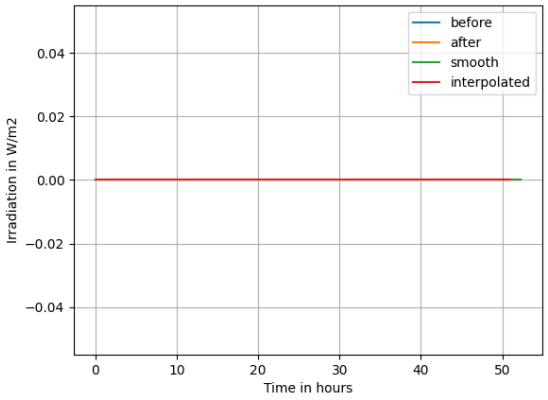

Figure 185: 2 - day irradiation short sequence

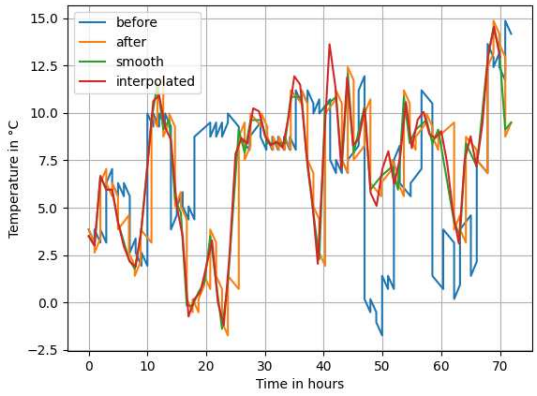

Figure 186: 3 - days temperature short sequence

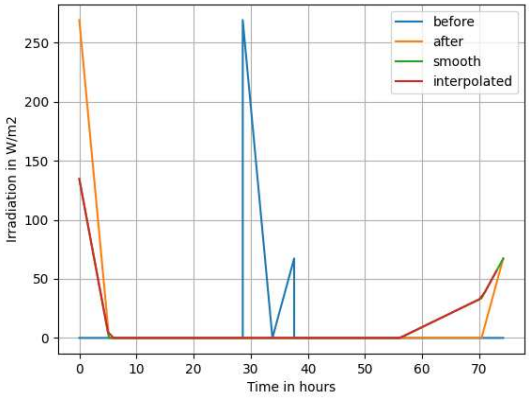

Figure 187: 3 - day irradiation short sequence

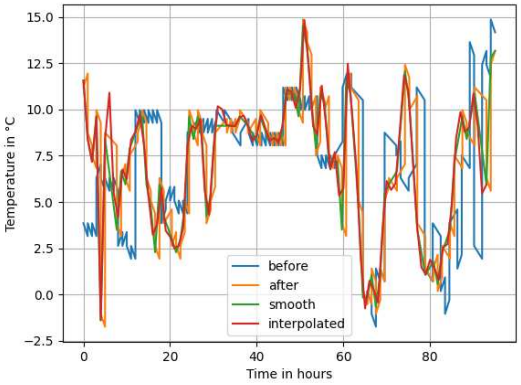

Figure 188: 4 - day temperature short sequence

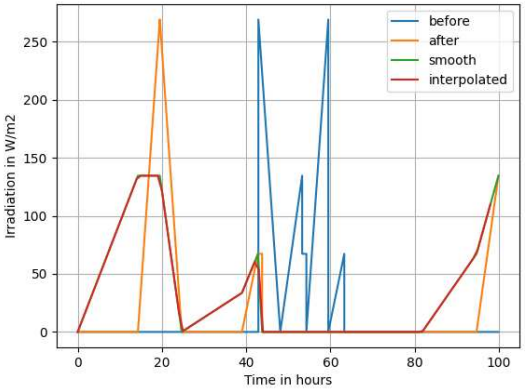

Figure 189: 4 - day irradiation short sequence

The idea is to generate the signals that are representative of the heating signal hence, the shape of the signal is not considered. Also, one can observe that as one increases the number of days better the representation of the short signal in terms of the heating season signals. This is the reason why from the third day onwards the signal contains the part that has radiation while the short sequences for 1 day and 2 days do not have the radiation. In short, there should be no radiation during the night and the early mornings, while there should be radiation in the mid-day, but the idea is to consider only the slopes of the

signal to have a representative short signal that can be used for the reducing the simulation time. So, this method should be capable of producing the desired results for the KPIs under consideration starting from a 1-day short sequence onwards. The signals obtained by the smoothening of the signals using the cubic splines method are used for the simulation since the segmented signals have unrealistic temperature differences for each hour. The results obtained for the segmentation method are shown in the next section.

6.7 Simulation result analysis for segmentation methods

The idea is to only check if the segmentation approach can reproduce the KPIs under the 5% error. The use case for the heat pump and the boiler is chosen for the building with the least insulated building model. The results for 1-day to 5-day short sequences are shown in Figure 190 and Figure 191, as one can see that the error as one could observe that 2 days are enough to reproduce the same results. But, for the two days use case one earlier was able to observe that the irradiation levels were completely zero. Hence, a minimum of three days is needed to make a suitable representation of the heating season. The results show that from the second day onwards the results remain the same for all the KPIs.

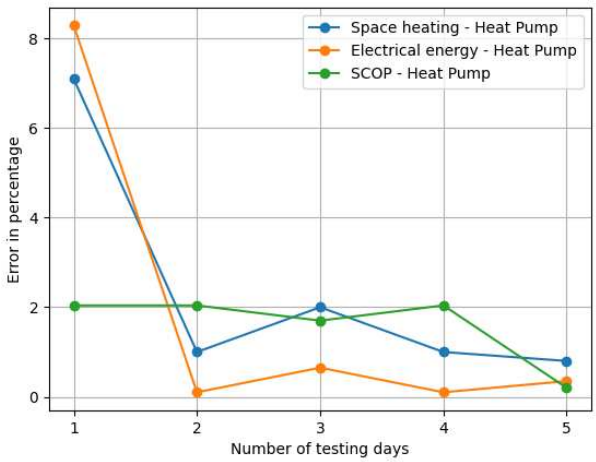

Figure 190:Results for heat pump use case

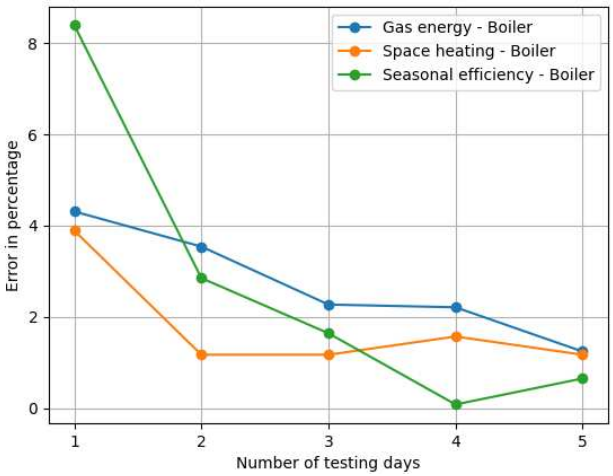

Figure 191: Results for the boiler use case

Since the shape of the signal is not maintained, the physical nature is compromised to reproduce the results for the heating season. In short, one would be able to reproduce the KPIs while it would remain unknown what exactly would be happening in the short sequence during simulation if it can reproduce the micro-details within the heating season. Hence in future work, one should be able to match the FFT of the signals while doing the segmentation as well. This should greatly improve the representation of the signal because the segmentation would consider the non-linearities, while the FFT would take into account the frequency-based dynamics of the temperature and the irradiation signal during the heating season. Hence, in the future, it would be useful to look at the segmentation method since it represents the non-linearity of the parts of the heating season while also reducing the testing time by a considerable time.

6.8 Chapter Conclusion

One could confirm from the simulations that there is not a lot of uncertainty produced by the methodology of short sequence reduction. The real uncertainty could be due to the experimental uncertainty but also due to the testing environment. As explained in the [59] a round robin testing in different labs could lead one to quantify the actual experimental uncertainty related to the methodology. Also, one could come to conclude that the philosophy of the methodology holds intact with different optimization algorithms but, with the change of the optimization algorithm one could see an uncertainty related to the number of testing days. For which one needs to perform the same simulation studies across a lot of optimization algorithms for different classifications to quantify the uncertainty based on the number of days from the least number of days required.

The other problem that one could identify with this method is that the fictitious sequence generation methods is able to reproduce the criteria under consideration for the heating season. But, whether it does represent the micro details within the heating season remains a big question. One reason is that it could be because one adopts a black box methodology to produce the testing sequence based on the temperature and the global irradiation sequence while only an objective function that is able to reproduce the criteria within the 5% error. Hence for a future step it would be important to identify one or many objectives that would be able to reproduce the micro details from heating season. The immediate next steps would be performing an experimental analysis with the generated short sequences to validate the results. Also, if the experiments are successful one could extend the same application to the weather data in other countries apart from France alone. The segmentation methodology evaluate the seasonal efficiency based on the slope of the temperature and the irradiation sequence. The methodology does not represent the usual short sequence where the shape of the profile is maintained. Hence, a lot of constraints would have to be added to replicate the physics of the system.

7. Conclusions on fictitious sequence generation methods

This chapter wishes to address the general conclusions based on the results obtained in the previous chapters and then give a brief overview of the segmentation followed by the future works that the short sequence needs to be addressed. In the previous chapter, one could conclude the following points about the fictitious sequence generation method, which are stated as follows:

1. The testing methodology could not reproduce all the micro details within the heating season.
2. The tests were carried on with a weather file having constant relative humidity, only the temperature and the irradiation short sequences were used for the testing methodology.
3. The clustering method is based on the grouping of similar days, while the fictitious sequence generation method reproduces the results based on the choice of the signal characteristics.
4. The methodology does not also consider the extremities, if the extremities are to be included one must make another constraint related to the extremities, but it would again increase the time taken for generating the short sequences.
5. The time taken for generating the short sequences are high but with a trade-off reducing the testing time taken for the real-time experimentation.
6. The method can produce the results irrespective of optimization algorithms pertaining only to the global optimization algorithms.
7. There could be uncertainty on the minimum number of testing days depending upon the type of the optimization algorithm and the chosen characteristics of the signal.

The previous section tried to propose a short method that would like to check if the shape of the signal is not maintained so that in the future one could reduce the testing time further. The idea was to generate a short signal that would be representative of the long-term sequence.

If one could look back at the results obtained from the fictitious sequence generation methods. One could find that the fictitious sequences based on the distribution method were able to reproduce only the seasonal efficiencies, while the PSD method was able to reproduce the results based on the energy levels and the seasonal efficiencies. The energy levels could be reproduced, and it highly depends on the method of extrapolation. But, in the case of the PSD method one was able to reproduce the energy levels as well because one was able to design the signal for both the temperature and the irradiation short sequence, hence one could see a reproduction of the energy levels as well.

Finally, the segmentation method was also able to reproduce the same results as well, but it completely lacked the micro-details to represent the season as well. In short, the PSD method better reproduces all the required KPIs and reproduces the seasonal efficiencies within the 5% limitations as

well. As explained in the third chapter. Also, the optimization process does not seem to produce that much uncertainty in the results due to the methodology adopted as explained in Chapter 4. The uncertainty in the method can be quantified practically by performing real-time experiments with the HIL setup as explained in [59], the round-robin method could also ensure if the method is capable of reproducing the same results across different HIL platforms as explained in [59]. Based on the simulation results and the results that are reproduced the PSD method is chosen.

7.1.1 Missing links and future works

This section is used to address the missing links in the short sequence method that could be addressed in the future or possibly found as the areas that one could improve to proceed with the fictitious sequence of producing results.

- **Generating multiple short sequences for other weather variables**

One of the main important hypotheses was that the simulations were done based on constant relative humidity. Hence, for the short sequence generation, the relative humidity was always kept at a constant value as in the original weather data file. Therefore, in the future depending upon the application for example a cooling system application would have to generate the relative humidity short sequences as well. In the future, ENGIE would be installing a climatic chamber to test out the heat pumps, hence it would be imperative to generate the short sequences for the relative humidity as well. Also, it would be important to find a workaround to produce many other weather variables in the short sequence so that it could faithfully reproduce the micro details within the heating season.

- **Choice of signal characteristics and generalization on weather data**

The results obtained, especially the energy levels and the seasonal efficiency are a direct result of the choice of the signal characteristics. For example, reproducing the seasonal efficiency demands the most representative periods need to be present in the short sequence. Hence, to do this the rationale was to use the PSD method. For example, if one wanted to include the extremities and use one average day in between then one would have to find other signal characteristics to do the simulations. This then translates to the other weather data sets as well, the method held good for the weather data in France. One would have to check if the same then applies to the weather data from other countries. The other question will also be to check if the weather data then holds good for use cases having tropical climatic conditions where the cooling system is of primary importance. It would also be important to see if the same method could reproduce the results for indirect efficiency evaluation methods where the combustion is also considered during the real-time simulation environment. Another important part of future work would be to consider the weather and climatic conditions of other countries/regions.

- **Uncertainty in the number of minimum days required for the short sequence**

The DE and DA algorithms were able to reproduce more or less similar results for the PSD methods. But the only proceeding issue was that the DE algorithm was able to reproduce the results for a 4-days short sequence. While the DA algorithm was able to reproduce the results for a 5-days short sequence meaning based on different optimization algorithms that solve a non-linear problem. Hence, in the future, it would also be important to ensure that a study based on different possible optimizations is also done. This would ensure what would be the minimum number of days that would guarantee the results obtained in the heating season.

If all the above problems could be answered then in the future the short sequence testing could pose much viability for reducing the testing time drastically when compared to the other available methods. Although, it remains to be seen if such a short sequence would be able to reproduce all the micro details of the heating season in the short sequence.

8 References

[1] C. M. Chini, K. L. Schreiber, Z. A. Barker, and A. S. Stillwell, "Quantifying Energy and Water Savings in the U.S. Residential Sector," *Environ. Sci. Technol.*, vol. 50, no. 17, pp. 9003–9012, Sep. 2016, doi: 10.1021/acs.est.6b01559.

[2] "Assessment of Seasonal Boiler Efficiency in Individual Buildings." https://www.esmagazine.com/articles/101464-assessment-of-seasonal-boiler-efficiency-in-individual-buildings (accessed Mar. 16, 2022).

[3] E. Mmk, "Hardware-in-the-loop simulering av motorservon på ett inbyggt system," p. 80.

[4] "ieee-thesaurus.pdf." Accessed: Feb. 15, 2022. [Online]. Available: https://www.ieee.org/content/dam/ieee-org/ieee/web/org/pubs/ieee-thesaurus.pdf

[5] S. Raman, N. Sivashankar, W. Milam, W. Stuart, and S. Nabi, "Design and implementation of HIL simulators for powertrain control system software development," in *Proceedings of the 1999 American Control Conference (Cat. No. 99CH36251)*, Jun. 1999, vol. 1, pp. 709–713 vol.1. doi: 10.1109/ACC.1999.782919.

[6] T. Hwang *et al.*, "Development of HILS Systems for Active Brake Control Systems," in *2006 SICE-ICASE International Joint Conference*, Oct. 2006, pp. 4404–4408. doi: 10.1109/SICE.2006.314663.

[7] "5th IFAC Workshop on Algorithms & Architecture for Real Time Control (AARTC'98), Cancun, Mexico, 15-17 April 1998."

[8] M. Schlager, W. Elmenreich, and I. Wenzel, "Interface Design for Hardware-in-the-Loop Simulation," Jul. 2006. doi: 10.1109/ISIE.2006.295703.

[9] O. Gietelink, J. Ploeg, B. De Schutter, and M. Verhaegen, "Development of advanced driver assistance systems with vehicle hardware-in-the-loop simulations," *Vehicle System Dynamics*, vol. 44, no. 7, pp. 569–590, Jul. 2006, doi: 10.1080/00423110600563338.

[10] H. K. Fathy, Z. S. Filipi, J. Hagena, and J. L. Stein, "Review of Hardware-in-the-Loop Simulation and Its Prospects in the Automotive Area". Modeling and Simulation for Military Applications, edited by Kevin," in *Proc. of SPIE*, 2006, pp. 1–20.

[11] L. Michaels *et al.*, "Model-Based Systems Engineering and Control System Development via Virtual Hardware-in-the-Loop Simulation," Oct. 2010, doi: 10.4271/2010-01-2325.

[12] P. Baracos, G. Murere, C. A. Rabbath, and W. Jin, "Enabling PC-based HIL simulation for automotive applications," in *IEMDC 2001. IEEE International Electric Machines and Drives Conference (Cat. No.01EX485)*, Cambridge, MA, USA, 2001, pp. 721–729. doi: 10.1109/IEMDC.2001.939394.

[13] S. Nidhra, "Black Box and White Box Testing Techniques - A Literature Review," *IJESA*, vol. 2, no. 2, pp. 29–50, Jun. 2012, doi: 10.5121/ijesa.2012.2204.

[14] M. Ehmer and F. Khan, “A Comparative Study of White Box, Black Box and Grey Box Testing Techniques,” *International Journal of Advanced Computer Science and Applications*, vol. 3, Jun. 2012, doi: 10.14569/IJACSA.2012.030603.

[15] M. Iacob and G.-D. Andreescu, “Implementation of hardware-in-the-loop system for drum-boiler-turbine decoupled multivariable control,” Jun. 2011, pp. 45–50. doi: 10.1109/SACI.2011.5872971.

[16] “A.Bouscayrol, ‘Hardware-In-the-Loop simulation’, Industrial Electronics Handbook, second edition, tome Control and mechatronics, Taylor and Francis March 2011, Chapter M33 - Google Search.” https://www.google.com/search?q=A.Bouscayrol%2C+%E2%80%9CHardware-In-the-Loop+simulation%E2%80%9D%2C+Industrial+Electronics+Handbook%2C+second+edition%2C+tome+Control+and+mechatronics%2C+Taylor+and+Francis+March+2011%2C+Chapter+M33&rlz=1C1GCEA_enFR965FR965&oq=A.Bouscayrol%2C+%E2%80%9CHardware-In-the-Loop+simulation%E2%80%9D%2C+Industrial+Electronics+Handbook%2C+second+edition%2C+tome+Control+and+mechatronics%2C+Taylor+and+Francis+March+2011%2C+Chapter+M33&aqs=chrome..69i57.1368j0j7&sourceid=chrome&ie=UTF-8 (accessed Jan. 25, 2022).

[17] “What is Hardware-in-the-Loop (HIL) Testing?” https://www.genuen.com/blog/what-is-hardware-in-the-loop-hil-testing (accessed Jan. 25, 2022).

[18] “M.Lauritzsen, ‘Hardware-in-the-Loop Testing Systems for ROV Control Systems’, Master Thesis, Dep. of Marine Technology, Norwegian University of Science and Technology, Trondheim, Norway, 2014 - Google Search.” https://www.google.com/search?q=M.Lauritzsen%2C+%E2%80%9CHardware-in-the-Loop+Testing+Systems+for+ROV+Control+Systems%E2%80%9D%2C+Master+Thesis%2C+Dep.+of+Marine+Technology%2C+Norwegian+University+of+Science+and+Technology%2C+Trondheim%2C+Norway%2C+2014&rlz=1C1GCEA_enFR965FR965&oq=M.Lauritzsen%2C+%E2%80%9CHardware-in-the-Loop+Testing+Systems+for+ROV+Control+Systems%E2%80%9D%2C+Master+Thesis%2C+Dep.+of+Marine+Technology%2C+Norwegian+University+of+Science+and+Technology%2C+Trondheim%2C+Norway%2C+2014&aqs=chrome..69i57.1397j0j7&sourceid=chrome&ie=UTF-8 (accessed Jan. 25, 2022).

[19] D. Mayer, T. Jungblut, J. Millitzer, and S. Wolter, “Hardware-in-the-Loop Test Environments for Vibration Control Systems,” Nov. 2015.

[20] B. Aleksandrov *et al.*, “Review of hardware-in-the-loop -a hundred years progress in the pseudo-real testing,” vol. 54, pp. 70–84, Dec. 2019.

[21] Institute of Electrical and Electronics Engineers, Ed., *2009 IEEE Vehicle Power and Propulsion Conference: VPPC 2009 ; Dearborn, Michigan, USA, 7 - 11 September 2009*. Piscataway, NJ: IEEE, 2009.

[22] J. Khan, "A Standardized Process Flow for Creating and Maintaining Component Level Hardware in the Loop Simulation Test Bench," Apr. 2016, pp. 2016-01–0052. doi: 10.4271/2016-01-0052.

[23] T. Vo-Duy and M. C. Ta, "A signal hardware-in-the-loop model for electric vehicles," *Robomech J*, vol. 3, no. 1, p. 29, Dec. 2016, doi: 10.1186/s40648-016-0068-9.

[24] R. Vijayagopal, L. Michaels, A. Rousseau, S. Halbach, and N. Shidore, "Automated Model Based Design Process to Evaluate Advanced Component Technologies," 2010. doi: 10.4271/2010-01-0936.

[25] W. Adiprawita, A. Ahmad, and J. Sembiring, "Hardware in the Loop Simulation for Simple Low Cost Autonomous UAV (Unmanned Aerial Vehicle) Autopilot System Research and Development," Jan. 2007.

[26] R. Yulnandi, C. Machbub, A. Prihatmanto, and E. Hidayat, "Design and implementation of hardware in the loop simulation for electric ducted fan rocket control system using 8-bit microcontroller and real-time open source middleware," *Journal of Mechatronics, Electrical Power, and Vehicular Technology*, vol. 8, p. 60, Jul. 2017, doi: 10.14203/j.mev.2017.v8.60-69.

[27] O. Jiménez, I. Urriza, L. A. Barragán, D. Navarro, J. I. Artigas, and O. Lucía, "Hardware-in-the-loop simulation of FPGA embedded processor based controls for power electronics," in *2011 IEEE International Symposium on Industrial Electronics*, Jun. 2011, pp. 1517–1522. doi: 10.1109/ISIE.2011.5984385.

[28] O. Lucía, O. Jiménez, L. A. Barragán, I. Urriza, J. M. Burdío, and D. Navarro, "Real-time FPGA-based Hardware-in-the-Loop development test-bench for multiple output power converters," in *2010 Twenty-Fifth Annual IEEE Applied Power Electronics Conference and Exposition (APEC)*, Feb. 2010, pp. 309–314. doi: 10.1109/APEC.2010.5433653.

[29] M. Short and M. Pont, *Hardware in the loop simulation of embedded automotive control system*. 2005, p. 431. doi: 10.1109/ITSC.2005.1520052.

[30] "256172.pdf." Accessed: Jan. 28, 2022. [Online]. Available: https://publications.lib.chalmers.se/records/fulltext/256172/256172.pdf

[31] T. Furukawa, L. C. Mak, K. Ryu, and X. Tong, "The platform- and hardware-in-the-loop simulator for multi-robot cooperation," Sep. 2010, pp. 347–354. doi: 10.1145/2377576.2377639.

[32] M. Schlager, R. Obermaisser, and W. Elmenreich, "A Framework for Hardware-in-the-Loop Testing of an Integrated Architecture," May 2007, vol. 4761, pp. 159–170. doi: 10.1007/978-3-540-75664-4_16.

[33] M. Santos *et al.*, “Rapid control prototyping for automotive software in power windows systems,” vol. 11, pp. 1341–1356, Jul. 2015.

[34] “Open Architecture Solution for Hardware-in-the-Loop Testing.” https://www.mathworks.com/company/newsletters/articles/open-architecture-solution-for-hardware-in-the-loop-testing.html (accessed Jan. 28, 2022).

[35] “Produit.” https://www.ni.com/fr-fr/shop/software/products/hil-and-real-time-test-software-suite.html (accessed Jan. 28, 2022).

[36] G. Schneider, J. Oppermann, A. Constantin, R. Streblow, and D. Müller, “Hardware-in-the-Loop-Simulation of a Building Energy and Control System to Investigate Circulating Pump Control Using Modelica,” 2015. doi: 10.3384/ECP15118225.

[37] A. Cruz, P. Rivière, D. Marchio, O. Cauret, and A. Milu, “Hardware in the loop test bench using Modelica: A platform to test and improve the control of heating systems,” *undefined*, 2017, Accessed: Jan. 28, 2022. [Online]. Available: https://www.semanticscholar.org/paper/Hardware-in-the-loop-test-bench-using-Modelica%3A-A-Cruz.-Rivi%C3%A8re/5c529bd3c60c96234edced9175a82c521567de14

[38] A. Piazzi, I. Grossi, M. Magni, M. Dongellini, J. P. Campana, and G. Morini, “The ‘Hardware-in-the loop’ approach for the experimental test of an innovative dual-source heat pump,” Jul. 2017.

[39] “Building Controls Virtual Test Bed | Simulation Research.” https://simulationresearch.lbl.gov/projects/building-controls-virtual-test-bed (accessed Feb. 14, 2022).

[40] S. Huang, W. Wang, M. R. Brambley, S. Goyal, and W. Zuo, “An agent-based hardware-in-the-loop simulation framework for building controls,” *Energy and Buildings*, vol. 181, pp. 26–37, Dec. 2018, doi: 10.1016/j.enbuild.2018.09.038.

[41] “Dynamic whole system testing of combined renewable heating systems – The current state of the art | Elsevier Enhanced Reader.” https://reader.elsevier.com/reader/sd/pii/S037877881300443X?token=241A3BA837B69B16D4032B4E11B03B43030AAFF15BF92393BD3C419E9EE4A061E396EBFF3B53FEDE11C26D706D57CC1C&originRegion=eu-west-1&originCreation=20220214145554 (accessed Feb. 14, 2022).

[42] A. Soltani and F. Assadian, “A Hardware-in-the-Loop Facility for Integrated Vehicle Dynamics Control System Design and Validation,” *IFAC-PapersOnLine*, vol. 49, no. 21, pp. 32–38, Jan. 2016, doi: 10.1016/j.ifacol.2016.10.507.

[43] P. J. King and D. G. Copp, “Hardware in the loop for automotive vehicle control systems development,” in *2004 Mini Symposia UKACC Control*, Sep. 2004, pp. 75–78. doi: 10.1049/ic:20040651.

[44] M. A. A. Sanvido, “Hardware-in-the-loop simulation framework,” ETH Zurich, 2002. doi: 10.3929/ETHZ-A-004317368.

[45] “Isermann and Scha - 1999 - Hardware-in-the-loop simulation for the design and.pdf.” Accessed: Mar. 14, 2022. [Online].

[46] P. Sarhadi and S. Yousefpour, “State of the art: hardware in the loop modeling and simulation with its applications in design, development and implementation of system and control software,” *International Journal of Dynamics and Control*, vol. 3, Jan. 2014, doi: 10.1007/s40435-014-0108-3.

[47] F. Gu, W. S. Harrison, D. M. Tilbury, and C. Yuan, “Hardware-In-The-Loop for Manufacturing Automation Control: Current Status and Identified Needs,” in *2007 IEEE International Conference on Automation Science and Engineering*, Sep. 2007, pp. 1105–1110. doi: 10.1109/COASE.2007.4341787.

[48] J. Ortiga, J. C. Bruno, and A. Coronas, “Selection of typical days for the characterisation of energy demand in cogeneration and trigeneration optimisation models for buildings,” *Energy Conversion and Management*, vol. 52, no. 4, pp. 1934–1942, Apr. 2011, doi: 10.1016/j.enconman.2010.11.022.

[49] “EN 14825:2018 - Air conditioners, liquid chilling packages and heat pumps, with electrically driven.” https://standards.iteh.ai/catalog/standards/cen/304fe3bd-b611-4f34-8ca2-8ace2d476d89/en-14825-2018 (accessed Apr. 19, 2022).

[50] “EN 15316-4-2:2008 - Heating systems in buildings - Method for calculation of system energy requirements and system efficiencies - Part 4-2: Space heating generation systems, heat pump systems,” *iTeh Standards Store*. https://standards.iteh.ai/catalog/standards/cen/79ff052a-0fc6-4d40-a8a0-f8c64e4ff8b5/en-15316-4-2-2008 (accessed Aug. 31, 2022).

[51] 14:00-17:00, “ISO 9459-5:2007,” *ISO*. https://www.iso.org/cms/render/live/en/sites/isoorg/contents/data/standard/03/98/39820.html (accessed Apr. 19, 2022).

[52] “EN 12976-2:2019 - Thermal solar systems and components - Factory made systems - Part 2: Test methods,” *iTeh Standards Store*. https://standards.iteh.ai/catalog/standards/cen/966d5d9c-a730-4840-b61d-d328d485bd3c/en-12976-2-2019 (accessed Apr. 19, 2022).

[53] D. J. Naron, “USING THE DST TEST METHOD FOR TESTING ‘SOLAR-ONLY’ AND ‘PREHEAT’ SOLAR DOMESTIC HOT WATER SYSTEMS,” p. 7.

[54] G. Panaras, E. Mathioulakis, and V. Belessiotis, “A method for the dynamic testing and evaluation of the performance of combined solar thermal heat pump hot water systems,” *Applied Energy*, vol. 114, pp. 124–134, Feb. 2014, doi: 10.1016/j.apenergy.2013.09.039.

[55] “ISO 9459-4 - Solar heating - Domestic water heating systems - Part 4: System performance characterization by means of component tests and computer simulation | Engineering360.” https://standards.globalspec.com/std/1575992/iso-9459-4 (accessed Apr. 19, 2022).

[56] “EN 12977-2:2018 - Thermal solar systems and components - Custom built systems - Part 2: Test methods for solar water heaters and combisystems,” *iTeh Standards Store*. https://standards.iteh.ai/catalog/standards/cen/ff762123-af35-4cef-9e76-97a5fef7346a/en-12977-2-2018 (accessed Apr. 19, 2022).

[57] D. Menegon, A. Vittoriosi, and R. Fedrizzi, “A new test procedure for the dynamic laboratory characterization of thermal systems and their components,” *Energy and Buildings*, vol. 84, pp. 182–192, Dec. 2014, doi: 10.1016/j.enbuild.2014.07.085.

[58] M. Y. Haller *et al.*, “Dynamic whole system testing of combined renewable heating systems – The current state of the art,” *Energy and Buildings*, vol. 66, pp. 667–677, Nov. 2013, doi: 10.1016/j.enbuild.2013.07.052.

[59] P. Mehrfeld *et al.*, “Dynamic evaluations of heat pump and micro combined heat and power systems using the hardware-in-the-loop approach,” *Journal of Building Engineering*, vol. 28, p. 101032, Mar. 2020, doi: 10.1016/j.jobe.2019.101032.

[60] D. Menegon, “Development of a Dynamic Test Procedure for the Laboratory Characterization of HVAC systems,” p. 183.

[61] H. Persson, B. Perers, and B. Carlsson, “Type12 and Type56: a Load Structure Comparison in TRNSYS,” Nov. 2011, pp. 3789–3796. doi: 10.3384/ecp110573789.

[62] “ASHRAE Standard 140 Maintenance and Development,” *Energy.gov*. https://www.energy.gov/eere/buildings/ashrae-standard-140-maintenance-and-development (accessed Aug. 30, 2022).

[63] E. Bertram, D. Carbonell, B. Perers, M. Haller, M. Bunea, and S. Eicher, *Models of Sub-Components and Validation for the IEA SHC Task 44 / HPP Annex 38 Part B: Collector Models*. 2012.

[64] W. Streicher, “Report on Solar Combisystems Modelled in Task 26 (System Description, Modelling, Sensitivity, Optimisation),” p. 13.

[65] “EN 16147:2017 - Heat pumps with electrically driven compressors - Testing, performance rating and requirements for marking of domestic hot water units,” *iTeh Standards Store*. https://standards.iteh.ai/catalog/standards/cen/94e7aca8-ef04-4c14-b33f-815ae9d86e04/en-16147-2017 (accessed Aug. 31, 2022).

[66] H. Sayegh, G. Fraisse, A. Leconte, E. Wurtz, O. Ouvrier Bonaz, and S. Rouchier, “Determination Of A Short Simulation Sequence For The Multi-Criteria Optimization Of Buildings: A Case Study,” Rome, Italy, pp. 1280–1287. doi: 10.26868/25222708.2019.210214.

[67] A. Belderbos and E. Delarue, “Accounting for flexibility in power system planning with renewables,” *International Journal of Electrical Power & Energy Systems*, vol. 71, pp. 33–41, Oct. 2015, doi: 10.1016/j.ijepes.2015.02.033.

[68] J. Ortiga, J. C. Bruno, and A. Coronas, “Selection of typical days for the characterisation of energy demand in cogeneration and trigeneration optimisation models for buildings,” *Energy Conversion and Management - ENERG CONV MANAGE*, vol. 52, pp. 1934–1942, Apr. 2011, doi: 10.1016/j.enconman.2010.11.022.

[69] A. Leconte, G. Achard, and P. Papillon, “Solar Combisystem Characterization with a Global Approach Test and a Neural Network Based Model Identification,” *Energy Procedia*, vol. 30, pp. 1322–1330, Dec. 2012, doi: 10.1016/j.egypro.2012.11.145.

[70] A. Leconte, G. Achard, and P. Papillon, “Global approach test improvement using a neural network model identification to characterise solar combisystem performances,” *Solar Energy*, vol. 86, no. 7, pp. 2001–2016, Jul. 2012, doi: 10.1016/j.solener.2012.04.003.

[71] “Master’s Thesis Hannes Engel - RWTH AACHEN UNIVERSITY Institute for Energy Efficient Buildings and Indoor Climate - English.” Accessed: Apr. 21, 2022. [Online]. Available: https://www.ebc.eonerc.rwth-aachen.de/go/id/nqkp/lidx/1

[72] “Integer Programming and the Theory of Grouping on JSTOR.” Accessed: Apr. 21, 2022. [Online]. Available: https://www.jstor.org/stable/2283635

[73] T. Madhulatha, “Comparison between K-Means and K-Medoids Clustering Algorithms,” 2011, pp. 472–481. doi: 10.1007/978-3-642-22555-0_48.

[74] “Buildings.Fluid.Boilers.BoilerPolynomial.” https://build.openmodelica.org/Documentation/Buildings.Fluid.Boilers.BoilerPolynomial.html (accessed Apr. 29, 2022).

[75] “3. Simulation Performance — Buildings Library User Guide.” https://simulationresearch.lbl.gov/modelica/userGuide/performance.html#numerical-solvers (accessed May 02, 2022).

[76] H. Abdi and L. J. Williams, “Principal component analysis,” *WIREs Computational Statistics*, vol. 2, no. 4, pp. 433–459, 2010, doi: 10.1002/wics.101.

[77] N. S. Malan and S. Sharma, “Feature selection using regularized neighbourhood component analysis to enhance the classification performance of motor imagery signals,” *Computers in Biology and Medicine*, vol. 107, pp. 118–126, Apr. 2019, doi: 10.1016/j.compbiomed.2019.02.009.

[78] “Snapshot.” Accessed: May 03, 2022. [Online]. Available: http://www.sthda.com/english/articles/31-principal-component-methods-in-r-practical-guide/112-pca-principal-component-analysis-essentials/

[79] D. A. Batra, “Analysis and Approach: K-Means and K-Medoids Data Mining Algorithms,” p. 6.

[80] P. Mehrfeld, K. Huchtemann, and D. Mueller, *Influences of Hot Water Tank States and the Order of Test Days to Gain the Annual Efficiency of Heat Pump Systems Evaluated Using Modelica*. 2017.

[81] P. Conti, C. Bartoli, A. Franco, and D. Testi, “Experimental Analysis of an Air Heat Pump for Heating Service Using a ‘Hardware-In-The-Loop’ System,” *Energies*, vol. 13, p. 4498, Sep. 2020, doi: 10.3390/en13174498.

[82] H. Geng, W. Kong, and Y. Wang, “Research on Uncertainty Analysis Method of Aircraft’s HWIL Simulation,” in *Theory, Methodology, Tools and Applications for Modeling and Simulation of Complex Systems*, Singapore, 2016, pp. 524–532. doi: 10.1007/978-981-10-2672-0_54.

[83] W. Tian and P. de Wilde, “Uncertainty and sensitivity analysis of building performance using probabilistic climate projections: A UK case study,” *Automation in Construction*, vol. 20, no. 8, pp. 1096–1109, Dec. 2011, doi: 10.1016/j.autcon.2011.04.011.

[84] I. Macdonald and P. Strachan, “Practical application of uncertainty analysis,” *Energy and Buildings*, vol. 33, no. 3, pp. 219–227, Feb. 2001, doi: 10.1016/S0378-7788(00)00085-2.

[85] X. Chen, H. Yang, and K. Sun, “Developing a meta-model for sensitivity analyses and prediction of building performance for passively designed high-rise residential buildings,” *Applied Energy*, vol. 194, no. C, pp. 422–439, 2017.

[86] M. Mottahedi, A. Mohammadpour, S. S. Amiri, D. Riley, and S. Asadi, “Multi-linear Regression Models to Predict the Annual Energy Consumption of an Office Building with Different Shapes,” *Procedia Engineering*, vol. 118, pp. 622–629, Jan. 2015, doi: 10.1016/j.proeng.2015.08.495.

[87] S. Wei, R. Jones, and P. de Wilde, “Driving factors for occupant-controlled space heating in residential buildings,” *Energy and Buildings*, vol. 70, pp. 36–44, Feb. 2014, doi: 10.1016/j.enbuild.2013.11.001.

[88] H. Janssen, “Monte-Carlo based uncertainty analysis: Sampling efficiency and sampling convergence,” *Reliability Engineering & System Safety*, vol. 109, pp. 123–132, Jan. 2013, doi: 10.1016/j.ress.2012.08.003.

[89] W. Tian, S. Yang, Z. Li, S. Wei, W. Pan, and Y. Liu, “Identifying informative energy data in Bayesian calibration of building energy models,” *Energy and Buildings*, vol. 119, pp. 363–376, May 2016, doi: 10.1016/j.enbuild.2016.03.042.

[90] W. Tian and R. Choudhary, “A probabilistic energy model for non-domestic building sectors applied to analysis of school buildings in greater London,” *Energy and Buildings*, vol. 54, pp. 1–11, Nov. 2012, doi: 10.1016/j.enbuild.2012.06.031.

[91] L. V. Gelder, P. Das, H. Janssen, and S. Roels, “Comparative study of metamodelling techniques in building energy simulation: Guidelines for practitioners,” *Simul. Model. Pract. Theory*, 2014, doi: 10.1016/j.simpat.2014.10.004.

[92] R. C. Smith, *Uncertainty Quantification: Theory, Implementation, and Applications*. SIAM, 2013.

[93] C. Chen, W. Xu, T. Guo, and K. Chen, “Analysis of actuator delay and its effect on uncertainty quantification for real-time hybrid simulation,” *Earthq. Eng. Eng. Vib.*, vol. 16, no. 4, pp. 713–725, Oct. 2017, doi: 10.1007/s11803-017-0409-6.

[94] S. Sankararaman, “Uncertainty Quantification and Integration in Engineering Systems.” 2012.

[95] E. Zio and N. Pedroni, “Literature review of methods for representing uncertainty,” p. 61.

[96] W. Tian *et al.*, “A review of uncertainty analysis in building energy assessment,” *Renewable and Sustainable Energy Reviews*, vol. 93, no. C, pp. 285–301, 2018.

[97] “Buildings.UsersGuide.” https://simulationresearch.lbl.gov/modelica/releases/latest/help/Buildings_UsersGuide.html (accessed May 19, 2022).

[98] “Monte Carlo Statistical Methods | SpringerLink.” https://link.springer.com/book/10.1007/978-1-4757-4145-2 (accessed May 19, 2022).

[99] B. Petersen, K. Gernaey, and P. Vanrolleghem, “Practical Identifiability of Model Parameters by Combined Respirometric-Titrimetric Measurements,” *Water science and technology : a journal of the International Association on Water Pollution Research*, vol. 43, pp. 347–55, Feb. 2001, doi: 10.2166/wst.2001.0444.

[100] “What is Linear Programming (LP)? - Definition from Techopedia,” *Techopedia.com*. http://www.techopedia.com/definition/20403/linear-programming-lp (accessed Aug. 24, 2022).

[101] “What is the difference between linear and non-linear programming - euresisjournal.org.” https://euresisjournal.org/en/what-is-the-difference-between-linear-and-nonlinear-programming (accessed Aug. 24, 2022).

[102] “Signal Features - MATLAB & Simulink.” https://www.mathworks.com/help/predmaint/ug/signal-features.html (accessed May 25, 2022).

[103] “SignalCharacteristics.pdf.” Accessed: May 25, 2022. [Online]. Available: http://wwwcourses.sens.buffalo.edu/mae334/notes/SignalCharacteristics

[104] G. H. Li, Z. Pei, R. Chen, and D. L. Hu, "The Principal Component Analysis of Signal Characteristic Parameters," *Applied Mechanics and Materials*, vol. 128–129, pp. 1269–1272, 2012, doi: 10.4028/www.scientific.net/AMM.128-129.1269.

[105] "Understanding and Choosing the Right Probability Distributions," in *Advanced Analytical Models*, John Wiley & Sons, Ltd, 2012, pp. 899–917. doi: 10.1002/9781119197096.app03.

[106] A. J. Hallinan, "A Review of the Weibull Distribution," *Journal of Quality Technology*, vol. 25, no. 2, pp. 85–93, Apr. 1993, doi: 10.1080/00224065.1993.11979431.

[107] J. Proakis and D. Manolakis, "Digital Signal Processing: Principles, Algorithms, and Applications," *undefined*, 1992, Accessed: May 29, 2022. [Online]. Available: https://www.semanticscholar.org/paper/Digital-Signal-Processing%3A-Principles%2C-Algorithms%2C-Proakis-Manolakis/cb5206cf9ee6a4eb5d1f2deb9736883850fcf310

[108] R. N. Youngworth, B. B. Gallagher, and B. L. Stamper, "An overview of power spectral density (PSD) calculations," in *Optical Manufacturing and Testing VI*, Aug. 2005, vol. 5869, pp. 206–216. doi: 10.1117/12.618478.

[109] D. F. Elliott, "Chapter 7 - Fast Fourier Transforms," in *Handbook of Digital Signal Processing*, D. F. Elliott, Ed. San Diego: Academic Press, 1987, pp. 527–631. doi: 10.1016/B978-0-08-050780-4.50012-6.

[110] M. Affenzeller, S. Winkler, and S. Wagner, "Evolutionary System Identification: New Algorithmic Concepts and Applications," 2008, pp. 29–48.

[111] "Continuous optimization | Combinatorics and Optimization | University of Waterloo." https://uwaterloo.ca/combinatorics-and-optimization/research-combinatorics-and-optimization/research-areas/continuous-optimization (accessed Aug. 04, 2022).

[112] "What is Combinatorial Optimization?" https://www.cs.cmu.edu/afs/cs.cmu.edu/project/learn-43/lib/photoz/.g/web/glossary/comb.html (accessed Aug. 04, 2022).

[113] S. Das and P. N. Suganthan, "Differential Evolution: A Survey of the State-of-the-Art," *IEEE Transactions on Evolutionary Computation*, vol. 15, no. 1, pp. 4–31, Feb. 2011, doi: 10.1109/TEVC.2010.2059031.

[114] *Adaptive Differential Evolution*. Accessed: Jun. 08, 2022. [Online]. Available: https://link.springer.com/book/10.1007/978-3-642-01527-4

[115] M. R. Islam, H. H. Lu, M. J. Hossain, and L. Li, "A Comparison of Performance of GA, PSO and Differential Evolution Algorithms for Dynamic Phase Reconfiguration Technology of a Smart Grid," in *2019 IEEE Congress on Evolutionary Computation (CEC)*, Jun. 2019, pp. 858–865. doi: 10.1109/CEC.2019.8790357.

[116] "Taxonomy-of-optimization-methods.jpg (850×1007)." https://www.researchgate.net/profile/D-Nagesh-Kumar/publication/342112667/figure/fig1/AS:901407657967616@1591923741187/Taxonomy-of-optimization-methods.jpg (accessed Aug. 05, 2022).

[117] D. KARABOĞA and S. ÖKDEM, "A Simple and Global Optimization Algorithm for Engineering Problems: Differential Evolution Algorithm," *Turkish Journal of Electrical Engineering and Computer Sciences*, vol. 12, no. 1, pp. 53–60, Jan. 2004, doi: -.

[118] "Frontiers | A Comparative Study of Differential Evolution Variants in Constrained Structural Optimization | Built Environment." Accessed: Jun. 08, 2022. [Online]. Available: https://www.frontiersin.org/articles/10.3389/fbuil.2020.00102/full

[119] T. Eltaeib and A. Mahmood, "Differential Evolution: A Survey and Analysis," *Applied Sciences*, vol. 8, p. 1945, Oct. 2018, doi: 10.3390/app8101945.

[120] "wolpert96.pdf." Accessed: Jun. 08, 2022. [Online]. Available: http://delta.cs.cinvestav.mx/~ccoello/compevol/wolpert96.pdf

[121] A. Hassanat, K. Almohammadi, E. Alkafaween, E. Abunawas, A. Hammouri, and S. Prasath, "Choosing Mutation and Crossover Ratios for Genetic Algorithms-A Review with a New Dynamic Approach," p. 390, Dec. 2019, doi: 10.3390/info10120390.

[122] J. R. S. PhD, "Why Is Cross Entropy Equal to KL-Divergence?," *Medium*, Feb. 12, 2022. https://towardsdatascience.com/why-is-cross-entropy-equal-to-kl-divergence-d4d2ec413864 (accessed Aug. 24, 2022).

[123] "Power spectral density estimates (LTPDA Toolbox)." https://www.lisamission.org/ltpda/usermanual/ug/sigproc_psd.html (accessed Aug. 24, 2022).

[124] R. Khandelwal, "Techniques to Measure Probability Distribution Similarity," *Geek Culture*, Jun. 13, 2021. https://medium.com/geekculture/techniques-to-measure-probability-distribution-similarity-9145678d68a6 (accessed Aug. 08, 2022).

[125] R. C. Smith, *Uncertainty Quantification: Theory, Implementation, and Applications*. SIAM, 2013.

[126] "SciPy documentation — SciPy v1.8.1 Manual." https://docs.scipy.org/doc/scipy/ (accessed Jun. 09, 2022).

[127] M. Centeno-Telleria, E. Zulueta, U. Fernandez-Gamiz, D. Teso-Fz-Betoño, and A. Teso-Fz-Betoño, "Differential Evolution Optimal Parameters Tuning with Artificial Neural Network," *Mathematics*, vol. 9, no. 4, Art. no. 4, Jan. 2021, doi: 10.3390/math9040427.

[128] P. Welch, "The use of fast Fourier transform for the estimation of power spectra: A method based on time averaging over short, modified periodograms," *IEEE Transactions on Audio and Electroacoustics*, vol. 15, no. 2, pp. 70–73, Jun. 1967, doi: 10.1109/TAU.1967.1161901.

[129] M. S. Bartlett, “Periodogram Analysis and Continuous Spectra,” *Biometrika*, vol. 37, no. 1/2, pp. 1–16, 1950, doi: 10.2307/2332141.

[130] Y. Xiang, D. Y. Sun, W. Fan, and X. G. Gong, “Generalized simulated annealing algorithm and its application to the Thomson model,” *Physics Letters A*, vol. 233, no. 3, pp. 216–220, Aug. 1997, doi: 10.1016/S0375-9601(97)00474-X.

[131] K. M. Mullen, “Continuous Global Optimization in R,” *Journal of Statistical Software*, vol. 60, pp. 1–45, Sep. 2014, doi: 10.18637/jss.v060.i06.

[132] C. Tsallis and D. A. Stariolo, “Generalized simulated annealing,” *Physica A: Statistical Mechanics and its Applications*, vol. 233, no. 1, pp. 395–406, Nov. 1996, doi: 10.1016/S0378-4371(96)00271-3.

[133] C. Tsallis, “Possible generalization of Boltzmann-Gibbs statistics,” *J Stat Phys*, vol. 52, no. 1, pp. 479–487, Jul. 1988, doi: 10.1007/BF01016429.

[134] “SciPy documentation — SciPy v1.8.1 Manual.” https://docs.scipy.org/doc/scipy/ (accessed Jul. 25, 2022).

[135] J. Brownlee, “Dual Annealing Optimization With Python,” *Machine Learning Mastery*, May 20, 2021. https://machinelearningmastery.com/dual-annealing-optimization-with-python/ (accessed Jul. 26, 2022).